A PARAMETRIC STUDY OF VESTIBULAR STIMULATION DURING CENTRIFUGATION

by

Jeremie M. Pouly

French Engineering Degree, Supaéro
(École nationale supérieure de l'aéronautique et de l'espace, France, 2006)

SUBMITTED TO THE DEPARTMENT OF AERONAUTICS AND ASTRONAUTICS IN PARTIAL FULFILLMENT OF THE REQUIREMENTS FOR THE DEGREE OF

MASTER OF SCIENCE IN AERONAUTICS AND ASTRONAUTICS

AT THE
MASSACHUSETTS INSTITUTE OF TECHNOLOGY

FEBRUARY 2006

Signature of Author_____
Department of Aeronautics and Astronautics
January 20, 2005

Certified by_____
Professor Laurence R. Young
Department of Aeronautics and Astronautics
Apollo Program Professor of Astronautics
Professor of Health Sciences and Technology
Thesis Supervisor

Accepted by_____
Jaime Peraire
Professor of Aeronautics and Astronautics
Chair, Committee on Graduate Students

A PARAMETRIC STUDY OF VESTIBULAR STIMULATION DURING CENTRIFUGATION

BY
JEREMIE M. POULY

SUBMITTED TO THE DEPARTMENT OF AERONAUTICS AND ASTRONAUTICS ON JANUARY 23, 2006 IN PARTIAL FULFILLMENT OF THE REQUIREMENTS FOR THE DEGREE OF MASTER OF SCIENCE IN AERONAUTICS AND ASTRONAUTICS.

ABSTRACT

Artificial Gravity (AG) provided by short-radius centrifugation is a promising countermeasure to the health problems associated with long duration human spaceflight. Head-turns performed during centrifugation, however, trigger a disturbing vestibular response that is only qualitatively understood. In order to design an efficient incremental adaptation procedure, the present study investigates the quantitative aspect of the vestibular side effects associated with AG, in particular, the relationship among cross-coupled stimulation, vestibular response, and adaptation.

We tested 20 young adults with supine right-quadrant yaw head-turns performed in a dark environment during short-radius centrifugation. We studied the changes in vestibular response and adaptation to head-turns at different levels of cross-coupled stimulation. Nine combinations of head-turn angle (20°, 40° or 80°) with centrifuge-velocity (12, 19 or 30 rpm) were tested over two consecutive days.

There were four key findings:

1. All measures, except the slow-phase velocity (SPV) peak amplitude of the vestibulo-ocular reflex, decrease significantly between the two experimental days, which demonstrates that significant adaptation is achieved.
2. Large head-angles lead to longer vertical vestibulo-ocular reflex time-constants than smaller angles do, but do not lead to greater adaptation.
3. In the nose-up position, the perceived body-tilt is highly correlated with the true tilt of the gravito-inertial force at mid-chest level.
4. The SPV-peak amplitude and all subjective ratings except body-tilt show significant correlation with the intensity of the cross-coupled stimulus (CCS): the larger the CCS, the stronger the vestibular response.

Thesis Supervisor: Professor Laurence R. Young
Title: Apollo Program Professor of Astronautics
Professor of Health Sciences and Technology

This work was supported by the National Space Biomedical Research Institute (NSBRI) through a cooperative agreement with the National Aeronautics and Space Administration (NCC 9-58).

ACKNOWLEDGEMENTS

I am deeply indebted to Professor Laurence Young, my advisor, for giving me the opportunity to work on the AG project. Thank you for hiring me, for your support and for your interest in the French culture. I'm honored to be your student.

For funding this research I'm grateful to NSBRI and NASA. I thank MIT and SUPAERO for giving me the chance to study in the US. I thank Liz Zotos and the MVL faculty members for making MVL a great place to work. I give my sincere appreciations to Sophie Adenot who guided me in my journey to MIT.

I am most grateful to Thomas Jarchow for understanding me better than I do myself. Thomas, thank you for always caring for me, for your understanding in all situations and your valuable advice. I learned a lot from you. I am also grateful to Alan Natapoff for the uncountable hours spent reading through my thesis. I learned a lot from our discussions and your advice were always wise and most useful.

My special gratitude goes to all the MVL students for the wonderful time spent together. There is no other lab I would have preferred to join than MVL. Many thanks to Paul Elias and Jessica Edmonds for being awesome officemates. Paul, I really appreciated the time you spent to answer all my questions about the US, I hope I didn't screw up your English. Jessica, you're an amazing person, thank you for the energy and the craziness you brought to the office. A big *merci* to both of you for all the fun, the laugh and even the cynicism shared. I'll miss striking the cockroaches with you guys! My special thoughts to Jessica Marquez for your nice words and your *coucous*. My thoughts as well to Dan Buckland and Angela Karis, Kevin Duda, Kristen Bethke, Liang Sim and, in general, to all the students in the lab, including the undergrads: I really had a great time with all of you guys.

To my roommates: thanks you guys for all the fun and the time spent together. Thank you Anthony for your imitation of my French accent, thank you Luis for giving me so many kills at Halo and, above all, thank you Justin for your generosity and friendship. I was never by myself back in Tang and there's nothing worse more than that. Many thanks to all the other people I met here, you all participated in making my grad studies an unforgettable story.

All my love to my parents and brother: you always believed in me and it gave me the strength to succeed. *Vous m'avez toujours soutenu et poussé vers l'avant. Je suis arrivé où j'en suis grâce à vous.* My gratitude to my family in law as well, for your timeless support (a big thank you to my personal punching ball for enduring me). And last but not least, thank you to my girl: You've always been with me from the start – back in high school – and I could never have gone this far without you. When you hold my hands, nothing is out of reach, not even my dreams.

Table of Contents

List of Acronyms

The following acronyms are used:

AATM	Adaptative Asymmetric Trimmed-Mean (filter)
AG	Artificial Gravity
CCS	Cross-Coupled Stimulus
CSA	Context-Specific Adaptation
FIR	Finite Impulse Response (filter)
GIF	Gravito-Inertial Force
LBNP	Lower Body Negative Pressure
LBPP	Lower Body Positive Pressure
MS	Motion Sickness
NUP	Nose Up
PFMH	Predictive FIR-Median Hybrid (filter)
OS	Order-Statistic (filter)
RED	Right Ear Down
RMS	Root Mean Square
SCC	Semi-Circular Canals
SHP	Subjective Horizontal Position
SPV	Slow-Phase Velocity
NSPV	Normalized SPV
VOR	Vestibulo-Ocular Reflex
aVOR	angular VOR
lVOR	linear VOR

1 Introduction

Some believe that Terra is not only the cradle of humankind but also the only place in the nearby universe where the human race will ever be able to flourish. Unlike the hostile space environment, the Earth provides us with everything we need to survive: oxygen, liquid water, food, radiation protection, and gravity. For almost 50 years, NASA and the other international space agencies have made headway against this belief and have shown that humans are able to survive for more than a year in a Low Earth Orbit environment – as in MIR, Skylab and ISS. This success shows that the Moon is accessible and that Mars and even places beyond could also be [1].

Space exploration is only beginning, and although monumental progress has been made since the early days of Sputnik, challenges remain.

Further human space exploration will, of course, require a great many purely technological victories, but human-related challenges may represent the lion-share of what remains to be accomplished. The space environment is hostile to the human body. Over the 40 years since humans first flew in space, several hazards have been identified that form obstacles to space exploration [2, 3]. Space radiation, surveyed elsewhere [4, 5], and the lack of gravity are only some of the most important risk factors.

1.1 Deleterious effect of microgravity

On Earth, the human body is accustomed to Earth gravity. In space, the body's physiological systems try to adapt to the new zero-g environment: Exposure to long-duration weightlessness has dramatic effects on the body including muscle atrophy, bone loss, cardiovascular alteration and vestibular deconditioning [3]. This adaptation may result in unpleasant consequences upon returning to a steady-state gravitational environment (Earth, Moon or Mars).

The Musculo-Skeletal system is affected by the lack of gravity. In microgravity astronauts float in space and do not have to bear their own weight. Since there is no need for strong lower limbs or back muscles to maintain posture, those muscles weaken and reduce in size. In long-duration missions, a reduction of up to 25% in the mass of certain muscles may be expected [3]. Astronauts can also loose up to 20% of their bone mass. This decrease threatens astronauts on a Mars-exploration mission with osteoporosis. In weightlessness bone mineral density decreases due to the absence of compressive gravitational loads on the lower body segments.

The cardiovascular system is modified in microgravity as in Figure 1.1. In 1-g – or other steady-state gravity – the blood concentrates in the heart and lower limbs (Figure 1.1-a). On first exposure to microgravity, where there is no gravity to "pull" the blood toward the feet, fluid shifts upward creating a surplus of blood in the chest and head (Figure 1.1-b). Cardiovascular adaptation to weightlessness leads to a decrease in blood volume (Figure 1.1-c) that regulates body fluid volume at heart level. On return to a steady-state gravity environment, fluid shifts downward under influence of gravity (Figure 1.1-d), which depletes the blood in the brain and may lead to fainting. In addition to this orthostatic intolerance, microgravity could also lead to more serious cardiovascular incidents, such as cardiac dysrhythmia [6].

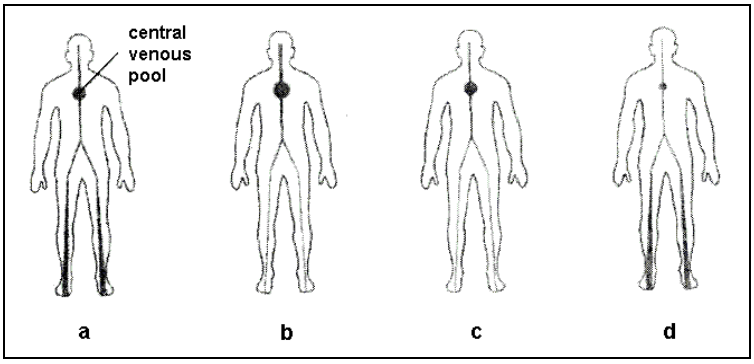

Figure 1.1. Changes in the cardiovascular system in response to changes in gravity load. (a) Earth – or any steady-state – gravity, normal conditions. (b) Microgravity, acute exposure. (c) Microgravity, chronic exposure. (d) Earth gravity, upon return. (modified from [7])

The vestibular system is also greatly influenced by the absence of gravity cues [8]. On Earth, the vestibular system measures head motions and uses gravity cues to assess

body orientation (Chapter 2). Since such cues are unavailable in space, after a period of space motion sickness [8, 9], vestibular function adapts to interpret only head motions. This space-adapted vestibular function becomes a problem after returning to planetary gravity since the vestibular system reinterprets (i.e. misinterprets) gravity cues as linear accelerations. This causes astronauts to experience vertigo, motion sickness and difficulty in maintaining posture and gaze.

1.2 Existing countermeasures

Most of the physiological modifications driven by exposure to weightlessness are appropriate adaptations of the human body to a novel environment. Internal processes typically minimize their own energetic cost and do not for example maintain an unnecessarily high bone density. Although these adjustments are appropriate in space, they create health hazards upon re-exposure to planetary gravity. Since any astronaut will some day return to Earth, this microgravity-related deconditioning has to be countered in order to reduce health hazards. For a mission to Mars this concern is even greater as the astronauts will have to maneuver in the 3/8-g Mars gravity without the medical assistance that could mediate recovery on Earth.

Classical exercise countermeasures include treadmills, ergometers and resistance devices. These exercise countermeasures attenuate deconditioning of the cardiovascular and musculo-skeletal systems. Musculo-skeletal deconditioning is partially countered [10]: Muscles are, of course, stimulated by any exercise, and bones undergo compressive loads during eccentric exercise (tension during muscle lengthening [11]). Cardiovascular deconditioning is not inhibited but the cardiovascular function is maintained globally by exercising the heart. The ISS currently offers the three different exercise devices, shown on Figure 1.2.

A less common countermeasure is the Lower Body Negative Pressure (LBNP) device shown in Figure 1.3. This attenuates cardiovascular deconditioning by applying a “negative” pressure to the lower part of the body. Decreased pressure shifts fluids toward the legs, as gravity would do.

Figure 1.2. Exercise facilities available on the ISS including (a) Treadmill with a Vibration Isolation and Stabilization System, (b) Cycle Ergometer with Vibration Isolation and Stabilization System, (c) Interim Resistive Exercise Devise. (reproduced from [12], NASA photography)

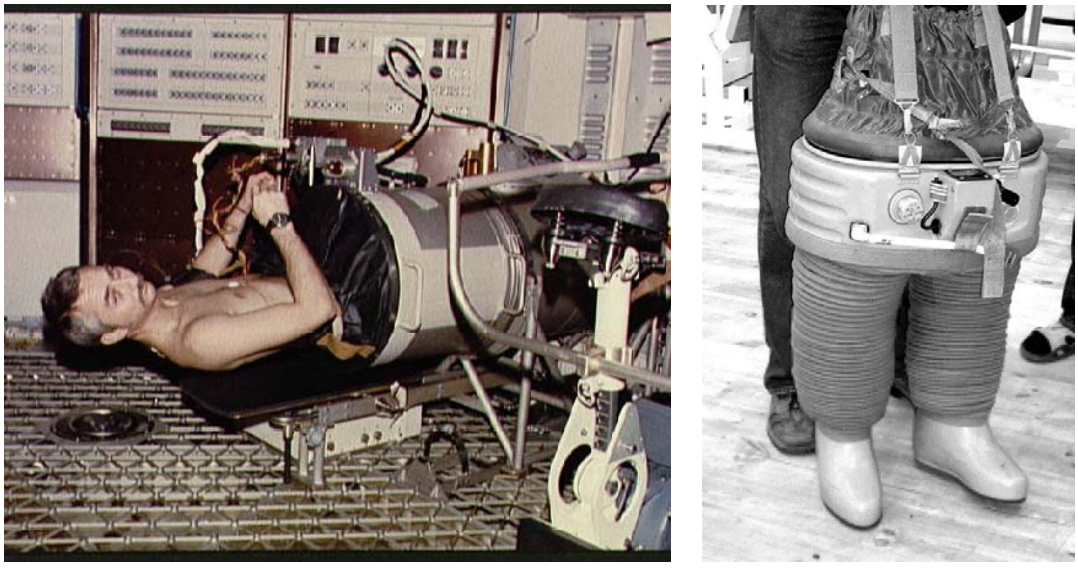

Figure 1.3. Cardiovascular alterations countermeasures. (a) Astronaut Owen Garriott lies in the Lower Body Negative Pressure Device during Skylab 3 (NASA photography). (b) Russian Lower Body Negative Pressure suit in its inactivated state (credits: Jessica Edmonds)

1.3 Artificial gravity

Existing countermeasures have not yet been proven to inhibit microgravity deconditioning. In the search for a more efficient way to reduce the adverse effects of weightlessness, Artificial Gravity (AG) has become the main challenger. Whereas exercise countermeasures aim at reducing symptoms, AG tries to remove their cause – if microgravity deconditioning leads to health hazards, the AG philosophy suggests that astronauts should remain conditioned to gravity. General AG considerations including human factor issues and spacecraft design are discussed by Young in [13, 14].

AG comes from Einstein's Equivalence Principle, which states that physics cannot distinguish gravity from acceleration [15]. Since any mechanical or physiological sensor identically interprets accelerations and gravity, accelerations can serve as "artificial" gravity (AG). In principle AG could be provided be any acceleration, but it classically refers to the sustained centripetal acceleration resulting from a rotational motion at a constant speed.

The notion of AG emerged at the beginning of the last century in the work of Tsiolkovsky, a Russian space visionary. Interestingly it was popularized more through science fiction than through conventional science and was long considered unfeasible. Indeed the early ideas for implementing AG – through rotating or tethered spacecraft – were over-challenging to technology (Figure 1.4).

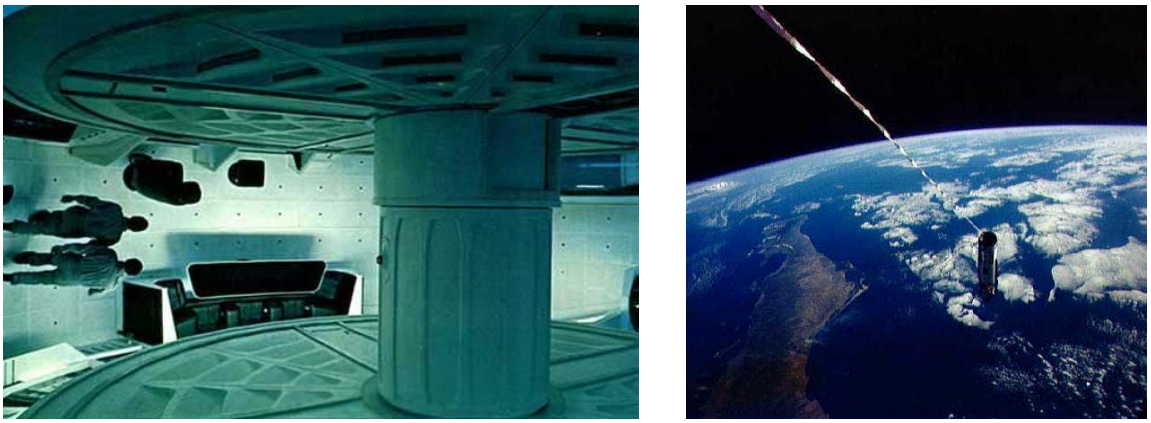

Figure 1.4. Early AG implementations. (a) Von Braun's concept of a rotating space station (from *2001: A Space Odyss*ey). (b) Gemini XI tethered Agena vehicle (NASA photography).

AG can be delivered by a short-radius centrifuge, rotating spacecraft or tethered vehicle. Von Braun's concept of a rotating space station requires launch capabilities still unavailable today, and the early attempts to test tethered-AG during Gemini were unsuccessful. At first, rotation rates near 10-rpm were considered to be the upper limit of human tolerance to vestibular stimulation [16]. For this reason, the rotator's radius had to be greater than 10 meters to provide the Earth-comparable gravity levels necessary to counter microgravity deconditioning. This dimensional constraint kept AG on the fiction side of science. It was finally shown in the 1990s that humans can tolerate intermittent exposure to rotation speeds greater than 20-rpm [17, 18]. This finding validated short-radius centrifugation as a physiologically bearable way to produce AG. Although technologically accessible, this new type of AG has not been extensively tested in orbit. To this day, implementation of short-radius centrifuges (SRCs) in space has been limited to shuttle missions STS-42 (Figure 1.5) and STS-90.

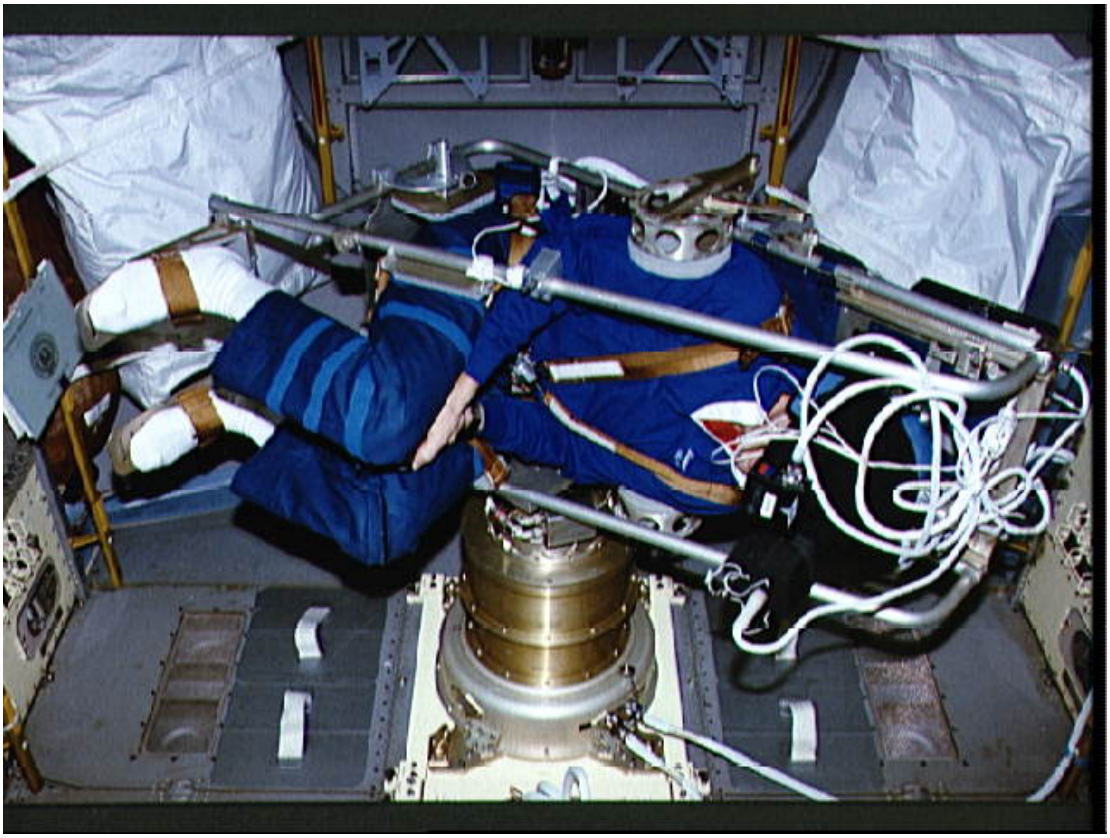

Figure 1.5. Mission specialist Hilmers in IML-1's MVI space rotator during STS-42. The rotator could be configured to spin the astronauts around two different body axes: interaural or vertical. The interaural axis configuration is shown. (NASA photography)

The results yielded by SRC testing in space are promising. Although AG SRC has had only limited tests to date, it has fulfilled some of its promises. It was found to counteract both the post-flight orthostatic intolerance [19] and the deconditioning of the otolith-ocular orienting reflex [20]. More data is necessary, however, to validate its general premises.

AG is a global countermeasure that, at one stroke, alleviates all the deleterious effects related to prolonged exposure to microgravity by eliminating their original source. Astronauts can be exposed to AG either continuously or intermittently. Continuous AG is created by a rotating spaceship, tethered or not, and provides a continuous gravity field in which the astronauts operate freely. By contrast, intermittent AG is created by a smaller rotating device onboard the spaceship (SRC) and is provided to the astronauts through time-limited daily sessions. Whereas continuous AG requires lower rotation rates and is less disturbing for the human body, intermittent AG is less constraining to the spaceship architecture and is technologically available. Intermittent AG might also be combined with exercise while spinning to enhance its effect [11]. While the effectiveness of AG as a countermeasure is well accepted, some side effects must be addressed. These potential drawbacks of AG include inherent gravity gradients, Coriolis forces induced by body movements, and cross-coupled effects generated by angular motions of the head. These problems increase in strength with rotation speed and are therefore more pronounced for intermittent AG than for continuous AG. This thesis focuses on intermittent AG generated by SRCs.

Gravity gradients may – or may not – have an adverse effect on physiological systems and require further study [21]. Alterations to the sensory-motor system are more problematic and have been studied carefully. In rotating artificial gravity environments, the body's dynamics are distorted by the effect of Coriolis forces. Experimental results suggest that the motor system can adapt to high rotation rate [22, 23] and that re-adaptation to Coriolis-free body dynamics upon cessation of rotation is quick [16]. Out-of-plane head movements performed during centrifugations generate disturbing cross-coupled effects. Although first exposures to AG are often associated with motion sickness, it has been shown that humans can adapt to this provocative stimulus [24]. This vestibular stimulation is the focus of this thesis.

1.4 Rationale and motivation

As part of a broader research project, this experimental thesis investigates the quantitative relation between the initial vestibular stimulation and the response to it. Indeed, AG is a new field of research and, although our understanding of the effect of centrifugation on neurovestibular function has been greatly enhanced by past studies, our knowledge remains mainly qualitative and approximate. In order to design efficient AG training, we need to know precisely how strong a stimulus is needed to trigger a given vestibular response, and how much adaptation is thereby generated. This is what this study seeks to contribute to.

Previous studies of the vestibular side-effects of AG have, generally, treated the parameters involved in vestibular disturbance one at a time. This was needed to gain the basic knowledge required to establish that humans can adapt to performing head-turns during high rotation-rate centrifugation and, thereby, validate the concept of AG. That first step has now been accomplished. This is proved by the increasing number of scientists that believe in AG as a countermeasure. If, then, we are to progress in our understanding of this inconvenient vestibular response we must vary our approach and design experiments that will deliver quantitative knowledge about the process. In particular, the first challenge, which has not been sufficiently addressed thus far, is to validate our model of initial stimulation. Based on the physiology of the semi-circular canals, the current model predicts that head-turns performed in a rotating environment trigger a cross-coupled stimulus (CCS) whose intensity drives the vestibular response (Section 2.2). But is this prediction verified experimentally?

As a foundation for further quantitative analyses of the vestibular disturbances associated with AG, this experimental thesis conducts a parametric study of the CCS. The goal of the thesis is to show the validity of the CCS parameter by experiment. In particular, this study compares the influence of the component parameters of the CCS, head-turn angle and centrifuge-velocity, on neurovestibular response and adaptation. The neurovestibular response is driven not only by the vestibular stimulation, but also by signals from other sensory systems, such as the somatosensory and proprioceptor

systems. The response might then be affected differently by head-angle and centrifuge-velocity since they might not be perceived similarly by the other sensory systems. It is then not given that the neurovestibular response and, above all, adaptation will be significantly correlated with the intensity of the CCS, and that has to be verified. This study, therefore, investigates the potential differences in the response along several iso-CCS lines: curves defining the intensity of the CCS with respect to centrifuge-velocity and head-angle (Section 3.2).

In addition, one of the current foci of general AG research is the design of an efficient incremental adaptation procedure. As opposed to sequential adaptation, which keeps a constant stimulus, incremental adaptation consists of exposing the subject to an increasing stimulus so that adaptation is achieved with minimal discomfort (Section 2.7). Optimization of incremental adaptation requires the quantitative knowledge mentioned previously. This thesis is a first step in that direction. In particular, it compares the relative effect of head-angle and centrifuge-velocity in order to make incremental adaptation more efficient: Where incremental adaptation procedures classically use centrifuge-velocity as the incremental variable, they might more appropriately use head-angle instead.

The question this study seeks to answer is, therefore, essential for our general understanding of the vestibular disturbance associated with AG. It is a prerequisite for the design of an efficient incremental adaptation procedure as well, and it is summarized by the single question: Are the iso-CCS lines also iso-neurovestibular-response and iso-adaptation lines?

1.5 Thesis organization

Chapter 1 – Introduction: Introduces artificial gravity as a countermeasure for the debilitating effects associated with long-term exposure to weightlessness.

Chapter 2 – Background: Provides general considerations underlying vestibular response and sensory adaptation to out-of-plane head-turns performed during centrifugation. The emphasis is on models relevant to this study.

Chapter 3 – Methods: Presents the experimental design and protocol, provides information on the equipment used and data collection.

Chapter 4 – Analysis: Describes eye-movements and subjective data analysis procedures with focus on the algorithm that extracts the slow-phase velocity component from the raw eye position.

Chapter 5 – Results: Describes trends in the data measured during the experiment – including statistical significance.

Chapter 6 – Discussion: Explores the experimental results and, when appropriate, suggests physiological reasons that may underlie the observed results.

Chapter 7 – Conclusion: Summarizes the key findings of this study and makes recommendations for future work.

2 Background

2.1 Vestibular physiology

This section describes the vestibular physiology that underlies the effect of different gravity environments (including artificial gravity) on the response of the vestibular system to head-turns.

2.1.1 Overview

The vestibular system is located in the inner ear (Figure 2.1) and measures the body orientation and acceleration in space. It provides the brain with data on linear and angular accelerations as well as orientation of the head with respect to gravity. Its function is essential to postural and gaze control, and people with a deficient vestibular apparatus experience difficulties in walking or in stabilizing gaze while moving [25].

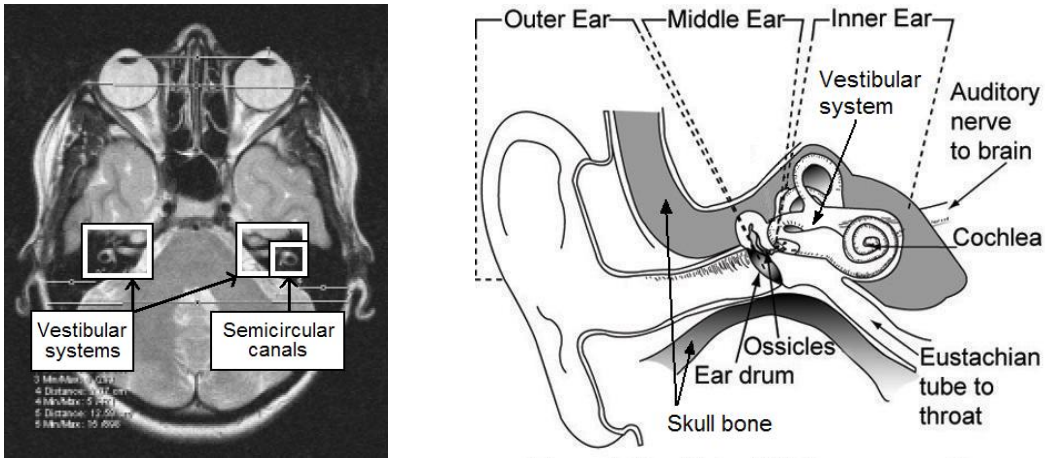

Figure 2.1. Position of the vestibular system. (a) Top view of the position of the vestibular systems in the head (modified from [26]). (b) Lateral view of the vestibular system in its surrounding organs (modified from [27]).

Any motion of the body is detected by the vestibular system, encoded as an electrical signal, and transmitted to the brain through the vestibular nerve. The brain integrates the vestibular, visual, and somatosensory inputs to estimate the orientation and motion of the body, and consequently elicit eye, head, or body movements that will stabilize gaze and maintain balance. The vestibular system consists of two symmetrical apparatuses located in the labyrinth of the temporal bone of the inner ear. Each is composed of three semicircular canals, the anterior, posterior, and lateral canal, and two otolith organs, the saccule and utricle. The canals are sensitive to angular acceleration whereas the otolith organs are primarily sensitive to linear accelerations and gravity. They are organized as on Figure 2.2.

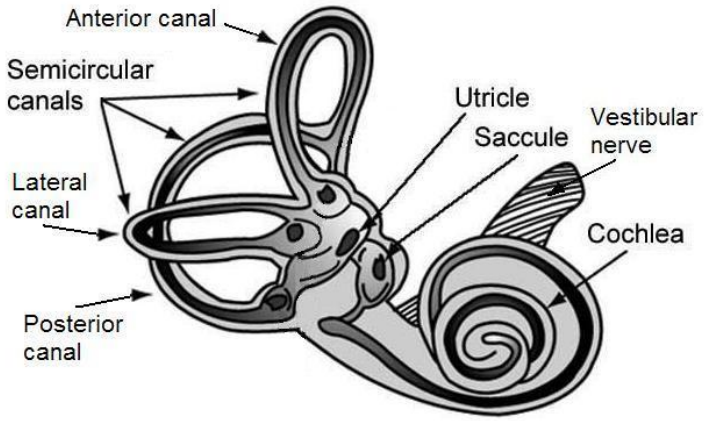

Figure 2.2. Human vestibular system (modified from [27]). The three tubular ducts of the semicircular canals are clearly visible in the left half of the drawing. The saccule and the utricle (otolith organs) are visible in the center of the picture.

As shown on the figure above, the vestibular system is very close to the auditory system (cochlea) and, in fact, those two systems present a lot of common properties.

2.1.2 The semi-circular canals

The semi-circular canals (SCC) are three approximately orthogonal, 2/3-ring-shaped canals filled with a fluid called endolymph. Each canal acts as an angular accelerometer and can only measure rotations in the plane in which it rests. The vestibular system

assesses any angular acceleration by combining the component measured by each of the three SCC. Orientation of the SCC with respect to the head has been accurately measured [28] and is represented on Figure 2.3. The lateral canals (RL or LL) are tilted approximately 30º from the head horizontal plane; the anterior (LA, RA) and posterior (LP, RP) canals, approximately 45º from the medio-lateral plane. However, as the vestibular system integrates the signals of the three SCC in a single 3D angular accelerometer, the angular accelerations can be described in terms of body components: roll, pitch, and yaw accelerations.

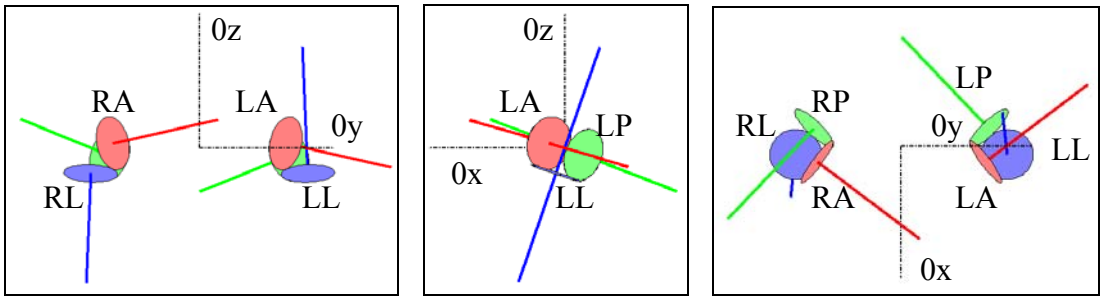

Figure 2.3. Orientation of the SCC: (a) front, (b) left side, and (c) top view in the coordinate system attached to the head. Using the right-hand rule, the vector coming out of each canal defines the direction of high sensitivity (increased discharge rate) of the canal [29, 30].

The basic layouts of the three SCC are identical, except that the vertical canals share a common wall. Each canal consists of a semicircular duct resting within the temporal bone in the perilymph fluid. The duct is filled with endolymph fluid and includes an enlarged region, the ampulla. As illustrated on Figure 2.4-b, the ampulla is a bulb-shaped chamber sealed by a flexible wedge known as the cupula. The cupula contains the cilia extremities of numerous hair cells implanted into the ampullary crest and directly connected to the nerve fibers (Figure 2.4-c). Section 2.1.4 provides more details about the hair cells. An important property of these sensory cells is their directional sensitivity: Stimulations of the cell can be separated, based on their directions, in excitations, to which the cell is very sensitive, and inhibitions, to which it is less sensitive.

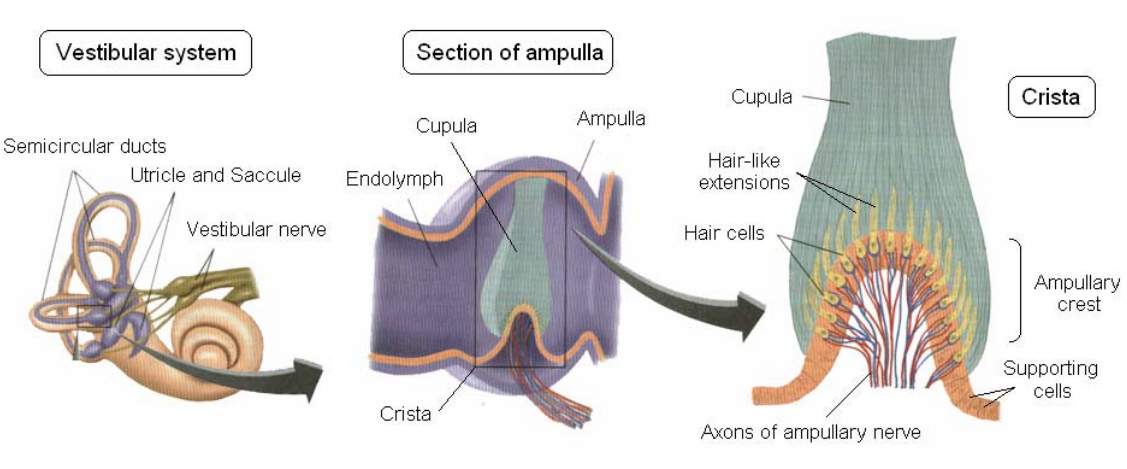

Figure 2.4. Anatomy of a semicircular canal. (a) Position in the vestibular system. (b) Section of ampulla showing how the cupula seals the duct. (c) Details of the crista and hair cells implantation (modified from http://www.colorado.edu/epob/epob3730rlynch/image/figure8-20.jpg).

In the crista (comprised of cupula and ampullary crest) the hair cells are oriented in the same direction. This uniform orientation of the hair cells, taken with their directional sensitivity, defines a direction of enhanced sensitivity for each canal. The canal measures the angular acceleration accurately in that direction and more approximately in the opposite direction [30]. To compensate for this anatomical asymmetry, the canals are paired so that in each pair the two canals rest approximately in the same plane and are sensitive to different directions. That is, if one canal is more sensitive to clockwise accelerations, the other will be more sensitive to counterclockwise stimulation. Resting in the same plane, the two lateral canals are functionally paired. The left anterior (LA) and the right posterior (RP) canals, resting in two planes almost parallel and sensitive to opposite directions, are naturally organized to be combined; as are the right anterior (RA) and the left posterior (LP) canals. Figure 2.3-c shows that crossed-pairing for the anterior and posterior canals.

Any rotation of the head projects onto the planes of the SCC and causes the motion of the endolymph in each stimulated canal to lag inertially behind the motion of the head itself. This inertia of the fluid with respect to the walls of the canals increases the pressure on one side of the cupula, which seals the ampulla, and decreases it on the other. This deflects the cupula as illustrated on Figure 2.5 and that deflection is transduced into

a nervous signal by the hair cells and transmitted to the brain, as explained in Section 2.1.4.

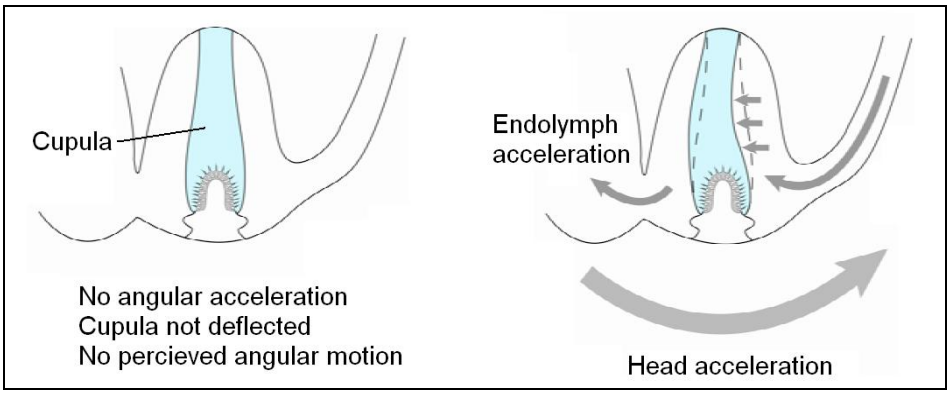

Figure 2.5. Detection of an angular acceleration by the SCC through inertia of the endolymph fluid relative to the canal motion (modified from [31]). (a) At rest. (b) Counterclockwise head angular acceleration: Inertia causes endolymph to lag behind, which deflects the cupula.

During sustained body rotations, the spring restoring force of the cupula will eventually damp the rotation sensation. For head-turns under normal conditions, the canal stimulation is not sustained long enough for this damping to occur[1]. However, for head-turns performed while spinning on a centrifuge, this decay of the canal response has a major influence on the sensation experienced by the subject.

The canal fluid dynamics can be represented by an overdamped torsion pendulum model. The model, first presented by Steinhausen in 1931, derives the angular displacement ξ of the cupula from the angular acceleration input α [32]. The model has been updated and experimentally verified by Fernandez and Goldberg [33], and has been described with variations by other authors [34, 35]. It is represented in the Laplace domain by the transfer function:

$$\frac{\xi}{\alpha} = \frac{\Theta}{\Delta} \times \frac{(1+\tau_L s)}{(s+\Delta/\Pi)(s+\Pi/\Theta)} \times \frac{\tau_A s}{1+\tau_A s}$$

[1] The dominant time-constant of the damping of cupular motion is 6s (as determined by Fernandez and Goldberg [33]) whereas head movements are typically shorter than 1s.

Where Θ represents the moment of inertia of the toroidal endolymph ring, Δ the spring constant of the cupular restoring force and Π the damping frictional drag of the endolymph. The original torsion pendulum model of the cupula's dynamics is defined by Θ, Δ, and Π. In addition τ_L accounts for the high frequency deviation from the torsion pendulum model and implies that the system is sensitive both to cupular displacement and to the velocity of the displacement. Finally τ_A corresponds to the adaptation process and is the frequency-domain representation of the Young-Oman adaptation operator [36]. The values of the four time-constants were determined in [33] as: $\tau_1 = \Pi/\Delta = 5.7s$, $\tau_2 = \Theta/\Pi = 0.003s$, $\tau_L = 0.49s$ and $\tau_A = 80s$.

2.1.3 The otolith organs

The otolith organs, the saccule and the utricle, are situated between the SCC and the cochlea in the temporal bone (Figure 2.2). They are sensitive to the direction of the gravito-inertial force (GIF) applied to the head, and consequently detect linear accelerations as well as changes in head orientation with respect to gravity. The saccule is dedicated to measuring primarily the vertical component of the GIF with respect to the head whereas the utricle measures primarily the horizontal component. They function similarly and both consist of a bed of hair cells known as the macula, a gelatinous matrix called the otolithic membrane, and numerous calcium carbonate crystals called otoconia that sit on the otolithic membrane, as shown in Figure 2.6. The otoconia layer is slightly differentiated along the median line of the macula, known as the striola: The otoconia are smaller than average there. The striola also defines the local polarization of the surrounding hair cells, which is different for the utricle and the saccule, as illustrated on Figure 2.7.

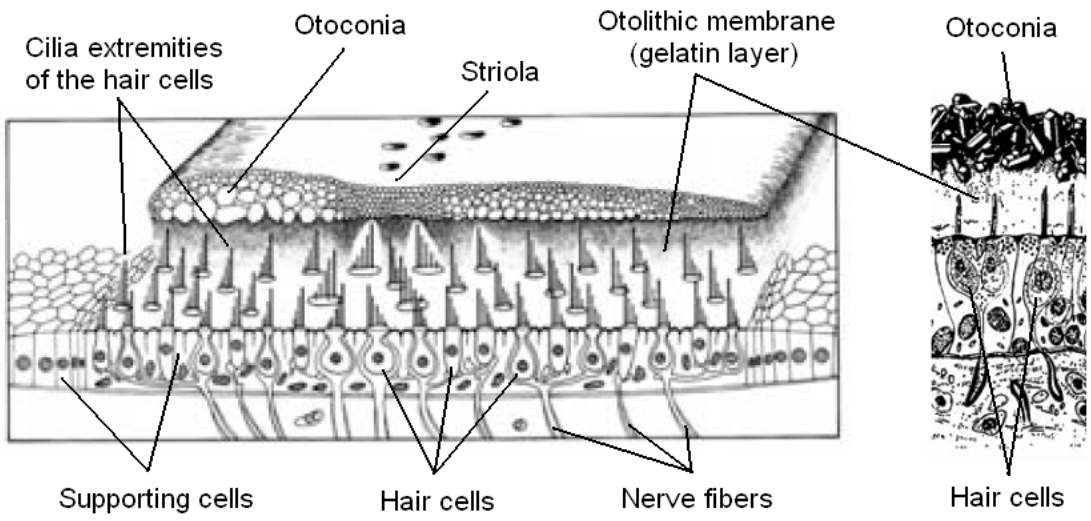

Figure 2.6. Physiology of the utricular macula (modified from [31]): (a) 3D perspective and (b) frontal view. Hair cells are embedded in the macula and can measure the deformation of the otolith membrane caused by the gravito-inertial motion of the otoconia with respect to the head.

The hair cells are anchored in the macula whereas their cilia extremities are embedded in the otolithic membrane. As in the crista of the SCC, the hair cells are locally polarized in the macula: Their direction of high sensitivity is orthogonal to the striola [37, 38]. The striola, however, follows the shape of the otolith organ and is not a straight line. The direction of polarization, thereby, varies gradually over the surface of the otolith. The saccule and the utricle, therefore, do not have a directional sensitivity. Figure 2.7 shows the global polarization of the hair cells in the saccule and utricle, as well as the orientation of the otolith organs in the head.

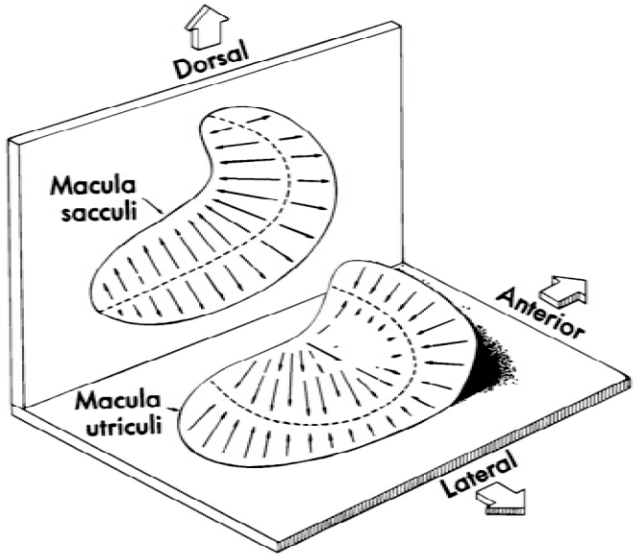

Figure 2.7. Orientation of the hair cells on the maculae of the otolith organs. The dashed line represents the striola and the arrows, the local direction of enhanced sensitivity of the hair cells. (reproduced from [31])

The otolith organs can detect the direction of the GIF via the deformation of the otolithic membrane. The otoconia, sensitive to the GIF applied to the head, are embedded in the membrane, which moves as a whole in response to changes in the GIF. The motion of the membrane relative to the macula, which is attached to the head, characterizes the GIF applied to the head. The otolith organs alone are not able to distinguish linear acceleration from changes in the gravity direction because they are sensitive only to the direction of the GIF and not its magnitude. Nevertheless, the brain uses other cues, such as the rotational acceleration sensed by the SCC, to differentiate the two sensations [39]. Figure 2.8 shows how head tilt or linear acceleration applied to the head are detected by the hair cells through the deformation of the otolithic membrane. The deformation of the membrane (symbolized by an "otolith displacement" on the figure) corresponds to the component of the GIF in the plane locally tangent to the macula (on the figure, for head-tilt this component is $G.\sin(\varphi)$ and for linear acceleration it is $-ma$).

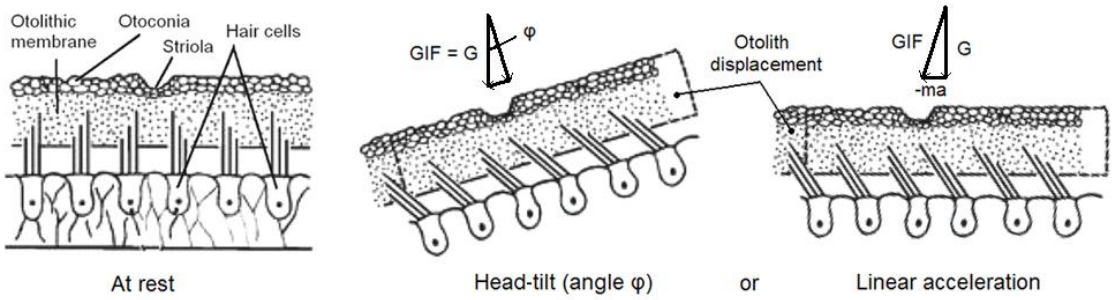

Figure 2.8. The GIF direction is detected in the otolith organs via the changes in the orientation of the hair cells' cilia (see next section). (a) shows the system at rest whereas (b) represents the effect of a head tilt and (c) the effect of a linear acceleration of the head. In both (b) and (c), the cilia bundle of the hair cells is clearly deflected to the right compared to the rest position (a). (modified from [31])

The exact position of the otolith organs in the head, unlike that of the SCC, is important and has been studied in [26]. Indeed, asymmetries in the position of the otolith organs on each side of the head may be one of the factors in space motion sickness and may also contribute to motion sickness during artificial gravity [40-44].

2.1.4 Hair cells

Hair cells respond to defection of their hairs by changing their potential, which allow them to measure tissue deformations. Both the SCC and the otolith organs use these sensory cells to estimate motion and orientation of the head. The hair-cell body is built into the ending of the vestibular nerve, as shown on Figure 2.9. Cilia protrude from the cell body and are sensitive to deformation of the surrounding tissues. A change in the configuration of the cilia bundle of the hair cell modulates its discharge rate by opening an ion channel that modifies the hair cell polarization. Among the cilia, the kinocilium is much longer than the stereocilia and indicates the direction of higher sensitivity of the cell. When the stereocilia are bent toward the kinocilium, an influx of alkali cations depolarizes the cell, inducing a nerve impulse. Conversely, when the cilia are bent away from the kinocilium, the influx of cations is blocked and the hair cell becomes hyperpolarized. The frequency of the action potential, specified by the cell polarization,

is directly encoded into the discharge rate by the vestibular nerve such that higher frequencies of action potentials lead to higher discharge rates [45].

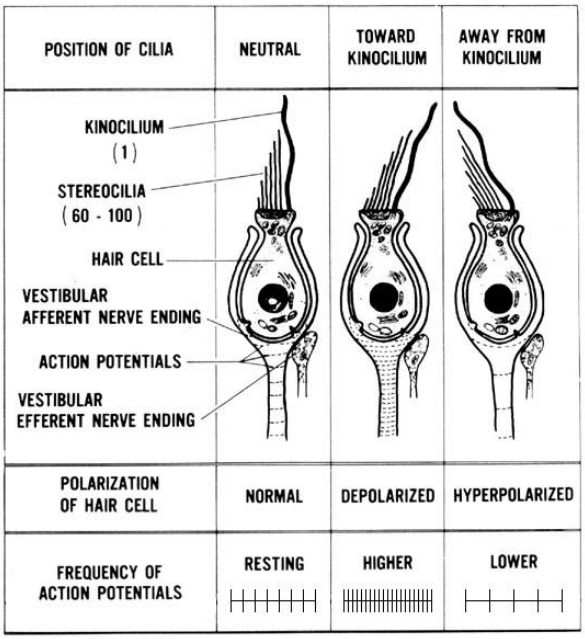

Figure 2.9. Physiology of the vestibular hair cells (reproduced from MIT class notes). The anatomical asymmetry of a hair cell allows it to detect both the intensity and the direction of any stimulation.

Hair cells present a directional specificity inherently associated with the morphological asymmetry of the cells (shown on Figure 2.9), but the quantitative difference in response to stimulation in opposite directions is explained by the cells electrophysiology [38]. First, the hair cells show a resting discharge rate, which allows each cell to respond bidirectionally to vestibular stimulation – by increasing or decreasing that rate. Positive mechanical stimulation (from the hair bundle of the hair cell to the kinocilium) increases the discharge rate of a hair cell from its resting rate to an upper limit that is seldom reached. Conversely, negative stimulation decreases the discharge rate of the cells from its resting rate to a residual (or minimum) discharge rate – which is easily reached. The input-output function of the hair cell is S-shaped and is characterized by inhibitory saturation [38], which explains the directional asymmetry in the cell's sensitivity.

Several hair cell[2] units coexist in the cristae and the maculae of the vestibular system; these units can be differentiated based on their resting and residual discharge rates. Figure 2.10 shows the force-response relation for active cells of the utricle with a resting discharge rate of 48 spikes/s. Intense inhibitory stimulation saturates the response and discharge rate does not falls below a residual 17 spikes/s. There is also a suggestion of an excitatory saturation near 300 spikes/s. For the hair cells of the utricle, therefore, there is a clear response asymmetry: The excitatory responses continue to grow as stimulation is increased, whereas relatively modest forces in the opposite direction lead to inhibitory saturation. The same conclusion can be expected from the hair cells of the cristae of the SCC, which explains the directional sensitivity of the canals.

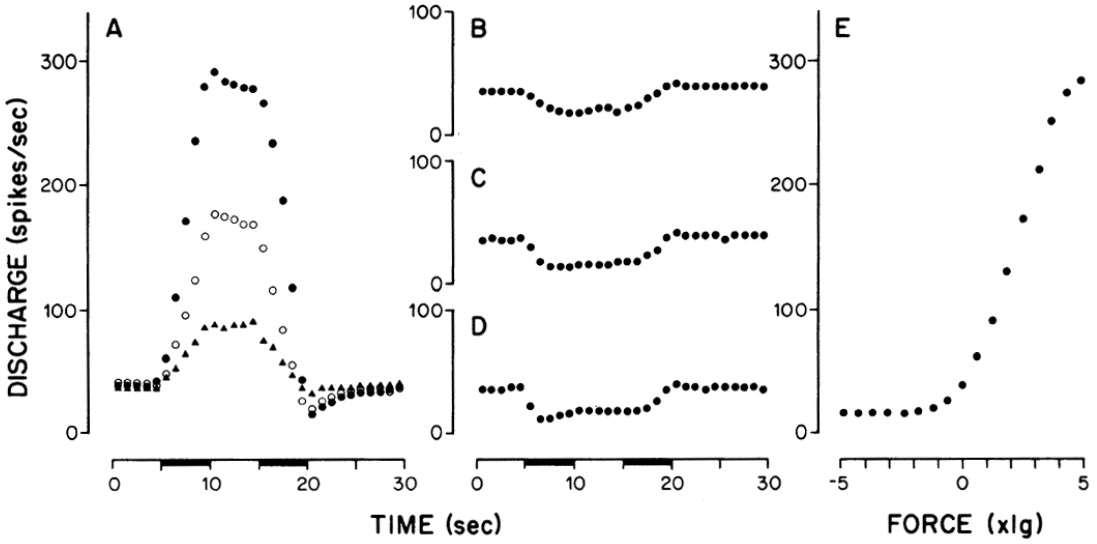

Figure 2.10. Asymmetry of sensory hair cells response to stimulation of opposite direction (force-response relations for utricle units). (A) Excitatory response profile: 1.23 g (triangles); 2.46 g (empty circles); 4.92 g (plain circles). (B-D) Inhibitory response profiles for 1.23, 2.46, 4.92 g, respectively. (E) Extended force-response relation. (reproduced from [38])

On the crista of the horizontal semicircular canal the kinocilia are on the sides of the cells nearest the utricle. On the cristae of the vertical canals the kinocilia are on the sides of the cells farthest from the utricle or facing the canal [30]. On the macula of the utricle,

[2] These hair cell units cannot be associated with the two structural types I and II.

the kinocilia are toward the striola, whereas on the macula of the saccule they are away from the striola (Figure 2.7) [37].

The hair cells are extremely numerous in the vestibular system: There are approximately 33000 hair cells in the utricle, 17000 in the saccule, and 8000 in each semi-circular canal's crista. This is very large compared to the 19000 hair cells that can be found in the cochlea. This large number of hair cells illustrates the importance of the vestibular system to the human body.

2.2 Artificial gravity and vestibular stimulation

The vestibular physiology described previously gives a straightforward explanation for the vestibular stimulation associated with head-turns in a rotating environment.

2.2.1 The Cross-Coupled Stimulus

Head-turns performed in an inertial frame of reference (normal conditions) stimulate the SCC only during the motion of the head. The cupula is deflected in one direction by the angular acceleration at the beginning of a brief head-turn, and is deflected back in the rest position by the head deceleration at the end. Head-turns performed during centrifugation create, in addition to this transient stimulus, a more sustained stimulus that lasts until damped by the canal dynamics (Section 2.2.3). This stimulus is due to the cross-coupled effect created by the composition of two non-coplanar angular motions. In this thesis, the name Cross-Coupled Stimulus (CCS) has been used for this vestibular stimulation. The next two sections explain how the CCS is generated mechanically and how it is interpreted physiologically.

2.2.2 Physics of the CCS

When a rotating body undergoes an angular motion in a plane different from the plane of initial rotation, its total motion with respect to the inertial reference frame is the three-dimensional rotation resulting from the composition of those two motions. During centrifugation, therefore, a head-turn stimulates the SCC beyond the simple rotation of the head commanded by the neck muscles. The head-turn leads to an extra stimulus, the CCS, interpreted by the SCC as a motion with respect to the rotating reference frame, although it is actually a motion relative to the inertial space. The disturbance created by the CCS comes from the fact that the vestibular system loses track of sustained angular motion in less than a minute. During centrifugation it detects motion cues relative to the inertial frame, but interprets them with respect to the rotating (non-inertial) frame. The CCS, then, is a true vestibular stimulation that is processed in the wrong reference frame and, thereafter, appears anomalous to the subject.

Peters performed a detailed derivation of the mathematical equations describing the CCS [30] (appendix section). The results to follow use the notation of Adenot [35]. The analysis focuses on yaw head-turns performed by a subject lying supine on a rotating bed with a constant angular velocity.

As established in [35], the expression for the angular acceleration of the head with respect to the inertial reference frame (0), written in the coordinate frame attached to the head (2) is:

$$\left[\overrightarrow{\alpha_{2/0}}\right]_2 = \begin{bmatrix} \dot{\psi}\,\omega_c \sin(\psi) \\ \dot{\psi}\,\omega_c \cos(\psi) \\ \ddot{\psi} \end{bmatrix}$$

with $\overrightarrow{\alpha_{2/0}}$: angular acceleration of the head with respect to the inertial reference frame, ω_c: centrifuge-velocity in the Earth's reference frame, ψ: yaw angle in head's reference

frame ($\psi = 0$ corresponding to the nose-up position), (0x), (0y) and (0z): respectively sagittal, lateral and vertical axes, defining the head's coordinate frame.

A simple head-turn performed in a rotating environment stimulates the three SCC and generates motion sensations in several directions. Figure 2.11 shows the total acceleration applied on the SCC resulting from a simple yaw head-turn performed while spinning. The CCS, created by the composition of head and centrifuge angular motion, adds roll and pitch components to the initial yaw angular acceleration.

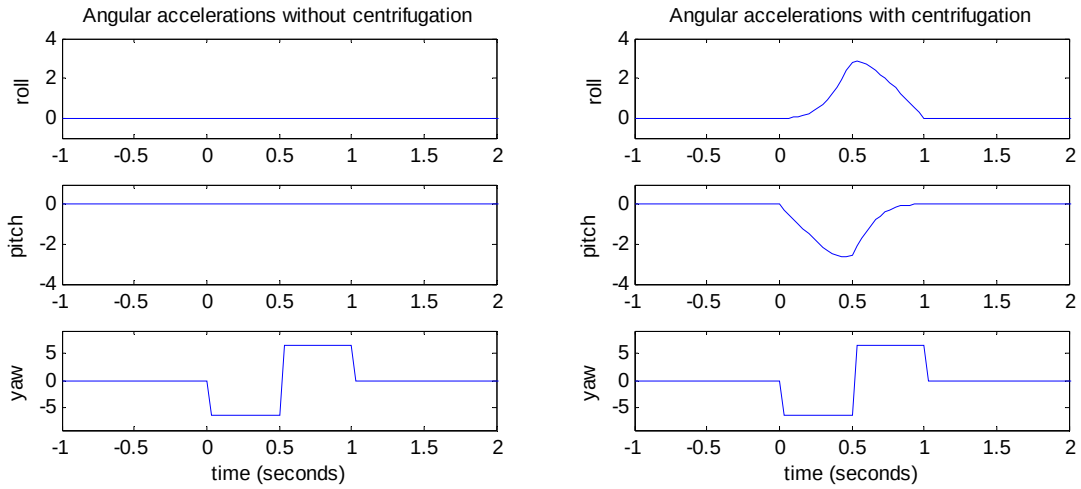

Figure 2.11. Angular accelerations (in rad/sec^2) corresponding to a simple yaw head-turn from 0° to 90° performed while spinning at 23 rpm. (a) Without centrifugation. (b) With centrifugation: The real acceleration of the head (yaw component) leads to roll and pitch component through the CCS.

Although the cupular deflection measures angular acceleration, the SCC response is better described in terms of changes in angular velocity. The angular velocity is easily derived from the angular acceleration. For a yaw head-turn made between the angles ψ_1 and ψ_2 at the centrifuge-velocity ω_c, the angular velocity stimulus is defined by:

$$Angular\ velocity\ stimulus = \begin{bmatrix} -\omega_c\left(\cos(\psi) - \cos(\psi_1)\right) \\ \omega_c\left(\sin(\psi) - \sin(\psi_1)\right) \\ \dot{\psi} \end{bmatrix}$$

with $\psi \in [\psi_1, \psi_2]$. This expression shows that there is a transient velocity component in the yaw direction that lasts only during the head-turn, and two persistent components in the roll and pitch directions that continue even after the head-turn is finished. The amount of stimulus generated by a head-turn is characterized by the change in angular velocity due to the head-turn. The magnitude of the angular velocity change is defined by:

$$CCS_{velocity} = \omega_c \sqrt{(\cos(\psi_1) - \cos(\psi_2))^2 + (\sin(\psi_2) - \sin(\psi_1))^2}$$

This expression specifies the total angular stimulus applied on the physiological systems after a head-turn.

2.2.3 Interpretation of the CCS by the vestibular system

After the CCS is created by head-turns in a rotating environment, the semi-circular canals detect the total angular acceleration applied to the head. The response of the canals can be calculated from the canal fluid dynamics model described earlier and is shown in Figure 2.12 separately for each component of the head acceleration (roll, pitch and yaw). There is no self-regulation possible at this level of the response and, therefore, adaptation to cross-coupled stimulation must occur at higher levels of the interpretation of the stimulus. The curves shown on Figure 2.12 have been generated with Matlab® using the open-loop transfer function presented in Section 2.1.2:

Angular acceleration $\longrightarrow$ $\boxed{\frac{\xi}{\alpha} = \frac{K(1+\tau_L s)\tau_A s}{(1+\tau_1 s)(1+\tau_2 s)(1+\tau_A s)}}$ $\longrightarrow$ Cupular deflection[3]

where ξ is the angular displacement of the cupula and α the angular acceleration input. The cupular displacements[3] plotted in Figure 2.12 use the values from [33]: $\tau_1 = 5.7s$, $\tau_1 = 0.003s$, $\tau_L = 0.49s$, $\tau_A = 80s$, and $K = 0.017s^2$.

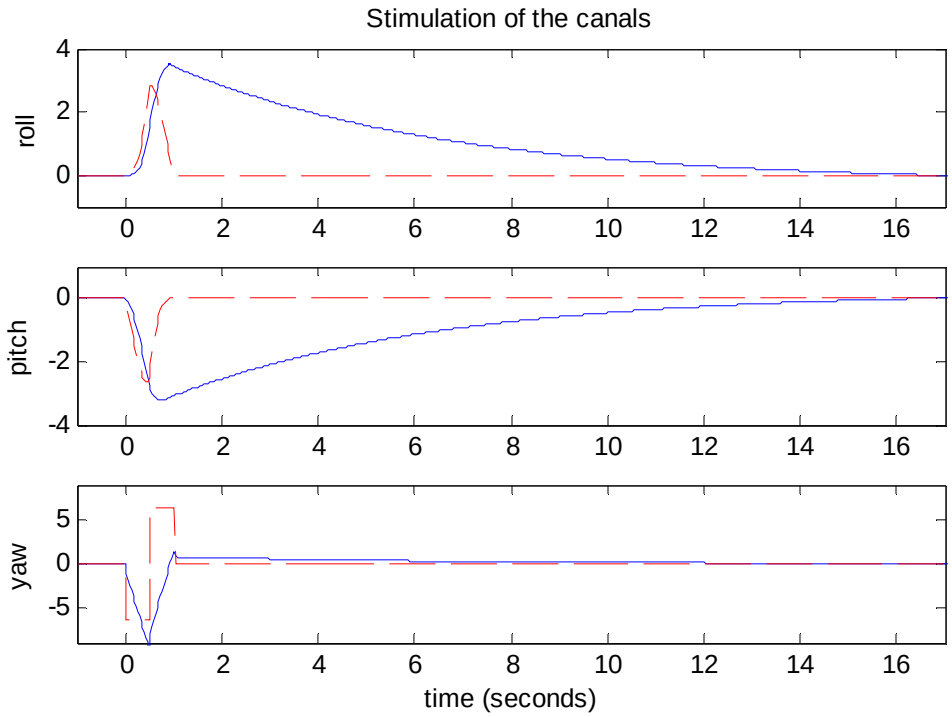

Figure 2.12. Cupular displacement[3] (solid line) in response to the angular acceleration (dashed line) corresponding to a yaw head-turn performed while spinning. Note that 1 unit corresponds to 10^{-3}rad for the cupular displacement and 1rad/sec^2 for the angular acceleration.

The cupular deflection in the yaw plane clearly shows that the original head acceleration (yaw component) leads only to a transient stimulus and hence a transient vestibular response. On the other hand, the two accelerations created by the CCS (roll and pitch components) continue to affect the vestibular response after the head-turn is finished: This stimulation triggered by the CCS lasts more than 10 seconds, until the signal is finally damped by the SCC dynamics, as shown on Figure 2.12.

Note that there is confusion sometimes about the contribution of the CCS to the vestibular response created by a head-turn while spinning. Some authors define another effect that depends only on the position of the canals with respect to the plane of centrifugation (often called canals in/out-of-plane effect). This new effect supposedly explains the stimulation of the SCC that follows the head-turn, while the CCS is reduced to a transient stimulus that dies when the head-turn stops. Actually, as illustrated on

[3] Note that this is not a real cupular displacement since there is no roll, pitch or yaw canals. It is a measure of the vestibular stimulation in the roll, pitch and yaw planes.

Figure 2.12, the CCS alone explains perfectly the canals' stimulation that continues after the head-turn is finished and therefore there is no need to posit any other effect to explain the vestibular response.

2.3 VOR response

The most commonly observed response to vestibular stimulation during AG is the vestibulo-ocular reflex (VOR) – reflexive compensatory eye-movements.

2.3.1 Dynamics of the VOR

Eye movements aim at stabilizing the image on the retina of the scene being observed. In addition to pursuit, there are two kinds of compensatory eye movements: the optokinetic nystagmus that stabilizes gaze for a moving scene and the vestibulo-ocular reflex (VOR) that stabilizes gaze for a moving observer. They are both controlled almost entirely by subcortical centers. The optokinetic nystagmus, beyond this study, is driven by passive motion of the retinal image and compensates for movements of the visual surroundings when the head is stable. The VOR (vestibular nystagmus) is driven by the vestibular response to head motion and compensates for motions of the head in a stable external environment. If the head is rotated to the right, the VOR drives the eyes to the left to compensate for the motion of the head and maintain a stable gaze[4]. There are two kinds of VOR: the angular VOR (aVOR) compensating for rotational head movements, driven mainly by the SCC, and the linear VOR (lVOR), driven mainly by the otolith organs. It appears, however, that otolith stimulation influences the aVOR as suggested in [46, 47] and the separation between aVOR and lVOR may be more theoretical than actual.

[4] The velocity of the eyes appears to be slower than the head velocity. The gain of eye velocity compared to head velocity depends on the direction of motion of the eyes but is no greater than 0.7 in the dark [69]. There is also a short lag between head and eye movements of approximately 35 ms.

The movement of the eyes during the VOR is characterized by two phases: the actual compensatory eye movement and the saccades. During the compensatory eye movements, also called slow-phase nystagmus, the eyes are driven at nearly the same velocity as the head motion in the opposite direction in order to stabilize the retinal image. As the eyes cannot keep on rotating in the same direction, after a certain angle they jump backward to begin another slow-phase nystagmus. This quick motion of the eyes, called a saccade, lasts about 20–200 milliseconds[5], and is also referred to as fast-phase eye-motion.

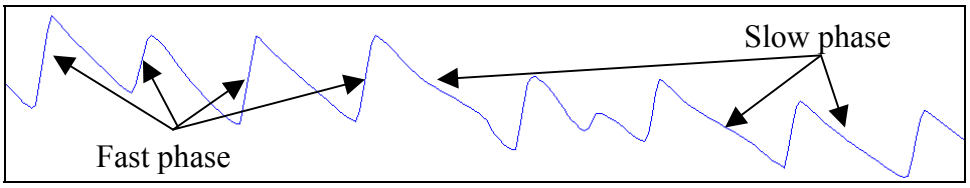

Figure 2.13. Slow and fast-phase components of the compensatory eye movements (real data).

The slow-phase component of the VOR stabilizes the retinal image, whereas the fast-phase repositions the eye to enable repeated compensatory eye movements. Since the fast-phase component of the VOR represents only a resetting of the eye position, the slow-phase of the eyes during the VOR is often considered more interesting for vestibular research.

This study investigates the aVOR, specifically the slow-phase velocity (SPV) of the compensatory eye movements during the aVOR. Based on our understanding of the physiology of the VOR, the SPV should be proportional to the head velocity felt by the SCC and is, therefore, a direct measurement of the state of the vestibular system. The SPV can be well described by a gain and a dominant time-constant (i.e. a single exponential mode). The gain is the ratio between the peak-value of the induced SPV and the CCS. The time-constant is defined as the time necessary for the SPV response to fold to $1/e$ of its peak- value.

[5] The peak angular speed of the eye during a saccade reaches up to 1000 degrees per second and is the fastest movement of an external part of the human body.

However, as argued by Dai in [48], the SPV is more accurately represented by two exponential modes. The use of two time-constants allows for separation of peripheral and central time dynamics and may lead to a better understanding of the phenomenon. The peripheral time-constant, discussed in [49], depends on cupular dynamics. It is also the called cupular time-constant and has limited adaptation capabilities. The central time-constant, discussed in [50], characterizes the velocity storage integrator. Dai found a mean value of 4.2s for the cupular time-constant [48]. The time-constant of the velocity storage integrator is longer and able to adapt to the environment. It decreases upon repeated stimulations.

2.3.2 Head-turns during centrifugation and VOR

Eye movements are generated by vestibular stimulation. For the aVOR, yaw angular acceleration will generate horizontal eye movements; pitch accelerations, vertical eye movements; and roll accelerations, torsional eye movements.

For yaw head-turns performed during centrifugations, the stimulus applied to the SCC carries both the normal yaw angular acceleration stimulus and the CCS, as described in Section 2.2. For a yaw head-turn between the angles ψ_1 and ψ_2 at the centrifuge-velocity ω_c, the equation defining the angular velocity stimulus[6] has been established in Section 2.2.2 as:

$$Angular\ velocity\ stimulus = \begin{bmatrix} -\omega_c\left(\cos(\psi) - \cos(\psi_1)\right) \\ \omega_c\left(\sin(\psi) - \sin(\psi_1)\right) \\ \dot{\psi} \end{bmatrix}$$

with $\psi \in [\psi_1, \psi_2]$. This expression shows that, during the head-turn, there is a transient compensatory nystagmus in the yaw direction, which elicits horizontal eye movements, but when the head-turn stops, this horizontal aVOR vanishes. By contrast, the two other

[6] Physiologically, the velocity storage integrator generates the velocity stimulus from cupular deflection – acceleration stimulus.

components of the angular velocity stimulus, generated by the CCS, reach their maximum value at the end of the head-turn ($\psi = \psi_2$). For a head-turn performed from the nose-up position ($\psi_1 = 0$) to an angle ψ_2, the angular velocity stimulus at the end of the head-turn, or angular velocity change, is given by:

$$Angular\ velocity\ change = \begin{bmatrix} -\omega_c\left(\cos(\psi_2) - 1\right) & (roll) \\ \omega_c \sin(\psi_2) & (pitch) \\ 0 & (yaw) \end{bmatrix}$$

This expression predicts that the angular velocity stimulus contains persistent components applied in the roll and pitch planes. These stimuli will generate torsional and vertical compensatory eye movements even after the head-turn is finished. The vertical aVOR can be measured in the head coordinate frame (roll, pitch, yaw) using the ISCAN® eye-tracking system described in Section 3.3.3. The torsional aVOR can theoretically be measured too, but not with the device used in this study.

2.4 Illusory motion response

Head-turns performed during centrifugation generate a stimulus (CCS) that head-turns performed in an inertial coordinate frame do not. Whereas in the rotating reference frame the CCS is only an artifact created by the head-turn, it is sensed by the vestibular system as an angular acceleration, and consequently activates the vestibular nerve. The velocity storage integrator processes the signal and triggers compensatory eye movements (described in the previous section) which would be appropriate with respect to an inertial frame, but are inappropriate for retinal stabilization in a rotating frame. The signal is also inputted into the balance and movement control loops and tricks the brain into thinking that the head is actually rotating as described by the CCS, hence the illusory motion sensation. This motion is referred to as illusory because it does not correspond to a real rotation of the head in the rotating frame of reference. This motion sensation would

be persistent if the CCS were not damped by the SCC fluid dynamics, as illustrated on Figure 2.12.

When the illusory motion stops, the vestibular system is left with a persistent body-tilt sensation that depends on the gravito-inertial force applied to the head. The goal of AG is to simulate the Earth gravity, therefore, it is a proof of the success of AG that a human being lying supine on a rotator feels tilted compare to the Earth-horizontal. In space this perceived body-tilt would be replaced by the normal "standing" sensation, but on Earth the total GIF includes Earth gravity. The perceived tilt is irrelevant for space applications and is therefore less important than the other responses.

In summary, head-turns performed in a rotating environment trigger transient illusory motion sensations that last until the CCS is damped by the SCC dynamics and persistent body-tilt sensations.

2.5 Motion Sickness response

Motion sickness is the most dramatic potential disadvantage associated with artificial gravity. If short radius centrifugation is to be used as a countermeasure to the deleterious effects of microgravity on the human body, we must understand what causes motion sickness and how to diminish it. Two different theories describe the case of motion sickness: sensory conflict and neural mismatch.

2.5.1 What is motion sickness

As described by Oman, motion sickness is a general term describing a group of common nausea syndromes attributed to conflict between different perceptual sources [51]. Indeed, the human brain integrates inputs from the vestibular, visual and somatosensory systems to estimate the actual state of the body. Usually the signals are concordant but in certain situations a conflict may emerge between the different inputs. Reading in a car, traveling on a boat without looking at the sea or performing head

movements in a rotating environment are all situations in which sensory conflicts emerge. During seasickness, for example, the conflict arises when a passenger is within the boat and cannot look at the sea. The vestibular system feels the undulations of the boat with respect to the sea while the visual system is provided an unchanging boat-based frame of reference. If the passenger goes on the deck, the sea becomes his visual frame of reference and the conflict disappears. For head-turns performed in a rotating environment, the sensory conflict arises between the SCC that interprets the CCS as describing the head motion, and the otolith organs and somatosensory system that are not sensitive to the CCS.

2.5.2 Neural mismatch theory

The widely accepted neural mismatch theory is based on a generalization of the sensory conflict idea. The neural mismatch theory hypothesizes that the main conflict is between the expectation of the internal model and the actual sensory inputs rather than directly between the sensory inputs [52]. This theory assumes that the brain constantly updates an internal model of the sensory inputs that are expected to accompany body orientation or motion. If a situation leads to a discrepancy between the internal model and the external perception, the responses are twofold. The internal model is gradually updated so as to diminish the conflict if the same situation were to recur and a sensation of nausea (or any other motion sickness syndrome) is generated. Paradoxically, the first response is the key to the adaptation process whereas the second impedes the use of AG.

Figure 2.14 presents the model developed by Oman for the neural mismatch conflict theory [53]. The sensory cues from the body receptors are compared to the internal prediction of these same cues and the discrepancy is fed back into the internal model (box labeled “Orientation brain”) to refine it. A limitation of the Oman model may be that it allows conflicts only between actual and predicted sensory signals. Brown found head-turns performed with or without visual feedback were as provocative of motion-sickness [54], which agrees with the choice made by Oman. Although the neural mismatch is

certainly essential to the building of motion sickness, simple sensory conflicts might, however, also contribute to the general conflict.

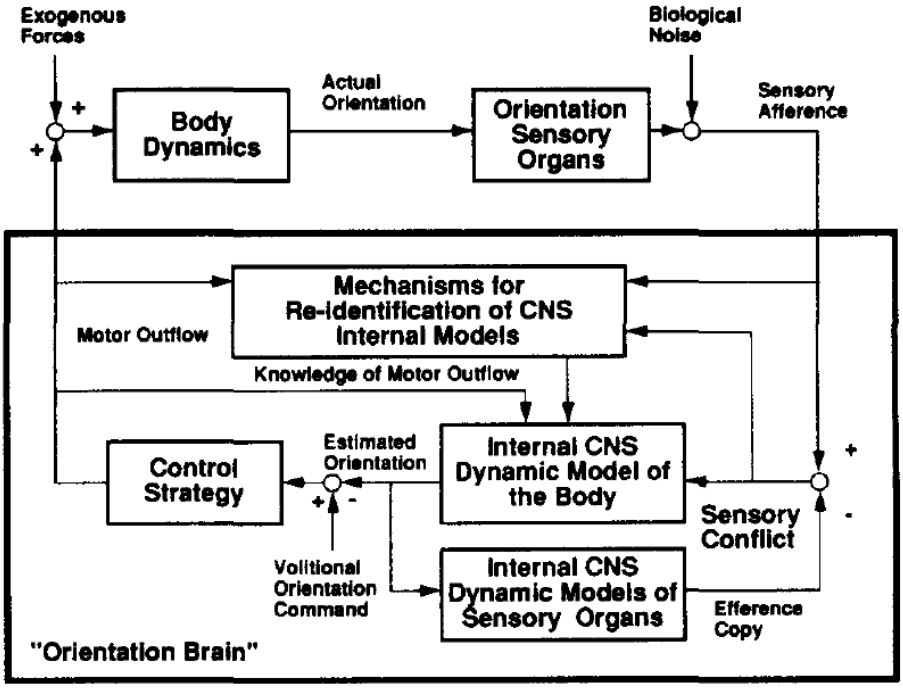

Figure 2.14. Mathematical model for sensory conflict and movement control based on observer theory (reproduced from [53]). The actual transfer function corresponding to each block is detailed elsewhere [53].

2.5.3 Symptom dynamics

The conflict model described above establishes the dynamics of the stimulus (neural mismatch or sensory conflict regrouped under the term "conflict") that generates motion sickness. However, the relation between conflict and motion sickness needs to be established as well. Oman developed an heuristic model to predict motion-sickness dynamics [51]. The external input to the model is the conflict (as defined in the model of the previous section), the output is the motion sickness generated. The model, described in Figure 2.15, presents two parallel pathways that participate to the building of motion sickness. The fast path response, with a time-constant <1min, accounts for virtually instantaneous increment in nausea levels produced by a single conflict stimulus. The slow

path, time-constant >10min, sets the overall nausea threshold and set the gain for the fast path. Motion sickness is generated from the sum of the two pathways using a threshold power law.

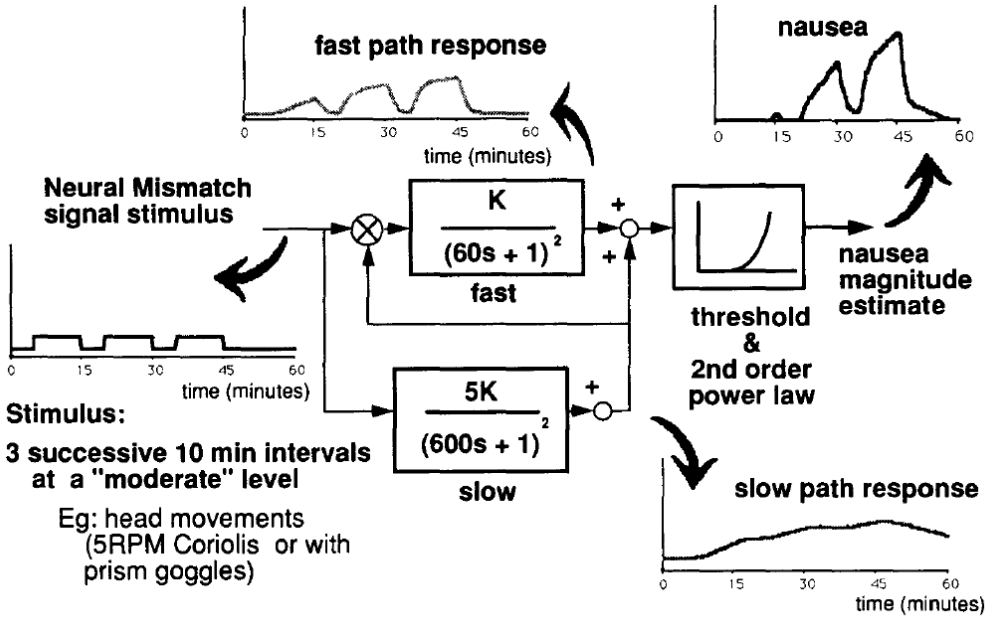

Figure 2.15. Mathematical model for nausea path symptom dynamics (reproduced from [51]). The second order power law was established on psychophysics basis.

2.5.4 How to measure motion sickness

Measuring motion sickness is a challenge because of the diverse combinations of symptoms it may generate: nausea, sleepiness, dizziness, stomach awareness, headache, pallor, abnormal sweating. Historically motion sickness has been assessed directly by the subject. Many different scales have been use to evaluate motion sickness. The scale commonly used in the MIT Man-Vehicle Laboratory is a 0-20 scale similar to the Well-Being Ratings or Pensacola scales [52, 55]. This scale is convenient because it is quicker and easier to rate than are most of the other existing motion sickness scales.

Because motion sickness is so hard to measure directly researchers have sought another physiological parameter, easier to measure, that correlates with motion sickness. The gain or time-constant of the VOR would be attractive candidates since they can be

measured directly and relatively easily from the eye movements. Although the results of [56] suggest a possible correlation between the time-constants of the aVOR and the maximum number of head-turns performed while spinning (correlated with motion sickness), no exact relation has been proven so far.

2.6 Vestibular adaptation to centrifugations

How are humans able to adapt to the disturbing vestibular side-effect generated by cross-coupled stimulation during AG?

2.6.1 Feasibility of adaptation

Several studies have proven that humans can adapt to the effects of head-turns during centrifugation at speed up to 23-rpm [16, 18, 23, 54, 57-59]. In these studies, the decrease in the intensity of the vestibular responses shows that the subjects adapted to the cross-coupled effect. When AG was first introduced it was thought that humans would not tolerate rotation rates above 10-rpm. That expectation led to the testing of adaptation to slow rotation. Early experiments in the Pensacola slow motion rotating room showed that VOR, disorientation, and motion sickness significantly decreased over days [16, 60]. More recently Young and co-workers demonstrated that humans can also adapt to stronger CCS generated by intermittent exposure to the high rotation speeds (23 rpm) provided by short-radius centrifuges [18, 54, 59]. It is now clear that humans with a normal vestibular function are able to adapt to a rotating environment with angular velocity above 10 rpm – even up to 30 rpm.

High-speed centrifugation is obviously more provocative than slower rotation since the CCS is proportional to the angular velocity (Section 2.2). Short-radius centrifugation is consequently more provocative than larger radius because the short radius must be compensated by high rotation rates to achieve the same simulated gravity level. For this reason short-radius centrifuges might seem unnecessarily provocative as compared with

larger-radius, but one must keep in mind the technological challenge that a rotating spacecraft represents as compared to a simple rotator the size of a bed that could sit within a spacecraft. Moreover, since high-speed centrifugation creates a stronger stimulus, it may very well lead to quicker adaptation by maximizing sensory conflict. This idea of maximizing conflict in order to accelerate adaptation has been studied with ambiguous results [61].

2.6.1.1 Dual adaptation

The goal of MIT's AG research is not so much to show that humans can adapt to making head-turns in a rotating environment, but more generally to show that they can dual-adapt to the rotating and the inertial non-rotating environments. Indeed, the benefit of AG would be hindered if, after exposure to centrifugation, the astronauts had to spend hours or even days to again get used to doing head-turns in an inertial environment. This would clearly be a safety issue in case of an emergency and would compromise the profit of short-radius centrifugations.

Fortunately, all the studies done so far have found that dual adaptation did occur or at least that re-adaptation to a normal environment was quick and painless. In particular, the early Pensacola experiments showed that out of the 4 subjects that spent 12 days in a rotating room spinning at 10-rpm, only 1 experienced a mild nausea that lasted a short time upon cessation of rotation [16]. The same studies also showed that, upon repeated exposure to spinning and stationary environments humans can fully dual-adapt to both. Other experiments on high-speed artificial gravity found that humans can adapt to crossed-coupled stimulations while maintaining their adaptation to stationary environments [18, 54]. This result agrees with what is expected from our experience of everyday life: going to the movie-theater does not make us dizzy.

This dual adaptation process has been defined explicitly for short-radius centrifugation: Adaptation driven by repeated exposure to cross-coupled stimulation must remain context-specific in order not to corrupt adaptation to stationary environments [18]. This "context-specific adaptation" (CSA) refers to the ability of the human sensory

system to modify its response to a repeated perturbation, while remaining unchanged for normal stimulation.

2.6.1.2 Adaptation vs. habituation

The term habituation is sometimes used instead of adaptation and one may confuse these two processes. While habituation refers to a decrease of the response to repeated stimulus, adaptation suggests a purpose-driven modification of the response.

According to its physiological use, habituation occurs when the human body is subject to a sustained or repeated stimulus. The body passively minimizes its response because a repeated stimulus reduces the sensitivity of the body to similar stimuli. If the stimulus disappears, habituation is rapidly lost.

By contrast, adaptation is an active process that aims at correcting a disturbing stimulus by changing the body's response. The key idea of adaptation is that it is driven by a functional goal and leads to a different interpretation of the signal. Adaptation typically occurs at higher level than habituation and causes the internal models of the human body to evolve with external conditions.

For exposure to short radius centrifugations over several days, habituation accounts for most of the decrease of the response within a day whereas adaptation accounts for the decrease between days.

2.6.2 Vestibular adaptation

By experiment, all specific vestibular responses – VOR, illusory motion, and motion sickness – show adaptation over a few days. In general, it was observed that motion sickness and illusory motion decrease more rapidly over experimental days than VOR gain and time-constant do.

2.6.2.1 VOR adaptation

Adaptation of a physiological parameter occurs in response to a conflict somewhere in the system. Although the dynamics of the VOR are well understood, the reasons for its adaptation in a dark environment remain to be explained. For head-turns performed with lights on, the visual feedback conflicts with the signal coming from the SCC, and this conflict justifies adaptation. By contrast, in the dark, there is no such conflict that could drive adaptation.

A possible explanation for VOR adaptation in a dark environment is the canal-otolith conflict that occurs in the velocity storage integrator following a head-turn during centrifugation [35]. The prediction of the otolith-canal conflict model is that smaller head-angles create smaller conflicts and should therefore lead to less adaptation than large angles.

By experiment, compensatory eye movements were found to decrease significantly over exposures to cross-coupled stimulation. Indeed, if the compensatory eye movements are appropriate for an Earth-fixed environment, only the horizontal component is appropriate for a centrifuge-fixed environment. In particular, the vertical eye movements are inappropriate and correspond to a canal-otolith conflict. It was found, as expected, that retinal slip substantially decreases the gain of the vertical VOR [61], and that virtually no adaptation of the VOR gain occurred without visual cues [58, 62]. Surprisingly, despite the dark environment, the normalized gain of the VOR was found to decrease in [57].

The dominant time-constant of the VOR usually decreases more on the first day of exposure to AG than on the following days. The reason the measured time-constant reaches a plateau lies in the dynamics of the VOR. As explained in Section 2.3, the VOR is accurately defined by two time-constants: the plastic time-constant of the velocity storage integrator, and the shorter cupular time-constant. Most experiments measure only the dominant time-constant that is the larger of these two (corresponding to the central one). After partial adaptation, the time-constant of the velocity storage integrator decreases to the level of the cupular time-constant, which is thought to be constant.

Consequently further exposure modifies the new dominant time-constant of the VOR only slightly.

2.6.2.2 Illusory motion adaptation

The perception of the SCC informs the brain about the current motion of the head. Because of the cross-coupled effect and its measurement by the SCC, the brain incorrectly believes that the body is in motion. Fortunately for the humans exposed to short radius centrifugation, the balance and movement control loops integrate signals not only from the SCC, but also from the otolith organs and the visual and the somatosensory systems. Upon repeated exposure to CCS, the conflict existing between these signals logically drives a re-evaluation of the original response that suppresses the inappropriate sensation. The illusory motion response thereby adapts to the CCS. Experimental results universally confirm a rapid decrease of the illusory motion sensation over time for a given level of CCS [35, 58, 61-63].

Illusory motion has often been associated with VOR since the CCS directly drives them both. However, while retinal slip appears to be necessary to adapt the VOR gain, vestibular and proprioceptive inputs provide sufficient conflict to diminish the illusory motion sensation [54]. This proves that there is no functional relation between the two responses.

As stated in Section 2.4, the illusory motion sensation is followed by a steady-state body-tilt sensation. This tilt sensation has little reason to adapt because it primarily comes from the detection of the GIF by the otolith organs and is a relevant response. However, it seems that the perceived body-tilt sensation is also affected by the preceding illusory motion sensation. Since the illusory motion response adapts, the perceived tilt might also adapt.

2.6.2.3 Motion sickness adaptation

As described in Section 2.5, motion sickness is the symptom of a conflict in the interpretation of a sensory signal. The conflict can be between two sensory inputs (sensory conflict) or between the actual and expected sensations following a motor command (neural mismatch). Since motion sickness is based on a conflict, it is only natural that it adapts as observed experimentally. Adaptation to motion sickness induced by out-of-plane head-turns during centrifugation is widely accepted as a fact.

Whereas VOR and illusory motion sensation usually show both habituation within an experimental day and adaptation over several days, motion sickness only shows adaptation. Motion sickness does not show habituation because it is a slow phenomenon compared to the other responses (time-constants of several minutes) and it is commonly observed to build up over time.

The very idea of an internal model in the brain associating sensory inputs to motor command leads to the assumption that cognitive training might be able to modify the internal model. This has already been studied with, unfortunately, no positive finding [64], and is currently being studied again at NASA.

Finally there might be a relation between the decrease of the dominant VOR time-constant and motion-sickness adaptation, as suggested by Dai [54, 56].

2.6.3 Transfer of adaptation

Now that it has been showed that humans can adapt to the disturbing cross-coupled effect created by head-turns in a rotating environment, the next step is to design a training procedure that exploits that finding. An important question that has to be answered before any training protocol can be designed is the one of transfer of adaptation. Will adaptation transfer from a protocol to another? According to the model of context-specific adaptation (Section 2.6.1.1) the answer to this question depends on the similarities between the two protocols. It also depends on the level at which adaptation occurs in the

internal pathway from stimulus to response. If adaptation occurs at the lower level, adaptation will be "stimulus-specific"; if it occurs at the higher level, adaptation will transfer from one type of CCS to any other type.

First, the idea of transfer of adaptation has to be defined: Adaptation is considered to transfer from a protocol to another if, after adaptation to the first, the response to the second protocol is lower than it would have been without the exposure to the first. The switch from the first to the second protocol might lead to short transition effects despite a successful transfer of adaptation. During these quick transition effects, the response to the second protocol's stimulus might not show any sign of pre-adaptation. When investigating transfer of adaptation, one must be careful not to mistake transition effects for failed transfer.

Transfer of adaptation between different conflict levels for a given type of head-turn has been shown in several experiments. Adaptation seems to transfer between centrifuge's directions of rotation [18, 61], centrifuge-velocities [62] and head-turn angles [35]. According to a recent project done in the Man-Vehicle Lab at MIT, adaptation also transfers between different otolith loadings (head aligned with the axis of rotation vs. head 15-inch off-center). The previous results were obtained for a subject lying supine on a rotating bed spun around an Earth-vertical axis through the center of his head, who performs only yaw head-turns in the right quadrant. On the other hand, transfer of adaptation between quadrants of motion (head-turns in the right quadrant vs. head-turns in the left quadrant) is less certain. Early experiments found that adaptation failed to transfer between quadrants for roll head-turns [60], but recent research done in the Man-Vehicle Lab suggests that transfer occurs at least partially for yaw head-turns. No transfer of adaptation was found between head-turns performed in the pitch and the yaw planes [58], which suggests that there is no transfer of adaptation between different planes of head motion in general. Head position with respect to gravity also plays an important role in the adaptation process of the vertical aVOR gain for monkeys [65]. As suggested by this study, adaptation of the gain includes a gravity-specific component that depends on the otolith loading and consequently does not transfer between two head positions.

As shown by the number of studies mentioned above and the diversity of the results, the question of transfer of adaptation is far from settled.

2.6.4 Validity of training on Earth

Questioning transfer of adaptation naturally leads to another essential question: Will adaptation achieved on Earth transfer to microgravity environments?

Perceptual disturbance in 0-g differs from that in 1-g. Specifically Earth gravity is known to influence the vestibular response to cross-coupled stimulations. Yaw head-turns performed in the right quadrant while lying supine on a rotating bed show a strong asymmetry between the two directions (to-NUP vs. to-RED) as measured by reported illusory motion sensation and motion sickness [66]. The authors conclude that since eye movements do not show any significant asymmetry the difference has to be specified in the brain processing centers. This result implies that pre-adaptation gained by the astronaut on Earth might not transfer to the 0-g environment because of a difference between the expected stimulus as constructed in the internal model through training on Earth and the actual stimulus in space.

The three-dimensional model developed by Holly [67] explains the experimentally-verified asymmetry between head-turn directions for off-axis rotation. The model is based on representation of the CCS with six degrees of freedom: the expected three rotations, but also the three translations. Heads turns can be characterized by the angular and linear displacements they generate. During centrifugation, the difference between the perceived and real motions is measured in terms of "twist" and "stretch". The twist factor is the difference between the angular displacements of the two motions whereas the stretch factor is the difference between the linear displacements. These two factors characterize the amount of conflict corresponding to a head-turn. The stretch factor for counterclockwise yaw head-turns being larger, the perceptual disturbance predicted by the model confirms the asymmetry between the two head-turn directions.

Interestingly enough, the model also suggests that cross-coupled stimulation should be weaker in 0-g than in 1-g. This prediction is confirmed by experiment. According to

biomedical results from Skylab and results from an experiment performed during parabolic flights [9], the CCS and the subsequent vestibular responses are much weaker in 0-g than in 1-g.

Although some surprises may still be expected as to the transfer of adaptation from Earth to 0-g, it appears that the disturbing vestibular response triggered by cross-coupled stimulation should be weaker in space.

2.6.5 Retention of adaptation

Humans can adapt to cross-coupled stimulation because of the plasticity of the internal pathways that interpret the stimulus. This plastic behavior implies, however, that if the vestibular system is not exposed to the stimulus for a certain time, it will lose its adaptation. No experiment has yet determined precisely how long adaptation is retained. Nevertheless, this knowledge is critical to the use of AG in space: If astronauts were, for some reasons, unable to use an onboard short-radius centrifuge for several days, they should know to what degree their adaptation to AG has fallen in the meantime.

A study found that adaptation was retained over a six-day rest period, but was not complete for all measures: VOR adaptation was fully maintained whereas adaptation for illusory motion and motion sickness was only partially maintained [59].

2.7 Choice of the adaptation procedure

There are many ways to induce adaptation to a stimulus. Depending on the reason that drives the need for adaptation, the procedure can be more or less distasteful for the subject, quick, expensive or even hazardous. Adaptation to artificial gravity classically follows sequential or incremental procedures.

2.7.1 Sequential adaptation

Sequential adaptation is the most widely studied adaptation procedure. It consists of repeated exposure to the same stimulus. Typically, for AG experiments, the subjects are exposed to the same head-turn protocol over several days [35, 58, 59, 63]. The main strength of sequential adaptation is that it allows a direct comparison of the results between the days since each day's trial deliver the same stimuli in the same order. Researchers usually prefer sequential adaptation because it permits a detailed and complex analysis. Specifically the effect of time is not confounded with changes in the experimental protocol.

2.7.2 Incremental adaptation

The concept of incremental adaptation is based on the belief that the first exposure to a stimulus is the most painful and that consequently a weaker stimulus should be presented upon first exposure. During such procedures the subjects are exposed to gradually increasing stimuli such that adaptation occurs while the discomfort of the subject remains low [62]. Incremental adaptation can reach the same goal as sequential adaptation in terms of strength of stimulus that the subject becomes adapted to. It will usually be slightly slower, but not necessarily, and will be substantially easier for the subject. The main advantage of incremental adaptation is that it maintains a low vestibular response during the whole adaptation process. Subjects who are more sensitive to the stimulus – and might have dropped out the sequential adaptation procedure – will be able to adapt to stimuli that are initially above their bearable threshold [68]. On the other hand, since the strength of the stimulus changes between days, the effect of time on the responses is confounded with the effect of stimulus increment. Incremental adaptation can be conducted by increasing centrifuge-velocity, head-angle, frequency of head-turns, or number of head-turns per day.

The experiment described in this thesis aims at finding whether the centrifuge-velocity or the head-angle should be the dominant increasing variable for an optimized incremental adaptation procedure.

3 Methods

3.1 Hypothesis

The main objective of this thesis is to quantify the relation between vestibular response and stimulus created by head-turns performed in a rotating environment. It focuses on the relative effect of the centrifuge-velocity and head-turn angle on the vestibular response itself and on the change in this response over a two-day period. Head-angle and centrifuge-velocity are two obvious candidate variables for increasing the stimulus intensity by incremental adaptation and the efficiency of an incremental adaptation procedure depends on our knowledge on the relative effect of those two variables.

Specifically, the thesis compares the vestibular response at five levels of stimulus in the pitch plane (CCS intensity), $\omega_c \sin(\psi_{\max})$, defined using three centrifuge-velocities, ω_c = 12, 19 and 30 rpm, and three different head-turn angles, $\psi_{\max}$ = 20, 40 and 80 degrees.

The hypotheses are:

1) Head-turns corresponding to the same CCS intensity yield the same vestibular response as measured by the amplitude of the eye movements, motion sickness and illusory motion sensations.
2) The subjective body-tilt depends only on the centrifuge-velocity, ω_c.
3) The stronger the stimulus, the more efficient the adaptation, but the less comfortable the process.
4) For a given CCS intensity, adaptation is quicker for head-turns corresponding to large angles, $\psi_{\max}$, than for those corresponding to high centrifuge-velocities, ω_c.

3.2 Experimental Design

This experiment is a part of a larger research plan whose goal is to set up efficient AG training. The protocol of this study was inspired by the work of Adenot on the effect of head-turn angle on the vestibular response [35]. The present study investigates the relative effect of centrifuge-velocity and head-angle on the vestibular response to head-turns in a rotating environment. Specifically, we looked for differences in the adaptation patterns over two consecutive days that might be related to different types of head-turn. We studied the vestibular response to nine combinations of three head-angles and three centrifuge-velocities.

The total stimulus applied to the SCC after a yaw head turn has both pitch and roll components (Section 2.2.2). It was observed, in a pilot study for this experiment, that the pitch sensation dominated over the roll sensation. This suggests that the vestibular response to yaw head-turns is dominated by the pitch signal that those turns generate. In addition, vertical eye-movements, elicited by the pitch canal, are much quicker than torsional eye-movements, elicited by the roll canal: It was observed that the gain for vertical eye-movements in the dark is twice the gain for torsional eye-movements [69]. Although this difference between the VOR components may reflect only that torsional eye-movements are smaller than vertical eye-movements, it might also be another observation that the pitch signal dominates over the roll signal in the vestibular response. Based on those hints, it is assumed in this study that the vestibular stimulus is substantially the pitch component of the CCS.

With this assumption, the expression for the angular velocity stimulus generated by a head-turn between the NUP position, $\psi = 0$, and an angle $\psi = \psi_{\max}$, performed while spinning at the velocity ω_c, simplifies to:

$$CCS_{pitch} = \omega_c \sin(\psi_{\max})$$

This experiment was designed to quantify the vestibular response in terms of angular velocity stimulus in the pitch plane (referred to as "CCS intensity"). The experiment is a parametric study of the effect of centrifuge-velocity and head-angle on the vestibular response to head-turns in a rotating environment. Figure 3.1 shows the range of the parametric study as well as the link between the combinations head-angle / centrifuge-velocity chosen and the CCS intensity in the pitch plane.

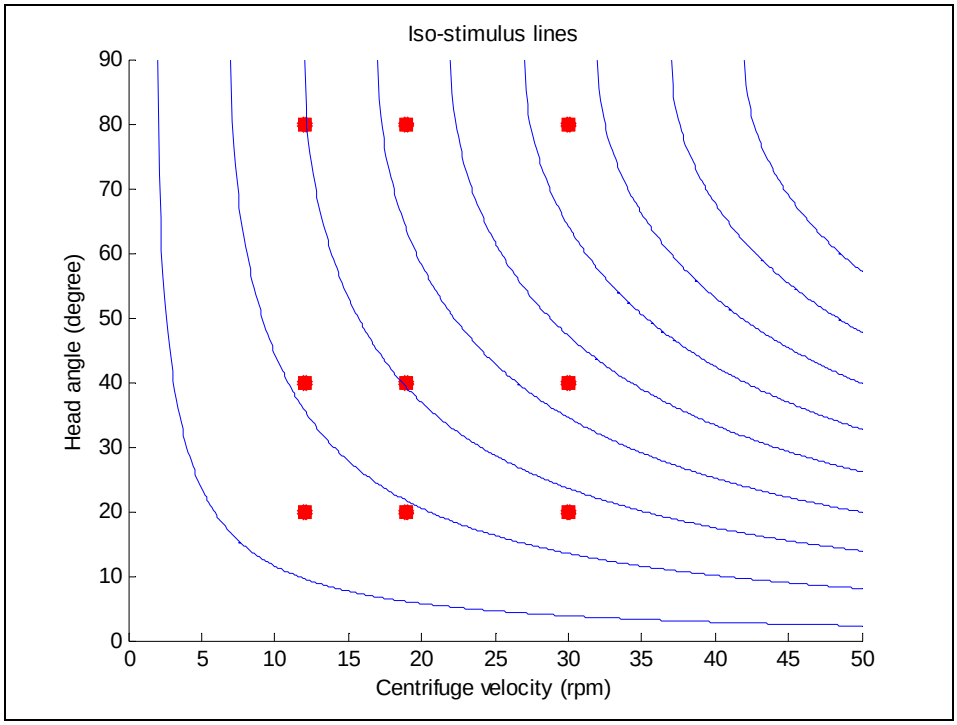

Figure 3.1. Lines of iso-stimulus and range of the parametric study. The lines correspond to combinations of head-angle and centrifuge-velocity that lead to the same CCS in the pitch plane. The dots represents the nine combinations of centrifuge-velocity and head-angle studied in the experiment.

Head-turn angles of 20, 40 and 80 degrees and centrifuge-velocities of 12, 19 and 30 rpm were combined in nine pairs of parameters representing five levels of CCS intensity, $\omega_c \sin(\psi_{\max})$, in the pitch plane as shown in Figure 3.1 and Table 3.1. Several criteria were used to choose the experimental head-angles: (1) Because past research found that the vestibular response was similar for 60 and 90-degrees [35], the experimental angles chosen were not in arithmetical sequence. (2) In order to be able to analyze the effect of

CCS intensity, head-turn angle, and centrifuge-velocity separately, the sines of the experimental angles were chosen according to a geometric progression. (3) Hardware restrictions constrained the head-angle to multiples of 10 degrees. (4) The span of the angles was maximized to increase the range of the results. Finally the values for the centrifuge-velocity were derived from the values of the head-turn angle using the equation defining the CCS intensity.

Table 3.1. CCS intensities in the pitch plane (in deg/sec) corresponding to the combinations of head-angles and centrifuge-velocities retained.

$CCS_{pitch} = \omega_c \sin(\psi_{\max})$		Head-angle (degrees)		
		20	40	80
Centrifuge-velocity (rpm)	12	24.6	46.3	70.9
	19	39.0	73.3	112.3
	30	61.6	115.7	177.3

The maximum head-angle was chosen to be 80° because most subjects are not flexible enough to perform head-turns to 90° and because there is little difference between the sines of 80° and 90° (0.98 instead of 1). Before each experiment it was tested that the subject was able to reach 80° and, in the rare cases this was too difficult, a cushion was placed below the subject's left shoulder to relieve the tension in the neck.

The ordering of centrifuge-velocities and head-turn amplitudes was a great concern because of the habituation to the stimulus that occurs within an experimental day [60, 61]. There were too many possible parameter combinations so it was not possible to test all the different permutations. The option of using a random sample of sequences was rejected because of this huge number of possible permutations. Further, performing head-turns to 80° at 30 rpm on the first experimental day is highly provocative and could lead to systematic drop-out of subjects if encountered before any habituation or adaptation occurred. We also decided to minimize the number of velocity changes during the experiment since accelerations and decelerations of the centrifuge are potentially provocative stimuli in themselves. For these reasons it was decided to start the experiment with the lowest centrifuge-velocity and increase the velocity during the

experiment so that the subjects could get used to the stimulus before experiencing the most provocative one. In order to partially decouple the effect of habituation from the effect of velocity, it was decided to repeat a sequence of eighteen head-turns twice within a day. Finally two sequences of head-turns were selected and the subjects were separated into two groups, each presented with the same set of stimuli in one of these two orders, as summarized in Table 3.2. Since the main objective of this experiment was to compare the combinations of centrifuge-velocity (ω_c) and head-turn angle ($\psi_{\max}$) that deliver the same CCS, the two sequences of head-turns were chosen so that those specific pairs were adjacent in the sequence:

Table 3.2: Order of CCS intensity for the two groups of the experiment. As indicated in bold type in the table, the velocity transitions allow a comparison of different pairs of parameters that create the same stimulus, controlled for habituation.

HT number	1 - 2	3 - 4	5 - 6	7 - 8	9-10	11-12	13-14	15-16	17-18
Centrifuge-velocity	12	12	12	19	19	19	30	30	30
				Group 1					
Head-angle	20	80	40	20	80	40	20	80	40
CCS intensity	25	71	**46**	**39**	112	**73**	**62**	177	116
				Groups 2					
Head-angle	40	20	80	40	20	80	40	20	80
CCS intensity	46	25	**71**	**73**	39	**112**	**116**	62	177

The stimulus was 36 yaw head-turns in the right quadrant, repeated for two consecutive days in the same order. Each type of head-turn was repeated four times during one experimental day – two head-turns from nose-up (NUP) to right-ear-down (RED) and two from RED to NUP. The full sequence of head-turns of the stimulus phase for one experimental day is shown on Figure 3.2.

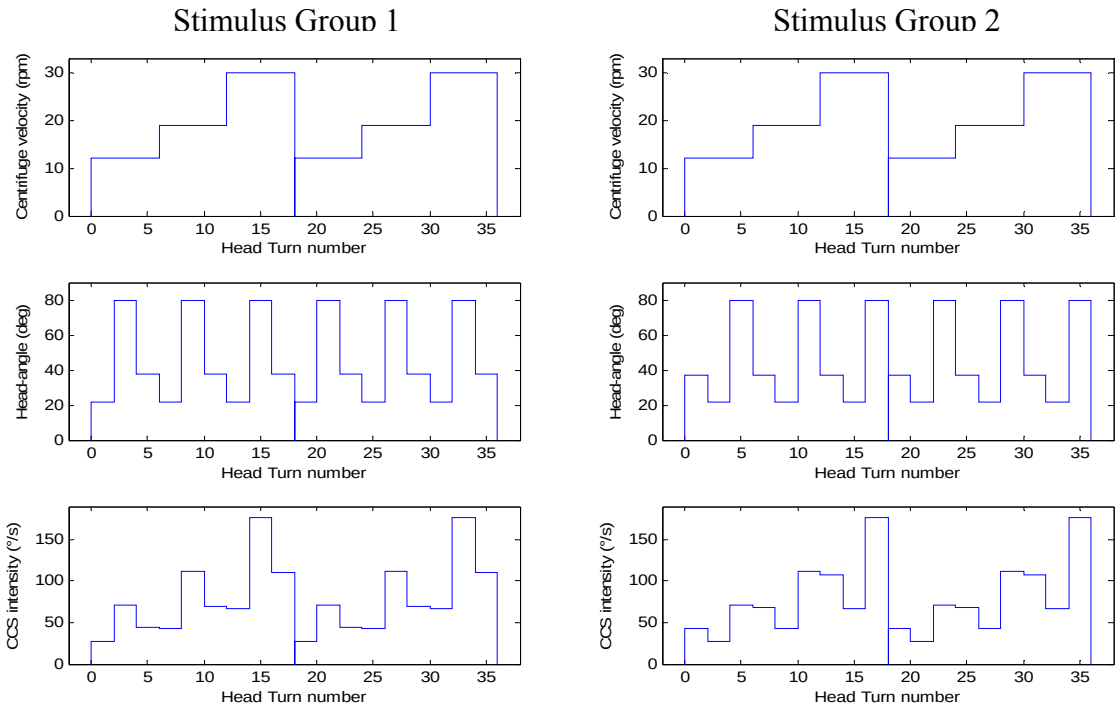

Figure 3.2. Characteristics of the sequence of head-turns for one experimental day, group 1 on the right and group 2 on the left.

During the stimulus phase, the subject lay supine on the bed in a dark environment with his head on the center of rotation. He was instructed to perform all the head-turns at the same head velocity of 50°/s: He was trained to move his head at that speed before the experiment and instructed to minimize erratic changes of speed during a head-turn.

3.3 Equipment

3.3.1 Centrifuge

The subjects were tested on the Man-Vehicle Laboratory (MIT) short radius centrifuge (see illustration on Figure 3.4). The centrifuge is a 2-meter-long rotating bed that was built in 1988 by Diamandis [70]. The control system was redesigned in 2000 by Cheung [71]. Since then the apparatus has been modified so that it can be used for

vestibular or cardiovascular experiments. An up-to-date technical description of the 2005 centrifuge can be found in [11].

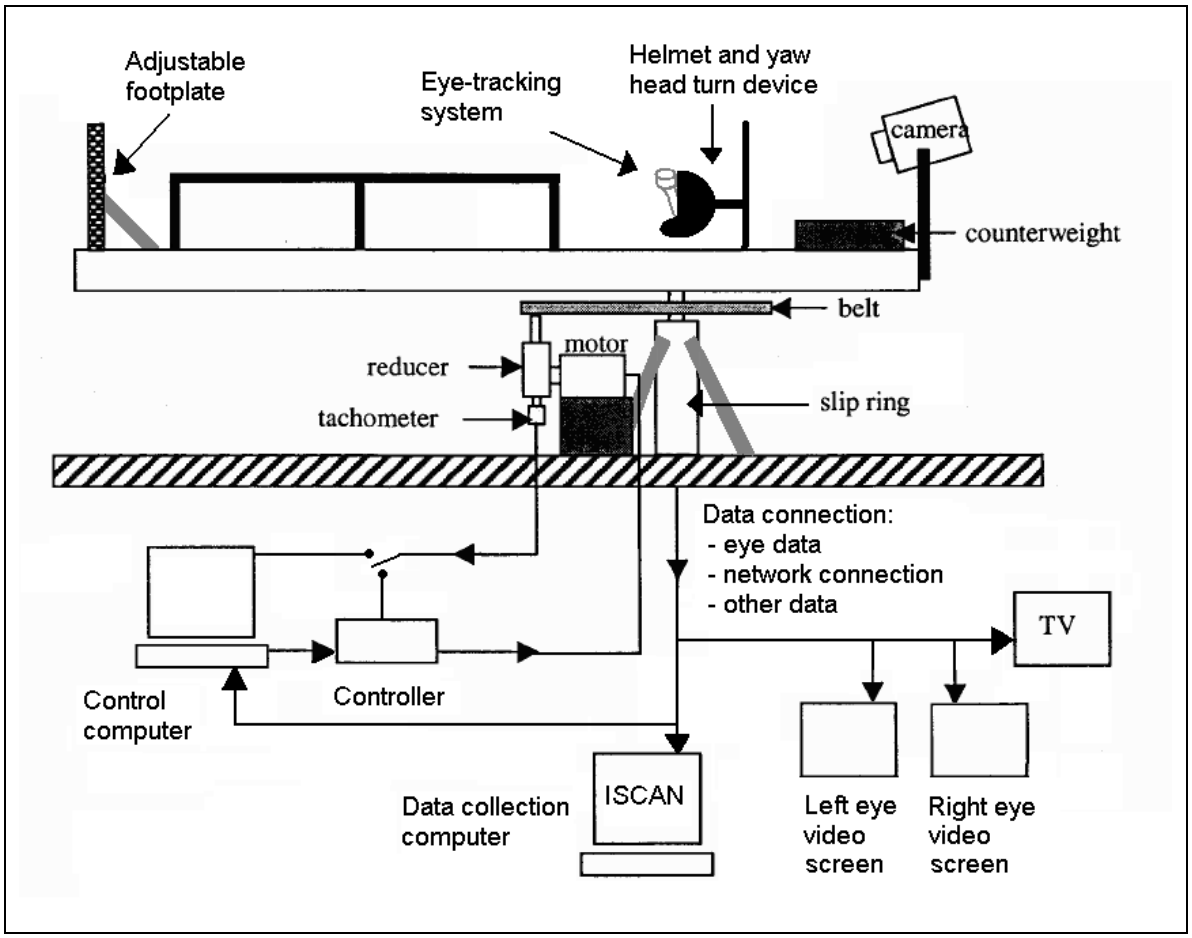

Figure 3.3. Schematic of the MIT Man-Vehicle Laboratory short-radius centrifuge (modified from [55]).

For this experiment, the centrifuge was configured to rotate the subjects clockwise about a vertical axis at rotation rates up to 30 rpm (180°/s). The centripetal acceleration created by the centrifuge produced no more than 1.7 g horizontally at foot level for a 1.75 m subject. The centrifuge is equipped with several safety features including a safety belt and an emergency-stop button onboard. The subject wore, throughout the experiment, a blindfold that ensured a dark environment; however, for this experiment, no canopy was used to isolate the subject from the air moving around him.

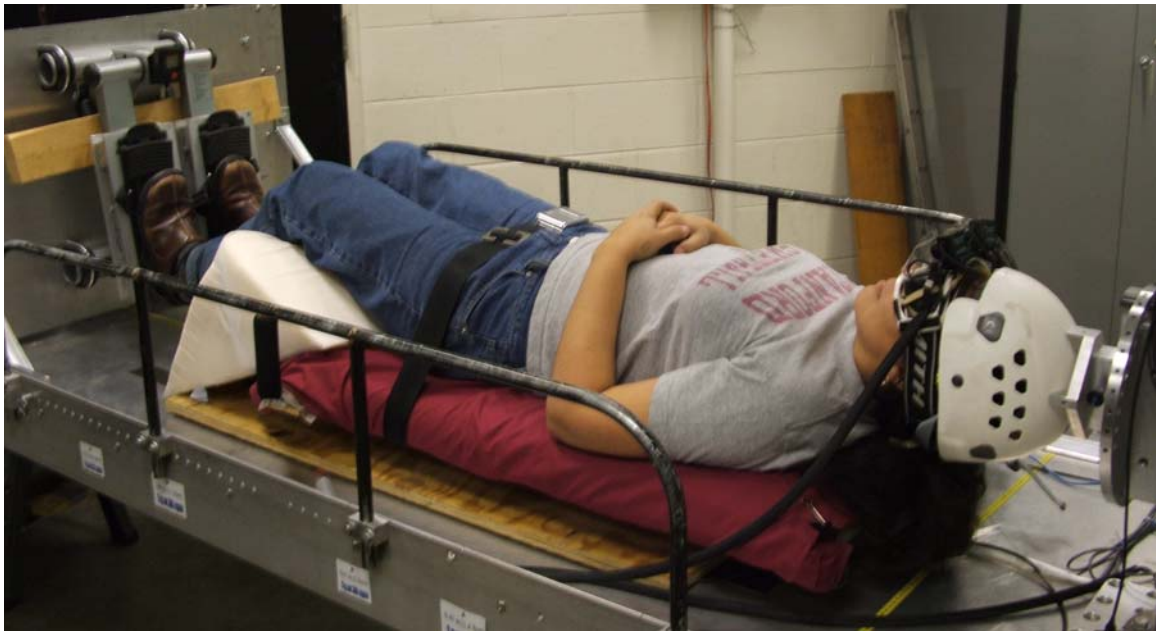

Figure 3.4. Subject lying on the Man-Vehicle Laboratory short-radius centrifuge at MIT (credits: Paul Elias).

3.3.2 Head monitoring

For safety reasons, the subject's head was secured in a helmet mounted on a yaw device, which kept the subject's head aligned with his body and restricted his head movements to the yaw plane [63]. In this experiment it was also used to control the amplitude of the head-turns made by the subjects. The helmet was equipped with a potentiometer that recorded head-angle in the yaw plane during the experiment. The head angular position – encoded as a voltage – was converted into degrees during the analysis and was differentiated to obtain the head velocity for each head-turn.

Since the experiment aimed at comparing the vestibular response elicited by head-turns whose amplitudes varied by only 20 degrees, we needed a device to monitor the head-angle closely. It was decided that using magnets to constrain the head-angle, as was previously done in a pilot experiment for this thesis and in [35], was not precise enough. We were concerned that the slight force applied by the magnets as the helmet passed by during a head-turn to a large angle would modify the vestibular response. Consequently a

new device was designed and built for this experiment. We used a set of aluminum bolts activated by a system of computer-controlled servomotors (Figure 3.5).

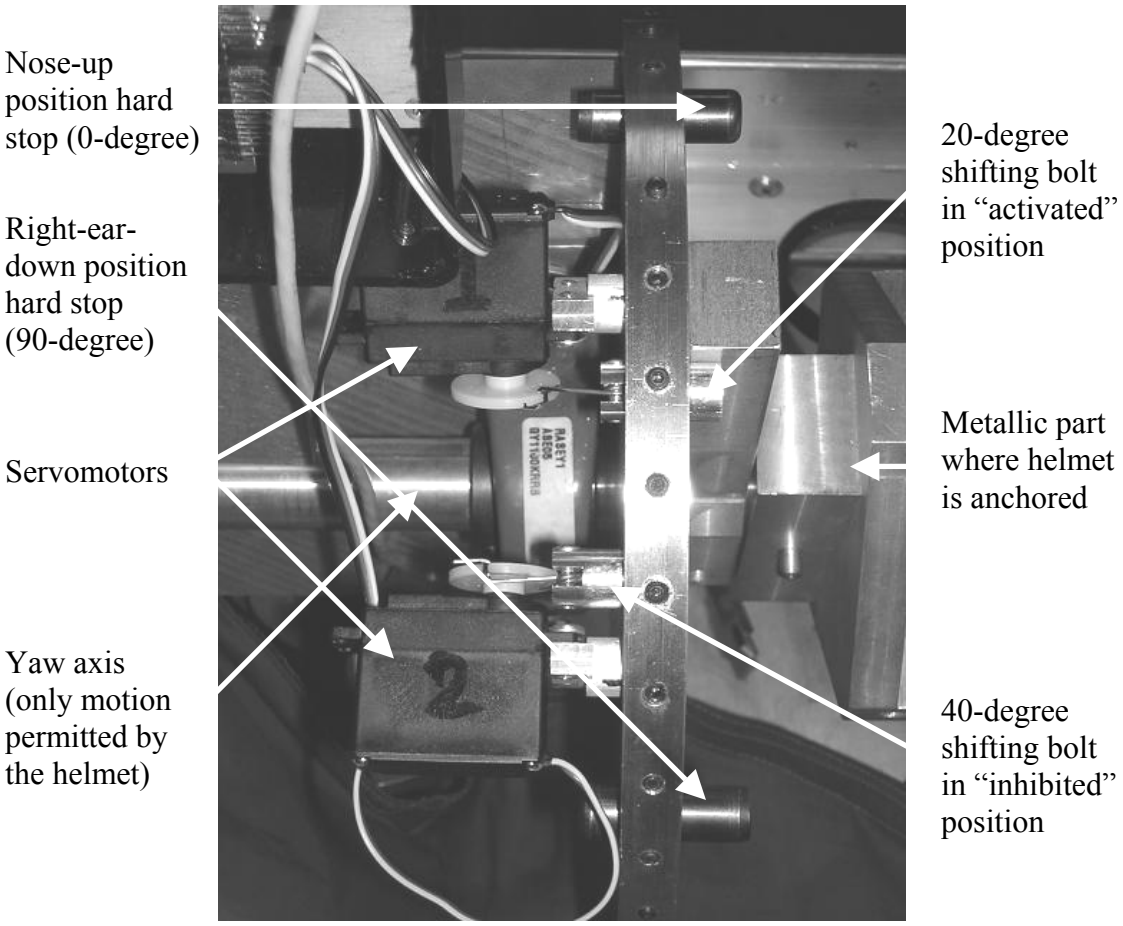

Figure 3.5. Device to control the maximum angle reached during a head-turn. The two servomotors that activate the two moveable bolts are attached on the device used to constrain head movements to yaw head turns.

The experimenter was able to change the configuration of the aluminum bolts, while the centrifuge was spinning, using a network connection going through the slip ring and a user interface written in Visual Basic®. The technical drawings for the hardware that was added specifically for this experiment can be found in Appendix A. Finally we used two stationary bolts for the 0 and 80-degree limits and two shifting bolts for 20 and 40 degrees. Overall this device allowed us to control reliably the maximum angle the subject could reach during a head-turn. Figure 3.6 demonstrates the different configurations of bolts used during the experiment.

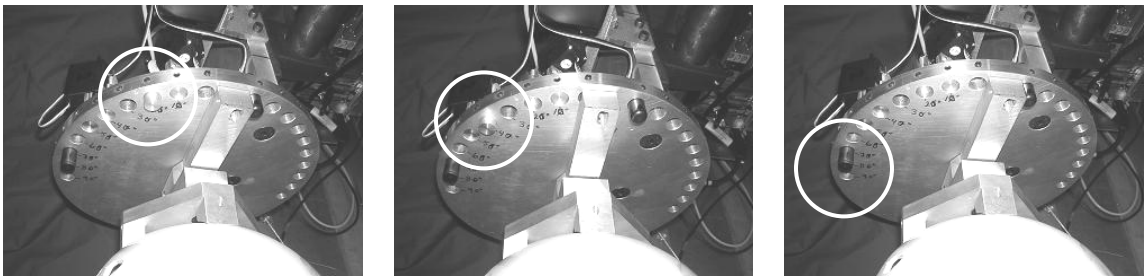

Figure 3.6. Positions of the device used to control the angle of a head-turn. (a) the servomotor corresponding to the 20-degree bolt is activated. (b) 40-degree bolt activated and 20-degree bolt inhibited. (c) 20-degree and 40-degreee bolts both inhibited.

The subjects had to perform all their head-turns at the same speed and were helped in the task by an audio signal that gave them the right pace for each head-turn. This idea was originally developed by Adenot [35] and is a simple way to help the subjects keep the same head velocity even for head-turns to different angles. The audio signal was a set of four rhythmic beeps whose cadence corresponded to the cadence of the head-turns. The two first beeps were used to remind the subject how much time was dedicated to the incoming head-turn. Then the third beep corresponded to a "start" signal and the last beep to a "stop" signal and the subject had to begin his head-turn with the third beep and hit the bolt corresponding to the angle of the head-turn as the fourth beep rang. The two last beeps had a slightly higher frequency than the two first ones to differentiate them. The head velocity was set to 50°/s and the frequencies of the beeps corresponding to the three different head-turn angles were calculated accordingly. The beeps were generated using Matlab® through a custom user interface.

3.3.3 Eye tracking

Eye movements were collected using an infrared (IR) miniature eye-tracking system and software developed by ISCAN®. The system illuminates each eye of the subject with an IR source. It uses the fact that the pupil absorbs a greater fraction of the IR than its surrounding area to create a "dark pupil" image of the eyes. The infrared cameras (Model EC-501) were mounted on a ski mask for a better and more comfortable fit on the

subject's face (Figure 3.7). The ski mask was also used to attach a blindfold to ensure a dark environment during the experiments. The blindfold was fixed using a pair of Velcro straps.

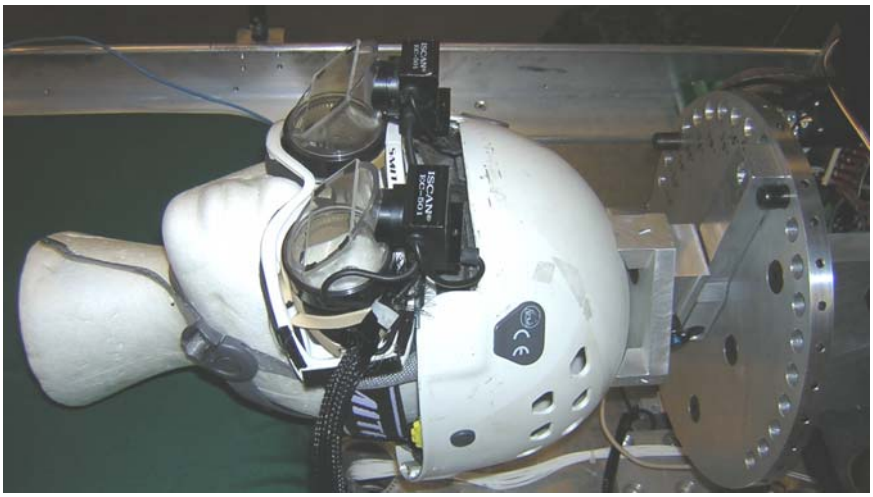

Figure 3.7. ISCAN® eye tracking system mounted into a ski mask. The helmet and the device to constrain the head-turns into the yaw plane are shown.

The video signals were transmitted to a computer via the slip ring and recorded at a sample frequency of 60 Hz with dedicated ISCAN® software. The software calculated the center of the dark area for both eyes and assumed that it was the center of the pupils. For each experiment it was possible to adjust manually the contrast of the dark-pupil images to make sure the center of the dark pupil corresponded to the actual center of the pupil. The software could only compute the 2D position of the eyes and recorded separately the vertical and horizontal components.

Before any head-turn, the eye-tracking software had to be calibrated in order to convert the eye position to degrees. As recommended in the ISCAN® documentation, we used a set of five LEDs 13 centimeters apart arranged as a cross (center, left, right, up and down), as shown on Figure 4.1. The calibration cross was placed 73 centimeters away from the subjects' eyes so that the four peripheral LEDs were 10° away from the center LED. The calibration applied by the ISCAN® software is slightly unstable and is detailed in Section 4.1.2.

It appeared that too much makeup interfered with the dark pupil recognition system and therefore the female subjects were asked to wear only light makeup on the days of the experiment. The subjects wearing contact lenses were asked to remove them if they blinked more often than usual because of the lenses.

3.4 Measurements

Each head-turn performed during the experiment was characterized by six different measures. Two came from a post-experiment analysis of the eye movements measured by the eye-tracking system (physiological measurement). The other four were subjective assessments made by the subjects after the VOR and all the transient sensations had vanished.

Eye-movement parameters are often considered more accurate because they are a physiological measure of the vestibular response, whereas the subjective assessments depend on the subject's ability to express them accurately. However, the eye-tracking system used in this experiment is not perfect, and the algorithm that extracts the slow-phase velocity from the eye position also introduces some errors (listed in Section 4.1.9). The contrast between the reliability of the two kinds of measure, therefore, is less dramatic than one might expect.

3.4.1 Eye movements (A & TAU)

Subjects wore the ISCAN® goggles during the entire experiment and eye movements were recorded for all the head-turns. Each subject was instructed not to change the position of the goggles after calibration and to open his eyes wide during and at least 20 seconds after each head-turn. A Matlab® routine developed at the MIT Man-Vehicle Laboratory was used to infer the slow-phase velocity from the measurements of eye position. Each head-turn, clearly identifiable as a slow-phase velocity step followed by a decline, was then fit with a single exponential mode. The eye movements for each head-

turn are characterized by the two parameters of the fit: the peak amplitude (A) and the time-constant (τ) of the decay. A more detailed explanation of the eye-movement analysis is given in the next chapter.

3.4.2 Illusory motion sensation (INT & DUR)

Each subject was asked to rate his sensation of illusory motion[7] in terms of two separate metrics: duration and intensity. The duration was indicated by holding down a button in order to measure the time elapsed between a head-turn and the moment when the subject feels stable again. The subject was instructed to press the button just as he stopped his head motion at the end of a head-turn and to hold it until the sensation of illusory motion vanished. The intensity, often referred to as the speed or strength of the illusory motion, was rated on an open-ended scale: The intensity of the first head-turn from NUP to RED performed while spinning (at 23 rpm) on the first experimental day was arbitrarily set to 10. The other sensations were scaled in proportion to that first value. Since the illusory motion is a transient sensation, it was the first rating solicited from the subject after he released the duration button.

3.4.3 Motion sickness (MS)

The motion sickness was rated on a scale from 0 to 20, 0 corresponding to "I feel fine" and 20 to "I am about to vomit." This is a measure of the discomfort of the subject following out-of-plane head-turns made in a rotating environment. As described by the subject, motion sickness often presents a sustained component that builds up relatively slowly as the experiment progresses and a transient component that boosts the motion sickness level during or just after the head-turns. In this experiment the subjects were

[7] This illusory motion is also referred to as "tumbling sensation" in other studies. In this thesis the term "illusory motion" has been retained over "tumbling sensation" because of its more general meaning (subjects can get confused by the word "tumbling" and not report potential spinning sensations).

asked to report the sustained component. The experiment was stopped at once if the subject reported a motion sickness value of 13.

3.4.4 Perceived body-tilt (TILT)

After the illusory motion sensation stopped, the subject was often left with a persistent sensation of body-tilt. This sensation is due both to sequels of the illusory motion sensation, as well as to the centripetal acceleration that tilts the GIF away from Earth vertical. This perceived body-tilt would remain unchanged indefinitely if the subject continued spinning without turning his head. For this reason the subject was asked about his perceived body-tilt last, after being asked about tumbling intensity and motion sickness. The perceived tilt was assessed using a clock analogy as described on Figure 3.8. The subject was asked to assume that he was the minute hand on a clock, with his head at the center of the clock, and had to report the position of his feet in minutes. If the subject thinks he is lying flat his feet will point to 45 minutes; if he feels pitched forward, he would report a value between 30 and 45 minutes and if he feels pitched backward he would report a value between 45 and 60 minutes.

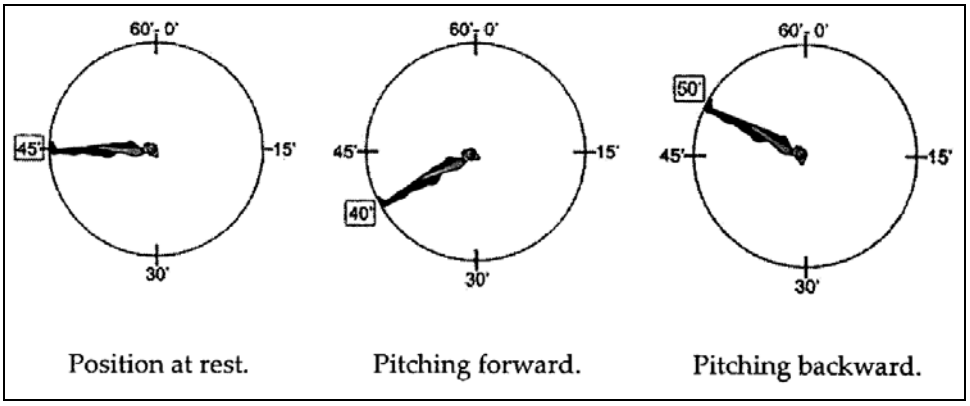

Figure 3.8. Illustration of the body-tilt assessment using a clock dial analogy (modified from [62]).

The values reported by the subject were then transformed into degrees during the analysis for a better visualization of the phenomenon.

3.5 Subjects

There were 27 subjects aged from 19 to 28 in the experiment, including 21 males and 6 females. They were all students, mostly from the MIT community, recruited either by informal presentation of the experiment or by announcements posted around campus. The head-turns to 80° at 30 rpm made this experimental protocol particularly provocative and two subjects dropped out during the first day of the experiment. Although they completed the first day three other subjects had bad experiences and did not come back for the second day. Technical problems with the centrifuge controller or the eye tracking system ruled two subjects out for the compete analysis. Finally one subject stopped the experiment before the post-adaptation phase on the first day but completed the protocol on the second day. This leads to the statistics presented in Table 3.3:

Table 3.3: Drop out rates and number of subjects used for each kind of analysis.

Gender	M	F
Total number of subjects	21	6
Number of subjects that completed the entire experiment	15	5
Percentage of drop outs (excluding technical problems)	26%	
Number of subjects with complete eye-data	11	5
Number of subjects with full data set for at least one day	15	5

The subjects were asked to come well rested and to abstain from any drugs that could alter the response of the vestibular system such as alcohol, nicotine and caffeine for 24 hours before the experiment. All subjects confirmed that they had no history of known vestibular disorders or any other disqualifying health problem as listed in the consent form (Appendix B). Before starting the experiment and after detailed explanations on the procedure, they all gave informed written consent to the protocol as required by the MIT Committee of the Use of Humans as Experimental Subjects (COUHES).

3.6 Protocol

3.6.1 Overview of the experiment

This experiment uses the same protocol as most of the other experiments on vestibular adaptation to short radius centrifugations conducted in the Man-Vehicle Laboratory. The protocol consists of five phases, four of which are the same for all experiments: Only the middle phase (stimulus) changes from experiments to experiments.

The first phase and the last phase consist of a sequence of 6 yaw head-turns in the right quadrant (3 to-NUP and 3 to-RED) performed with the bed is still. The first phase (pre-rotation) is a check "in-situ" of the vestibular system of the subject and it is also used to define the subject's baseline reference for the subjective measurements. The last phase (post-rotation) is used to assess the re-adaptation to a normal environment that occurs when the centrifuge is stopped and the subject performs head-turns without spinning.

The second and the fourth phases are a sequence of 6 yaw head-turns in the right quadrant performed while spinning at 23 rpm. The second phase (pre-adaptation) determines the initial vestibular response of the subject before applying the experimental treatment. In particular, the first head-turn performed in this second phase defines the scale for the tumbling intensity as described in Section 3.4.2. The fourth phase (post-adaptation) is used to characterize the amount of adaptation resulting from the experiment. These two spinning phases are especially important to allow us to compare different groups of subjects or different treatments.

Finally the middle phase (stimulus phase) is longer than the other phases and is described in Section 3.2. All phases were conducted in a dark environment with the subject lying supine on the bed with his head on-center. Table 3.4, presented further on, summarizes the main characteristics of the different phases. For safety reasons, an experimental protocol checklist was used during the experiment (Appendix C).

3.6.2 Preparation before the experiment

When a subject was first contacted he was asked if he had any of the disqualifying medical problems listed in the consent form (Appendix B). With the first email, the subject was provided a document containing a quick introduction to the experiment and a description of the different measurements (Appendix D). On the days of the experiment, the subject confirmed that he had not consumed any drugs, alcohol or caffeine in the previous 24 hours. It was checked that he was within the weight and height limitations of the centrifuge. If he qualified for the experiment the subject was informed of the potential hazards or discomfort related to the centrifuge. He was then introduced to the short-radius centrifuge and its safety equipment. The experiment's timeline as well as its main characteristics were described and a detailed consent form, approved by the MIT Committee of the Use of Humans as Experimental Subjects (COUHES), was provided. The subject was instructed to carefully read and sign the consent form and the experimenter checked that the subject fully understood what was expected from him. The subject was also reminded that his participation was voluntary and that he could withdraw from the experiment at any time.

After the subject signed the consent form, the experiment protocol was explained and a fair amount of time was dedicated to the explanations of the four subjective measures. The subject was asked to keep his eyes wide open for at least 20 seconds after each head-turn. When the subject was comfortable with the measurements to be used, he was helped onto the bed, was given the eye-tracking goggles and his footplate was adjusted. Then he was secured in the helmet, was given the tumbling and the emergency stop buttons and had his safety belt fastened. The subject was trained to rate the subjective measurements and to perform the different types of head-turn using the audio signal. He continued practicing until he was proficient at performing head-turn to the three head-angles used at the same angular velocity. When the subject was ready to start the experiment the eye-tracking system was calibrated using the device described in Section 3.3.3 and his blindfold was put on. The centrifuge was "walked around" (manually rotated) to make sure nothing blocked the rotation. The lights were then turned off.

3.6.3 Experimental protocol

The subject started by making 6 head-turns without spinning to 80 deg (pre-rotation phase). The centrifuge was then spun up carefully to 23 rpm with the lights on so that the experimenter could react quickly in case of any safety issue. When the centrifuge speed stabilized at 23 rpm, the lights were turned off again and the subject performed 6 head-turns to 80 deg (pre-adaptation phase). Then, during the stimulus phase, depending on the group he belonged to, he went through one of the two sequences of head-turns described in Section 3.2 (see specifically Figure 3.2). Finally the subject made 6 more head-turns at 23 rpm to 80 deg (post-adaptation phase) and, after the centrifuge was slowly spun down and stopped, he made the 6 final head-turns without spinning to 80 deg (post-rotation phase). The complete sequence of head-turns performed by the subjects in Group 1 is shown on Figure 3.9 – Group 2 is similar except for the order of the head-angles in the stimulus phase – and the experimental conditions for each phase are shown in Table 3.4.

Table 3.4: Summary of experimental protocol.

Phase	Pre-rotation	Pre-adaptation	Stimulus (treatment)	Post-adaptation	Post-rotation
Number of HT	6	6	36	6	6
Centrifuge-velocity (rpm)	0	23	12, 19 or 30	23	0
Head-turn angle (degrees)	80	80	20, 40 or 80	80	80
CCS intensity	none	high	low to really high (5 levels)	high	none
Eye movements	yes	yes	yes	yes	yes
Verbal reports	yes	yes	yes	yes	yes

The cadence for the head-turns was one every 30 seconds except when the centrifuge speed was changed in which case a 30-second break was observed to allow eye-movements and other sensations to vanish. If the subject's motion sickness reached a value of 13 or if the subject requested it, the experiment was aborted and the centrifuge has gently spun down. Depending on the amount of data recorded, the subject was either totally excluded from the analysis or included for some of the statistics.

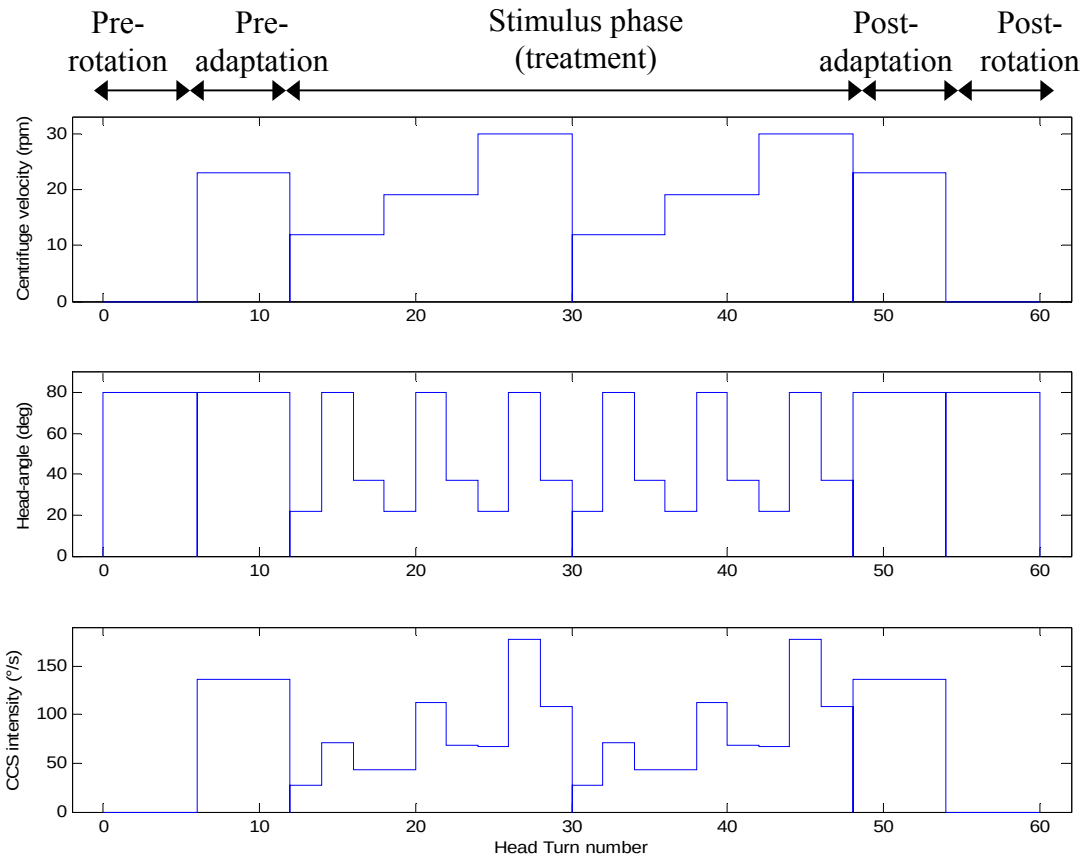

Figure 3.9. Characteristics of all the head-turns performed by Group 1 during one experimental day, from the pre-rotation phase to the post-rotation.

After the experiment – and before helping the subject out of the bed – another calibration sequence was recorded to check that the eye-tracking system was still correctly calibrated. The subject was allowed to lie down on the bed to recover from the experiment and was finally debriefed.

4 Data Analysis

4.1 Eye-movements

The eye-movements analysis package is a key software tool in the analysis of the physiological data. Each step of the analysis is given in detail in the paragraphs to follow so that the algorithm may be modified if necessary.

4.1.1 Goal of the eye data analysis

The eye-movements analysis is a complicated process that analyzes the raw eye position and produces two parameters – amplitude and time constant – characterizing the behavior of the VOR SPV. First, the algorithm filters the eye position data recorded by ISCAN®, differentiates the signal to obtain the eye velocity trace and extracts the slow-phase velocity component. Best exponential fits are then calculated for each head-turn separately.

Note that ISCAN® can record only the movements of the eyes in two dimensions and does not detect torsional eye-movements. It also breaks the 2D motion of the eyes down into vertical and horizontal components. The movements of each eye are recorded separately. The two components of each eye's movements are analyzed separately according to the same procedure. This section details the complete analysis process and points out its weaknesses.

4.1.1.1 History of the MVL eye-movements analysis package

Balkwill wrote in 1992 the first version of the eye analysis software used to extract the slow-phase velocity from the eye position [72]. He implemented a new algorithm based on order statistic filters developed by Engelken [73], using the computing software

Matlab®. This new algorithm' performance compared favorably in precision and speed to the corresponding classic procedure and became the core of the Matlab® eye-movements analysis package used in the Man-Vehicle Laboratory at MIT. One of the great strengths of this new robust procedure was that it is fully automated and does not require the user to have any knowledge of the algorithm. Since then the package has evolved to integrate several functions that make the analysis of the slow-phase velocity easier; the primary algorithm creating the slow-phase velocity, however, has only been little revised.

4.1.1.2 Recent revision of the package

For this thesis, the package was revised totally and while the primary algorithm was only slightly modified, the functionality of the software was greatly enhanced by the development of a graphical user interface (screenshots of the GUI are given in Appendix H). The slow-phase velocity analysis procedure was also converted into a semi-automatic routine that, on a single button press, analyzes the eye movements for all head-turns and allows manual modification of the exponential fits. The updated version of the software is described in the next sections. The organization of the Matlab® scripts of the eye-analysis package is given in Appendix I.

4.1.2 Note on ISCAN® calibration

The eye-movements analysis software requires the calibrated eye position recorded by the ISCAN® software. However the calibration process applied by ISCAN® is controversial and is worth commenting on. For the vertical eye-movements, for example, the calibration process asks for the y-coordinate of the center of the pupil in pixel units when the subject looks in these direction: straight ahead (LED#1), 10° up (LED#2) and 10° down (LED#3) – the three LEDs are labeled on Figure 4.1. Then it splits the sample of eye positions recorded during the experiment into two groups: The eye positions that are above the average line of gaze (whose pixel values is greater than that of LED#1) and the positions that are below. For each group, a separate normalization coefficient is

calculated: For the data points that correspond to gazes above the average line, the normalization coefficient is defined by the difference between the pixel values of LED#2 and LED#1 divided by 10; similarly the normalization coefficient for the other half of the data points is defined by the difference between the pixel values of LED#3 and LED#1 divided by -10.

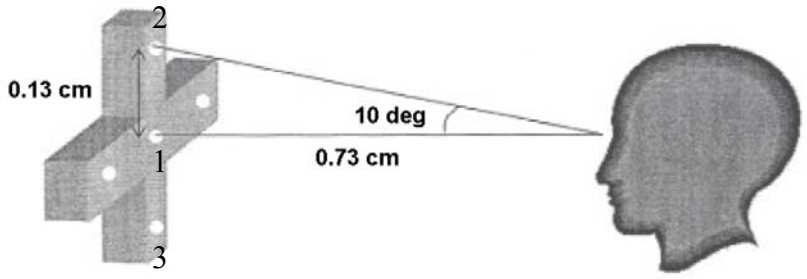

Figure 4.1. Eye-tracking system's calibration settings (modified from [35]). Each one of the five white dots represents a LED.

This "two-level" normalization should be more precise than a normal calibration (with only one normalization coefficient for all the data points) because of the curved shape of the eye ball – the curved motion of the center of the pupil is projected onto the planes of the eye-cameras. In practice, however, it appears that the goggles often drift during the experiments and this two-level calibration process may hinder the quality of the eye-movements. Therefore the calibration should be checked for each eye-movements recording, and if it were found to be deficient, the eye position would have to be recalibrated from the raw data using a customized process.

4.1.3 Organization of the Matlab® eye-analysis package

The eye-analysis package is separated into two sets of functionalities as illustrated in Figure 4.2. The first set extracts the slow-phase velocity (SPV) component of the eye movements from the eye position signal recorded by ISCAN® and the second analyzes the SPV and produces the best exponential fit for each head-turn. While the

differentiation of the SPV is fully automated, the human operator ultimately validates the fitting process. This description of the eye-analysis package focuses on the algorithm that extracts the SPV.

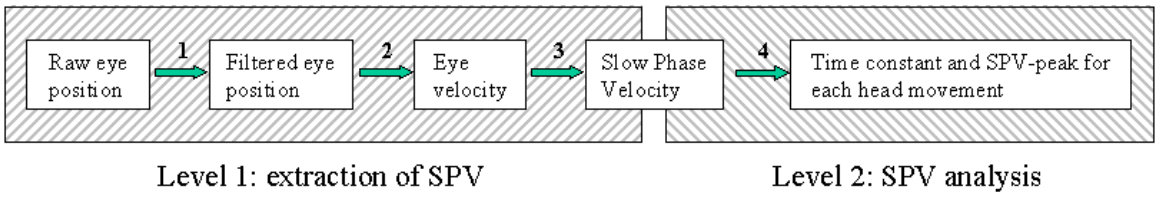

Figure 4.2. High-level organization of the eye-analysis package. The procedure comprises the four main steps indicated on the figure. These steps (1-4) are detailed in the next sections.

Note that this linear process has a built-in limitation since each new step uses the output from the previous step. If the result of a step is poor in quality it may corrupt the next step. The early steps, therefore, must be carefully optimized in order not to distort the later.

4.1.3.1 Introduction to order-statistic filters

Order-statistic (OS) filters are a class of nonlinear digital filters that show properties highly valuable for filtering the nystagmus signal [73]. They operate on a sliding window of input data usually centered on the current point of interest. The samples in the window are rank-ordered by amplitude and a linear combination of the ordered sample forms the filter's output. Median filters belong to the OS filter class (the linear combination defining the output is 1 for the center sample and 0 for all the others). The definition of the OS filters can be extended to include FIR-Median Hybrid (FMH) filters for which the data is first processed by a set of FIR subfilters and then the median of the FIR subfilter outputs is taken as the FMH filter output. The key element in all OS filters is the data ordering operation, which is a data dependent, nonlinear process.

The important property of some OS filters is the existence of "root signals" toward which the signal being filtered will converge on repeated filtering.

4.1.4 Pre-processing - Remove blinks

Since the ISCAN® eye-tracking system records eye movements by analyzing the dark pupil image of the eyes, blinks lead to a loss of signal. In order not to interfere with the filtering process, blinks must be isolated and removed before any other analysis is applied. The ISCAN® software has an integrated algorithm that provides an arbitrary value of 0 to the blinks it can detect, and most of them can be removed from the eye position signal using this 0-flag. Then the blinks that were missed can be removed based on the statistical properties of the signal: Samples that are more than 4 standard deviation away from the mean can be treated as blinks. The signal is then interpolated to fill the gaps created by removing the blinks.

4.1.5 Step 1 - Filter eye position

The blink-free position signal must be filtered before any differentiation process can be applied. The filtering of eye movements is done using a smoothing nonlinear filter designed to preserve the transitions between the slow- and fast-phase components of the signal [73, 74]. The VOR eye position always presents the same succession of linear segments representing alternatively compensatory movements (slow-phase) and saccades (fast-phase). Since the goal of the algorithm is, eventually, to separate the two components, this early filtering operation must preserve the transitions. The class of OS filters used, Predictive FIR-Median Hybrid (PFMH) filters, has been designed for this purpose [74].

The PFMH filter operates on a sliding window as described in Section 4.1.3.1. Several predictive FIR filters, each designed to predict the value at the center of the window, are applied separately to the upper and lower halves of the window. All the FIR filters applied on the lower half of the window are forward predictors and all the filters applied on the upper half are backward predictors The PFMH filter delivers the median of the set of values including the outputs of these filters and the actual central value of the

sliding window. The fact that all the FIR filters used are either pure forward or pure backward predictors is the key to preserving the transitions in the signal.

The VOR signal can be modeled as a sequence of second-order polynomial segments. The PFMH filters have the essential property of possessing root signals that are invariant under the action of the filter [74]. If the predictors constituting the PFMH filter are chosen so that the noise-free VOR is one of the root signals, the filter may be applied several times and the experimental VOR will eventually converge to the ideal noise-free VOR. Practically, noise-free VOR are root signals for any PFMH filter based on zero-, first- and second-order FIR predictors.

The eye position filtering process used in the eye-analysis package contains a PFMH filter and a classic FIR low-pass filter. The low-pass filter reduces the noise of the signal and makes the PFMH filter more efficient. The PFMH filter is first applied once, then the low-pass filter is applied, and finally the PFMH filter is applied three more times. Figure 4.3 shows the results of the eye-position filter.

The PFMH filter used in the eye-movements analysis package is based on three first-order predictors of size N=3, N=5, and N=7, and a second-order predictor of size N=5 (see [72-74] for the expression of the filters). The low-pass filter has a cutoff frequency of 28Hz.

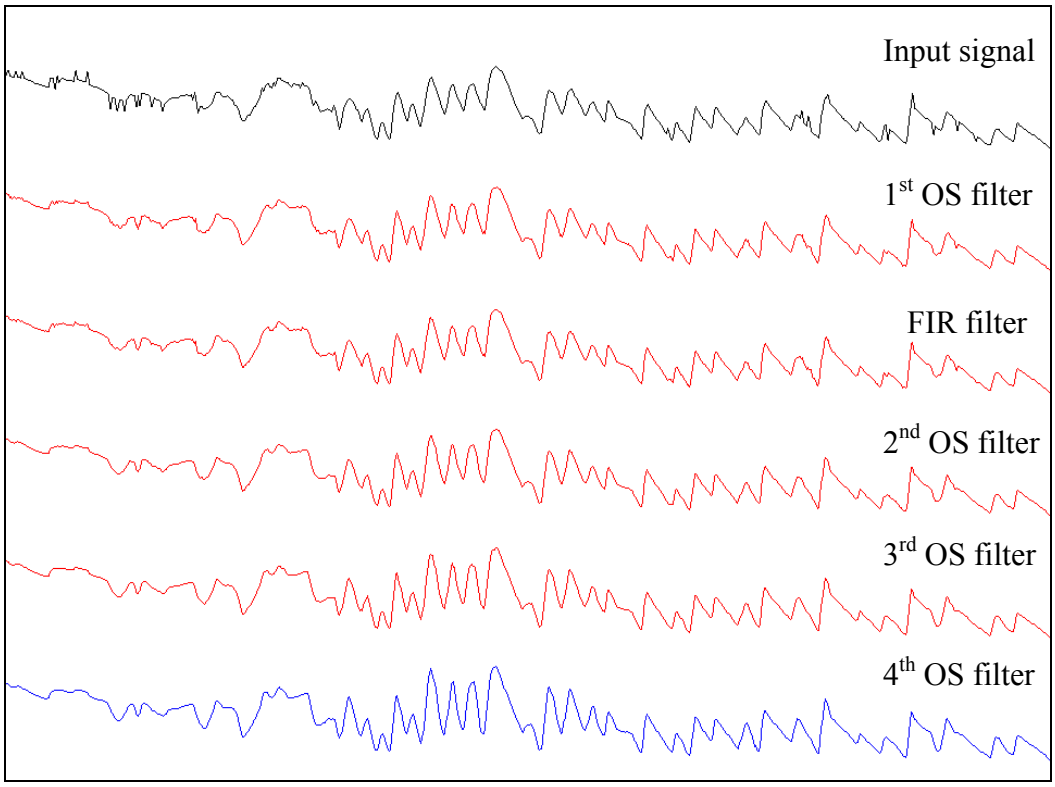

Figure 4.3. Smoothing filter results. The top trace is the noisy signal, the bottom trace is the output of the filter. After the last pass, most of the noise has disappeared and the signal is closer to an ideal nystagmus signal. Transitions between slow- and fast-phase components are well preserved.

4.1.6 Step 2 - Differentiate eye position

Two different filters can be used to differentiate the filtered eye-position.

The first filter is a nine-point FIR filter calculated by Merfeld and applied with zero phase shift. The filter is a convolution of a three-point differentiator and a seven-point low path filter with a 10Hz corner frequency. Using Matlab® convention and for a sample frequency of 60Hz, this standard band-limited filter is defined by:

$$A = [1/60]$$

$$B = [0.0077 \quad 0.0714 \quad 0.1078 \quad 0.0870 \quad 0 \quad -0.0870 \quad -0.1078 \quad -0.0714 \quad -0.0077]$$

The alternative filter is an OS filter developed specifically for differentiating the VOR eye-position signal to produce the eye velocity. It is called "Robust Differentiator" (RD) [75]. The RD differentiates the position signal by taking an odd number of two-point differences around the point of interest and then selecting the median of the differences. The derivative of the input signal is then obtained by dividing the median difference by the time interval. In the eye-analysis package, the default number of two-point differences is 7.

The performances of the RD were found to be slightly worse than those of the nine-point FIR filter that, therefore, was set as the default differentiating filter in the algorithm. Nonetheless, it is possible to have the algorithm use the RD instead of the FIR filter by changing the settings of the eye-movements analysis package.

4.1.7 Step 3 - Extract SPV

The SPV is extracted from the eye velocity signal using an Adaptative Asymmetrical Trimmed-Mean (AATM) filter [72, 73, 76]. Whereas classical methods rely on pattern recognition methods, this approach uses the local statistical properties of the velocity signal. The AATM filter does not require any intervention by the operator, or any assumption as to the direction of the nystagmus. This property is essential since the direction of the fast-phase component of the VOR not only redirects gaze in the direction of the head motion, but also reorients the eyes with respect to Earth-vertical [77]. Note that in the eye-analysis package, the output of the AATM undergoes further processing before final estimation of the SPV (see diagram on Figure 4.5). This is not strictly necessary since the AATM is already supposed to output the SPV trace, but it yields better results.

The AATM filter operates on a sliding window of data centered on the point of interest. Based on the assumption that, on average, the eyes spend more time in slow-phase than in fast-phase, the SPV at the center of the window is approximated as the value of the dominant mode of the eye-velocity frequency distribution The AATM filter

is a computationally efficient way to estimate the true dominant mode. The filter presents three main characteristics that are described in the paragraphs to follow.

The AATM filter is based on a trimmed-mean filter that operates on a sliding window of data samples. The samples of the window are sorted by amplitude, and a fraction of the samples are "trimmed" away from each end. The output of the filter is the average of the remaining data samples. This trimmed-mean filter is made asymmetric by trimming an unequal number of data samples from the two ends. Finally the filter becomes adaptative as the shift index defining the asymmetric trimming is made a function of the data sample in the window. The block diagram of the filter is presented on Figure 4.4.

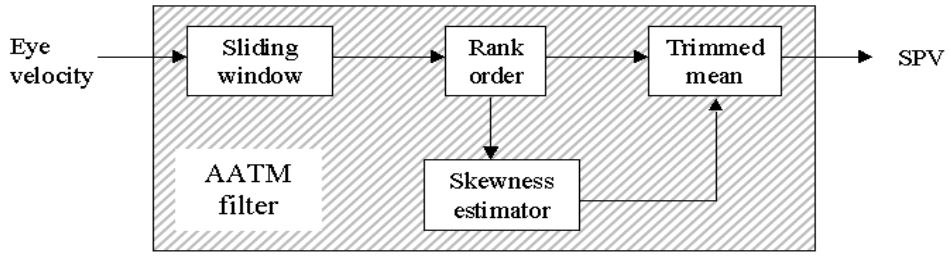

Figure 4.4. Block diagram of the AATM filter. From the rank-ordered distribution of the velocity sample from a sliding window the filter calculates a skewness estimator. The customized-skewness is then used to select a number of samples whose average constitute the output of the filter.

The AATM filter is defined on a window of length L by the expression:

$$AATM_{\alpha,K} = \frac{1}{L - 2\lfloor L\alpha \rfloor} \sum_{j=\lfloor L\alpha \rfloor + 1 + K}^{L - \lfloor L\alpha \rfloor + K} x_j$$

where α is the trimming fraction, K is the shift index that makes the filter asymmetric, and $\lfloor\ \rfloor$ means "integer part of". The shift index, K, is a function of the window samples and is defined by:

$$K = \lfloor MS_\beta \rfloor$$

where M is the maximum shift index permitted, and S_β is the skewness estimator. The skewness estimator is defined by a parameter β chosen to balance noise immunity against sensitivity, and is given by:

$$S_\beta = \frac{MAX_\beta + MIN_\beta - 2\,MED}{MAX_\beta - MIN_\beta}$$

$$MAX_\beta = x_{L-[L\beta]},\ \text{the trimmed maximum}$$
$$MIN_\beta = x_{[L\beta]},\ \text{the trimmed minimum}$$
$$MED = x_{[L/2]+1},\ \text{the median}$$

In the eye-movements analysis package, the AATM filter operates on a 1-second sliding window (L = 60) and is defined by the parameters $\alpha = 0.44$, $M = 24$ and $\beta = 0.12$.

The output of the AATM filter is already an approximation of the SPV trace, but it was found that, for noisy data, the quality of the SPV could be improved with further processing. Functionally, the SPV is the envelope of the velocity trace as shown on Figure 4.6. Indeed, the compensatory eye movements are triggered by a velocity signal and they consist essentially of the slow-phase. The purpose of the saccades is simply to reposition the eyes.

The SPV-extraction algorithm uses the AATM filter output as a first approximation of the SPV. Since the SPV is the envelope of the velocity trace, this approximation of the SPV is used to detect the velocity samples that are part of the fast-phase. Finally the true SPV signal is obtain by lifting the fast-phase samples from the eye-velocity signal, and interpolating the signal that remains through the gaps. The complete process for extracting the SPV is summarized on Figure 4.5.

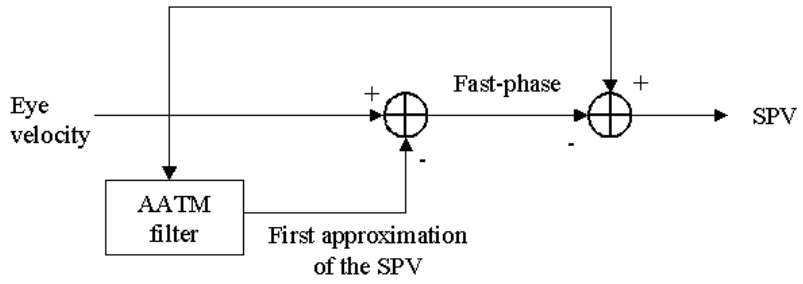

Figure 4.5. Diagram of the process that extracts the SPV from the eye-velocity. The AATM filter is used to recognize the fast-phase using a first approximation of the SPV. The real SPV is then obtained by interpolation of the fast-phase-free velocity trace.

In the eye-movements analysis package, the samples of the velocity trace that are too far from the SPV approximation outputted by the AATM filter are considered as part of the fast-phase. The threshold to separate the phases is defined by the root mean square (RMS) of the difference between the velocity and the SPV-approximation traces. In the algorithm, the velocity samples that are more than ½ RMS away from the SPV approximation are considered as being part of the fast-phase[8]. The results obtained by the SPV-extraction algorithm are shown on Figure 4.6.

[8] Actually, the threshold to separate the fast-phase from the slow-phase is ½ RMS except if this value is greater than 30°/s, in which case 30°/s is used instead.

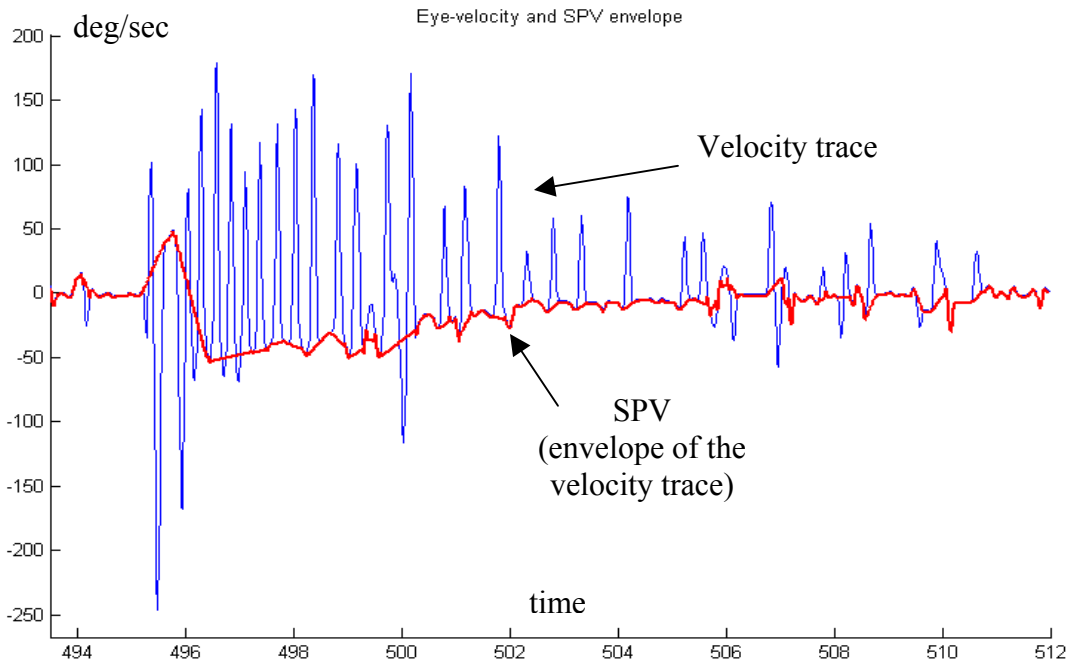

Figure 4.6. Results yielded by the SPV-extraction algorithm. The thin line is the eye-velocity trace; the thick line is the SPV component, which corresponds to the envelope.

Although this method of extracting the SPV is robust and, as claimed in [76], outperforms the more complex pattern-recognition algorithms, there are some limitations, discussed in Section 4.1.9.

4.1.8 Step 4 - Analyze SPV

This final step of the eye-movements analysis procedure requires a SPV signal of high quality and consequently relies greatly on the results of the previous steps in the analysis. The goal of the SPV-analysis is to fit a single exponential mode on the decay in the SPV that follows each head-turn.

4.1.8.1 Objective of the SPV-analysis

During the VOR, the behavior of the SPV is characterized by two primary parameters: the initial amplitude (A) of the SPV and the time constant (τ) of the VOR. A single exponential mode, $A\,e^{-t/\tau}$, can therefore be fit to the data. Although a higher order model could be used to fit the SPV (Section 2.3.1) [48], the single exponential mode used is more robust and is found, by experiment, to fit the data with a good accuracy.

4.1.8.2 Automatic analysis

The SPV analysis procedure consists of two steps. First the eye-movements corresponding to every head-turn are isolated from one another. Then an exponential curve is fit to the SPV decay, separately for each head-turn. Both steps are equally important and are equally challenging to automate.

The first objective of the automatic SPV-analysis routine is to detect when each head-turn occurs in order to determine when the compensatory eye-movements start. This step is necessary in order to split the SPV trace into chunks that corresponds to the SPV decay that follows a head-turn. There are three ways to perform this operation depending on the data available.

4.1.8.3 Detect head-turns based on head-velocity

The obvious way to determine when the head-turns occurred is to map the eye-movement trace to the head-position trace. The process requires a recording of head-position that is synchronized with the recording of the eye-movements. Note that head-velocity is used instead of head-position because it is more robust. Indeed, most experiments use a constant head-velocity for all head-turns but sometimes use different head-angles. The head-velocity trace is obtained by differentiating the filtered head-position. The head-velocity signal is intentionally made smooth and contains only the

samples that were above a given noise-level, as shown on Figure 4.7. The head-velocity signal is then processed to detect the head-turns. The operator can adjust the parameters N, A and T defined later to optimize the head-turn recognition process. The spikes in the head-velocity trace that have more than N samples above a threshold A (or below threshold "-A") are considered potential head-turns. If the time elapsed between two head-turns so detected is shorter than T the second head-turn is discarded. The first samples and the sign of the remaining spikes are recorded as the starting time and direction of the head-turns. For each head-turn, the beginning of the compensatory eye-movements is the time associated to the largest value of the SPV in the 12 seconds that follow the starting time of the head-turn. The direction of the SPV must be opposed to the direction of the head-velocity spike: Depending on the sign of the head-velocity spikes, the SPV largest value is either the maximum value of the SPV, or the minimum. The result of this procedure is shown on Figure 4.7.

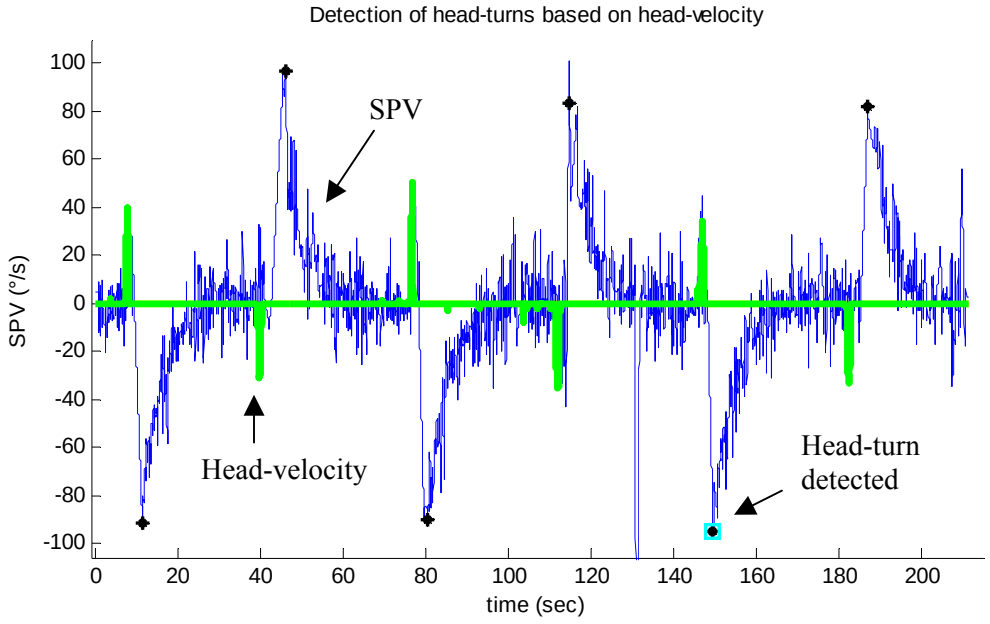

Figure 4.7. Detection of head-turns based on head-velocity. The thick line corresponds to the head-velocity signal (not normalized on this graph), the thin line is the SPV trace, and the six black stars are the head-turns as detected by the procedure.

The head-velocity is the most reliable way of detecting the head-turns, but differentiating the head-position (raw data) in head-velocity may be difficult for noisy signals.

4.1.8.4 Detect head-turns based on the duration button

The second way to find the beginning of the compensatory eye-movements for each head-turn is to use the data from the illusory-motion duration button[9]. The duration-button signal is a square-wave whose lower baseline corresponds to the "button not activated" state and upper baseline (square parts) to the "button activated" state. The times when the subject felt a motion, which are correlated to the compensatory eye-movements, are easy to detect from the duration-button trace. As shown on Figure 4.8, the distribution of the duration-button samples is clearly bimodal. The mean of the two modes is used as a threshold to separate the times when the subject felt a motion (button pressed) from the times when he felt stable. For each head-turn, it is assumed that the beginning of the compensatory eye-movements occurs during the time the button was pressed. With only the duration-button signal, however, there would be no way to predict the direction of the SPV. There are two options for resolving this ambiguity. Assuming the subject did not forget to press the button for some of the head-turns, the direction of the SPV must alternate as the direction of the head-turns alternates between "to-NUP" and "to-RED". The beginning of the eye-movements for each head-turn is then alternatively the time corresponding to the minimum or the maximum value of the SPV during the interval the button was pressed. The second option uses the assumption that the SPV trace itself contains the information on the direction of the VOR. For each interval for which the button was pressed, the beginning of the eye-movements is simply the time corresponding to the largest SPV in magnitude. The result of this second procedure is shown on Figure 4.8.

[9] The duration button is pressed by the subject during each head-turn. The subject is instructed to press the button when he starts moving his head and to hold it as long as he feels a motion sensation.

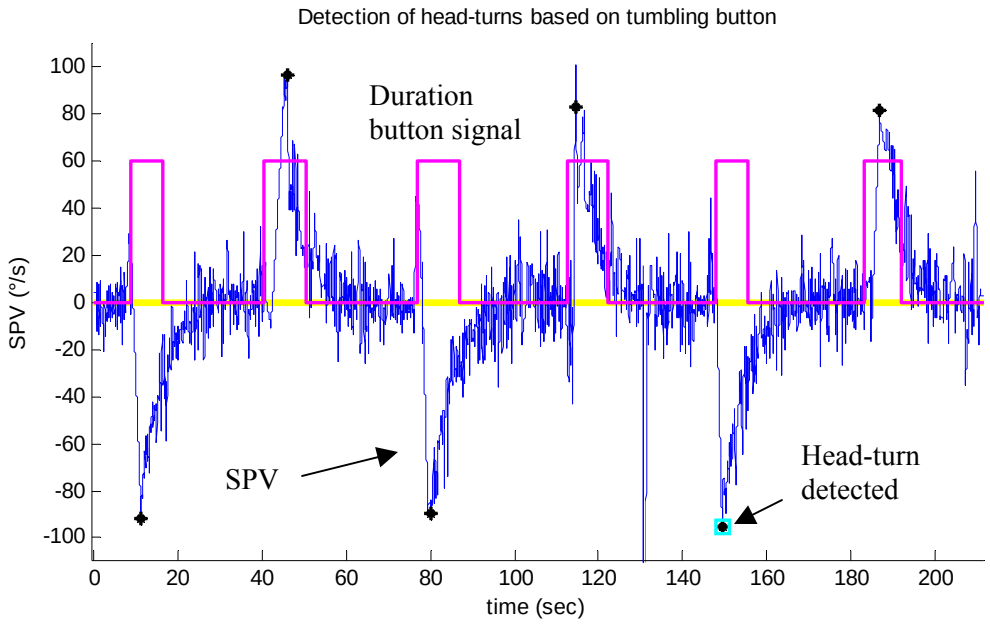

Figure 4.8. Detection of head-turns based on duration button. The square line corresponds to the duration button signal, the thin line is the SPV trace, and the six black stars are the head-turns as detected by the procedure.

Using the duration-button signal is the default way of detecting the head-turns in the eye-movements analysis package. Although it relies on the subject to press the button as instructed, using the duration-button signal enables to map robustly the eye-movement data with the illusory motion duration data.

4.1.8.5 Detect head-turns based only on the SPV

Finally head-turns can be detected directly from the SPV trace without any other information. Indeed, without vestibular stimulation – no head-turn – there are no compensatory eye-movements and the SPV is null. Just after a head-turn the SPV is the fastest and it decays with time until it vanishes. These properties of the SPV trace can be used on a filtered approximation of the SPV to detect when the eye-movements start after a head-turn. Again, the operator can adjust the parameters F, N, A, and T defined later to optimize the procedure (N, A, and T are the same as defined for the head-velocity analysis). The SPV signal is filtered at the frequency F, and the spikes in the filtered SPV

that have more than N samples above a threshold A (or below threshold "-A") are flagged as potential head-turns. If the time elapsed between two head-turns so detected is shorter than T the second head-turn is discarded. Figure 4.9 shows the process to detect head-turns using the filtered SPV signal (low-pass digital filter with a cutoff frequency of 0.3Hz). Finally the results on the filtered SPV are tweaked a little to find the true beginning of the eye-movements corresponding to each head-turn

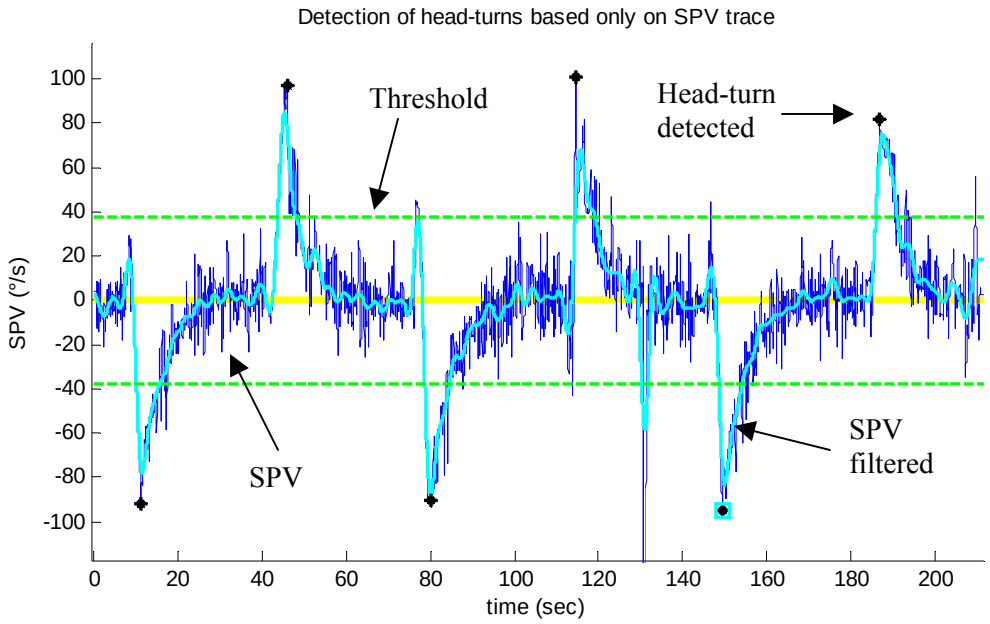

Figure 4.9. Detection of head-turns based only on the SPV trace. The dark line is the SPV trace, the light line corresponds to the SPV trace filtered at 0.3Hz, the dashed line is the threshold (A) for head-turn detection, and the six black stars are the head-turns as detected by the procedure.

This last way of detecting head-turns is only used if no other data is available. Although it yields good results for the SPV analysis, it misses information on illusory-motion duration and head velocity.

4.1.8.6 Automatic fit of the SPV decays

At this point, the beginning of the eye-movements for each head-turn has been detected by one of the methods described above. The last step is to fit a single

exponential mode separately on the SPV-decay that follows each head-turn. The algorithm assumes that compensatory eye-movements last about 20s after a head turn and fits the model on the 20-second chunks of SPV that follow the peak-SPV. The procedure to obtain the best exponential fit is iterative. The model is first fit to the initial 20-second SPV signal. At each iteration, the SPV samples that are too far from the previous best fit are discarded and the resulting signal is fit again. Discarding the outliers refines the fit and makes it more robust against noise. The process iterates until every SPV sample used for the fit is within an acceptable range of the best-fit curve. In the algorithm, the threshold used to determine if a sample should be discarded for the next fitting iteration is based on the standard deviation of the SPV of the current iteration. The threshold is time-dependent: The samples close to the start of the eye-movements are allowed more variation – six standard deviations – than those towards the end – only three standard deviation. The user can modify the threshold through the graphical user interface to make the process more efficient. As shown on Figure 4.10, this automatic procedure leads to high quality fits for most head-turns, and still gives decent results for the others (such as the fourth fit on the figure).

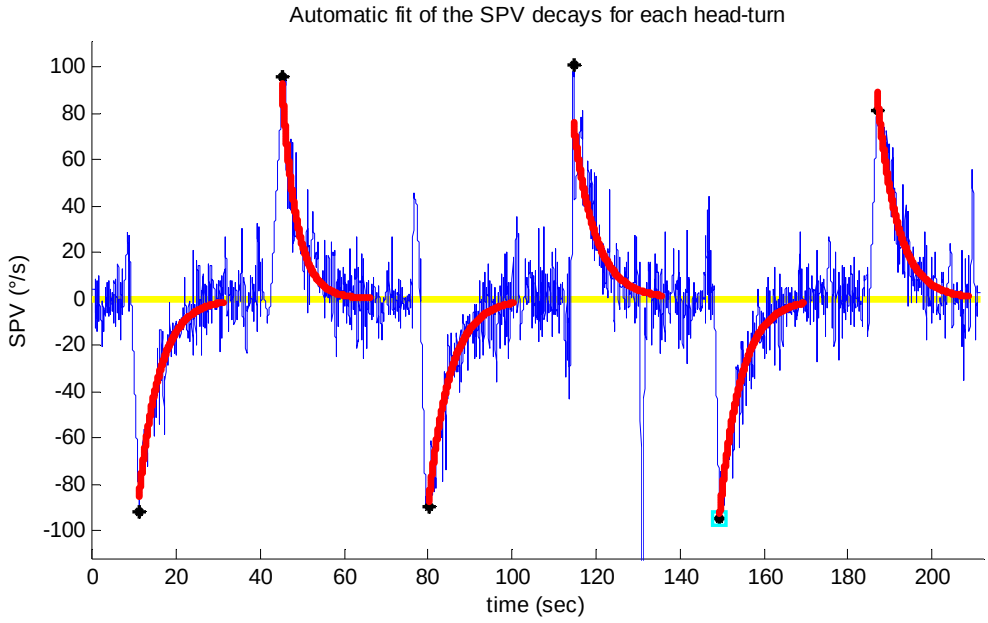

Figure 4.10. Automatic fits of the SPV decays for six head-turns. The fits corresponding to the fourth and last head-turns are close to the optimal fit but seem to be slightly off. All the other fits are perfect and do not need any manual modifications.

This step is the last in the automatic-analysis procedure. In the eye-movements analysis package, the operator can modify manually the results of the automatic routine. He can intervene at two stages of the analysis procedure: before the fitting operation or after. Before the fitting process, the operator can change the results of the head-turn detection procedure. He can add, remove, or move head turns to correct for malfunctions or inaccuracies. Similarly, after the automatic fitting process, the operator can check if the fits are correct and he can easily modify those that are not perfect. More details about the manual fitting operation can be found elsewhere [58, 62].

The results of the whole eye-movements analysis process – including filtering, differentiating, SPV-extraction, fitting and manual checking – are shown on Figure 4.11.

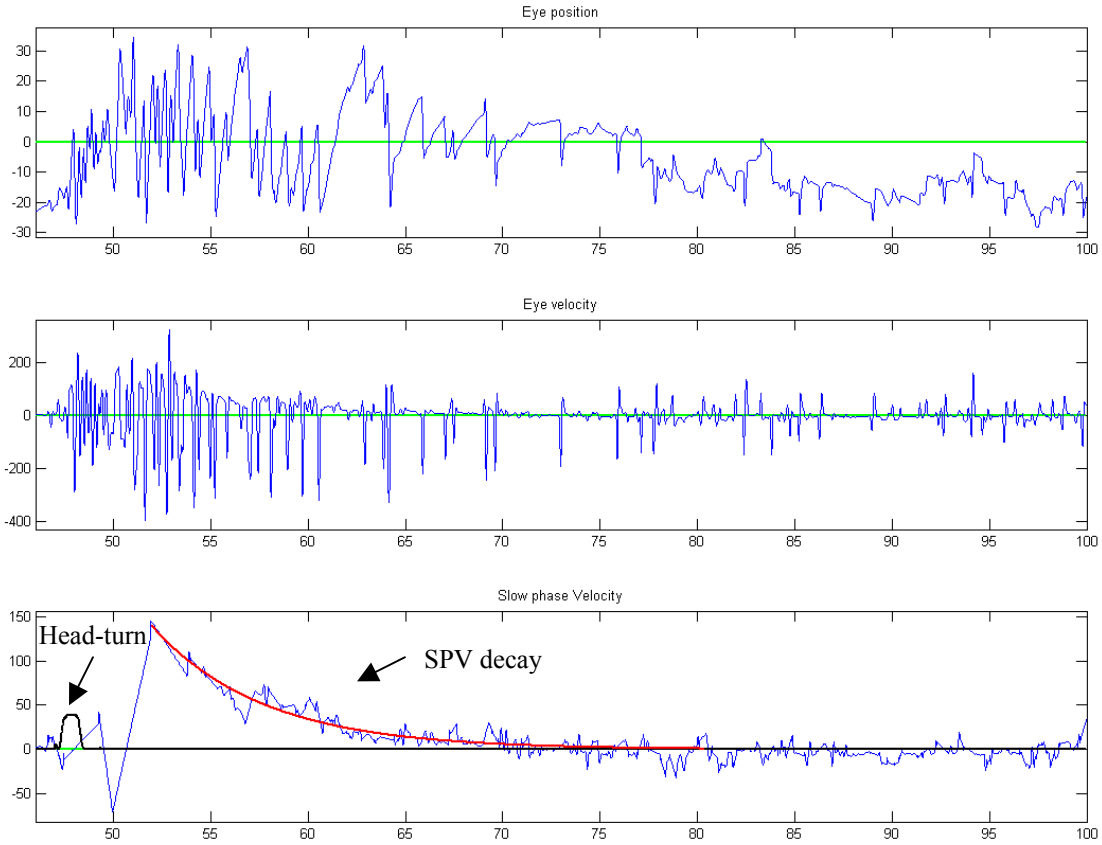

Figure 4.11. Results yielded by the eye-analysis package (deg or deg/sec with respect to time in sec). The top plot corresponds to the eye position after blink removal and filtering. The middle plot is the velocity trace obtained using the FIR differentiating filter (Section 4.1.6). The bottom plot represents the SPV – as calculated by the algorithm – with its best exponential fit. The head velocity of the head-turn (not normalized) is shown with the SPV plot.

4.1.9 Recommendations for improvement

The analysis of the VOR is a real challenge that depends not only on the hardware but also on the analysis methods. The eye-analysis package used in the Man-Vehicle Laboratory yields relatively good results, but could still be improved. This section summarizes the limitations of the package.

4.1.9.1 Miscellaneous

First, as pointed out in Section 4.1.2, the ISCAN® calibration process may introduce errors and calibration should, therefore, be checked manually for each data set. A systematic recalibration of the raw data could, thereby, lead to better results. The blink-removal, position-filtering and differentiation procedures are already efficient.

The SPV-fitting process does not present any substantial obstacle to achieving good eye-data quality. The automatic routine that analyzes all the head-turns at once yields good results when the SPV is only modestly erratic at the beginning of the head-turn. Failure of the automatic routine does not, however, impede the analysis since the operator ultimately validates each exponential fit separately.

4.1.9.2 SPV extraction

The more challenging part of the package is the classification of the eye-velocity samples as slow-phase vs. fast-phase. This classification is conducted through the AATM filter. As opposed to the other procedures of the package, the dissection of the velocity sample into physiologic components requires more than signal processing knowledge. It is built on the physiological assumptions that the eye spends more time in slow-phase than in fast-phase. This assumption is not always fulfilled experimentally, especially at the beginning of the VOR when the slow-phase is the quickest. As shown on Figure 4.12, when this requirement is not met the estimate of the slow-phase velocity is poor. There

are two known situations in which the algorithm yields mitigate results: If the stimulation is too strong or if the sample frequency is too low.

The intensity of the CCS (velocity stimulus) commands the slow-phase velocity of the eyes. If the stimulation is strong enough, the SPV can be almost as fast as the fast-phase (before any damping occurs). The eye will then spend equal times in each phase and the algorithm will not be able to distinguish between slow- and fast-phases. For experiments with a centrifuge-velocity below 30-rpm this should not be a real concern because slow-phase velocities are at most as fast as the centrifuge-velocity (180 deg/sec) whereas fast-phase velocities are typically 500 deg/sec.

The 60-Hz sample frequency of the ISCAN® eye-tracking system is a more pressing problem. Indeed, the fast-phase can be as short as 20 ms: Figure 4.12 shows an average fast-phase amplitude of 15 deg/sec, which leads to duration of 30 ms per fast-phase beat. Fast-phase beats are, therefore, represented by about 2 data samples, which obviously leads to degradation of the nearby slow-phase. It also routinely leads to under-estimation of the fast-phase velocity, which increases the concern that the algorithm will not be able to distinguish between slow- and fast-phase.

Figure 4.12 illustrate a failure of the algorithm to accurately estimate the SPV for an 80-degree head-turn while spinning at 30 rpm. Although the head-turn occurs at the beginning of the recording (thick bumpy line in the SPV window), the SPV is correctly estimated only 6 seconds later.

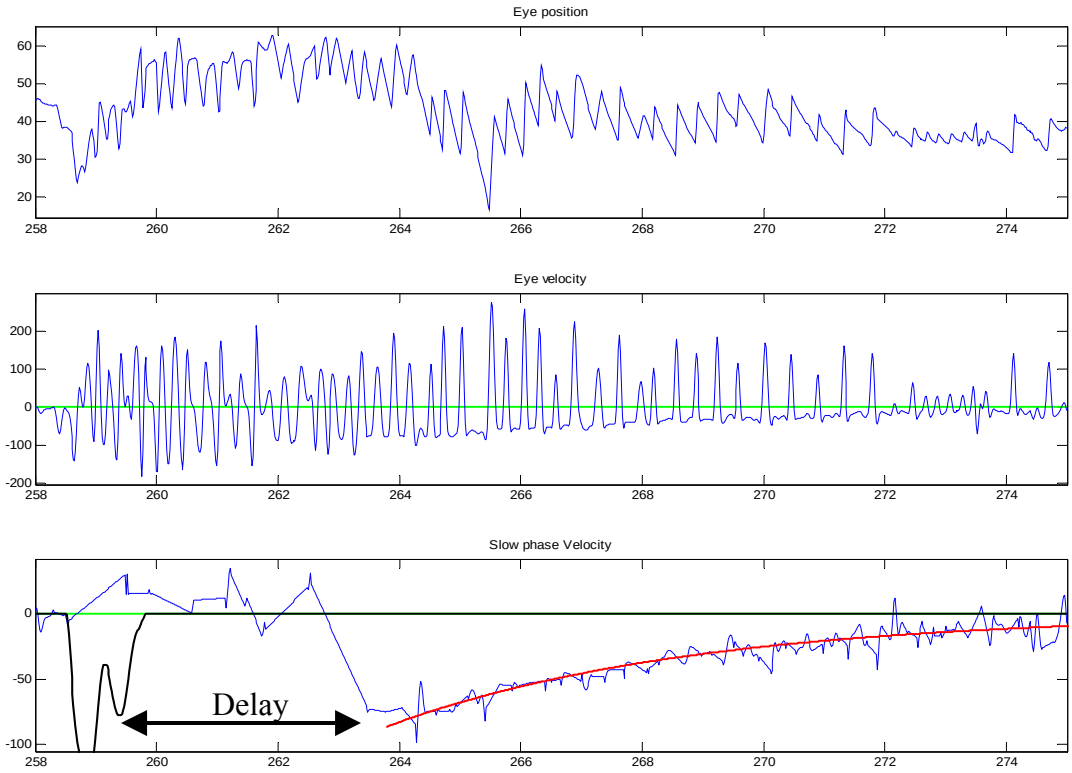

Figure 4.12. Typical result showing the limitation of the eye-analysis package. Top plot: eye position (deg), middle plot: eye velocity (deg/sec), and bottom plot: SPV (deg/sec vs. time in sec). The algorithm is able to classify the phases of the velocity trace only if the eye spends more time in the slow-phase than in the fast-phase. This graph shows that this assumption is not always satisfied. As long as the assumption is not met, the algorithm is not able to pick up the slow-phase. The recognition of the SPV is delayed and the estimation of the SPV-peak amplitude is void.

Since the model used to fit the data is a single exponential mode, the problem mentioned above should not interfere with the estimate of the time-constant of the SPV. Indeed, if the SPV-extraction algorithm is not able to recognize the SPV signal within a few seconds, the exponential fit will have different amplitude but same time-constant as the fit on the ideal SPV signal. This property is easy to demonstrate. Let t_1 be the delay between the real start of the compensatory eye-movements (ideal SPV signal) and the time when the algorithm starts recognizing the SPV. The best exponential fit to the ideal SPV signal is $A e^{-t'/\tau}$, and the best fit to the actual SPV signal $B e^{-t/\tau_1}$. The time t and t' are connected by the delay t_1 such that $t'=(t+t_1)$. Then the two exponential fit must agree

for the SPV value at time $t'=0=t+t_1$, which relates the two amplitudes A and B, and finally leads to equality of the two time-constants τ and τ_1.

$$A\,e^{-(t+t_1)/\tau} = B\,e^{-t/\tau_1}$$
$$\Leftrightarrow \begin{cases} A = B\,e^{t_1/\tau_1} \\ \tau = \tau_1 \end{cases}$$

In conclusion, the limitations of the SPV-extraction algorithm affect primarily the amplitude of the exponential fit and might not affect the estimate of the time-constant of the VOR.

4.2 Data normalization

Subjective assessments of motion sickness, illusory motion intensity, illusory motion duration and body-tilt are recorded during the experiment and compiled into a single spreadsheet. The physiological data (amplitude and time-constant characterizing of the VOR decay) are then added to the spreadsheet. The vestibular response depends on the centrifuge-velocity and the head-angle (Chapter 2). For each head-turn, therefore, the measurements may be normalized during the analysis to the centrifuge-velocity, to the head-angle (actually the sine of the head-angle as demonstrated in Section 2.2.2), or to the CCS intensity (Section 2.2.2). In this study, the eye-movement data were normalized to the CCS intensity to obtain the normalized SPV or NSPV (Section 5.3.3).

4.3 Statistical analysis

Data were analyzed using with the SYSTAT® 11 software package. Unless stated otherwise, all variables were analyzed using either the General Linear Model (GLM) univariate repeated measures ANOVA or the mixed regression model with hierarchical

subject factor. The significance level $p<0.05$ was used. Correlation coefficients were obtained using Microsoft® Excel®.

5 Results

5.1 Overview

Significant adaptation to head-turns performed during centrifugation is achieved, as indicated by both the physiological measurements and the subjective ratings. As expected, the vestibular response is highly correlated to the CCS intensity. In particular, the sensation of illusory motion is almost proportional to the CCS intensity. The relation between the SPV-peak amplitude and the CCS intensity is less clear-cut and seems to follow a logarithmic pattern. The time-constant of the VOR depends mainly on the head-angle. The body-tilt depends on the centrifuge-velocity but not on the head-angle. Finally, the increment of the motion sickness level after a head-turn appears to be related to the CCS intensity of the head-turn.

The goal of this study was to find quantitative relations between the CCS intensity and the vestibular response, and, accordingly several regression tests were conducted. The effects of day (Day), replication (Replication or Rep), head-turn direction[10] (Direction or Dir), gender (Gender), motion sickness susceptibility[11] (MSgroup), head-angle (Angle), and centrifuge-velocity (Velocity) were also analyzed. In this chapter, those variables will be referred to using the single word in parentheses. The effects of head-velocity and of the order in which the different kinds of head-turn appeared were also tested preliminarily.

As described in Section 2.6.1.2, two phenomena, adaptation and habituation, change the value of the neurovestibular response with time. Our primary interest in this study is in adaptation: Day is the variable that corresponds to adaptation, whereas Replication corresponds to habituation.

[10] The head-turns investigated in this study are turns between the right-ear-down (RED) and the nose-up (NUP) positions. The two turns directions are, therefore, from NUP to RED and from NUP to RED.
[11] Susceptibility to motion sickness seems to affect eye-movements and subjective assessments, and the subjects were, therefore, separated into two groups based on their average motion sickness score during the experiment. The difference between the two groups was then statistically evaluated.

5.2 Preliminary analysis

5.2.1 Head velocity

According to the expression describing the stimulus (CCS) created by head-turns performed during centrifugation, the head-velocity does not affect the vestibular response (Section 2.2.2). Nonetheless, the subjects were instructed to keep a constant velocity during a head-turn and to perform all head-turns at the same velocity. This precaution was taken to minimize the range of head-velocities used because, although head-velocity is not supposed to affect the vestibular response in general, very low or very high velocities might. Despite the instructions, the subjects used a non-negligible range of head-velocities during the experiment, as shown on Figure 5.1. That range was large enough to study the effect of head-velocity on vestibular response. We investigated the effect of the maximum velocity reached during a head-turn instead of the averaged head-velocity. This velocity-peak value was chosen as metric because potential irregularities in the head-turns' velocity profiles make it sometimes difficult to define a meaningful average velocity. Overall, in this experiment, the peak head-velocity is 86.9±24.3°/s, and it is 96.6±22.8°/s for the head-turns of the pre- and post-adaptation phases only.

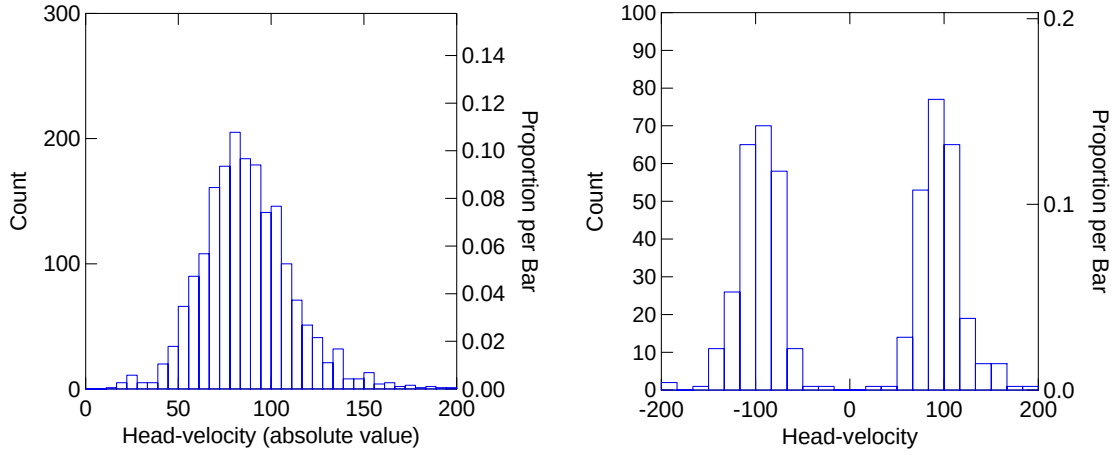

Figure 5.1. Histogram of measured peak head-velocity. (a) All head-turns performed during the experiment. (b) Only head-turns to 80 degrees at 23 rpm (pre- and post-adaptation phases).

For the pre-adaptation and post-adaptation phases, correlations between each measurement and peak head-velocity were tested. We studied the head-turns to 80 degrees at 23 rpm because they are repeated more times than the other kinds of head-turn. There is no significant correlation between the head-velocity and any of the measurements, as shown on Figure 5.2.

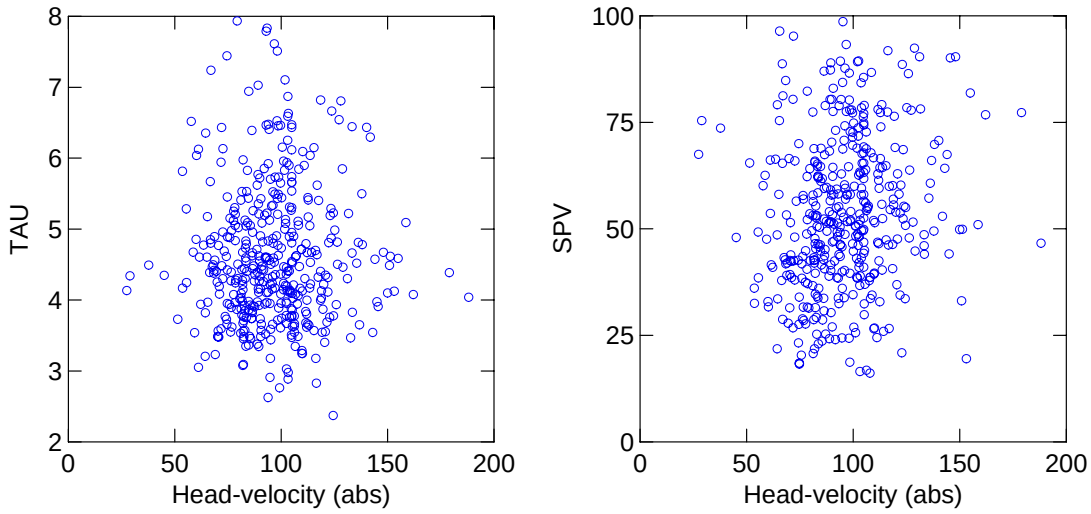

Figure 5.2. Correlation between head-velocity and physiological measurements. (a) VOR time-constant vs. head-velocity. (b) SPV-peak amplitude vs. head-velocity.

As expected, the head-velocity does not have an effect on the vestibular response to head-turns performed during centrifugation. This conclusion is, naturally, limited to the range of peak head-velocity tested – 50°/s to 130°/s.

5.2.2 Order effect (group)

For this experiment, the subjects were separated in advance into two groups. The two groups differed only in the ordering of the presentation of the various head-angles during the experiment (Section 3.2). It was hypothesized that the order of head-angle presentation would not have a significant effect on the measurements. The results confirm our hypothesis for all the measures except the SPV-peak amplitude (Table 5.1).

Table 5.1. Statistical significance of the effect of head-turn ordering on each measurement (p-value of paired t-tests).

	Effect of order (p-value)
VOR time-constant	0.551
SPV-peak amplitude	0.015
Illusory motion intensity	0.816
Illusory motion duration	0.830
Body-tilt sensation	0.062
Motion sickness	0.575

5.3 Physiological data

The eye-movement analysis is based on the eye movements of the 16 subjects for whom a complete data set was available. For these 16 subjects, there are no missing values for the stimulus phase. On the other hand, there are some values missing from the pre-adaptation and the post-adaptation phases.

5.3.1 VOR time-constant (τ)

The VOR time-constant statistics are based on a sample of 1152 VOR (16 subjects * 36 head-turns * 2 days) corresponding to head-turns performed during the stimulus phase. The distribution of τ for this sample is approximately normal, as shown on Figure 5.3, which justifies the use of the GLM ANOVA model. The mean VOR time-constant (4.168 ± 0.812 seconds) is substantially shorter than that found in past experiments: Adenot found a mean VOR time-constant of 4.9 seconds for an experiment using a similar protocol [35], and other studies found a mean value of 4.7 and 5.3 seconds [58, 63]. This difference in τ might be due to the revision of the eye-movements analysis software that was done between these previous studies and ours.

If all the head-turns for which an exponential fit was found (1792 head-turns) are included in the statistics, the mean is 4.263 ± 0.885 seconds, which is consistent with the results of the stimulation phase alone and approaches the cupular time-constant.

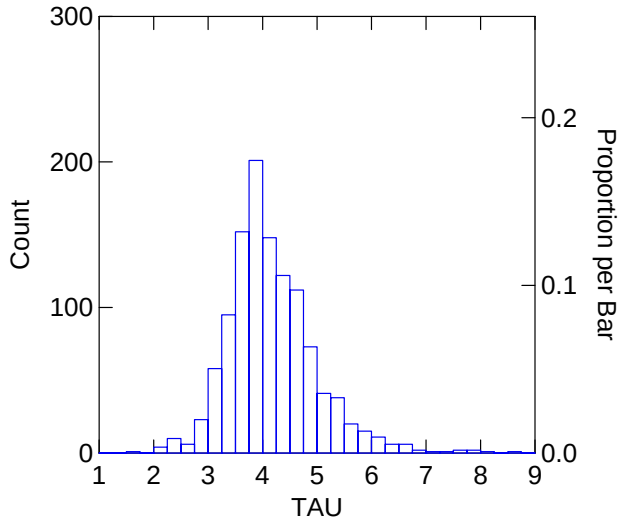

Figure 5.3. Histogram of τ values for the vertical VOR of the 16 subjects retained for statitical analysis of the eye-movements. The histogram shows the 1152 head-turns of the stimulus phase (mean = 4.168 ± 0.812).

We performed a GLM repeated-measures ANOVA on the VOR time-constant against the categories Direction and Angle, and the variables Day, Velocity and Replication. We also tested the effect of Gender and Msgroup (between-subject variables). As indicated in Table 5.2, there are significant effects of Day ($p = 0.006$), Replication ($p < 0.001$) and Angle ($p = 0.001$) on the VOR time-constant. Four cross effects are also significant.

Table 5.2. Significant main and cross effects on VOR time-constant. Results of a GLM ANOVA with a significance level of $p < 0.05$. Only the significant cross effects are shown.

	F-value	df	p-value
Gender	0.172	1, 13	0.685
MSgroup	0.592	1, 13	0.455
Direction	1.039	1, 13	0.327
Day	10.981	1, 13	0.006
Centrifuge-velocity	0.030	2, 26	0.951
Head-angle	8.839	2, 26	0.001
Replication	21.848	1, 13	< 0.001
Day*Rep	10.676	1, 13	0.006
Angle*Rep	6.927	2, 26	0.004
Day*Rep*Dir	12.395	1, 13	0.004
Angle*Velocity	2.603	4, 52	0.048

The VOR time-constant decreases significantly over Days and Replications, as expected from the results of past studies. The decrease of the time-constant over Replications, however, is less marked on the second day of the experiment (cross effect Day*Rep), as shown on Figure 5.4-a: Whereas much habituation occurs on the first day, there is almost no habituation on the second day. The two head-turn Directions do not follow the same adaptation pattern (cross effect Day*Rep*Dir): The τ values for head-turns from NUP to RED decreases significantly quicker than in the opposite direction (Figure 5.4-b).

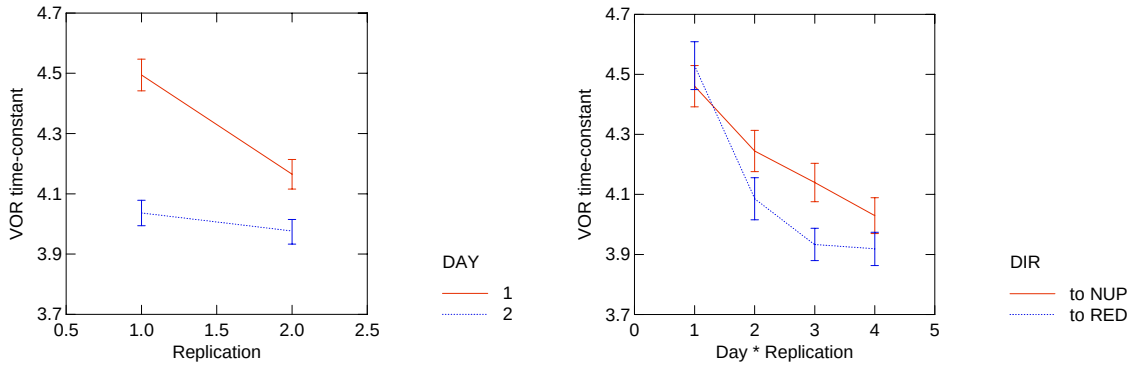

Figure 5.4. Adaptation and habituation of the VOR time-constant. (a) Decrease of τ over Replications and Days (cross effect Day*Rep clearly visible). (b) Difference in the adaptation pattern between the two head-turn directions (cross effect Day*Rep*Dir) – in this second graph (only), 1 and 2 represent replications during Day1whereas 3 and 4 are replications during Day2.

Head-angle has a significant effect on the time-constant: the bigger the head-angle, the longer the time-constant, as shown on Figure 5.5-a. This effect was suggested by the results found by Adenot [35], but it was not significant in this previous experiment, perhaps because of the smaller number of subjects in that study. Head-angle also has a stronger effect on the time constant for the later replication, as illustrated on Figure 5.5-b (cross effect Angle*Rep).

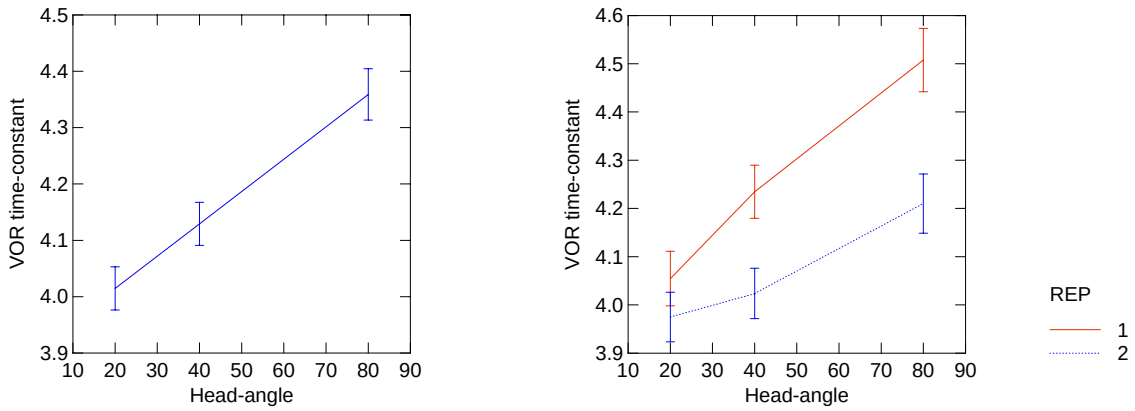

Figure 5.5. Effect of Head-angle on the VOR time-constant: the bigger the Angle, the longer the time constant. (a) Main effect of head-angle. (b) Cross effect Angle*Rep: the head-angle has less effect on the second replication than on the first one.

Finally, the effect of head-angle on the VOR time-constant depends significantly on the centrifuge-velocity (cross effect Angle*Velocity), as shown on Figure 5.6: the higher the centrifuge-velocity, the weaker the effect of head-angle on the VOR time-constant. The graph suggests that for head-angles greater than 60 degrees, the time-constant will be longer for slower rotation rates and that, conversely, for head-angles below 60 degrees, the time-constant will decrease with the centrifuge-velocity. It also predicts that for a head-angle of 60 degrees, the centrifuge-velocity will have no influence on the VOR time-constant. This finding, however, is only marginally significant. Figure 5.6 shows clearly that the standard errors on the data points are large compared to the gap between the points themselves. Nonetheless, this interaction between the effects of head-angle and centrifuge-velocity on the VOR time-constant raises several questions that should be addressed by future experiments.

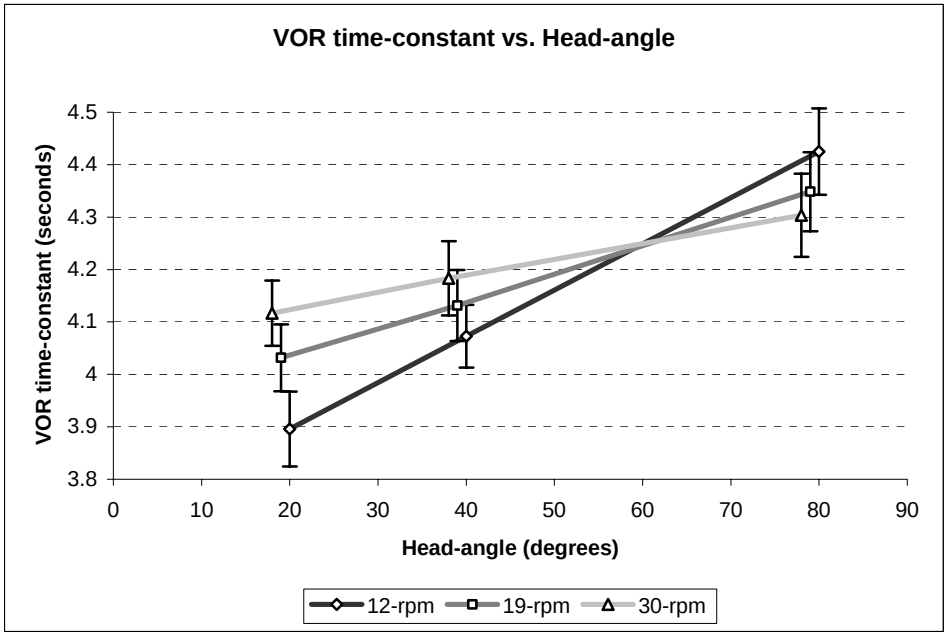

Figure 5.6. The higher the centrifugation speed, the lighter the effect of head-angle on the VOR time-constant (cross effect Angle*Velocity). The three linear fits are significant (p-values smaller than 0.017).

Based on the results (Table 5.2), the VOR time-constant does not depend on the centrifuge-velocity and, therefore, does not depend on the CCS intensity. This result was expected because the VOR time-constant characterizes the internal process commanding the VOR and has no reason to depend on the stimulus. There is no cross effect between Day and either centrifuge-velocity or head-angle. This suggests that there is no significant difference between the adaptation achieved for different head-angles and centrifuge-velocities.

5.3.2 SPV-peak amplitude (*A*)

The SPV-peak amplitude statistics are based on the stimulus phase data from 16 subjects (1152 head-turns). This sample of SPV-peak amplitude is approximately normally distributed, which justifies the use of the GLM ANOVA model. The mean SPV-peak amplitude for the head-turns of the pre-adaptation and post-adaptation phases

(359 head-turns to 80-deg at 30-rpm) is 55.6 ± 20.5 deg/sec. Figure 5.7 shows the SPV trace for the first replication of head-turns on the first day for subject 18.

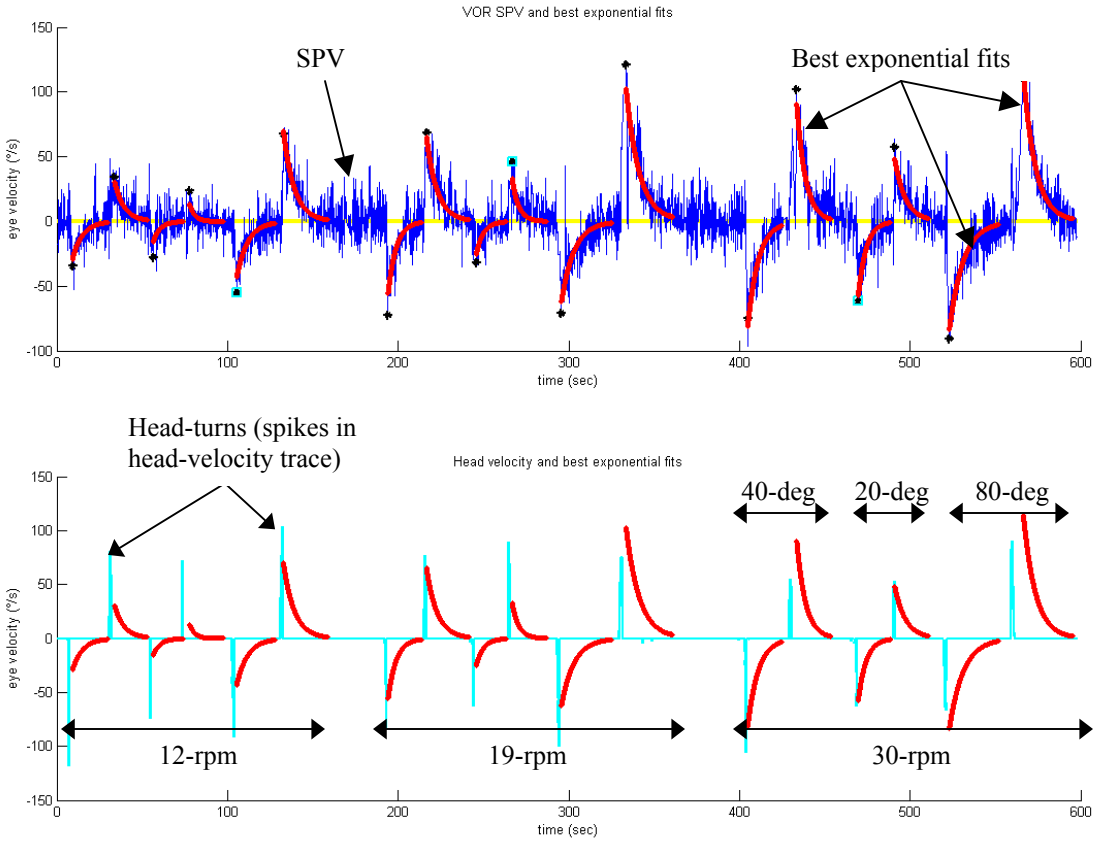

Figure 5.7. Typical SPV trace for a sequence of 18 head-turns. The graphs show the head-velocity trace (each spike corresponding to a head-turn), the SPV trace, and the best exponential fits to the VOR SPV for each head-turn.

We performed a GLM repeated-measures ANOVA on the SPV-peak amplitude against the categories Direction, Angle, Gender and MSgroup, and the variables Day, Velocity and Replication. As illustrated in Table 5.3, there are significant effects of Velocity ($p < 0.001$), Angle ($p < 0.001$) and Replication ($p = 0.004$) on the SPV-peak amplitude. Three cross-effects are also significant.

Table 5.3. Significant main and cross effects on SPV-peak amplitude. Results of a GLM ANOVA with a significance level of $p < 0.05$. Only the significant cross effects are shown.

	F-value	df	p-value
Gender	2.518	1, 13	0.137
MSgroup	1.734	1, 13	0.211
Direction	1.854	1, 13	0.196
Day	0.536	1, 13	0.477
Centrifuge-velocity	106.835	2, 26	< 0.001
Head-angle	77.266	2, 26	< 0.001
Replication	12.178	1, 13	0.004
Velocity*Angle	2.724	4, 52	0.039
Velocity*MSgroup	6.783	2, 26	0.004
Angle*MSgroup	3.871	2, 26	0.034

The SPV-peak amplitude decreases significantly over Replications, but was found not to decrease over Days, as shown on Figure 5.8. The figure indicates that the decrease over Replications might be a little smaller on the second day than on the first, but this cross effect is not significant. This finding suggests that, although the eye-movement response habituates to the vestibular stimulation, there is no adaptation over days.

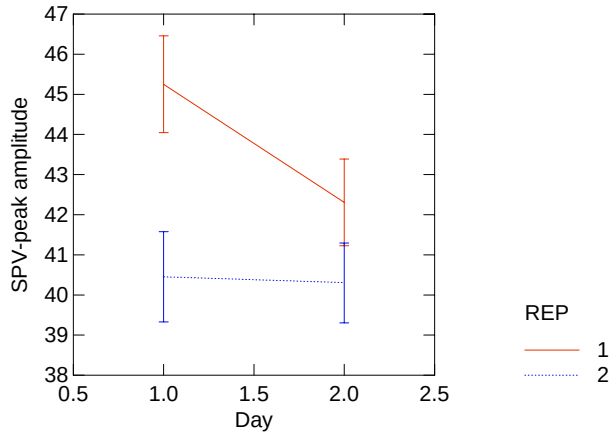

Figure 5.8. Effect of Day on the SPV-peak amplitude by Replication.

As expected, there is a significant effect of centrifuge-velocity and head-angle on SPV-peak amplitude: the stronger the stimulus, the bigger the SPV-peak amplitude. An increase of head-angle – or an increase of centrifuge-velocity – leads to a stronger CCS and, therefore, to faster compensatory eye-movements. According to our results, the

SPV-peak amplitude is proportional to the centrifuge-velocity, as shown on Figure 5.9. By contrast, the effect of the sine of the head-angle, $sin(\psi_{max})$, on the SPV-peak amplitude is not linear (Figure 5.10-b). It seems that being close to the NUP position enhance the effect of head-angle on the SPV-peak amplitude: The SPV-peak amplitude is more sensitive to $sin(\psi_{max})$ for small values of ψ_{max} (i.e. the graph is steeper). Figure 5.9 also shows that the influence of head-angle is more important for small centrifuge-velocities than for large one (cross effect Angle*Velocity).

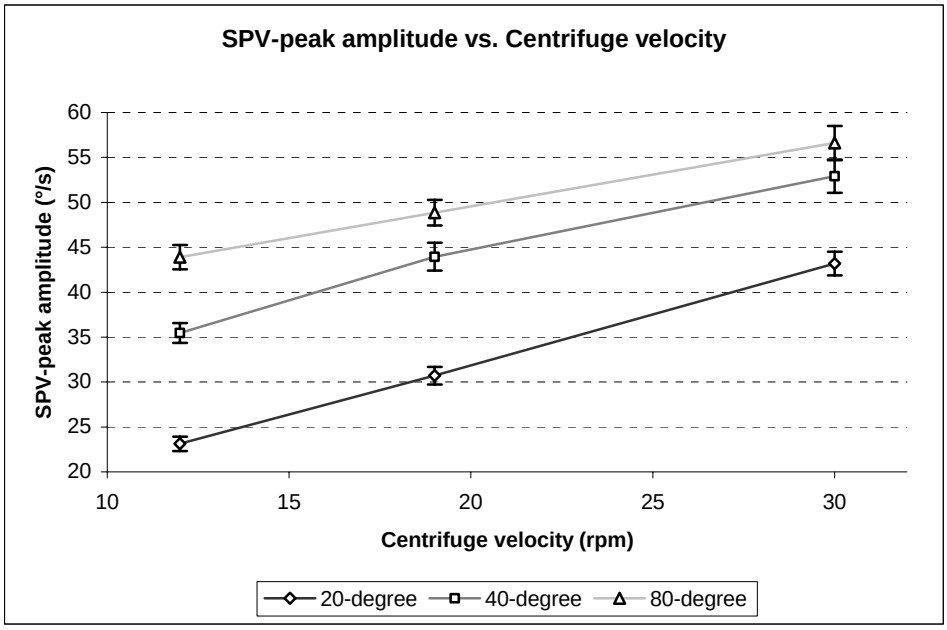

Figure 5.9. Effect of centifuge velocity on SPV-peak amplitude by head-angle.

In the course of the eye-movements analysis, we observed an unexpected time-delay between a head-turn and the beginning of its corresponding compensatory eye-movements. This delay is highly correlated with the CCS intensity ($R^2 = 0.98$), as shown on Figure 5.10-a. Such a phenomenon has dramatic consequences for the quality of the physiological data; in particular, it can blur the estimate of the SPV-peak amplitude: Several seconds after a head-turn is performed, the vestibular signal has already been substantially damped by the dynamics of the SCC and the SPV-peak amplitude measured is smaller than the true amplitude. The fact that the SPV-peak amplitude is not

proportional to the head-angle, as illustrated on Figure 5.10-b, might be a consequence of this time-delay.

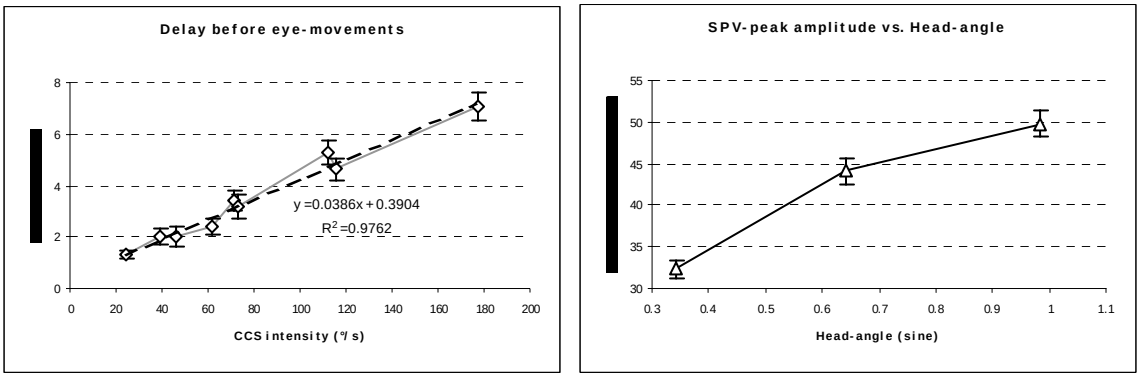

Figure 5.10. Limitations to the SPV-peak analysis. (a) Mean time-delays between the head-turns and the beginning of the compensatory eye-movements with respect to CCS intensity. (b) Effect of head-angle on SPV-peak amplitude.

Finally there are two significant effects involving the motion sickness susceptibility of the subjects (MSgroup). As shown on Figure 5.11, subjects that are more susceptible to motion sickness are also more sensitive to changes in centrifuge-velocity or head-angle (cross effects Velocity*MSgroup and Angle*MSgroup).

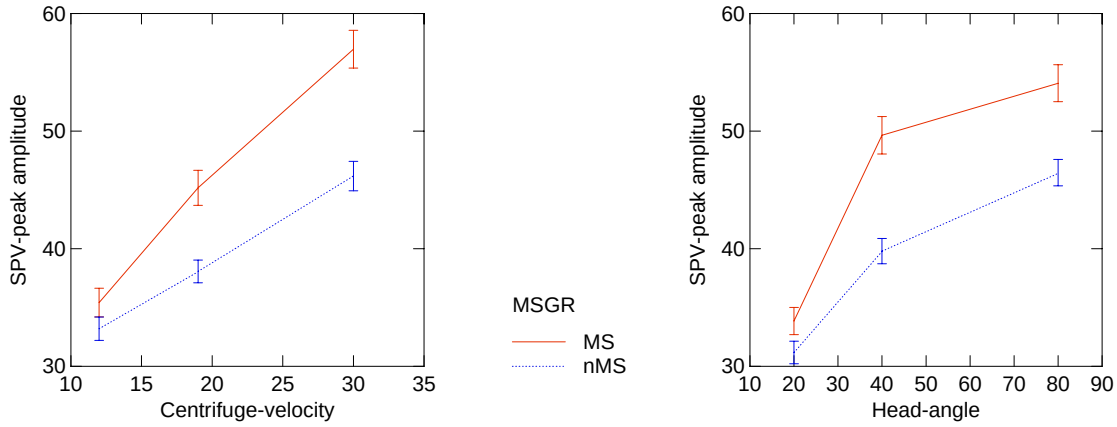

Figure 5.11. Influence of motion sickness susceptibility on the SPV-peak amplitude with respect to: (a) centrifuge velcoity and (b) head-angle.

MSgroup does not have a significant effect on SPV-peak amplitude during the stimulus phase, but for the pre-adaptation and post-adaptation phases, subjects more susceptible to motion sickness have significantly higher SPV-peak amplitude (mixed regression, $p = 0.044$).

5.3.3 NSPV (normalized SPV-peak amplitude)

As noted in Section 2.3, the VOR is well described by a time-constant (τ) and a gain (NSPV). The SPV-peak amplitude theoretically corresponds to the product of the gain of the VOR and the CCS intensity, but the experimental results do not support this prediction (see previous section). The analysis of the SPV-peak amplitude suggests that this prediction is not precisely verified experimentally (Figure 5.12). Indeed, although the SPV-peak amplitude is proportional to the centrifuge-velocity, it is not linearly related to the sine of the head-angle, $sin(\psi_{max})$. The relation between the SPV-peak amplitude and the CCS intensity is, therefore, not perfectly linear, as shown on Figure 5.12.

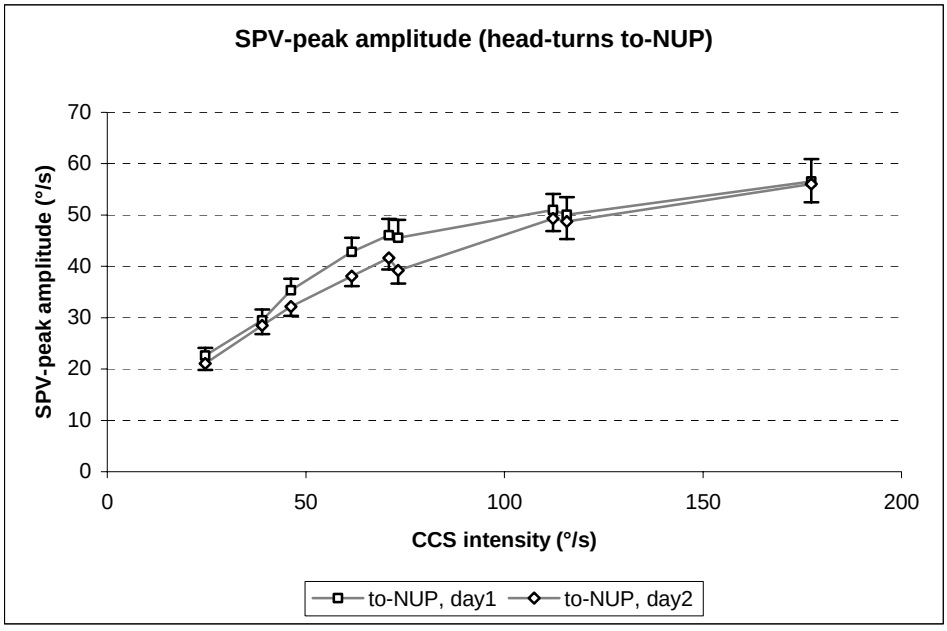

Figure 5.12. SPV-peak amplitude with respect to CCS intensity by Days. Only the results for the head-turns from RED to NUP are plotted but the other direction looks similar.

Despite what is suggested by the results, we investigated the effect of NSPV using its classical definition. The NSPV (gain of the VOR) is obtained by normalizing the SPV-peak amplitude to the vestibular stimulus (CCS intensity) created by a head-turn. The NSPV statistics are based on the stimulus phase data from 16 subjects (1152 head-turns). This sample of NSPV is approximately normally distributed, which justifies the use of the GLM ANOVA model. The mean NSPV for the head-turns of stimulus phases (vertical VOR) is 0.625 ± 0.302 which is slightly smaller but consistent with the average of 0.73 found in a previous experiment [69].

We performed a GLM repeated-measures ANOVA on the NSPV against the categories Direction, Angle, Gender and MSgroup, and the variables Day, Velocity and Replication. As illustrated in Table 5.4, there are the same significant main effects on NSPV as on SPV-peak amplitude: Velocity ($p < 0.001$), Angle ($p < 0.001$) and Replication ($p = 0.012$). Two cross-effects are also significant.

Table 5.4. Significant main and cross effects on NSPV. Results of a GLM ANOVA with a significance level of $p < 0.05$. Only the significant cross effects are shown.

	F-value	df	p-value
Gender	3.185	1, 13	0.098
MSgroup	0.603	1, 13	0.451
Direction	2.586	1, 13	0.132
Day	0.675	1, 13	0.426
Centrifuge-velocity	70.907	2, 26	< 0.001
Head-angle	100.069	2, 26	< 0.001
Replication	8.474	1, 13	0.012
Velocity*Angle	3.170	4, 52	0.021
Day*Dir	4.343	1, 13	0.057

The NSPV adaptation pattern is different for the two head-turns directions (marginally not significant). Whereas there is very little adaptation for head-turns from NUP to RED, there seems to be significant adaptation for the head-turns in the opposite direction (cross effect Day*Dir). In addition, there is, as for the SPV-peak amplitude, a significant effect of Replications and no effect of Day on the NSPV.

Although the NSPV should not depend on the parameters of the CCS, there are significant effects of centrifuge-velocity and head-angle on the NSPV. Indeed, the NSPV

is a gain and if the standard linear model used to explain the VOR (Section 2.3) is correct, the normalized SPV-peak amplitude (NSPV) should not depend on the CCS intensity. As shown on Figure 5.13, our results suggest that the NSPV decreases when the intensity of the CCS increases. Although this finding seems surprising, it is consistent with the results of Adenot who studied the effect of head-angle and found that the larger angles led to significantly smaller NSPV [35]. There is also a statistically significant interaction between centrifuge-velocity and head-angle (cross-effect Velocity*Angle), but it is numerically negligible.

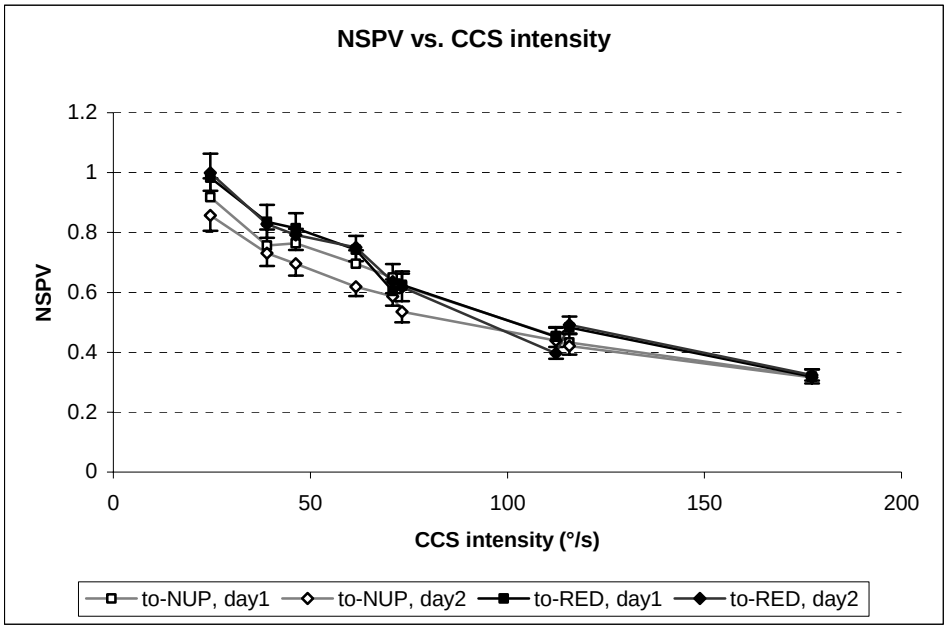

Figure 5.13. NSPV with respect to CCS intensity by Days and head-turn Directions.

The fact that the NSPV – supposed to be normalized – still depends significantly on the CCS intensity will be discussed in the next chapter. There could be several explanations to this finding; one of them is simply that our estimate of the SPV for strong CCS is erroneous, as mentioned in the previous section. On the other hand, previous studies already suggested that the NSPV is perhaps the wrong parameter and does not characterize the gain of the VOR: In particular, it has been found to depend significantly on the head-angle [35].

5.4 Subjective assessments

5.4.1 Motion sickness

The motion sickness statistics are based on the motion sickness ratings of 7 subjects. The analysis concentrates on the stimulus phase and excludes all subjects who did not feel motion-sick. The subjects were separated in two groups based on their motion sickness score: those who felt virtually no motion sickness and those who felt at least some motion sickness[12]. We tried to balance the groups but, because the experiment was highly provocative, many subjects who felt motion sick were actually too sick to complete all part of the experiment and, therefore, are missing some data points. Finally, 7 subjects qualified for the motion sickness analysis.

Figure 5.14 shows the profile of motion sickness for the 5 subjects of the group given the first sequence of angles (20° - 80° - 40°) who qualified for the motion sickness analysis. Adaptation is clearly visible since the level of motion sickness on the second experimental day is significantly lower than that on the first day. The motion sickness builds up between the two replications on the first day, but not on the second day, which is a sign that adaptation is achieved. The same figure also shows the effect of centrifuge-velocity on motion sickness: Higher velocities lead to higher motion sickness level. On the other hand, no effect of head-angle is evident on the figure.

[12] Only the subjects who had an average motion sickness score greater than 1 for the stimulus phase of the first experimental day were retained for the analysis.

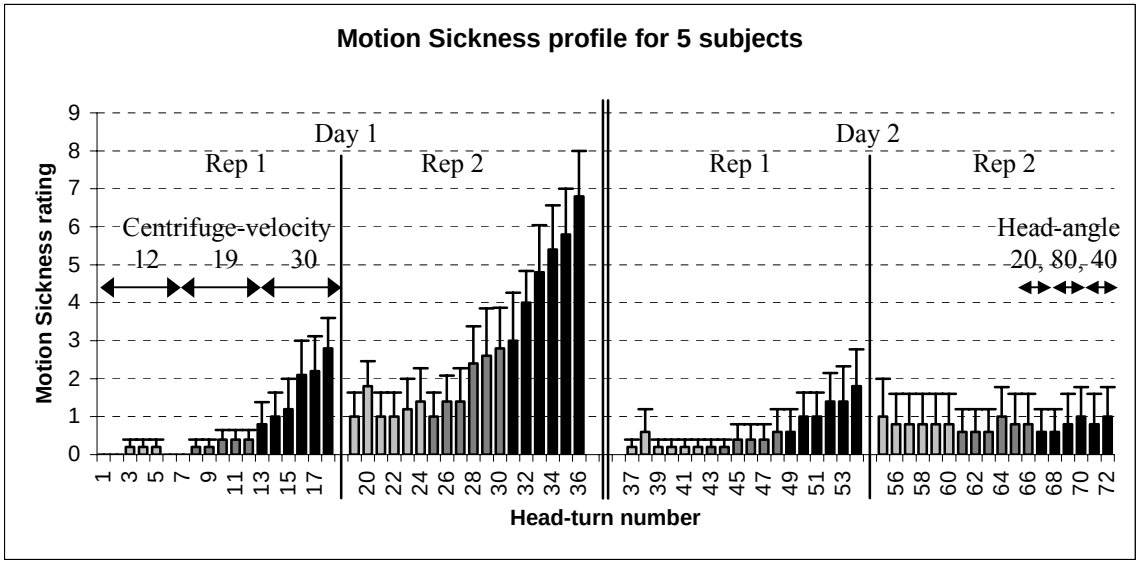

Figure 5.14. Change in motion sickness throughout the stimulus phases of the two experimental days. Average of the 5 subjects that qualified for the motion sickness analysis for the first ordering of head-turns. The order of head-angle for each centrifuge-velocity is: 20°, 80° then 40°.

Motion sickness builds up very slowly compared to the other measures (time-constants of 1 and 10 minutes as described in Section 2.5). Since in our experiment the subject alternated head-turns of different levels of stimulation over a short period of time, the normal motion sickness score does not measure the isolated effect of the each head-turn accurately: When a head-turn is performed, the motion sickness it creates is added to the current level of nausea and does not disappear for several minutes (according to the model presented in Section 2.5.3). The motion sickness score, therefore, measures the cumulative effects of all the head-turns performed in the preceding minutes, as shown by its autocorrelation plot (Figure 5.15): For a given head-turn, the motion sickness score is significantly correlated with the scores of the 16 previous head-turns (and the correlation coefficients for the most recent head-turns are close to 1). The autocorrelation plot is also consistent with a long time-constant for motion sickness of about 10 minutes. Indeed, the motion sickness is positively correlated to the 16 previous head-turns and since head-turns are performed every 30 seconds approximately, motion sickness shows a positive correlation with the motion sickness scores of the 8 previous minutes.

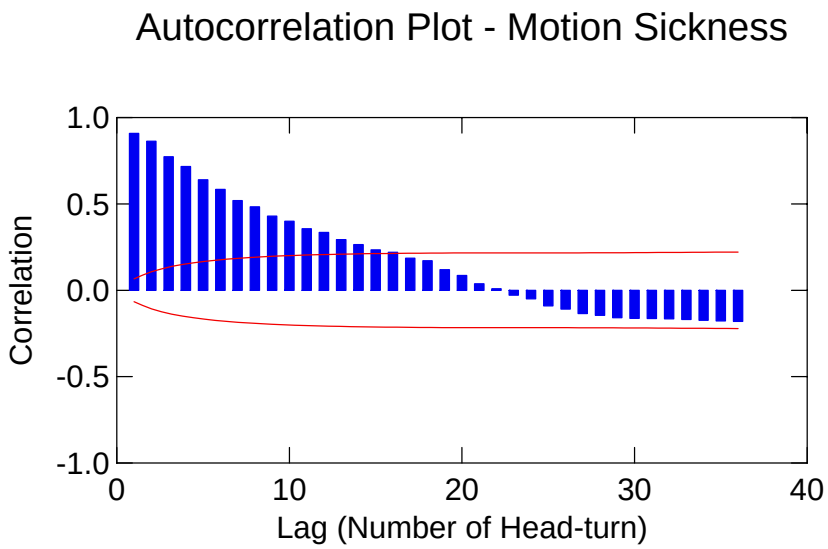

Figure 5.15. Autocorrelation of motion sickness. The bars are the correlation between the motion sickness scores and the line indicates the p=0.05 level of significance. The graph takes into account all the head-turns performed during the experiment, from the pre-rotation to the post-rotation phases.

Due to this correlation between the motion sickness scores, we decided to study also the motion sickness increment due to each head-turn separately – the difference between the motion sickness score after the head-turn and the motion sickness score before. This additional measure helps in isolating the true amount of motion sickness induced by head-turns of different CCS intensity. The motion sickness increment is far less autocorrelated ($r < 0.25$) than the simple score (see autocorrelation plot in Appendix E). Increment is, therefore, a useful measure of the amount of motion sickness induced by a single head-turn.

A Kruskal-Wallis nonparametric test was performed on motion sickness scores and increments for the usual within-subject categories: Direction, Day, Velocity, Angle and Replication. As illustrated in Table 5.5, there are significant effects of Direction, Day and Velocity on both motion sickness score and motion sickness increment.

Table 5.5. Significant main and cross effects on motion sickness increment. Results of Kruskal-Wallis nonparametric test (significance level: p < 0.05).

		Chi-square	df	p-value
Motion sickness score	Direction	5.805	1	0.016
	Day	41.240	1	< 0.001
	Centrifuge-velocity	-	2	< 0.001
	Head-Angle	-	2	0.195
	Replication	38.559	1	< 0.001
Motion sickness increment	Direction	43.273	1	< 0.001
	Day	7.256	1	0.007
	Centrifuge-velocity	-	2	< 0.001
	Head-Angle	-	2	0.146
	Replication	0.405	1	0.524

First, there is a significant effect of head-turn Replication on motion sickness score, but not on motion sickness increment. This finding demonstrates that using the "motion sickness increment" metric makes it possible to control for some of the time effects associated with motion sickness: There is no "build-up" of motion sickness on this new metric. This observation suggests that the effect of centrifuge-velocity on motion sickness increment is decoupled from the effect of head-turn replication.

There is a significant effect of head-turn Direction on both motion sickness score ($p = 0.016$) and motion sickness increment ($p < 0.001$): the head-turns from RED to NUP are more provocative than the turns to-RED. This result, shown on Figure 5.16, is consistent with the findings of past studies [35, 62, 63]. Figure 5.16-a shows that, on average, the head-turns to-RED lead to improvement in motion sickness (MS score decreases) whereas the head-turns to-NUP lead to a greater motion sickness. There is also a significant effect of Day on motion sickness that appears more clearly on the analysis of motion sickness score ($p < 0.001$, Figure 5.16-b) than on the motion sickness increment ($p = 0.007$, Figure 5.16-a).

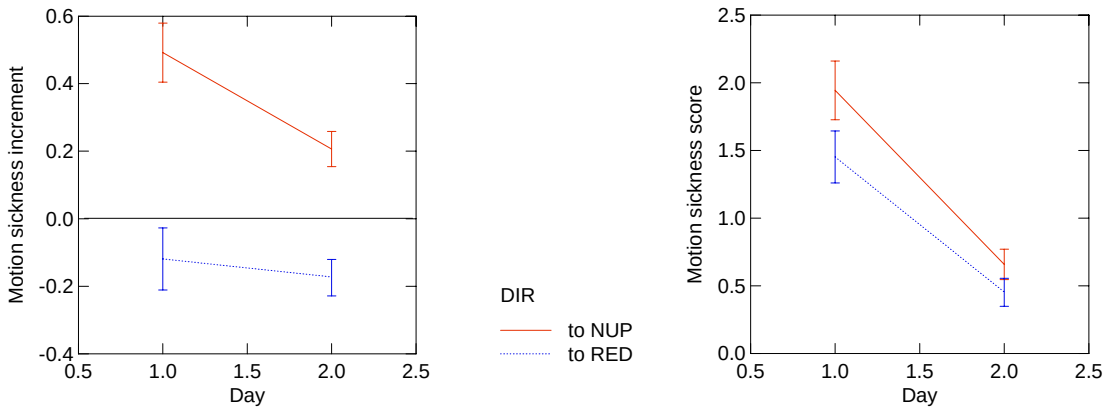

Figure 5.16. Effect of day on motion sickness by head-turn directions. (a) Variations of motion sickness increment. (b) Variations of motion sickness score.

There was a significant effect of centrifuge-velocity on motion sickness increment: the higher the centrifuge-velocity, the greater the motion sickness created by a single head-turn. The data suggests the same trend between head-angle and motion sickness increment, and although it was found not to be significant overall, it was marginally significant on the second experimental day ($p = 0.065$). Since the motion sickness increment following a head-turn depends on centrifuge-velocity and to a lesser extent on head-angle, we tested for correlation between motion sickness increments and CCS intensity. The result, shown on Figure 5.17, suggests that the amount of motion sickness created by a head-turn depends linearly on the CCS intensity. Linear regressions on each curve yield correlation coefficients greater than 0.73, with a slope significantly smaller for the second experimental day than for the first (0.0025 vs. 0.005). These results, however, are only suggestive since the standard errors on each point are large, as shown on the figure (especially for the first experimental day).

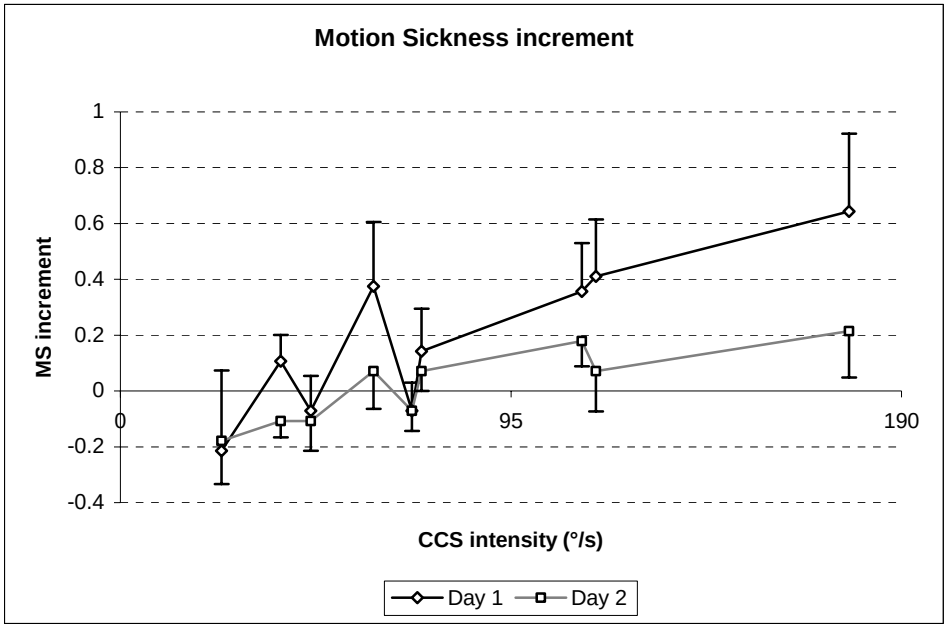

Figure 5.17. Effect of CCS intensity on motion sickness increments (amount of motion sickness created by head-turns) by day. The decrease of motion sickness increments between the two days (adaptation) is clearly visible.

The amount of motion sickness created by each head-turn (motion sickness increment) seems to be a more appropriate metric to analyze the motion sickness induced by head-turns of different CCS intensity. In fact there was a correlation between CCS intensity and motion sickness increments, whereas there is no such trend between CCS intensity and motion sickness score.

5.4.2 Illusory motion intensity

The data for the 20 subjects who completed the experiment were retained for the analysis of the illusory motion sensation. The statistics are based on the stimulus phase (1440 head-turns). We performed a GLM repeated-measures ANOVA on the illusory motion intensity against the categories Direction, Angle, Gender and MSgroup, and the variables Day, Velocity and Replication. As illustrated in Table 5.6, there are significant effects of Direction ($p = 0.003$), Velocity ($p < 0.001$), Angle ($p < 0.001$) and Day ($p < 0.001$) on the illusory motion intensity. Three cross-effects are also significant.

Table 5.6. Significant main and cross effects on illusory motion intensity. Results of a GLM ANOVA with a significance level of $p < 0.05$. Only the significant cross effects are shown.

	F-value	df	p-value
Gender	2.715	1, 17	0.118
MSgroup	1.380	1, 17	0.256
Direction	11.554	1, 17	0.003
Day	20.142	1, 17	< 0.001
Centrifuge-velocity	65.821	2, 34	< 0.001
Head-angle	35.673	2, 34	< 0.001
Replication	2.622	1, 17	0.124
Angle*Dir	8.951	2, 34	0.001
Angle*Day	3.418	2, 34	0.044
Angle*Velocity	8.772	4, 68	< 0.001

The illusory motion intensity decreases significantly over Days (Figure 5.18), but not over Replications. This suggests that, as opposed to the SPV-peak amplitude, the illusory motion sensation does adapt over days but does not habituate within a day. The results also confirm the asymmetry between the two head-turn directions: The head-turns from RED to NUP trigger a more intense illusory motion sensation that the head-turns from NUP to RED. This has been observed in several other studies [35, 62, 63] and is illustrated on Figure 5.18. In addition, head-turns performed from NUP to RED are significantly less sensitive to increase in the head-angle than head-turns performed in the opposite direction (cross effect Dir*Angle).

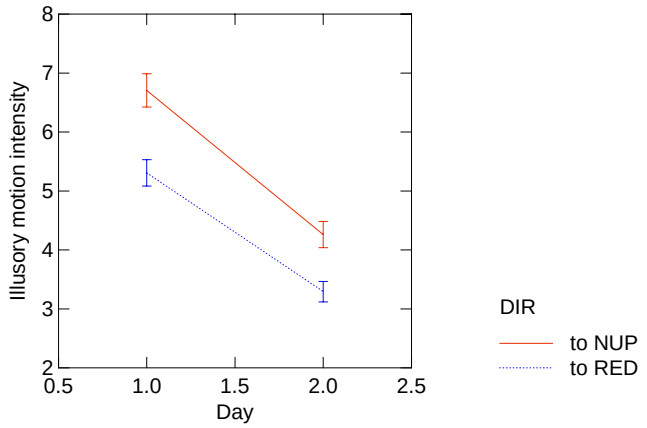

Figure 5.18. Effect of Direction and Day on the intensity of the illusory motion sensation.

As expected (Section 2.4), there are significant effects of head-angle and centrifuge-velocity on the intensity of the illusory motion, which increases when the head-angle or the centrifuge-velocity increases. Figure 5.19 illustrates this finding and also shows that the head-angle has significantly less effect on the illusory motion intensity for low centrifuge-velocities (cross effect Velocity*Angle).

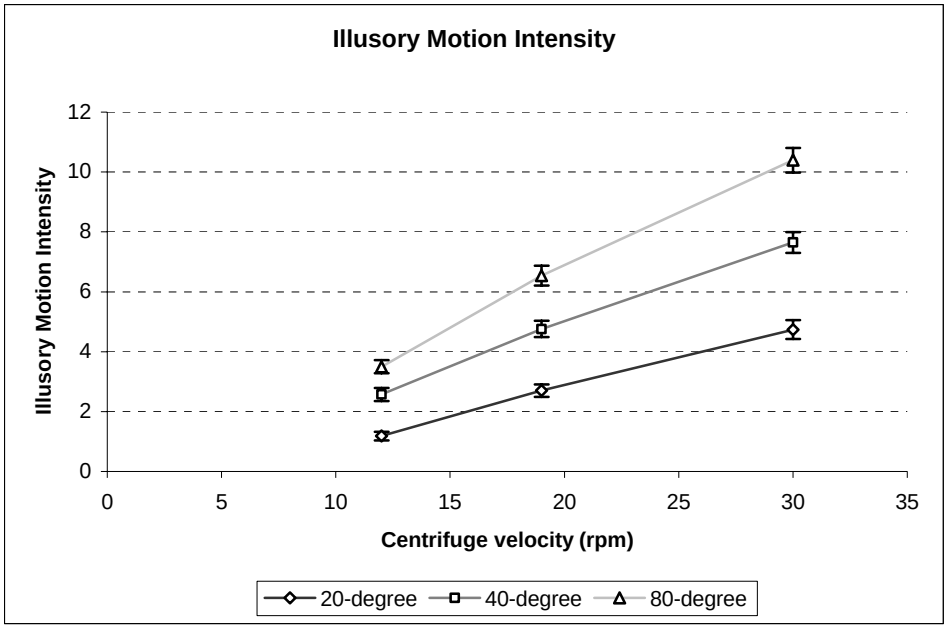

Figure 5.19. Effect of centrifuge-velocity and head-angle on the intensity of the illusory motion.

The intensity of the illusory motion depends both on head-angle and centrifuge-velocity, and actually seems to depend linearly on the CCS intensity, as shown on Figure 5.20. This result was one of our initial hypotheses and it reinforces the idea that the illusory motion is a direct response to the vestibular stimulation – as opposed to motion sickness – and is, therefore, proportional to the CCS intensity. Table 5.8 (next section) gives the linear regression coefficients for the four curves in the figure below.

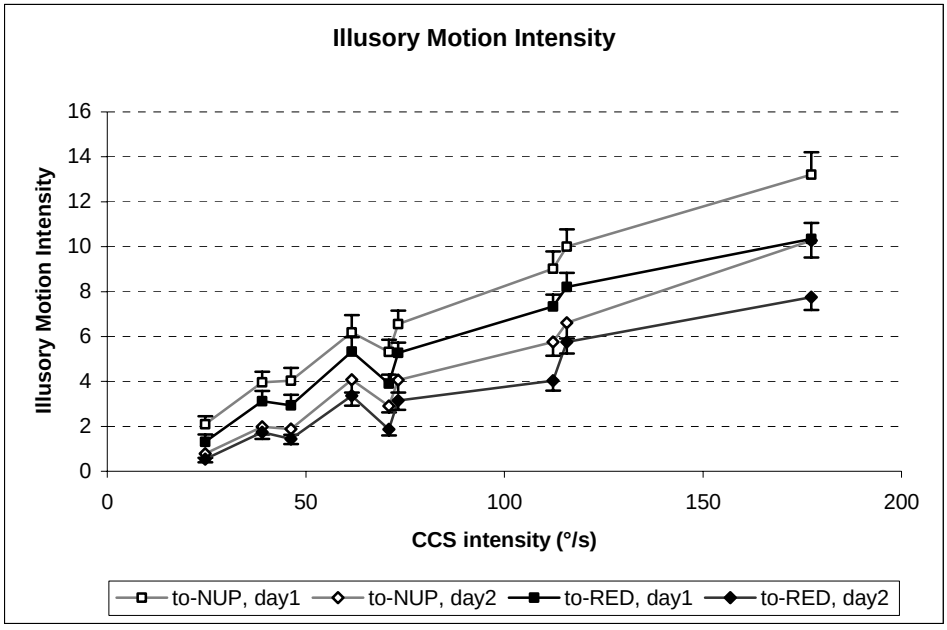

Figure 5.20. Effect of CCS intensity on the intensity of the illusory motion by day and head-turn direction.

Finally there is a significant interaction between the effects of head-angle and day on the intensity of the illusory motion: the decrease of intensity between days is smaller for small head-angles than for larger ones. This result is important because is shows a difference in the pattern of adaptation by head-angle and centrifuge-velocity despite the linear relation that exists at first between the illusory motion intensity and the composite CCS intensity. It is, however, only marginally significant ($p = 0.044$) and needs to be confirmed by other experiments.

5.4.3 Illusory motion duration

The statistics for the duration of the illusory motion are based on the same pool of subjects as the illusory motion intensity: 20 subjects, 1440 head-turns (only in stimulus phase). We performed the same GLM analysis as for the illusory motion intensity (previous section): The significant main effects are the same but are accompanied by more significant cross effects. As illustrated in Table 5.7, there are significant effects of

Direction ($p < 0.001$), Velocity ($p < 0.001$), Angle ($p < 0.001$) and Replication ($p < 0.001$) on the VOR time-constant. There are eight significant cross-effects, but three of them can be discarded (three last cross effects in the table) because they are negligible compared to their main effects.

Table 5.7. Significant main and cross effects on illusory motion duration. Results of a GLM ANOVA with a significance level of $p < 0.05$. Only the significant cross effects are shown.

	F-value	df	p-value
Gender	1.240	1, 17	0.283
MSgroup	0.567	1, 17	0.463
Direction	32.639	1, 17	< 0.001
Day	25.460	1, 17	< 0.001
Centrifuge-velocity	40.925	2, 34	< 0.001
Head-angle	49.812	2, 34	< 0.001
Replication	1.215	1, 17	0.288
Day*Velocity	7.988	2, 34	0.002
Day*Angle	11.912	2, 34	< 0.001
Dir*Velocity	11.554	2, 34	< 0.001
Dir*Angle	11.871	2, 34	< 0.001
Velocity*Angle	6.317	4, 68	< 0.001
Angle*Rep	5.204	2, 34	0.011
Day*Velocity*Dir	4.711	2, 34	0.017
Velocity*Angle*Rep	3.197	4, 68	0.019

The duration of the illusory motion follows the same pattern as its intensity. There is a significant effect of head-turn direction: The head-turns from RED to NUP trigger a longer illusory motion than the head-turns from NUP to RED (Figure 5.21-a). In addition, the head-turns from NUP to RED are significantly less affected by increases of centrifuge-velocity or head-angle than are the head-turns to-NUP (cross effect Dir*Angle and Dir*Velocity). There is a significant decrease over experimental days of the duration of the illusory motion (adaptation), but no effect of replication (habituation). The adaptation to the illusory motion, however, is significantly different for the various head-angles and centrifuge-velocities used: The higher the centrifuge-velocity, the greater the adaptation, as shown on Figure 5.21-b (cross effect Day*Velocity). The same adaptation pattern also applies to the head-angle: the larger the head-angle, the greater the adaptation (cross effect Day*Angle).

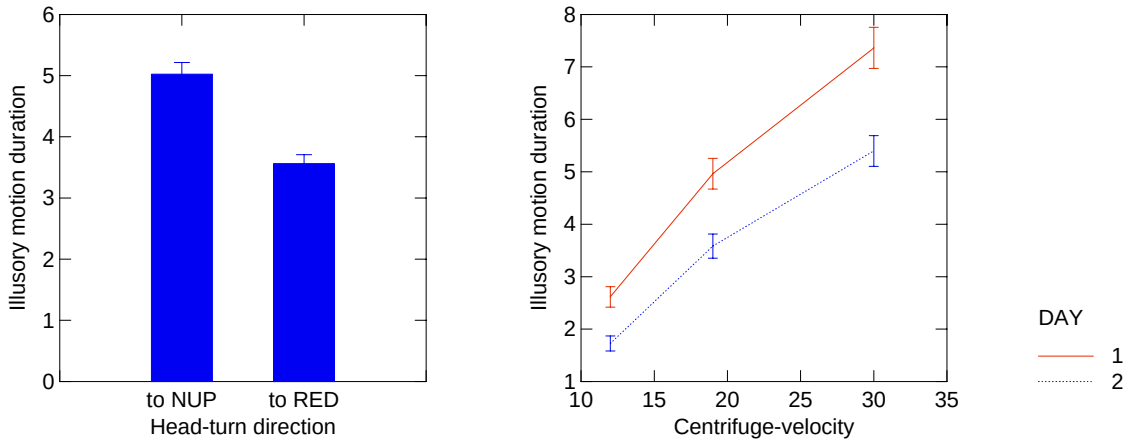

Figure 5.21. Significant effects on the duration of the illusory motion. (a) Effect of head-turn direction. (b) Effect of centrifuge-velocity by days.

There is a significant effect of centrifuge-velocity and head-angle on the duration of the illusory motion: the larger the stimulus, the longer the illusory motion sensation. There is the same interaction between the effects of centrifuge-velocity and head-angle as there was for the illusory motion intensity: Increase in head-angle has less effect for low centrifuge-velocities than for higher velocities. Finally the duration of the illusory motion sensation depends linearly on the CCS intensity, as shown on Figure 5.22. The linear regression coefficients – all above 0.94 – demonstrate that the duration of the illusory motion sensation is almost perfectly proportional to the CCS intensity (details can be found in Table 5.8). In addition, Figure 5.22 clearly shows the significant effects of head-turn direction and day.

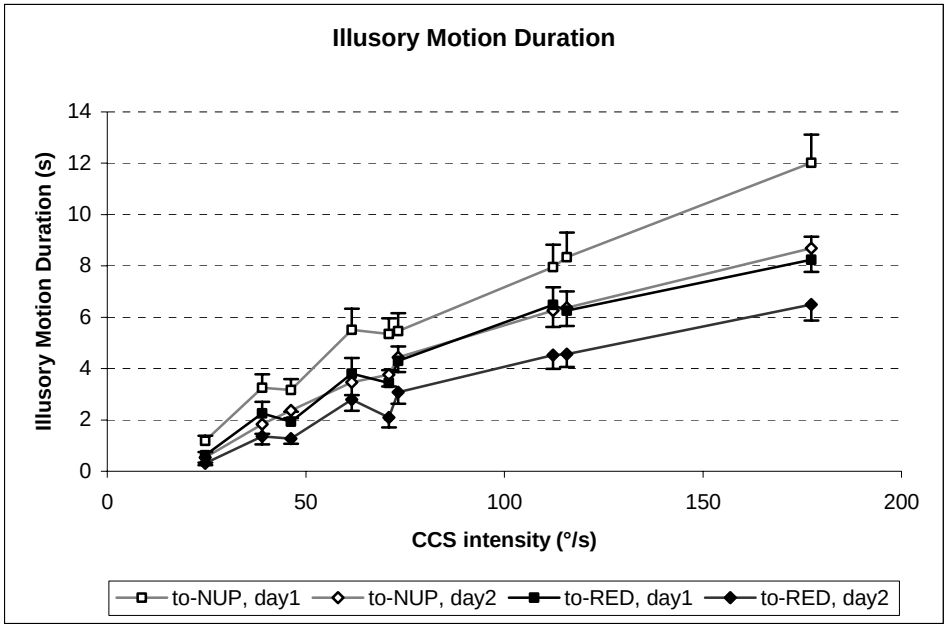

Figure 5.22. Effect of CCS intensity on the duration of the illusory motion by day and head-turn direction.

The results of the linear regression for the illusory motion are summarized in Table 5.8. The high correlation coefficients prove that the linear fits are really close to the experimental data. The changes in slopes and intercepts over the two experimental days show clearly how adaptation occurs: Not only does the gain of the illusory motion sensation decrease with adaptation (change in slope), but the threshold of the vestibular response increases (change in intercept). This finding will be discussed further in the next chapter.

Table 5.8. Summary of the linear regression coefficients for the illusory motion sensation (intensity & duration) by head-turn Directions and Days.

		Slope	Intercept	R^2
Illusory motion intensity	to-NUP, day 1	0.072	0.932	0.973
	to-NUP, day 2	0.061	-0.601	0.971
	to-RED, day 1	0.059	0.616	0.940
	to-RED, day 2	0.046	-0.406	0.920
Illusory motion duration	to-NUP, day 1	0.068	0.388	0.976
	to-NUP, day 2	0.053	-0.039	0.969
	to-RED, day 1	0.050	0.135	0.943
	to-RED, day 2	0.040	-0.287	0.959

The results show that duration and intensity of the illusory motion are affected similarly by the different parameters investigated in this study. In the next chapters, therefore, the illusory motion sensation will often be considered as a whole.

5.4.4 Perceived body-tilt

The perceived body-tilt statistics are based on the stimulus phase of 11 subjects (792 head-turns). Of the 20 subjects that completed both experimental days, 9 reported a constant body-tilt of 90 degrees (lying horizontal) and were, therefore, excluded from the analysis. The complete body-tilt plot for each subject can be found in Appendix F. For this sample of 11 subjects the body-tilt was approximately normally distributed. We performed a GLM repeated-measures ANOVA on the body-tilt against the categories Direction, Angle, Gender and MSgroup, and the variables Day, Velocity and Replication. As illustrated in Table 5.3, there are significant effects of Velocity ($p = 0.032$), Direction ($p = 0.007$) and Replication ($p = 0.004$) on the perceived body-tilt. Two cross-effects are also significant.

Table 5.9. Significant main and cross effects on perceived body-tilt. Results of a GLM ANOVA with a significance level of $p < 0.05$. Only the significant cross effects are shown. Although the table lists the effect of Day as insignificant, it does so only because the values for the two head-turn directions (both significant) have opposite "signs" compared to the 90-degree reference, which cancel the two significant effects (see text for more details).

	F-value	df	p-value
Gender	0.048	1, 8	0.832
MSgroup	0.911	1, 8	0.368
Direction	13.049	1, 8	0.007
Day	0.035	1, 8	0.855
Centrifuge-velocity	4.312	2, 16	0.032
Head-angle	2.252	2, 16	0.138
Replication	10.954	1, 8	0.011
Day*Dir	4.969	1, 8	0.056
Velocity*Dir	7.423	2, 16	0.005

There is a significant effect of replication on the perceived body-tilt: The tilt sensation decreases significantly over replications (ie. comes back to the initial "lying

horizontal" feeling). There is a significant effect of Direction on the body-tilt: The head-turns from NUP to RED led to a significantly smaller tilt sensation than the head turns from RED to NUP – as previously observed in several studies [35, 62]. This finding is shown on Figure 5.23, along with the marginally significant cross effect Day*Direction. The head turns to-RED initially lead to a "feet upward" tilt sensation whereas the turns to-NUP lead to a clear "feet downward" tilt sensation. The effect of Day on both head-turn directions is to diminish the tilt sensation, as illustrated on Figure 5.23. Since the effect of Day on the body-tilt is opposite for the two turn-directions, the GLM showed only a significant cross effect Day*Dir instead of a significant effect of Day alone. We conducted, therefore, a mixed regression on each direction separately and found that there is a significant effect of Day on the perceived body-tilt ($p = 0.033$ for head-turns to-RED and $p = 0.038$ for head-turns to-NUP). This finding shows that the body-tilt as perceived by the subjects adapts over the experiment, as already observed [62].

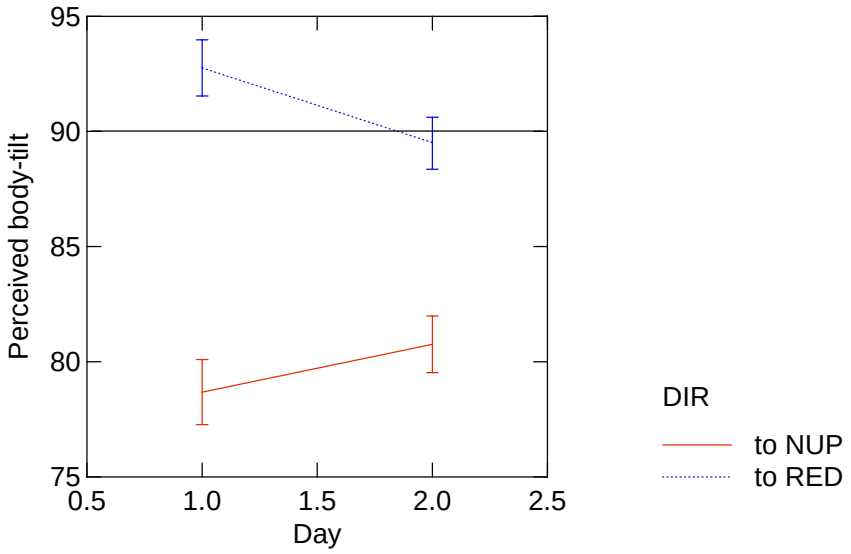

Figure 5.23. Effect of day on the perceived body-tilt by head-turn directions. The main effect of Direction and the cross effect Direction*Day are clearly visible.

Finally there is a significant effect of centrifuge-velocity on the body-tilt perceived by the subject during centrifugation, as shown on Figure 5.24. There is a significant interaction between the effects of head-turn direction and centrifuge-velocity: Changes in

centrifuge-velocity have a greater influence on the tilt sensation for head-turns from RED to NUP than for turns in the opposite direction. For head-turns to-NUP, the average body-tilt experienced by the subjects during 30-rpm centrifugation is 25° in the feet downward direction. This result demonstrates that the artificial gravity created by centrifugations is interpreted by the human body as a real gravity would be, which clearly illustrates the success of AG.

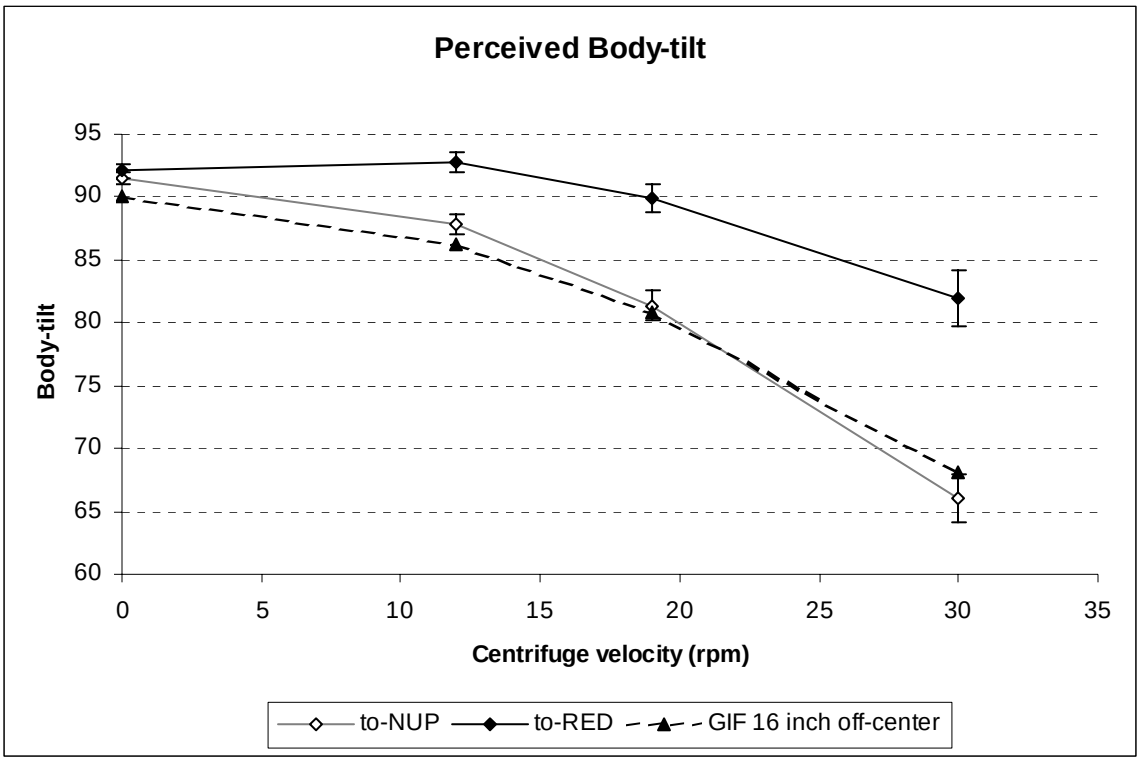

Figure 5.24. Effect of centrifuge-velocity on the perceived body-tilt by head-turn direction. The dashed line represents the theoretical tilt of the GIF at mid-chest level (16-inch from head center).

Although the head of the subject was on-axis (no artificial gravity loading on the otolith organs), the subject felt a strong body-tilt sensation for high centrifuge-velocity. This result confirms that there are other gravity-receptor organs than those in the vestibular system. Furthermore, for the head-turns in the "to-NUP" direction, the perceived body-tilt (as rated by the subjects) is very close to the true tilt of the GIF 16-inch away from the center of rotation – which corresponds approximately to mid-chest

level. According to this finding one of these other gravito-receptor organs could very well lie at chest level [78].

In addition, the fact that there is no effect of head-angle on the body-tilt whereas there is an effect of head-turn direction, suggests that the head position with respect to the trunk has no influence on the tilt sensations experienced by the subjects after a head-turn.

6 Discussion

When humans perform head-turns in a rotating environment, they experience a strong vestibular response that includes illusory motion sensation, vestibulo-ocular reflex, and possibly motion sickness. For yaw head-turns performed in the dark during head on-axis supine clockwise horizontal rotations, the pitch component of the vestibular stimulation, $\omega \sin(\psi_{max})$, dominates the vestibular response. We expected to find a strong correlation between the CCS intensity and the vestibular response – as indicated by physiological measures and subjective ratings. We also expected, based on the conflict theory (Section 2.5.2), that stronger CCS would drive greater adaptation.

6.1 Overview of key findings

From the results described in the previous chapter, four key findings stand out and require further explanation:

1) As already observed in past experiments, all measures except SPV-peak amplitude decrease significantly over experimental days, which proves that there is significant adaptation to vestibular stimulation.
2) There is a significant effect of head-angle on the VOR time-constant. High angles lead to longer time-constant than smaller angles, but do not lead to greater adaptation – decrease of the VOR time-constant.
3) In subjects that perceived a non-stationary body-tilt during the experiment the tilt sensation depends significantly on the centrifuge-velocity. Moreover, the perceived tilt angle reported in the NUP position is highly correlated with the true tilt of the GIF at mid-chest level.
4) The SPV-peak amplitude and all measures of subjective response except body-tilt show significant correlation with the CCS intensity: the larger the CCS, the stronger the vestibular response. The subjective ratings are linearly dependent on the CCS intensity and show greater relative adaptation for smaller stimulus. By

contrast, the SPV-peak amplitude seems to depend linearly on the logarithm on the CCS and does not show any adaptation.

6.2 Analysis of key findings

6.2.1 Adaptation and head-turn direction asymmetry

Key finding 1: As already observed in past experiments, all measures except SPV-peak amplitude decrease significantly over experimental days, which proves that there is significant adaptation to vestibular stimulation.

Previous work conducted in the Man-Vehicle Laboratory showed that vestibular adaptation is possible to head-turns performed during short-radius centrifugation. Our experimental results, once again, confirm that adaptation to high rotation rates is achieved in a period as short as two days.

There is a significant decrease in all subjective ratings between the two experimental days. Motion sickness, especially, shows a dramatic decrease over days: Of the seven subjects that feel significantly motion sick on the first day, only one has non-negligible motion sickness scores on the second day – still lower than his scores on the first day. The susceptibility to motion sickness greatly diminishes on the second day, as indicated by the absence of motion sickness build-up (see individual graphs in Appendix G). Indeed, according to the symptoms dynamics model (Section 2.5.3), motion sickness undergoes a gradual increase, on repeated vestibular stimulation, due to the long time-constant (10 min) that characterizes the internal pathway. This steady increase leads to the build-up of motion sickness that is clearly observed on the first experimental day. By contrast on the second day, the subjects' susceptibility to motion sickness is greatly reduced and the intensity of conflict generated by most head-turns does not trigger any nausea. The results suggest that the adaptation of the motion sickness response is two-fold: the amount of motion sickness generated by a single head-turn is smaller on the second day than on the first, and the rate of the motion-sickness build-up is reduced.

The illusory motion sensation shows a clear decrease between the two experimental days and so does the body-tilt sensation. These sensations, estimated by subjective ratings, adapt because they are associated to well-identified conflicts, as explained in Section 2.6.2. Susceptibility to motion sickness decreases because of the conflict between the sensory inputs and the prediction of the internal model – same conflict that initially triggered the motion sickness response. Similarly, the illusory motion and body-tilt sensations are accompanied by obvious conflicts between the signals from the canals on one side and the signals from the otolith organs and the somatosensory system on the other side.

The analysis of eye-movements indicates that whereas the VOR time-constant shows adaptation, the SPV-peak amplitude does not. This lack of adaptation for the gain of the VOR has already been verified by previous studies for head-turns in a dark environment and agrees with the conclusion of Brown [54]: Retinal slip is necessary to decrease the gain of the VOR for head-turns performed during centrifugations. By contrast, the VOR time-constant decreases significantly between the two experimental days and shows clear signs of adaptation despite the dark environment. This adaptation of the VOR time-constant for head-turns performed in a dark environment has already been observed [58, 61, 62]. As suggested by Dai, the VOR time-constant might be related to motion sickness [56]. Since motion sickness susceptibility decreases dramatically between the two days, it might explain why the VOR time-constant adapts even for head-turns performed in a dark environment.

6.2.2 VOR time-constant and CCS

Key finding 2: There is a significant effect of head-angle on the VOR time-constant. High angles lead to longer time-constant than smaller angles, but do not lead to greater adaptation – decrease of the VOR time-constant.

Although one might think that the VOR time-constant characterizes only the internal process that commands the VOR and does not depend on the stimulus, it was found to depend significantly on the head-angle. The time-constant does not depend on the

centrifuge-velocity and, therefore, does not depend directly on the CCS intensity. It is not surprising that the VOR time-constant is not directly affected by the CCS intensity: The duration of the compensatory eye-movements is defined by the dynamics of the velocity storage integrator and not by the magnitude of the input – CCS intensity – to the system. In addition, as shown on Figure 6.1, our results strongly suggest that the time-constant is linearly dependent on the head-angle – and not on the sine of the head-angle. As mentioned in the Section 5.3.1, there is a marginally significant ($p = 0.048$) interaction between centrifuge-velocity and head-angle, but since this finding is very surprising and because it might only be an artifact of the eye-movement analysis, further investigation is necessary before any conclusion can be drawn.

Adenot had already studied the effect of head-angle on the VOR time-constant in an experiment conducted at MIT. Her results[13], also shown on Figure 6.1, are consistent with ours: the VOR time-constant increases linearly with the head-angle. One can notice that the ranges of the VOR time-constants are clearly separated on the graph, a difference that can be explained by the revision of the eye-movements analysis algorithm that took place between the two experiments (Section 4.1). In her results, the VOR time-constant already seemed to be linearly dependent on the sine of the head-angle – but there was no significant effect. On the other hand, she did not observe a decrease of the VOR time-constant between the two experimental days. The differences between the results of the two studies – effect of head-angle and day – might be explained by the smaller number of subject that participated in Adenot's experiment, or by the different experimental setup used to control the head-angle: Whereas Adenot used magnets, much imprecise, to indicate the different head-angles and relied on the subject to stop his head-turn at the right angle, we used a system of moving rods that prohibited the subject from going beyond the targeted angle.

[13] The results shown for Adenot's experiment have been recalculated from her raw data for this analysis.

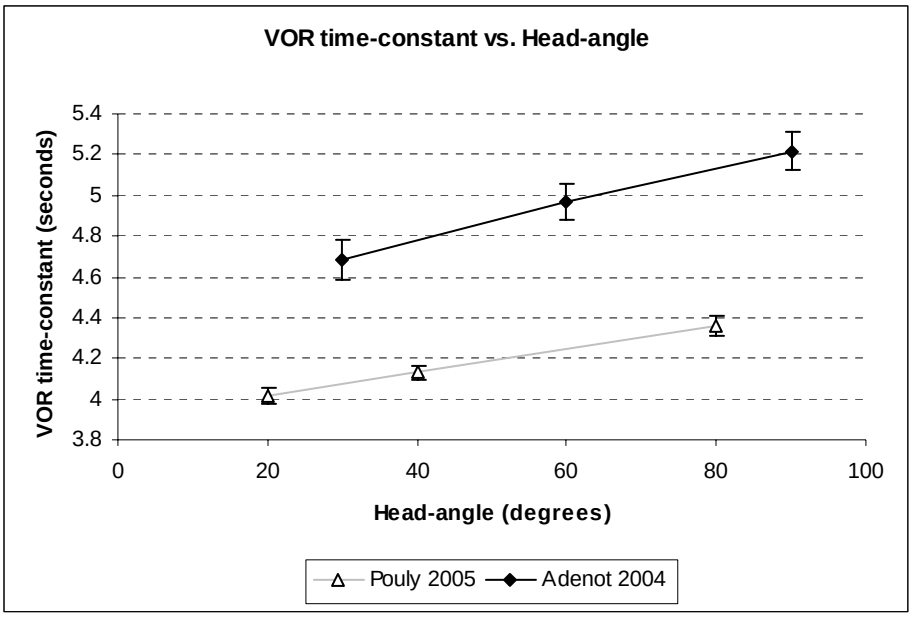

Figure 6.1. VOR time-constant with respect to head-angle: comparison of our results with Adenot's.

The linear relation between the VOR time-constant and the head-angle suggested on Figure 6.1 confirms what Adenot had previously observed: smaller head-angles trigger shorter VOR. The current model of the VOR involves inputs from only the vestibular system aside from internal parameters – gain and time constant(s) – that adapt to repeated stimulation. Within this model, the VOR time-constant should not be affected by the head-angle. Nonetheless, the true dynamics of the VOR are certainly more complicated. Under the assumption that proprioceptor signals are also inputs to the system, one might have a hint as to how to explain the observed variations. It may be that in our experiment, the VOR is damped more quickly for small head-angles than for large because smaller movements lead to faster reflexes. This suggestion, however, requires more experimental verification. Although the trend is fairly clear in our results – small standard errors – it is less obvious in Adenot's results and remains lightly backed by theoretical considerations.

The small inconsistencies between the conclusions of the two experiments and the lack of physiological explanation call for further investigation to understand this linear relation between VOR time-constant and head-angle. Research should especially be conducted to establish the true effect of proprioceptor inputs on the VOR. An experiment could, for example, compare the time-constant of the true VOR – elicited by whole body

angular acceleration without any proprioceptor input – with the time constant of VORs elicited by head-turns to different angles performed during centrifugation.

6.2.3 Body-tilt and GIF

Key finding 3: In subjects that perceived a non-stationary body-tilt during the experiment the tilt sensation depends significantly on the centrifuge-velocity. Moreover, the perceived tilt angle reported in the NUP position is highly correlated with the true tilt of the GIF at mid-chest level.

The experimental results confirm the prediction that the body-tilt experienced by the subjects after head-turns during centrifugation depends on centrifuge-velocity, but not on head-angle. The faster the centrifuge velocity, the larger the body tilt experienced by the subject. This is expected from the behavior of the true tilt of the GIF, which increases when centrifuge velocity increases. There is also a significant effect of turn-direction on the estimate of body-tilt. For the head-turns from NUP to RED, the body-tilt experienced by the subjects is closer to horizontal than for the head-turns from RED to NUP. It is also less sensitive to centrifuge-velocity. Indeed, for values below 15 rpm, there is no effect of centrifuge velocity on the body-tilt for the head-turns to-RED. Although it had been observed several times, this directional asymmetry has not yet been explained. Our finding, however, suggests that it is not the head position with respect to the trunk that interferes with the estimation of the body-tilt in the RED position – since head-angle does not have any effect. The sequels of the illusory motion sensation that follows a head-turn might help in explaining the effect of turn direction on perceived body-tilt, but further investigation is necessary.

During the experiment, subjects were spun with the center of their head aligned with the axis of centrifugation. Because the head is positioned on-center, there is no otolith loading associated with the artificial gravity created by the rotation of the bed. Nonetheless, the subjects experience a persistent sensation of body-tilt that confirms that there are extravestibular graviceptors in the human body. Indeed, although it is widely acknowledged that vestibular and visual information are primary sources for the

perception of posture, it has been shown recently that there are other graviceptors in the human body – perhaps located in the trunk – that are sensitive to fluid shift [78-80]. This finding makes it possible to explain why many bilaterally labyrinthectomized patients – or other that are vestibularly deficient – are able to control their body posture.

This somatic graviception has been demonstrated by Vaitl in 1997 using Lower Body Negative or Positive Pressures (LBNP, LBPP) on a tilt-table [80]. In the experiment, subjects were exposed to lower body pressure changes while lying supine on the tilt-table and were instructed to set the angle of the table so that they feel horizontal. The tilt-table was used as a direct way to assess the Subjective Horizontal Position (SHP) perceived by the subject. The experiment, replicated by the same authors with similar results in 2002 [78, 79], strongly suggests that there are somatic truncal graviceptors in the human body. Figure 6.2 shows the results of both experiments: The lower body pressure changes led to fluid shift in the trunk of the subject that led to changes in the SHP. The experiment shows that LBPP and LBNP have a static effect on graviception. Since the subjects had neither vestibular nor visual information about their actual body position throughout the experiment, the changes in SHP were most likely triggered by the manipulation of blood – or more generally body fluid – distribution.

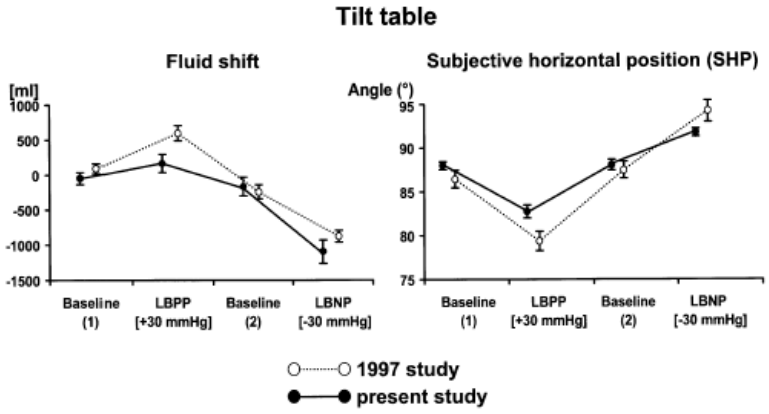

Figure 6.2. Experimental results suggesting that fluid shifts induced by lower body pressure manipulation trigger changes in SHP (1997 and 2002). (a) Mean change in fluid shift of thoracic blood volume. (b) Mean changes in SHP measured by the angle of the tilt-table with respect to different lower body pressures (reproduced from [78]).

In 2002, Vaitl and coworkers designed an experiment specifically to differentiate the effect of the otolith organs from the effect of changes in fluid distribution on the perception of body position. They combined a sled centrifuge with LBNP and LBPP. The experimental protocol was the same as that of the tilt-table experiment previously described except that instead of changing the angle of the tilt-table, the subject assessed his SHP by moving the sled radially along his spinal axis, as illustrated on Figure 6.3.

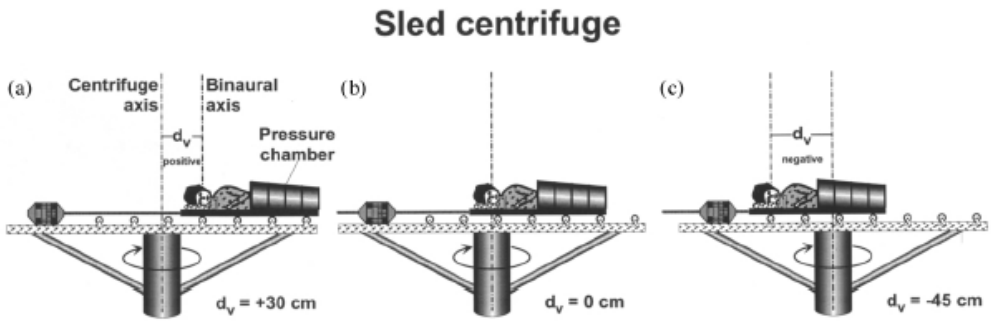

Figure 6.3. SHP on a rotating sled (36 rpm). Due to the centripetal acceleration, the subject feels tilted, depending on the distance between the centrifuge axis and the otolith organs (binaural axis). On exposure to LBNP or LBPP, the SHP of the subject changes and the subject is required to move the sled until he or she feels horizontal. (reproduced from [78])

In this experiment, the subject assessed his SHP by adjusting his "otolithic input" – the distance between his otolith organs and the axis of centrifugation. As expected, LBNP and LBPP modified the SHP and led to active changes of the otolithic input by the subject: The authors found that changes in SHP due to LBNP and LBPP were cancelled out by otolith input, as shown on Figure 6.4.

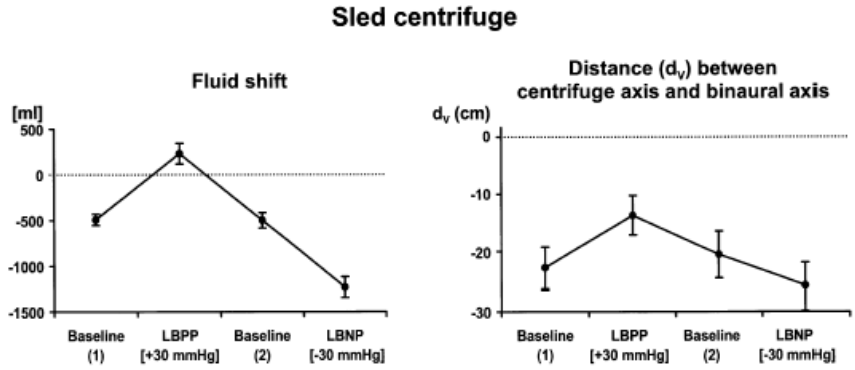

Figure 6.4. Sled centrifuge. (a) Mean change in fluid shift of thoracic blood volume. (b) Mean changes in SHP measured by the distance of the centrfigue axis from the binaural axis with respect to different lower body pressures. (reproduced from [78])

These remarkable findings demonstrate that, during centrifugations in a totally dark environment (no visual input), the SHP is estimated from both the blood distribution – somatic graviception – and the otolithic input – vestibular graviception. Indeed, during centrifugation, the artificial gravity "pulls" the blood of the subject towards his feet as normal gravity would for a standing subject. This phenomenon modifies the blood distribution in the subject's body and this change is perceived by somatic graviception. On the other hand, the angle between the GIF applied on the otolith organs and the spinal body axis is perceived by vestibular graviception.

One can notice that, for baseline lower body pressure, the subjects adjusted to 20 cm approximately the distance between centrifuge and binaural axes (Figure 6.4-b). This distance can be interpreted as describing the position of the mathematical center of the body graviceptors – center of graviception. Interestingly, during centrifugation, the position of this center of graviception is near the mid-point between mid-chest and vestibular system.

Under our experimental conditions – subject lying supine in the dark with his head on-center – there is no otolithic input and thus body-tilt estimation is driven by somatic graviception alone. Interestingly, for the head-turns from RED to NUP, the mean body-tilt estimate is well fit by the true tilt of the GIF 16 inches away from the center of rotation, as shown on Figure 5.24. Since 16 inches from the center of the head corresponds to mid-chest level (on average), our result suggests that the somatic

graviceptors rest at mid-chest level. This result is also consistent with the conclusion of a previous study that the somatic graviceptors of the cardiovascular system are located below the upper torso [79].

6.2.4 CCS intensity and vestibular response

Key finding 4: The SPV-peak amplitude and all measures of subjective response except body-tilt show significant correlation with the CCS intensity: the larger the CCS, the stronger the vestibular response. The subjective ratings are linearly dependent on the CCS intensity and show greater relative adaptation for smaller stimulus. By contrast, the SPV-peak amplitude seems to depend linearly on the logarithm on the CCS and does not show any adaptation.

As expected, there is a strong correlation between CCS intensity and several measurements: illusory motion (both intensity and duration), SPV-peak amplitude and motion sickness increment. These results confirm the hypothesis that, for head-turns performed during centrifugation, the pitch component dominates the roll component in the vestibular response. Indeed, as observed experimentally, the vestibular response is significantly correlated with the part of the CCS applied in the pitch plane[14], $\omega_c \sin(\psi_{max})$, but not with the total magnitude of the CCS. That this conclusion holds for both head-turn directions suggests that the pitch canal is morphologically more sensitive than the roll canal: On Earth, otolith inputs are different for the two head-turn directions and the roles of the pitch and roll canals are exchanged when the head-turn direction is changed. This rules out most possible explanations and leaves the morphological one.

The illusory motion sensation is proportional to the CCS intensity, as shown on Figure 6.5. The experimental data, fit well by straight lines ($R^2 > 0.95$), demonstrate that the illusory motion sensation is directly proportional to the vestibular stimulus. The graphs, however, suggest that for very weak stimulations, the linear behavior does not describe the data accurately and the same phenomenon can also be expected for very strong stimuli. These deviations from the linear relationship for extreme stimulations are

[14] In this thesis, the pitch component of the CCS is, by convention, referred to as "CCS intensity".

not surprising and are typical of most human sensory systems. The adaptation pattern of the illusory motion sensation, shown on Figure 6.5, is interesting and appears clearly in the coefficients of the linear fits (y = ax+b). The illusory motion sensation adapts both in threshold and in sensitivity: On the second experimental day, the (theoretical) minimum stimulation that can trigger a response is larger than on the first day – the coefficient "b" is smaller – and the increase of the response for a given increase of the stimulus is reduced – coefficient "a" smaller. This adaptation pattern provides us with information on how the internal models that define the vestibular response are modified by adaptation.

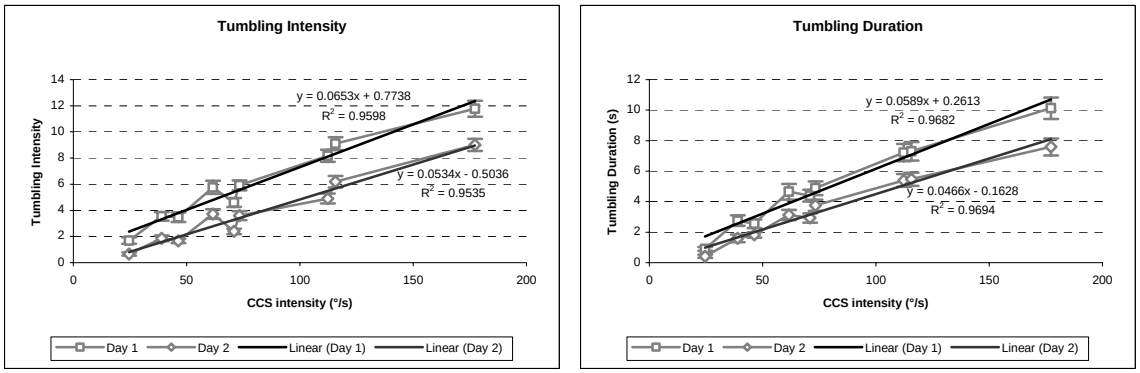

Figure 6.5. Illusory motion sensation vs. CCS intensity, including linear fit. (a) Intensity of the illusory motion. (b) Duration of the illusory motion.

The motion sickness increment – change in motion sickness score after a head-turn – is also linearly dependent on the CCS intensity. The relation is less marked than for the illusory motion sensation ($R^2 \sim 0.75$), certainly because of the smaller number of subjects used for the motion sickness analysis (only 7 subjects). Nonetheless, as shown on Figure 5.17, the linear trends are still visible, as well as the adaptation pattern mentioned previously: Over the two days, the motion sickness response changes both in sensitivity and in the minimum CCS that increases the motion sickness score.

The SPV-peak amplitude is, by contrast, linear in the logarithm of the CCS intensity, as shown by the quality of the logarithmic fits ($R^2 > 0.96$). Figure 6.6 shows the experimental data and the best fits and shows that there is no significant adaptation of the SPV-peak amplitude over the experiment.

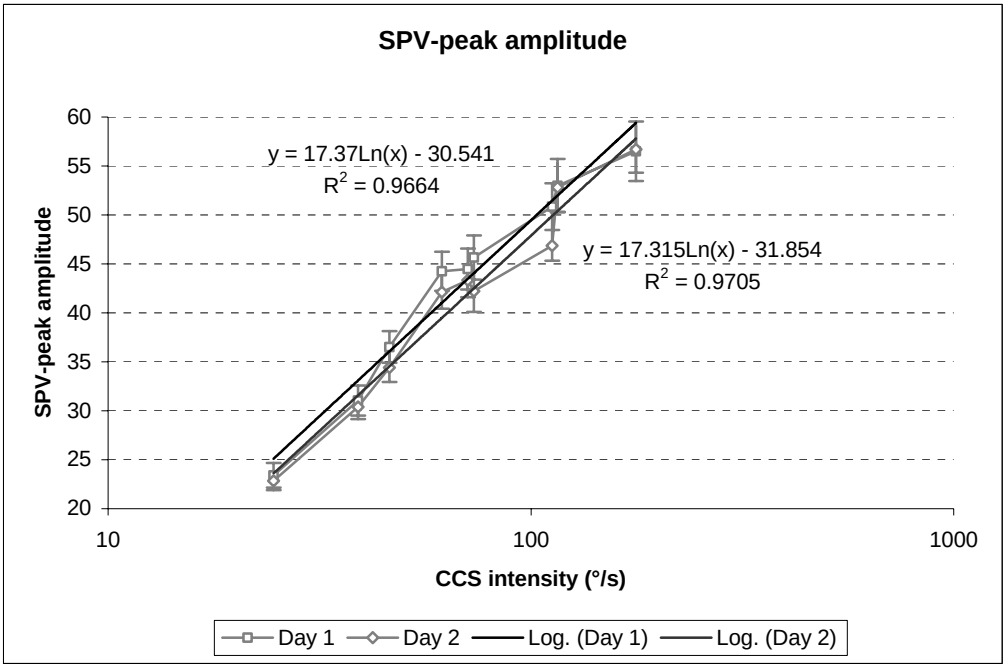

Figure 6.6. SPV-peak intensity vs. CCS intensity (semi-log scale), including best logarithmic fit.

This logarithmic relation is surprising because SPV-peak amplitude is the one measure that, according to the model used to describe the aVOR, should be proportional to the CCS intensity. Indeed, the vertical aVOR – whose SPV-peak amplitude is measured – is directly triggered by the pitch component of the CCS and aims at counterbalancing the illusory motion perceived by the vestibular system. In order to truly compensate for the motion of the body and maintain a stable visual field, the initial amplitude of the aVOR – before any damping occurs – must be proportional to the CCS intensity. Although this logarithmic behavior could have a physiological reality[15], the most probable explanation is the substantial time delay in the data between the head-turns and the beginning of the corresponding compensatory eye-movements (Sections 5.3.2). This time delay is proportional to the CCS intensity and could very well alter the true trend of the SPV-peak amplitude – the measured peak amplitude is obviously smaller than the true peak amplitude if read several seconds after the beginning of the eye-movements. Whether this delay is a true physiological phenomenon or merely an artifact

[15] There are other sensory systems in the human body that respond logarithmically to their associated stimulations – like the auditory system (dB). On the other hand, a logarithmic dependence of the SPV of the VOR on stimulation would impede its apparent function.

of the eye-movement analysis algorithm must be investigated to better understand the relation between SPV-peak amplitude and CCS intensity.

6.3 Limitations and recommendations for future work

This study gives a first indication of the quantitative relation that connects intensity of initial stimulation, strength of vestibular response and degree of adaptation. Replicating this experiment with a larger number of subjects would certainly allow us to resolve some of the marginally significant – or insignificant – results that have been found. In particular, more subjects are needed for the analysis of motion sickness: Only the 7 subjects who had non-negligible motion sickness could be used for the statistical analysis, which is too few to obtain meaningful results. The number of subjects used for the analysis of the body-tilt is also small (11 subjects) and, although the trends found for the perceived body-tilt are significant, more subjects would allow a more reliable generalization of the findings to a larger population.

With more subjects, more types of head-turns could be studied. The current parametric study concentrates on five levels of CCS intensity defined from nine combinations of head-angle with centrifuge-velocity. This design gives a first approximation to the true quantitative relationship among CCS, neurovestibular response and adaptation. Although the present results can be generalized to any CCS, the generalization would be more reliable if it were based on a larger sample of CCSs.

This experiment was designed to ensure a precise control of the head-angle – using servomotor devices – in order to determine precisely the CCS intensity corresponding to each type of head-turn, based on the assumption that the centrifuge-velocity was set accurately. It turned out that the centrifuge velocity often drifted during the experiment by up to 1 rpm. The next series of experiments should fix this problem either by revising the centrifuge controller to make it more precise, or by monitoring the centrifuge-velocity closely during the experiment and correcting for its variability in the analysis.

There is an apparent correlation in the data between the perceived body-tilt for the head-turns to-NUP and the true angle of the GIF 16 inch away from the center of rotation. As already mentioned, however, it would be very helpful for the analysis to know the truncal anthropometric data of each subject in order to correlate the perceived tilt with the angle of the GIF at mid-chest level – or at some other appropriate position anthropometrically scaled separately to each subject. In case of a successful correlation, such data would potentially allow us to determine the true position of the center of the somatic graviceptors in the human body.

Finally, the severest limitation of this study arises from the eye-movement analysis package used. Several past studies performed in the Man-Vehicle Laboratory already mentioned some erratic problems related to this package. The time delay measured in this experiment between head-turns and detected eye-movements, however, suggests that the estimation of the SPV-peak amplitude obtained from the package is largely approximate and that the package itself might be outdated. This issue is a big concern not only because it leads to physiological measurements – supposed to be direct and accurate measures of the vestibular response – of poor quality, but also because there is no quick fix to the problem. As detailed in Section 4.1.9.2, the algorithm used to extract the SPV may not be adapted to the eye-movements analysis for head-turns that stimulates the SCC beyond a velocity threshold. There is no perfect solution to this problem, but future experiments could try to extrapolate the true SPV-peak amplitude from the measured SPV-peak amplitude, the VOR time-constant and the time delay between head-turn and eye-movements. Another solution would be to try to find a better algorithm, if possible, to analyze eye-movements.

6.4 Implication for incremental adaptation

This study was specifically designed to find out whether head-angle or centrifuge-velocity is the best choice for the incremental variable in an incremental adaptation procedure. As expected from our model of vestibular stimulation during centrifugation, the results show that centrifuge-velocity and head-angle (actually sine of the head-angle)

have a similar effect on the neurovestibular response: Changing the centrifuge-velocity or the sine of the head-angle by the same factor leads to a similar vestibular response change (Figure 6.10). This shows the validity of the CCS parameter and, thereby, demonstrates that centrifuge-velocity and head-angle are equally attractive candidates for the incremented variable during incremental adaptation.

The most important result is the connection between the amount of motion sickness created by a head-turn (motion sickness increment) and the intensity of the CCS. Figure 6.7 and Figure 6.8 show the quantitative relation between centrifuge-velocity, head-angle and motion sickness increment for the two experimental days. The motion sickness threshold[16] – level of CCS that preserves the degree of motion sickness level – is emphasized on the graph (thick black line). The motion sickness threshold – as well as the other contour lines – shifts substantially toward the top-right corner from Day 1 to Day 2. The shift demonstrates that adaptation occurs.

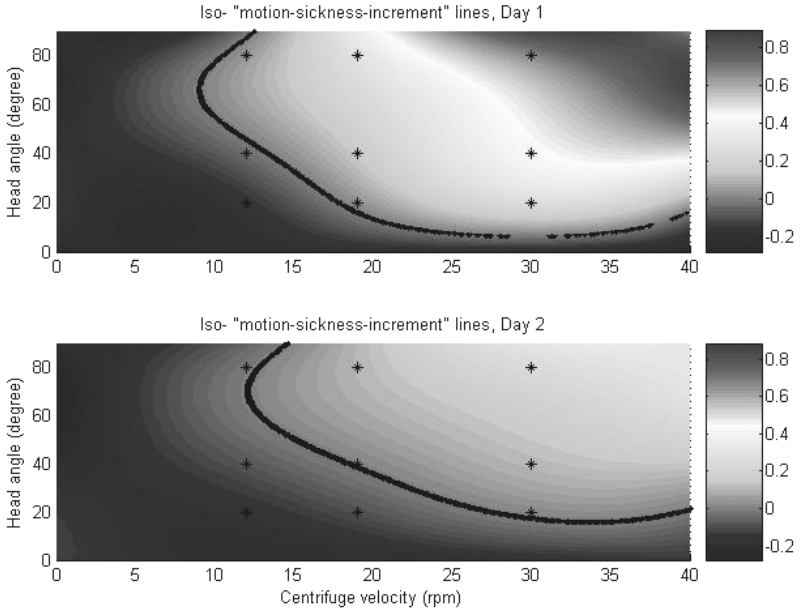

Figure 6.7. Motion sickness induced by a head-turn with respect to centrifuge-velocity and head-angle: (top) day 1, (bottom) day 2. Prediction based on the experimental results (third order polynomial extrapolation from both the raw data and the best linear fit). The thick black line marks the motion-sickness threshold and the nine stars the points actually tested in the experiment.

[16] The motion sickness threshold defines the CCS intensity for which the contribution of a head-turn to the motion sickness level is null. This is the limit between the head-turns that create motion sickness (above the threshold) and those that allow an amelioration of overall motion sickness score (below the threshold).

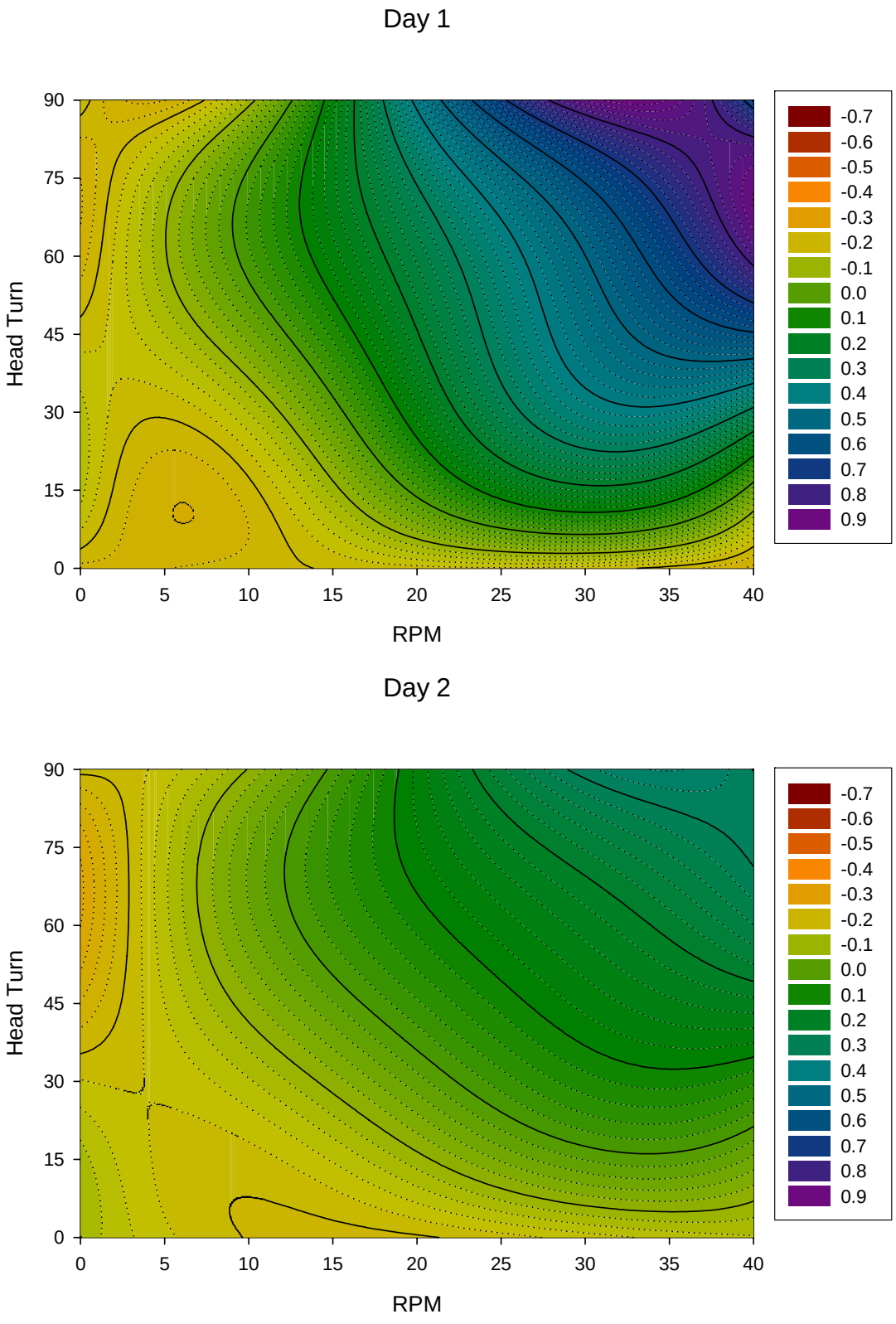

Figure 6.8. Contour map of motion sickness induced by a head-turn with respect to centrifuge-velocity and head-angle by day. The top-right corner is the highest point; the bottom-left, the lowest.

The quantitative results shown on Figure 6.7 and Figure 6.8 can be used to design an efficient incremental adaptation procedure: For any CCS intensity, the graphs give the discomfort associated with head-turns on the two experimental days. For example, the graphs suggest that a head-turn to 30° at 15 rpm on day 1 does not generate any motion sickness. Assuming the adaptation achieved is the same as in this experiment, the subject will be able to perform head-turns to 50° at 15 rpm – or to 30° at 22 rpm – on day 2 without experiencing any discomfort. An incremental adaptation procedure based on the head-angle could, therefore, require the subject to perform head-turns to 30° at 15 rpm on the first day, and to 50° at the same centrifuge-velocity on the second day. The subject will then adapt with no discomfort.

The amount of adaptation to each type of head-turn can be characterized, for a given measure, by the ratio of the result on the second day to that on the first. This ratio represents the fraction of the vestibular response on the first day that remains on the second: the smaller the ratio, the greater the adaptation. These adaptation coefficients for three measurements are shown on Figure 6.9.

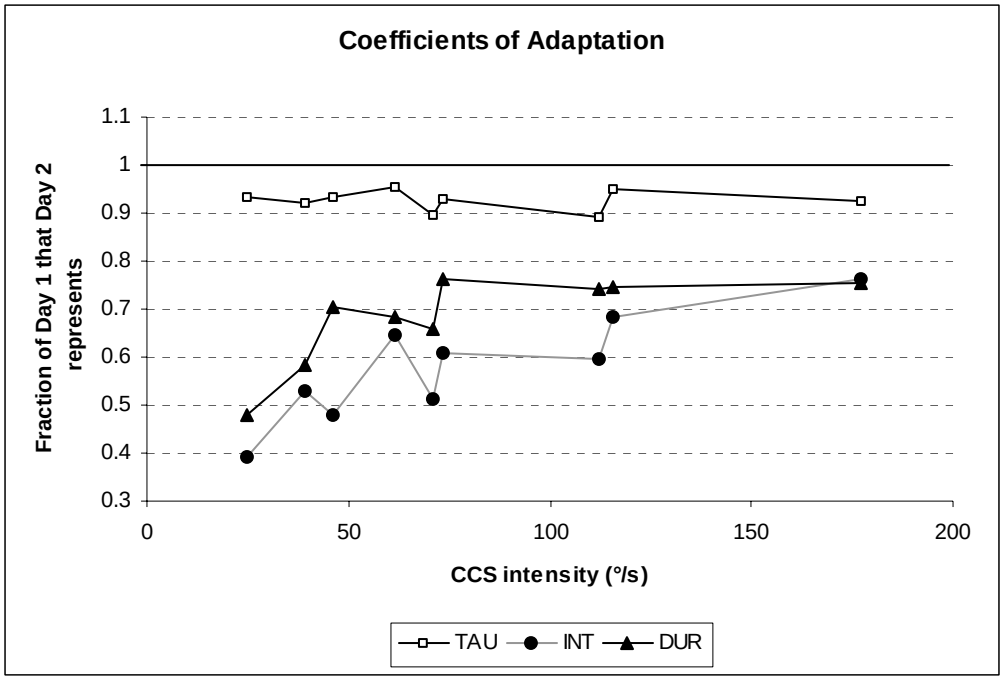

Figure 6.9. Coefficients of adaptation for three of the measurements: VOR time-constant (TAU), illusory motion intensity (INT), and duration (DUR). A coefficient of "1" means that no adaptation occurred.

To design an efficient incremental adaptation procedure, it is desirable to choose the CCS intensity that optimizes the gain of adaptation with respect to the discomfort. The adaptation pattern found – adaptation in both threshold and sensitivity – leads to the conclusion that smaller CCS intensity leads to stronger adaptation. This result, however, is misleading because in this experiment it is not possible to separate out the true amount of adaptation associated with each CCS intensity: The adaptation observed is not achieved by a single level of CCS, but is due to all of them at the same time. The next step, therefore, would be to determine the degree of adaptation corresponding to each level of CCS separately, and ultimately obtain the same plots as in Figure 6.8 and Figure 6.9 after adaptation to each level of CCS exclusively. A possible experiment could study three groups of subjects participating in a three-consecutive-day experiment. During the first and the third experimental days, the subjects would follow the protocol used in the present study; during the second day, each group would be exposed to a different CCS intensity (group 1 exposed to small CCS intensity, group 2, to medium CCS, and group 3, to high CCS). The adaptation coefficients found between the first and the last days would allow a comparison of the adaptation achieved by the different levels of CCS applied on day 2. This extension of the present experiment would allow us to find the CCS intensity that optimizes adaptation with respect to discomfort.

There is no difference between the effect of centrifuge-velocity and of head-angle on the adaptation pattern of the vestibular response: The amount of adaptation is, according to the experimental results, driven only by the CCS intensity. On the other hand, head-turns to small head-angles lead to shorter VOR time-constants than do head-turns to larger angles. Based on the hypothesis that the VOR time-constant is an indicator of the subject's motion sickness [56], head-turns to small head-angles at large centrifuge-velocity might lead to the same amount of adaptation as head-turns to large angles at small velocity – but with less discomfort. This finding suggests that it might be better to choose head-angle as the incremented variable. Unfortunately, the high variability in motion sickness seen in this experiment makes it hard to validate or reject this hypothesis.

Although it does not prove that head-angle is a better choice than centrifuge-velocity, the present study demonstrates that either one can be chosen as the incremented variable

to conduct incremental adaptation. As shown on Figure 6.10, the vestibular response is indeed driven by the CCS intensity, which regroups centrifuge-velocity and head-angle.

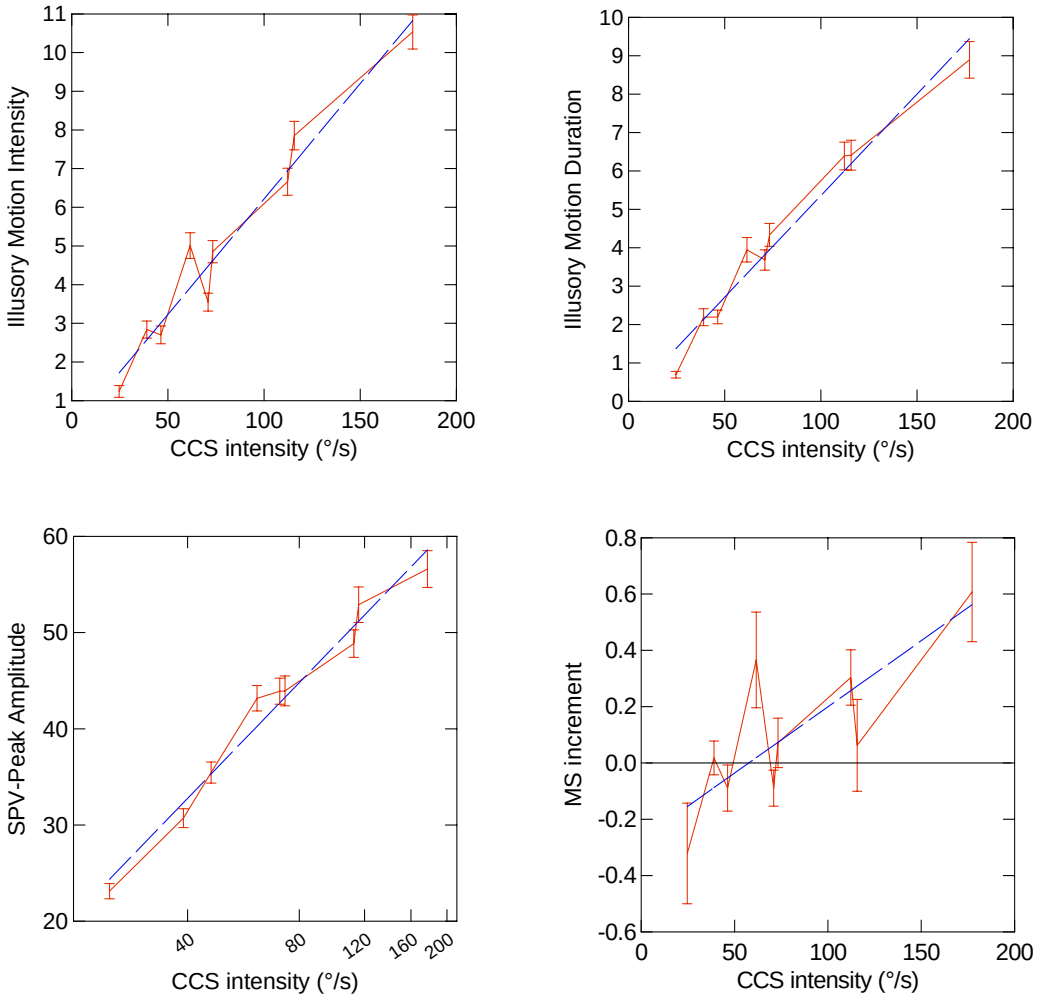

Figure 6.10. Validity of the CCS parameter: (a) illusory motion intensity, (b) illusory motion duration, (c) SPV-peak amplitude, (d) motion sickness increment. Experimental results in plain line and best linear fit in dashed line.

The validity of the CCS parameter has now been established and the next step toward developing an efficient incremental adaptation procedure is to establish the quantitative relationship between CCS intensity and adaptation.

7 Conclusion

One of the greatest technological challenges to human space exploration lies in the deconditioning of several vital body functions as a result of prolonged exposure to weightlessness. AG is a promising countermeasure to this deleterious effect because it treats all the symptoms at once, by attacking the problem at its root. Current technological constraints, however, restrict space applications of AG to short-radius centrifugation and correspondingly high rotation speeds. Unfortunately, head-turns performed while spinning at high rotation rates trigger, through cross-coupled stimulation, a disturbing vestibular response that includes disorienting sensations of self-motion, improper compensatory eye-movements and motion sickness.

The goal of this parametric study of vestibular stimulation was to investigate the quantitative aspect of the relationship among cross-coupled stimulus (CCS) intensity, neurovestibular response and adaptation. It aimed at demonstrating experimentally that the CCS, as defined in this thesis, is a valid model for the semi-circular canals stimulation by head-turns performed during centrifugation. The other objective was to contribute to the design of an efficient incremental adaptation procedure.

There was a very high correlation between CCS intensity and neurovestibular responses. This finding validates the use of the CCS parameter and shows that head-angle and centrifuge-velocity are equally attractive candidates for the incremented variable during incremental adaptation. Small head-angles were found to lead to shorter VOR time-constant than larger angles, which suggests that small head-angles could lead to less discomfort than larger angles would. This prediction, however, was not supported by the motion sickness results. Adaptation to the vestibular stimulation was, once again, successfully achieved over the two experimental days. There was no difference between the effect of centrifuge-velocity and sine of head-angle on vestibular adaptation but, surprisingly, adaptation was stronger to weaker CCS intensities. Finally the perceived body-tilt experienced by the subjects in the NUP position was very highly correlated with the true tilt of the GIF at mid-chest level.

These results support the hopes for using AG as a countermeasure to weightlessness since, on one hand, the human body interprets it as real gravity and, on the other hand, it seems possible to train humans to ignore the disturbing vestibular effects it generates. In addition, this study suggests that head-angle might be a better choice for the incremented variable during incremental adaptation. The quantitative relation investigated in this thesis demonstrates the centrality of the CCS parameter, further study, however, is necessary to gain a global quantitative understanding of the vestibular side-effect associated with AG. Future work, in particular, should establish the quantitative relation between CCS intensity and adaptation in order to empower the design of an efficient incremental adaptation procedure.

References

1. NASA, *The Vision for Space Exploration.* 2004.

2. Beckers, F., B. Verheyden, and A.E. Aubert, *Space Physiology.* Encyclopedia of Biomedical Engineering (in press), 2005.

3. NSBRI, *http://www.nsbri.org/.* Website, 2005.

4. Schimmerling, W., F.A. Cucinotta, and J.W. Wilson, *Radiation risk and human space exploration.* Adv Space Res, 2003. **31**(1): p. 27-34.

5. Wilson, J.W., et al., *Issues in deep space radiation protection.* Acta Astronaut, 2001. **49**(3-10): p. 289-312.

6. Grenon, S.M., et al., *Simulated microgravity induces microvolt T wave alternans.* Ann Noninvasive Electrocardiol, 2005. **10**(3): p. 363-70.

7. Howard, P., *The Vestibular System.* In "Handbook of Perception and Human Performance", New York: John Wiley, 1986.

8. Young, L.R., *Space and the vestibular system: what has been learned?* J Vestib Res, 1993. **3**(3): p. 203-6.

9. Lackner, J.R. and A. Graybiel, *The effective intensity of Coriolis, cross-coupling stimulation is gravitoinertial force dependent: implications for space motion sickness.* Aviat Space Environ Med, 1986. **57**(3): p. 229-35.

10. Shackelford, L.C., et al., *Resistance exercise as a countermeasure to disuse-induced bone loss.* J Appl Physiol, 2004. **97**(1): p. 119-29.

11. Edmonds, J.L., *Exercise in Artificial Gravity.* Unpublished SM Thesis, Department of Aeronautics and Astronautics, MIT - MVL, 2005.

12. Cavanagh, P.R., A.A. Licata, and A.J. Rice, *Exercise and pharmacological countermeasures for bone loss during long-duration space flight.* Gravit Space Biol Bull, 2005. **18**(2): p. 39-58.

13. Young, L.R., *Artificial Gravity.* Encyclopedia of Space Science and Technology, 2003. **1**: p. 138-151.

14. Young, L.R., *Artificial gravity considerations for a mars exploration mission.* Ann N Y Acad Sci, 1999. **871**: p. 367-78.

15. Marmet, P., *Einstein's Theory of Relativity Versus Classical Mechanics.* Newton Physics Books, http://www.newtonphysics.on.ca/EINSTEIN/Chapter10.html, 1997.

16. Graybiel, A., et al., *Effects Of Exposure To A Rotating Environment (10 Rpm) On Four Aviators For A Period Of Twelve Days.* Aerosp Med, 1965. **36**: p. 733-54.

17. Burton, R.R. and L.J. Meeker, *Physiologic validation of a short-arm centrifuge for space application.* Aviat Space Environ Med, 1992. **63**(6): p. 476-81.

18. Hecht, H., E.L. Brown, and L.R. Young, *Adapting to artificial gravity (AG) at high rotational speeds.* J Gravit Physiol, 2002. **9**(1): p. P1-5.

19. Moore, S.T., et al., *Artificial gravity: a possible countermeasure for post-flight orthostatic intolerance.* Acta Astronaut, 2005. **56**(9-12): p. 867-76.

20. Moore, S.T., et al., *Ocular counterrolling induced by centrifugation during orbital space flight.* Exp Brain Res, 2001. **137**(3-4): p. 323-35.

21. Hastreiter, D. and L.R. Young, *Effects of a gravity gradient on human cardiovascular responses.* J Gravit Physiol, 1997. **4**(2): p. P23-6.

22. DiZio, P. and J.R. Lackner, *Sensorimotor aspects of high-speed artificial gravity: III. Sensorimotor adaptation.* J Vestib Res, 2002. **12**(5-6): p. 291-9.

23. Lackner, J.R. and P.A. DiZio, *Adaptation to rotating artificial gravity environments.* J Vestib Res, 2003. **13**(4-6): p. 321-30.

24. Young, L.R., et al., *Artificial gravity: head movements during short-radius centrifugation.* Acta Astronaut, 2001. **49**(3-10): p. 215-26.

25. Pavlou, M., et al., *Simulator based rehabilitation in refractory dizziness.* J Neurol, 2004. **251**(8): p. 983-95.

26. Nowe, V., et al., *The interutricular distance determined from external landmarks.* J Vestib Res, 2003. **13**(1): p. 17-23.

27. NASA, *http://weboflife.nasa.gov/learningResources/vestibularbrief.htm.* Website, 2005.

28. Della Santina, C.C., et al., *Orientation of Human Semicircular Canals Measured by Three-Dimensional Multiplanar CT Reconstruction.* J Assoc Res Otolaryngol, 2005: p. 1-16.

29. Highstein, S.M., R.R. Fay, and A.N. Popper, *The Vestibular System.* Springer Verlag New York, Inc, 2003.

30. Peters, R.A., *Dynamics of the vestibular system and their relation to motion perception, spatial disorientation, and illusions. NASA CR-1309.* NASA Contract Rep NASA CR, 1969: p. 1-223.

31. Carey, J., *http://www.bme.jhu.edu/labs/chb/courses/strucfunc/2004_10_05.pdf.* Whitaker Institute at Johns Hopkins, Class notes, 2006.

32. Steinhausen, W., *Ber die beodachtung der cupula in den bogengangsampullen des labyrinths des lebenden hechts.* Pflgers Arch, 1933. **232**: p. 500-512.

33. Fernandez, C. and J.M. Goldberg, *Physiology of peripheral neurons innervating semicircular canals of the squirrel monkey. II. Response to sinusoidal stimulation and dynamics of peripheral vestibular system.* J Neurophysiol, 1971. **34**(4): p. 661-75.

34. Oman, C.M., E.N. Marcus, and I.S. Curthoys, *The influence of semicircular canal morphology on endolymph flow dynamics. An anatomically descriptive mathematical model.* Acta Otolaryngol, 1987. **103**(1-2): p. 1-13.

35. Adenot, S., *Artificial Gravity: Changing the Intensity of Coriolis Cross-Coupled Stimulus with Head-Angle.* Unpublished SM Thesis, Department of Aeronautics and Astronautics, MIT - MVL, 2004.

36. Young, L.R. and C.M. Oman, *Model for vestibular adaptation to horizontal rotation.* Aerosp Med, 1969. **40**(10): p. 1076-80.

37. Fernandez, C. and J.M. Goldberg, *Physiology of peripheral neurons innervating otolith organs of the squirrel monkey. I. Response to static tilts and to long-duration centrifugal force.* J Neurophysiol, 1976. **39**(5): p. 970-84.

38. Fernandez, C. and J.M. Goldberg, *Physiology of peripheral neurons innervating otolith organs of the squirrel monkey. II. Directional selectivity and force-response relations.* J Neurophysiol, 1976. **39**(5): p. 985-95.

39. Bos, J.E. and W. Bles, *Theoretical considerations on canal-otolith interaction and an observer model.* Biol Cybern, 2002. **86**(3): p. 191-207.

40. Peterka, R.J., *Torsional vestibulo-ocular reflex measurements for identifying otolith asymmetries possibly related to space motion sickness susceptibility.* Acta Astronaut, 1994. **33**: p. 1-8.

41. Diamond, S.G. and C.H. Markham, *Ocular torsion as a test of the asymmetry hypothesis of space motion sickness.* Acta Astronaut, 1992. **27**: p. 11-7.

42. Diamond, S.G. and C.H. Markham, *Ocular torsion in upright and tilted positions during hypo- and hypergravity of parabolic flight.* Aviat Space Environ Med, 1988. **59**(12): p. 1158-62.

43. Diamond, S.G. and C.H. Markham, *Prediction of space motion sickness susceptibility by disconjugate eye torsion in parabolic flight.* Aviat Space Environ Med, 1991. **62**(3): p. 201-5.

44. Markham, C.H. and S.G. Diamond, *Further evidence to support disconjugate eye torsion as a predictor of space motion sickness.* Aviat Space Environ Med, 1992. **63**(2): p. 118-21.

45. Goldberg, J.M. and C. Fernandez, *Physiology of peripheral neurons innervating semicircular canals of the squirrel monkey. III. Variations among units in their discharge properties.* J Neurophysiol, 1971. **34**(4): p. 676-84.

46. Curthoys, I.S., et al., *Off-center yaw rotation: effect of naso-occipital linear acceleration on the nystagmus response of normal human subjects and patients after unilateral vestibular loss.* Exp Brain Res, 1998. **123**(4): p. 425-38.

47. Raphan, T. and B. Cohen, *The vestibulo-ocular reflex in three dimensions.* Exp Brain Res, 2002. **145**(1): p. 1-27.

48. Dai, M., et al., *Model-based study of the human cupular time constant.* J Vestib Res, 1999. **9**(4): p. 293-301.

49. Goldberg, J.M. and C. Fernandez, *Physiology of peripheral neurons innervating semicircular canals of the squirrel monkey. I. Resting discharge and response to constant angular accelerations.* J Neurophysiol, 1971. **34**(4): p. 635-60.

50. Raphan, T., V. Matsuo, and B. Cohen, *Velocity storage in the vestibulo-ocular reflex arc (VOR).* Exp Brain Res, 1979. **35**(2): p. 229-48.

51. Oman, C.M., *Motion sickness: a synthesis and evaluation of the sensory conflict theory.* Can J Physiol Pharmacol, 1990. **68**(2): p. 294-303.

52. Reason, J.T. and J.J. Brand, *Motion Sickness.* Academic Press Inc (London) Ltd, 1975.

53. Oman, C.M., *A heuristic mathematical model for the dynamics of sensory conflict and motion sickness.* Acta Otolaryngol Suppl, 1982. **392**: p. 1-44.

54. Brown, E.L., H. Hecht, and L.R. Young, *Sensorimotor aspects of high-speed artificial gravity: I. Sensory conflict in vestibular adaptation.* J Vestib Res, 2002. **12**(5-6): p. 271-82.

55. Lyne, L.E., *Artificial Gravity: Evaluation of Adaptation to Head Movements During Short-Radius Centrifugation Using Subjective Measures.* Unpublished SM Thesis, Department of Aeronautics and Astronautics, MIT - MVL, 2000.

56. Dai, M., et al., *The relation of motion sickness to the spatial-temporal properties of velocity storage.* Exp Brain Res, 2003. **151**(2): p. 173-89.

57. Adenot, S., T. Jarchow, and L.R. Young, *Adaptation of VOR to Coriolis Stimulation.* Ann N Y Acad Sci, 2005. **1039**: p. 88-96.

58. Garrick-Bethell, I., *Cross plane transfer of vestibular adaptation to human centrifugation.* Unpublished SM Thesis, Department of Aeronautics and Astronautics, MIT - MVL, 2004.

59. Young, L.R., et al., *Adaptation of the vestibulo-ocular reflex, subjective tilt, and motion sickness to head movements during short-radius centrifugation.* J Vestib Res, 2003. **13**(2-3): p. 65-77.

60. Guedry, F.E., Jr., W.E. Collins, and A. Graybiel, *Vestibular Habituation During Repetitive Complex Stimulation: A Study Of Tranfer Effects.* J Appl Physiol, 1964. **19**: p. 1005-15.

61. Brown, E.L., *Artificial Gravity: The Role of Visual Inputs in Adaptation to Short-Radius Centrifugation.* Unpublished SM Thesis, Department of Aeronautics and Astronautics, MIT - MVL, 2002.

62. Bruni, S., *Artificial Gravity: Neurovestibular Adaptation to Incremental Exposure to Centrifugations.* Unpublished SM Thesis, Department of Aeronautics and Astronautics, MIT - MVL, 2004.

63. Newby, N.J., *Artificial Gravity: The Role of Graviceptive Information during Cross-Coupled Rotation in Context-Specific Adaptation.* Unpublished SM Thesis, Department of Aeronautics and Astronautics, MIT - MVL, 2002.

64. Meliga, P., et al., *Artificial gravity--head movements during short-radius centrifugation: influence of cognitive effects.* Acta Astronaut, 2005. **56**(9-12): p. 859-66.

65. Yakushin, S.B., T. Raphan, and B. Cohen, *Gravity-specific adaptation of the angular vestibuloocular reflex: dependence on head orientation with regard to gravity.* J Neurophysiol, 2003. **89**(1): p. 571-86.

66. Mast, F.W., N.J. Newby, and L.R. Young, *Sensorimotor aspects of high-speed artificial gravity: II. The effect of head position on illusory self motion.* J Vestib Res, 2002. **12**(5-6): p. 283-9.

67. Holly, J.E., *Perceptual disturbances predicted in zero-g through three-dimensional modeling.* J Vestib Res, 2003. **13**(4-6): p. 173-86.

68. Graybiel, A. and J. Knepton, *Bidirectional overadaptation achieved by executing leftward or rightward head movements during unidirectional rotation.* Aviat Space Environ Med, 1978. **49**(1 Pt 1): p. 1-4.

69. Tweed, D., et al., *Rotational kinematics of the human vestibuloocular reflex. I. Gain matrices.* J Neurophysiol, 1994. **72**(5): p. 2467-79.

70. Diamandis, P.H., *The artificial gravity sleeper: a deconditioning countermeasure for long duration space habitation.* Unpublished SM Thesis, Department of Aeronautics and Astronautics, MIT - MVL, 1988.

71. Cheung, C.C., *Regulator Control of a Short-Radius Centrifuge and Subjective Response to Head Movements in a Rotating Environment.* Unpublished SM Thesis, Department of Aeronautics and Astronautics, MIT - MVL, 2000.

72. Balkwill, M.D., *Changes in Human Horizontal Angular VOR After the Spacelab SLS-1 Mission.* Unpublished SM Thesis, Department of Aeronautics and Astronautics, MIT - MVL, 1992.

73. Engelken, E.J. and K.W. Stevens, *A new approach to the analysis of nystagmus: an application for order-statistic filters.* Aviat Space Environ Med, 1990. **61**(9): p. 859-64.

74. Engelken, E.J., K.W. Stevens, and J.D. Enderle, *Development of a non-linear smoothing filter for the processing of eye-movement signals.* Biomed Sci Instrum, 1990. **26**: p. 5-10.

75. Engelken, E.J., et al., *Application of robust data processing methods to the analysis of eye movements.* Biomed Sci Instrum, 1996. **32**: p. 7-11.

76. Engelken, E.J., K.W. Stevens, and J.D. Enderle, *Optimization of an adaptive nonlinear filter for the analysis of nystagmus.* Biomed Sci Instrum, 1991. **27**: p. 163-70.

77. Hess, B.J. and D.E. Angelaki, *Kinematic principles of primate rotational vestibulo-ocular reflex. I. Spatial organization of fast phase velocity axes.* J Neurophysiol, 1997. **78**(4): p. 2193-202.

78. Vaitl, D., et al., *Shifts in blood volume alter the perception of posture: further evidence for somatic graviception.* Int J Psychophysiol, 2002. **44**(1): p. 1-11.

79. Saborowski, R., D. Vaitl, and R. Stark, *Perception of posture and cerebral blood flow.* Int J Psychophysiol, 2002. **43**(2): p. 167-75.

80. Vaitl, D., H. Mittelstaedt, and F. Baisch, *Shifts in blood volume alter the perception of posture.* Int J Psychophysiol, 1997. **27**(2): p. 99-105.

Appendix A – Technical Drawings

Technical drawings of the servomotor device used to constraint the angle of the head-turns performed by the subject during the experiment. All dimensions are in tenths of an inch. All pieces were made out of aluminum. A piano wire was used to connect the shifting bolt to the servomotor. The stationary bolt was attached to the plate that was screwed to the servomotor.

The drawings were made using SolidWorks^{TM}, 2005 Educational Edition.

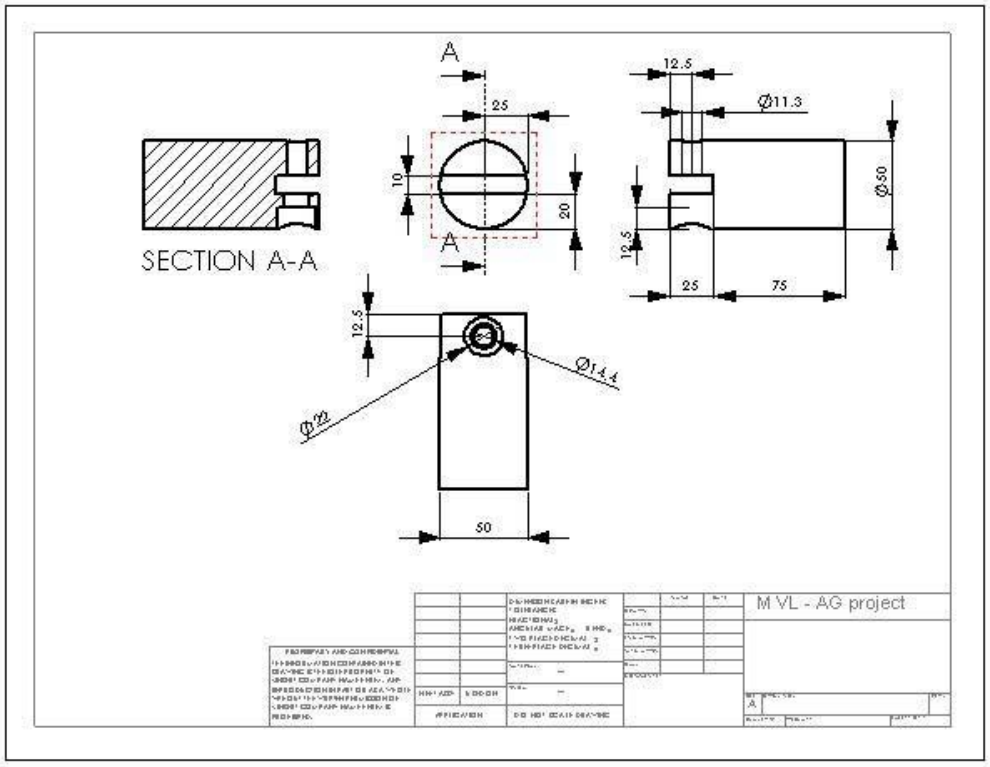

Shifting bolt

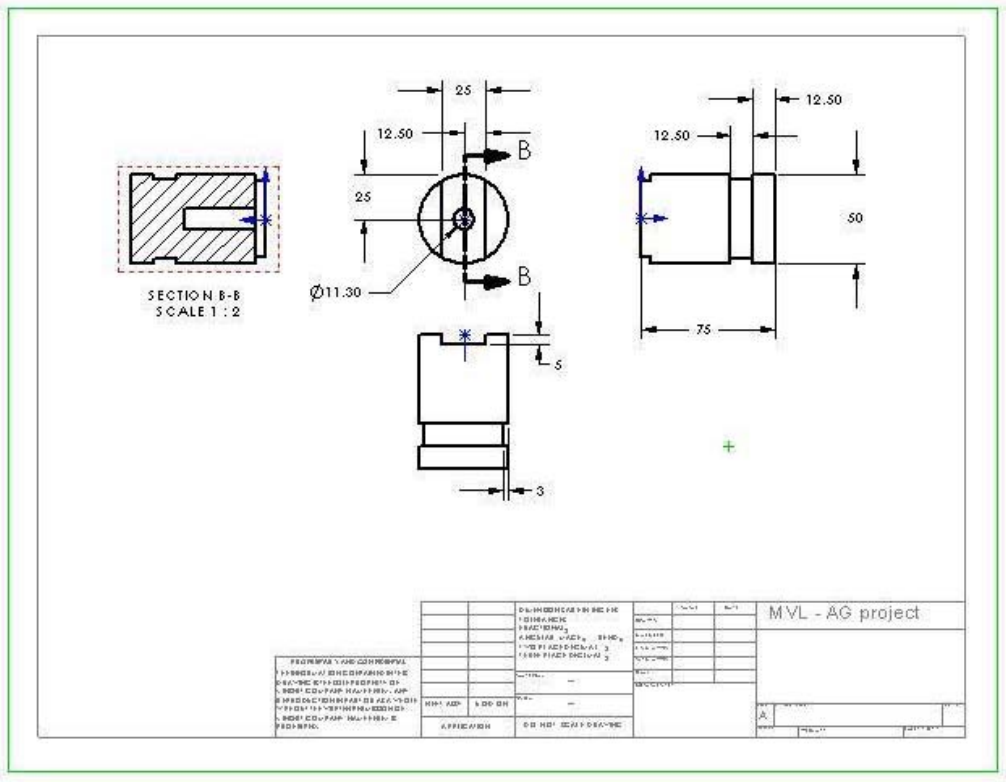

Stationary bolt

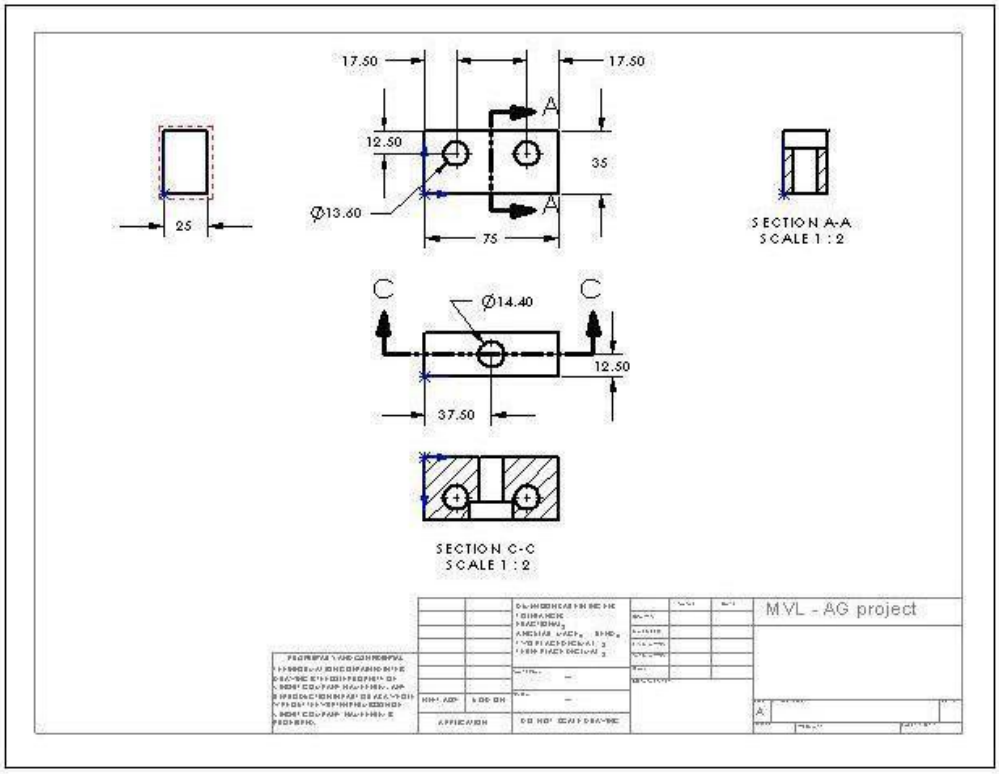

Plate

Appendix B – Consent Form

CONSENT TO PARTICIPATE IN NON-BIOMEDICAL RESEARCH

Neurovestibular Aspects of Artifical Gravity: Toward a Comprehensice Countermeasure.

You are asked to participate in a research study conducted by Laurence Young, Sc.D., from the Department of Aeronautics and Astronautics at the Massachusetts Institute of Technology (M.I.T.) The NASA Johnson Space Center is also participating in this study. The results of this study may be published in a student thesis or scientific journal. You were selected as a possible participant in this study because you volunteered and meet the minimum health and physical requirements. You should read the information below, and ask questions about anything you do not understand, before deciding whether or not to participate.

PARTICIPATION AND WITHDRAWAL

Your participation in this study is completely voluntary and you are free to choose whether to be in it or not. If you choose to be in this study, you may subsequently withdraw from it at any time without penalty or consequences of any kind. The investigator may withdraw you from this research if circumstances arise which warrant doing so. Such circumstances include evidence that you do not meet the minimum health and physical requirements, or that during the study it becomes clear to the experimenter that are becoming drowsy, unalert, or uncooperative.

You should not participate in this study if you have any medical heart conditions, respiratory conditions, medical conditions which would be triggered if you develop motion sickness, are under the influence of alcohol, caffeine, anti-depressants, or sedatives, have suffered in the past from a serious head injury (concussion), or if there is any possibility that you may be pregnant. The experimenter will check to see if you meet these requirements.

PURPOSE OF THE STUDY

The purpose of this study is to understand the cognitive and physiological effects of short-radius centrifugation used to produce Artificial Gravity (AG). Short radius centrifugation is currently being investigated as a countermeasure to the deleterious effects of weightlessness experienced during long duration spaceflight.

PROCEDURES USED IN THIS STUDY

If you volunteer to participate in this study, we would ask you to do the following things: When you arrive at the lab, you will be briefed on the background of centrifugation, disqualifying medical conditions, the experiment protocol, and the various components of the centrifuge, including the emergency stop button, restraining belt, and data collection devices. Data collection devices include goggles that monitor your eye movement, heart rate sensors, and sensors that detect your head movement. After your briefing, the experimenter will record your answers to basic questions about your health, and take your height, weight, blood pressure, and heart rate.

During the experiment you will he on the centrifuge In either the supine position, the prone position, or on the side on the rotator bed You may be asked to place your head Into a cushioned

pivoting helmet at the center of the centrifuge that limits your head movement to one or several rotational axes After lying down, the experimenter may collect some data while the centrifuge is stationary. The experimenter will ask you if you are ready before starting rotation. Your rotation on the AGs will not exceed the following parameters:

- Acceleration no greater than 5 revolutions per minute, per second
- G-level along you body axis will not exceed 2.0G at your feet (a "1G" is defined as the acceleration or force that you experience normally while standing on earth)
- Time of rotation not exceeding 1 hour

During rotation the experimenter may direct you to make voluntary head movements or to perform simple tasks such as adjusting a line of lights or reading portions of text. A possible protocol for an actual trial will consist of a short period of supine rest in the dark, followed by a period of head movements (ranging from 90 degrees to the left, to vertical, to 90 degrees to the right) In the dark, followed by a period of similar head movements In the light, and that this trial could be repeated many times. During these head movements, your head should move at approximately a speed of 0.25 meters per second.

During and after the experiment you will be asked to report your subjective experience (how you feel, how you perceive your head movements, etc.). During and after the experiment you will be asked to report your motion sickness rating. This data will be recorded anonymously.

When the experiment is complete, the centrifuge will be stopped, and the experimenter may collect some additional data.

As a participant in experimental trials, you tentatively agree to return for additional trials (at most 10) requested by the experimenter. You may or may not be assigned to a study group that performs similar tasks. Other than the time required for rotation, the time commitment is 20 minutes for the first briefing, and 10-60 minutes for other procedures before and after rotation.

POTENTIAL RISKS AND DISCOMFORTS

During rotation you may develop a headache or feel pressure In your legs caused by a fluid shift due to centrifugation You may also experience nausea or motion sickness, especially as a result of the required head movements You will not be forced to make any head movements If you experience any discomfort, you are free to discontinue head movements at any time. The experimenter will frequently ask you about your motion sickness to ensure your comfort. You may also feel sleepy during the experiment, and the experimenter will monitor your alertness through communication and through a video camera.

ANTICIPATED BENEFITS TO SUBJECTS

You will receive no benefits from this research.

ANTICIPATED BENEFITS TO SOCIETY

The potential benefits to science and society are a better understanding of how short radius centrifugation can enable long duration spaceflight.

PAYMENT FOR PARTICIPATION

Eligible subjects will receive payment of $10/hr for their participation. Checks wil1 be mailed within 4-6 weeks of participation. Subjects not eligible for compensation include international students who work more than 20 hours per week, or volunteers from the M.I.T. Man Vehicle Lab.

PRIVACY AND CONFIDENTIALITY

Any information that 1s obtained In connection with this study and that can be identified with you will remain confidentla1 and will be disclosed only with your permission or as required by law.

Some of the data collected in this study may be published In scientific journals and student theses, or archived with the National Space Biomedical Research Institute. The data may consist of measurements of your eye movement, subjective ratings of illusions experienced during centrifugation, subjective descriptions of your experience during centrifugation, measurements related to your subjective orientation in space, measurements of your cognitive abilities before, during, and after centrifugation, subjective ratings of your motion sickness, and heart rate.

During the experiment, the experimenter will monitor you through a video camera capable of imaging in darkness. You will be monitored to ensure your state of well being and compliance with the experiment protocol. In some cases the video data will be recorded on VHS tapes. You have a right to review and edit the tape. Any recorded videotapes will be accessible only by members of the current Artificial Gravity research team. Videotapes will be erased in *5* years, at most.

Research data collected during the experiment is stored in coded files that contain no personal information. This coding of the data will prevent linking your personal data to research data when it is analyzed or archived. Research data is stored in Microsoft excel files and ASCII files, and there is no certain date for destruction. The data is stored in Man Vehicle Lab computers that remain accessible only by Artificial Gravity team members, except data archived with the National Space Biomedical Research Institute. The investigator will retain a record of your participation so that you may be contacted in the future should your data be used for purposes other than those described here.

EMERGENCY CARE AND COMPENSATION FOR INJURY

"In the unlikely event of physical injury resulting from participation in this research you may receive medical treatment from the M.I.T. Medical Department, including emergency treatment and follow-up care as needed. Your insurance carrier may be billed for the cost of such treatment. M.I.T. does not provide any other form of compensation for injury. Moreover, in either providing or making such medical care available it does not imply the injury is the fault of the investigator. Further information may be obtained by calling the MIT Insurance and Legal Affairs Office at 1-617-253 2822."

IDENTIFICATION OF INVESTIGATORS

If you have any questions or concerns about the research, please feel free to contact:

Principle Investigator: Laurence Young (37-219) 77 Massachusetts Avenue Cambridge, MA 02139 (617) 253-7759	

RIGHTS OF RESEARCH SUBJECTS

You are not waiving any legal claims, rights or remedies because of your participation in this research study. If you feel you have been treated unfairly, or you have questions regarding your lights as a research subject, you may contact the Chairman of the Committee on the Use of Humans as Experimental Subjects, M.I.T., Room E23-230, 77 Massachusetts Ave, Cambridge, MA 02139, phone 1-617-253 4909.

SIGNATURE OF RESEARCH SUBJECT OR LEGAL REPRESENTATIVE

I have read (or someone has read to me) the information provided above. I have been given an opportunity to ask questions and all of my questions have been answered to my satisfaction. I have been given a copy of this form.

BY SIGNING THIS FORM, I WILLINGLY AGREE TO PARTICIPATE IN THE RESEARCH IT DESCRIBES.

_____
Name of Subject

_____
Name of Legal Representative (if applicable)

_____ _____
Signature of Subject or Legal Representative Date

SIGNATURE OF INVESTIGATOR

I have explained the research to the subject or his/her legal representative, and answered all of his/her questions. I believe that he/she understands the information described in this document and freely consents to participate.

_____
Name of Investigator

_____ _____
Signature of Investigator Date (must be the same as subject's)

SIGNATURE OF WITNESS (If required by COUHES)

My signature as witness certified that the subject or his/her legal representative signed this consent form in my presence as his/her voluntary act and deed.

_____ _____
Name of Witness Date

Appendix C – Protocol's Checklist

SET-UP

Go to the lab and check everything before the subject arrives

Turn on computers (ISCAN & control), power supply, eye cameras, control box	☐
Turn on onboard computer and make sure network connection works	☐
Unplug everything and secure wires	☐
Check if there is enough memory on HD (ISCAN), need about 200 megs	☐
Adjust the slider (with/without helmet), and fix it if necessary – Find the blindfold	☐
Ensure there is nothing unsafe on the bed	☐
Perform a test run, test in particular servomotors to switch head-angle configurations	☐

Explain the experiment, making sure the subject is eligible

Explain the experiment and the potential hazards to the subject	☐
Make sure the subject understands the risks and what is expected from him	☐
Ensure the consent form is signed and the MS questionnaire is completed	☐
Ask the subject to remove everything from his pockets	☐
Install the subject onto the bed (be sure the controller is off) with the iron horse in place	☐
Adjust the footplate (put pins in) and give the goggles to the subject	☐
Secure subject's feet, fasten the safety belt and give him the emergency button	☐
Explain emergency stop and run over the protocols again (practice HT)	☐
Put up experiment in progress sign, close the door and turn off centrifuge light	☐

PRE-PHASE

Run the calibration sequence (Center dot, L, R, C, U, D, C) once in calibration mode	☐
Start recording, do the calibration again 3 times (stop recording at the end)	☐
Blindfold subject, turn off all lights, close curtains	☐
Start recording eye data, do the pre-phase (6 HT) and stop recording at the end	☐

MAIN-PHASE *(Start the centrifuge)*

Check that the centrifuge speed is set to 0 and that the mode is on manual	☐
Manually do a whole turn with the bed to check that there is nothing in the way	☐
Ask the subject if he is ready to spin	☐
Start-up the centrifuge and slowly spin up the bed to the desired speed	☐
Start recording eye data before each phase (Pre / Stim / Post) and stop after	☐
Make sure the motion sickness of the subject does not go above 13	☐
Check that the subject is opening his eyes wide 20s after each head-turn	☐

POST-PHASE

Stop the centrifuge: set the speed to 0 and stop the controller (wait for complete stop)	☐
Turn off the controller	☐
Start recording eye data, do the post phase (6HT), stop recording	☐
Remove blindfold and do the calibration again 3 times while recording	☐
Lock the bed with the footstool and the C-clamp	☐
Save data (as *.raw and *.txt extensions for raw and ASCII files)	☐
Ask the subject his impressions especially on the illusory motion sensation	☐
Give the subject the compensation form to be completed	☐
Remove the experiment sign and turn everything off (plug the batteries back in)	☐

Appendix D – Basics of Centrifuge Tests

(Paul Elias, Man-Vehicle Lab)

-Artificial gravity resulting from centrifugation provides a potential countermeasure to the adverse effects of weightlessness experienced by astronauts.

- Head turns made in a rotating environment (e.g. on a centrifuge) elicit a vestibular response that sometimes leads to sensations of motion sickness, tumbling, and perceived body tilt.

- The Artificial Gravity Team in the Man-Vehicle Lab is interested in how people adapt to various types of head turns during centrifugation.

- The test protocol consists of making a series of head turns while lying supine and rotating on the centrifuge. The centrifuge is a 2-meter rotating bed that can accommodate subjects up to 220lb.

- To learn about the vestibular response and the process of adaptation, we record several measures throughout the centrifugation, including: a) motion sickness b) duration of tumbling sensation c) intensity of tumbling sensation d) perceived body tilt e) eye movements

- Motion sickness is recorded on a 0 – 20 scale, as verbally reported by the subject

- Duration of tumbling sensation is recorded by having the subject depress a button throughout the perceived sensation

- Intensity of tumbling sensation is reported relative to the first sensation perceived, as indicated by the subject (First sensation intensity = 10, all subsequent sensations relative to 10)

- Body tilt is reported based on the direction the feet are perceived to be pointing (Reference frame is to imagine one's body as a minute hand on a clock, feet pointing radially outward: Feet pointing at 45 minutes implies a sensation of being horizontal, feet at 30 minutes implies a sensation of standing up, etc.

- Eye movements are recorded using a monitoring system that involves the subject donning a pair of modified ski goggles

- Subjects should be well rested and in good health, with no history of vestibular, cardiovascular, respiratory, or hearing problems. Subjects should not participate if there is any possibility of being pregnant. Subjects should not consume alcohol or caffeine 24 hours prior to centrifugation, and should not be under the influence of anti-depressants or sedatives during the experiment.

Appendix E – Autocorrelation Plot

Motion sickness increment autocorrelation plot: the motion sickness increments are only slightly correlated with each other compared to the motion sickness scores.

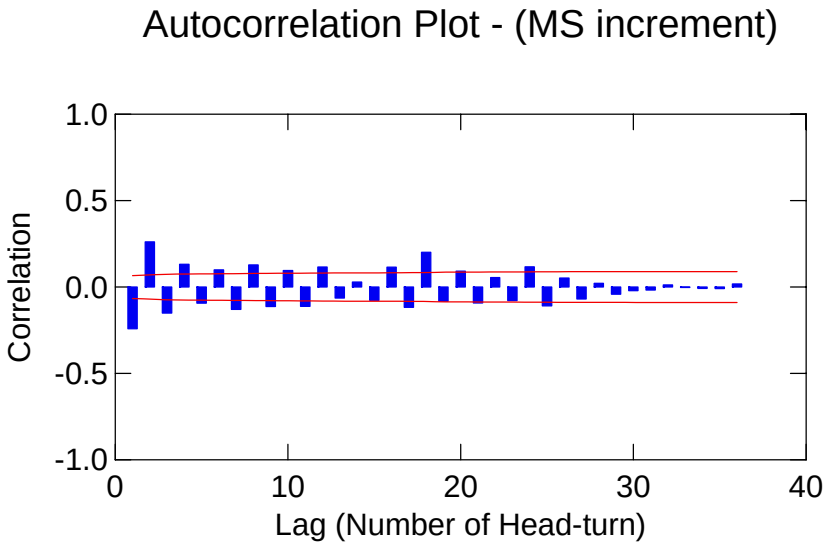

Appendix F – Body-tilt plots

Individual body-tilt plots for each subject during the whole experiment. The first 60 head-turns belong to the first experimental day and the last 60 to the second. The 11 subjects retained for the body-tilt statistical analysis are: 101, 105-107, 111, 114-117, 119 and 121.

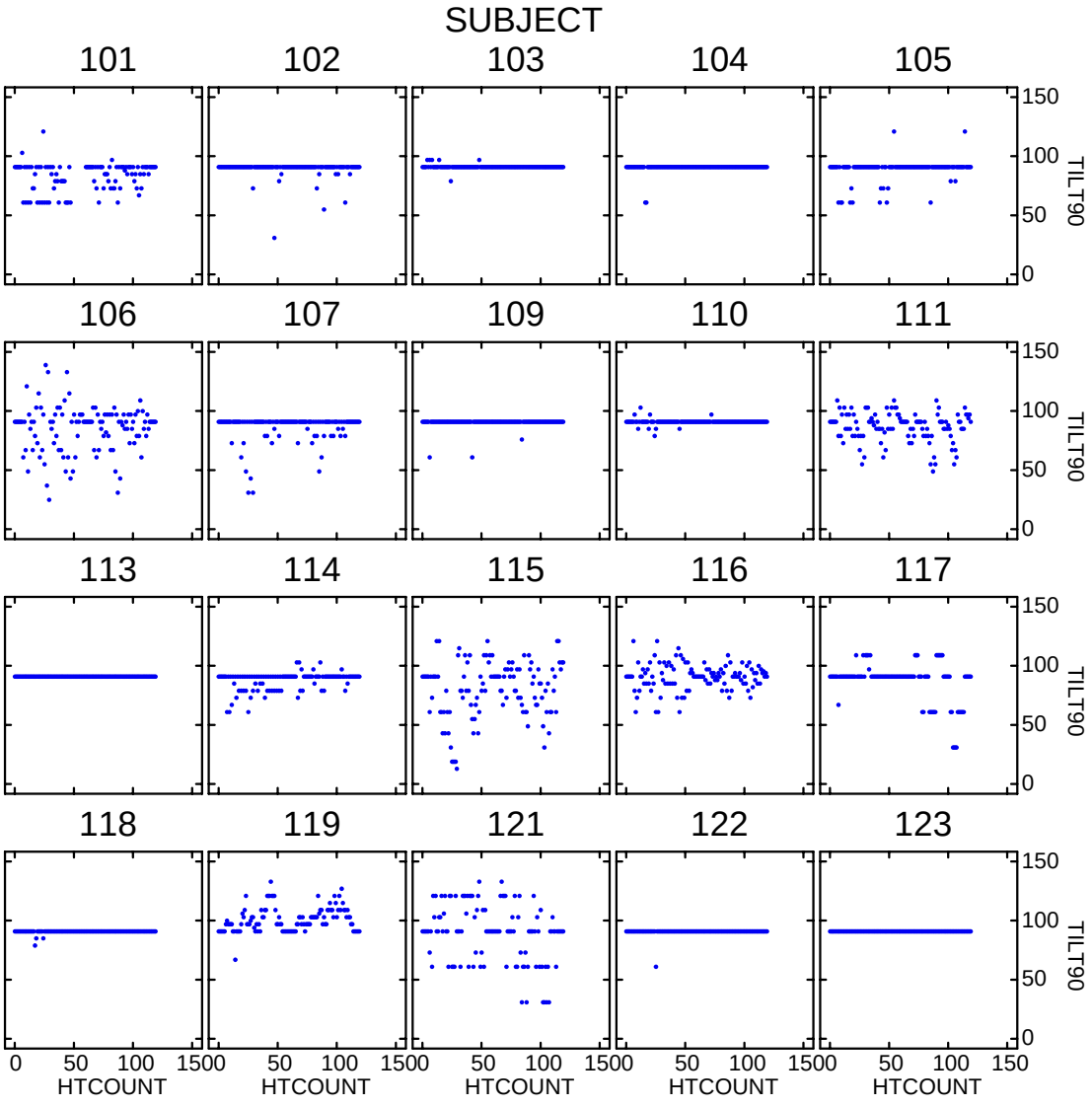

Appendix G – Motion Sickness plots

Individual motion sickness plots for each subject during the whole experiment (motion sickness scores). The first 60 head-turns belong to the first experimental day and the last 60 to the second. The 7 subjects retained for the motion sickness statistical analysis are: 101, 104, 113, 114, 116, 117 and 119.

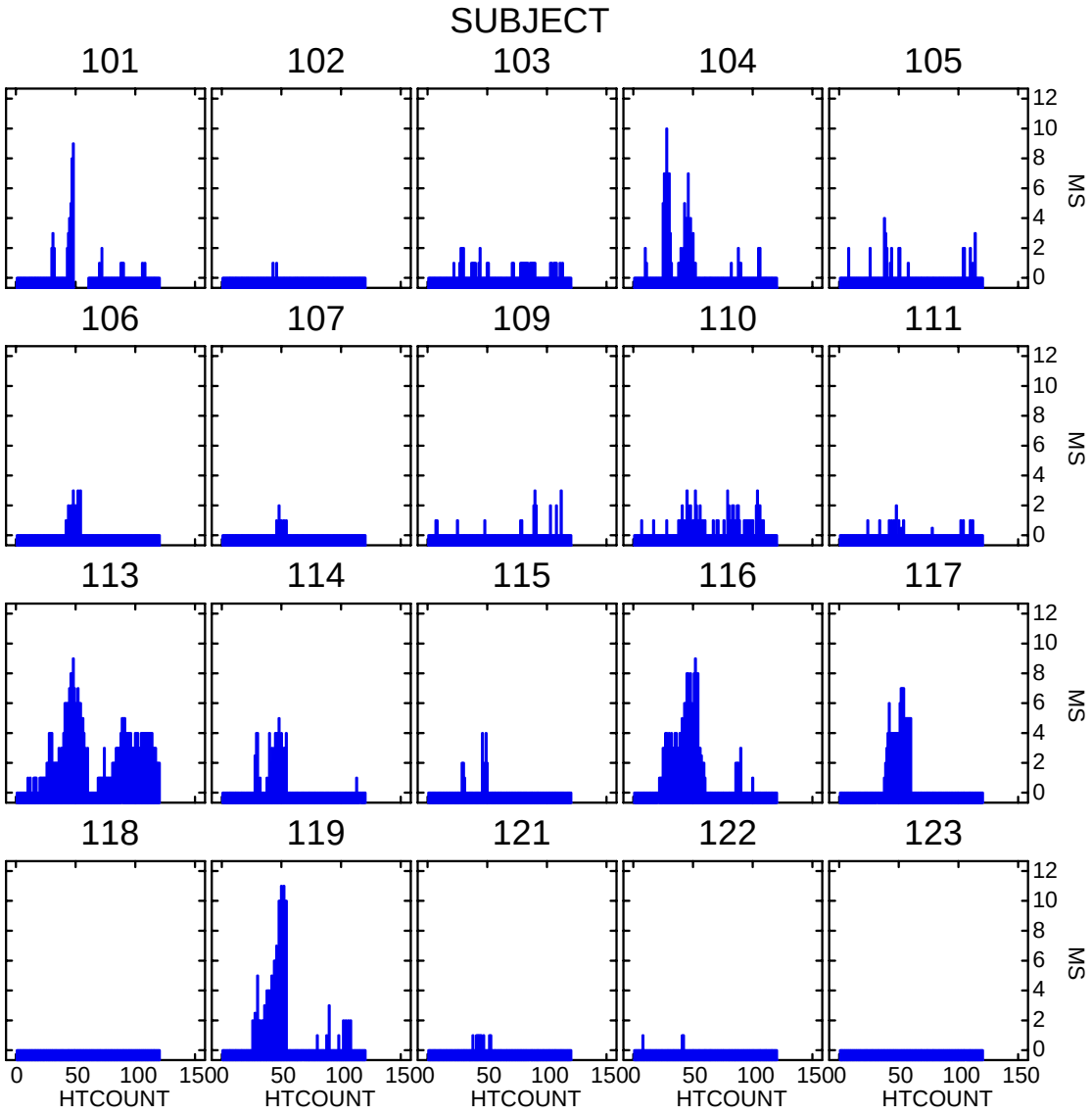

Appendix H – Matlab® code GUI

The following pictures are screenshots of some of the user interfaces developed for the eye-movements analysis package for this thesis.

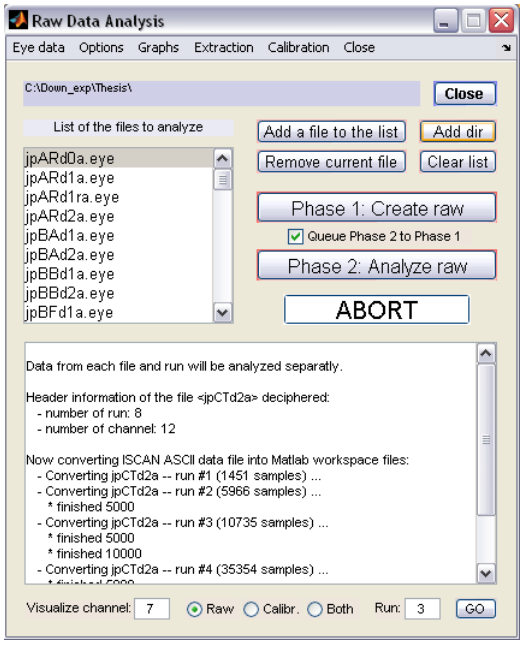

General interface used to create the SPV from the recording of the eye-movements

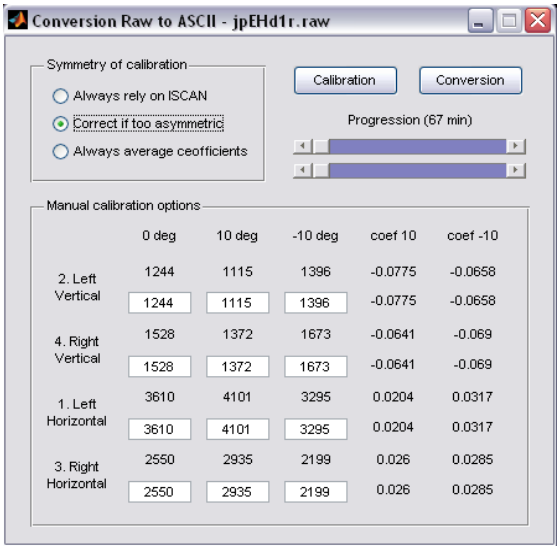

Interface used to recalibrate the eye-position from the raw eye-data using the calibration data

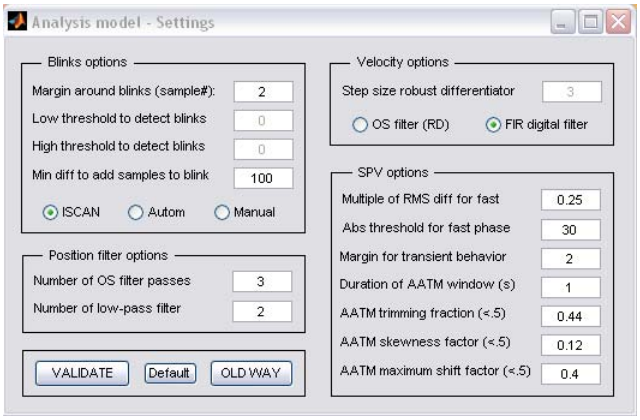

Interface used to change the parameters of the algorithm that creates the SPV from the eye-position

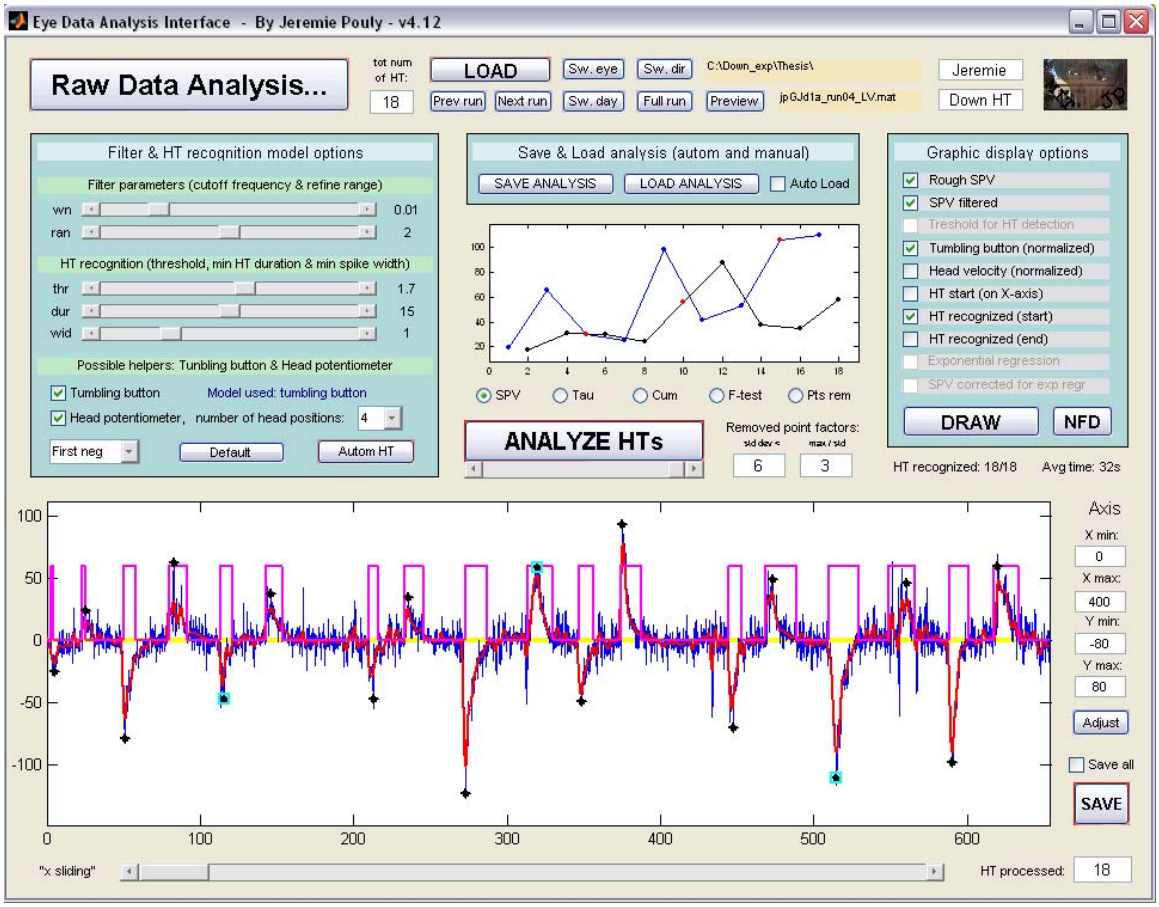

General interface used for the analysis of the SPV. Functionalities include automatic routine to detect the head-turns and fit the SPV with a single exponential mode as well as manual modifications of the automatic routines' results.

Appendix I – Matlab® code organization

Eye_analysis_step1 *

- Eye_channel_options *
- Eye_data_analysis_options *
- Extra_data_options *
- Recreate_ascii_from_raw *
  - Convert_raw_file
- Extraction Head Velocity
  - Head_potentiometer_analysis
- Extraction_step1
- Convert_bed_file_header
- Batch_bed_file
  - Init_bed
  - Batch_eye_channel
    - Init_bed
    - Deblink
      - Simple_blinks
      - Tresh_blinks
      - Interp_blinks
    - Filt_position (or filt_position_old…)
      - OS_filter
        - PHMH1
        - PFMH2
    - Differentiate
      - Zero_filter
    - Bed_classify_phases
      - AATM_filter
      - Min_threshold
    - Interpolate
- Show_creation_spv
  - Batch_eya_channel_bis

BBA_interface *

- Load_file_setup
- ***Eye_analysis_step1 ****
- Autom_HT_recognition
  - Head_potentiometer_analysis
- Autom_regression
  - Eye_analysis_interface
    - Exp_regression_interface
      - Exp_cost
- Manual_correction *
  - Data_eliminator
  - Exp_regression_manual
    - Exp_cost
- Save_results_eye_anal
  - Verify_HT_for_save

Appendix J – Data

The spreadsheet to follow gives each subject's raw data: the subjective ratings reported during the experiment and the physiological measurements processed from the data collected during the experiment. The columns in the spreadsheet are:

- **SUBJECT**: Subject number
- **SEX**: Gender of the subjects (F → female, M → male)
- **MSGr**: Motion sickness group ("MS" → motion sick subject, "nMS" → non motion sick subject), the two groups are detailed in Appendix G (only the subjects marked as "MS" were used for the motion sickness analysis)
- **TiltGr**: Tilt group (1 → subject experienced substantial body-tilt during the experiment, 2 → weak body-tilt, 3 → no body-tilt at all), the two groups are detailed in Appendix F (only the subjects in group 1 were used for the body-tilt analysis)
- **Day**: Experimental day
- **RPM**: Centrifuge-velocity (in rpm)
- **ANGLE**: Angle of the head-turn (in degree)
- **PHASES$**: Name of the experimental phases
- **DIR$**: Direction of the head-turn (to RED vs. to NUP)
- **MS**: Motion sickness score
- **TILT**: Body-tilt rating in the clock analogy (45 is the horizontal)
- **DUR**: Illusory motion duration (in seconds) measured by the tumbling button
- **INT**: Illusory motion intensity (first head-turn is 10)
- **SPV**: Absolute value of the peak amplitude of the SPV (in deg/sec)

- **`TAU`**: Primary time-constant of the VOR (in seconds)
- **`HeadVel`**: Head velocity as extracted from the head position measured by the potentiometer (in deg/sec)
- **`TimeHT_EM`**: Delay between a head-turn and the peak-amplitude of the eye-movements (in seconds)
- **`MS_DIFF`**: Motion sickness increments (difference between consecutive motion sickness scores)
- **`Tilt90`**: Body-tilt expressed compared to the Earth vertical (in degree, with 0° being standing on Earth and 90° lying horizontal on the bed)

SUBJECT	SEX	MSGr	TiltGr	DAY	RPM	ANGLE	PHASE$	DIR$	MS	TILT	DUR	INT	SPV	TAU	HeadVel	TimeHT_EM	MS_DIFF	Tilt90
101	F	MS	1	1	0	80	pre	to RED	0	45		0						90
101	F	MS	1	1	0	80	pre	to NUP	0	45		0					0	90
101	F	MS	1	1	0	80	pre	to RED	0	45		0					0	90
101	F	MS	1	1	0	80	pre	to NUP	0	45		0					0	90
101	F	MS	1	1	0	80	pre	to RED	0	45		0					0	90
101	F	MS	1	1	0	80	pre	to NUP	0	45		0					0	90
101	F	MS	1	1	23	80	PRE	to RED	0	47	0.85	10	59.5	4.8	96.3	3.4	0	102
101	F	MS	1	1	23	80	PRE	to NUP	0	40	6.92	20	53.1	8.2	-81.1	1.1	0	60
101	F	MS	1	1	23	80	PRE	to RED	0	45	4.7	10	74.2	4.9	96.1	2.5	0	90
101	F	MS	1	1	23	80	PRE	to NUP	0	40	12.12	20	81.2	7.2	-67.1	6.2	0	60
101	F	MS	1	1	23	80	PRE	to RED	0	45	6	15	77.4	5.4	81.1	1.9	0	90
101	F	MS	1	1	23	80	PRE	to NUP	0	40	13.17	20	60.3	4.8	-122.4	6.5	0	60
101	F	MS	1	1	12	20	STIM	to RED	0	45	0	0	17.7	4.9	102.6	2.1	0	90
101	F	MS	1	1	12	20	STIM	to NUP	0	40	0	0	14.1	6.5	-82.4	0.7	0	60
101	F	MS	1	1	12	80	STIM	to RED	0	45	1.22	10	39.5	5.8	94.9	2.1	0	90
101	F	MS	1	1	12	80	STIM	to NUP	0	42	7.55	15	37.2	6.2	-106.9	1.7	0	72
101	F	MS	1	1	12	40	STIM	to RED	0	42	0.98	5	29.5	4.6	115.9	1.7	0	72
101	F	MS	1	1	12	40	STIM	to NUP	0	44	6.7	15	26.4	5.9	-80.4	1.1	0	84
101	F	MS	1	1	19	20	STIM	to RED	0	45	0.73	5	21.5	4.1	84.2	1.5	0	90
101	F	MS	1	1	19	20	STIM	to NUP	0	40	3	5	28.9	4.4	-74.8	0.8	0	60
101	F	MS	1	1	19	80	STIM	to RED	0	45	7.5	15	47.2	5.1	100.1	2.3	0	90
101	F	MS	1	1	19	80	STIM	to NUP	0	40	17.27	20	54.1	5.5	-136.4	7.0	0	60
101	F	MS	1	1	19	40	STIM	to RED	0	45	4.33	10	48.9	4.2	99.8	1.8	0	90
101	F	MS	1	1	19	40	STIM	to NUP	0	40	5.12	10	44.0	5.1	-83.0	2.2	0	60
101	F	MS	1	1	30	20	STIM	to RED	0	50	1.05	10	58.2	3.1	76.1	1.7	0	120
101	F	MS	1	1	30	20	STIM	to NUP	0	40	11.68	15	65.8	5.4	-88.1	0.7	0	60
101	F	MS	1	1	30	80	STIM	to RED	0	45	9.07	15	32.0	4.8	107.0	3.7	0	90
101	F	MS	1	1	30	80	STIM	to NUP	0	40	23.47	28	47.3	4.0	-101.0	8.5	0	60

101	F	MS	1	1	30	40	STIM	to RED	0	45	10.28	15	49.9	4.2	111.8	2.0	0	90
101	F	MS	1	1	30	40	STIM	to NUP	2	40	14.53	20	65.0	3.6	-57.9	5.3	2	60
101	F	MS	1	1	12	20	STIM	to RED	3	45	1.5	5	17.9	4.4	72.2	1.3	1	90
101	F	MS	1	1	12	20	STIM	to NUP	2	44	4.25	5	14.2	4.8	-68.0	0.5	-1	84
101	F	MS	1	1	12	80	STIM	to RED	0	45	2.95	5	26.2	5.0	107.4	2.0	-2	90
101	F	MS	1	1	12	80	STIM	to NUP	0	42	9.62	10	26.3	6.1	-90.4	3.7	0	72
101	F	MS	1	1	12	40	STIM	to RED	0	43	2.38	7	28.3	3.7	104.9	2.0	0	78
101	F	MS	1	1	12	40	STIM	to NUP	0	44	5.87	10	37.5	3.8	-65.3	0.8	0	84
101	F	MS	1	1	19	20	STIM	to RED	0	43	0.67	5	21.0	3.9	69.4	1.6	0	78
101	F	MS	1	1	19	20	STIM	to NUP	0	40	5.68	5	12.3	4.8	-92.6	8.1	0	60
101	F	MS	1	1	19	80	STIM	to RED	0	45	11.43	12	29.2	4.9	110.7	3.5	0	90
101	F	MS	1	1	19	80	STIM	to NUP	0	43	16.65	20	33.1	3.9	-112.3	6.6	0	78
101	F	MS	1	1	19	40	STIM	to RED	0	43	6.63	10	38.6	3.7	77.4	1.9	0	78
101	F	MS	1	1	19	40	STIM	to NUP	0	43	10.28	15	14.7	4.9	-73.7	0.5	0	78
101	F	MS	1	1	30	20	STIM	to RED	2	43	5.03	10	35.4	3.5	65.5	1.5	2	78
101	F	MS	1	1	30	20	STIM	to NUP	3	40	10.95	17	29.1	3.6	-57.6	3.5	1	60
101	F	MS	1	1	30	80	STIM	to RED	4	40	14.97	20	28.4	4.4	102.3	5.6	1	60
101	F	MS	1	1	30	80	STIM	to NUP	5	40	21.92	28	10.8	4.7	-84.6	8.9	1	60
101	F	MS	1	1	30	40	STIM	to RED	8	45	11.6	16	41.6	4.1	108.3	2.4	3	90
101	F	MS	1	1	30	40	STIM	to NUP	9	40	15.9	21	59.6	3.3	-53.6	4.6	1	60
101	F	MS	1	1	23	80	POST	to RED										
101	F	MS	1	1	23	80	POST	to NUP										
101	F	MS	1	1	23	80	POST	to RED										
101	F	MS	1	1	23	80	POST	to NUP										
101	F	MS	1	1	23	80	POST	to RED										
101	F	MS	1	1	23	80	POST	to NUP										
101	F	MS	1	1	0	80	post	to RED										
101	F	MS	1	1	0	80	post	to NUP										
101	F	MS	1	1	0	80	post	to RED										
101	F	MS	1	1	0	80	post	to NUP										
101	F	MS	1	1	0	80	post	to RED										
101	F	MS	1	1	0	80	post	to NUP										
101	F	MS	1	2	0	80	pre	to RED	0	45		0						90
101	F	MS	1	2	0	80	pre	to NUP	0	45		0					0	90
101	F	MS	1	2	0	80	pre	to RED	0	45		0					0	90
101	F	MS	1	2	0	80	pre	to NUP	0	45		0					0	90
101	F	MS	1	2	0	80	pre	to RED	0	45		0					0	90
101	F	MS	1	2	0	80	pre	to NUP	0	45		0					0	90
101	F	MS	1	2	23	80	PRE	to RED	0	45	0	0	33.1	4.5	150.9	4.0	0	90
101	F	MS	1	2	23	80	PRE	to NUP	0	43	16.45	10	55.7	5.0	-113.5	8.0	0	78
101	F	MS	1	2	23	80	PRE	to RED	0	45	9.62	7	50.8	5.2	124.6	4.1	0	90
101	F	MS	1	2	23	80	PRE	to NUP	1	42	11.97	12	50.7	6.0	-101.1	7.1	1	72
101	F	MS	1	2	23	80	PRE	to RED	0	45	7.47	8	37.5	5.1	77.6	6.2	-1	90
101	F	MS	1	2	23	80	PRE	to NUP	2	40	12.9	15	48.3	4.5	-101.3	9.0	2	60
101	F	MS	1	2	12	20	STIM	to RED	0	45	0	0	20.4	3.2	87.2	1.8	-2	90
101	F	MS	1	2	12	20	STIM	to NUP	0	45	0	0	20.5	5.3	-44.5	3.0	0	90
101	F	MS	1	2	12	80	STIM	to RED	0	45	0	0	37.2	4.6	87.8	3.8	0	90
101	F	MS	1	2	12	80	STIM	to NUP	0	42	6.92	7	32.7	7.4	-109.7	5.5	0	72
101	F	MS	1	2	12	40	STIM	to RED	0	44	0.38	4	35.8	3.5	113.4	1.7	0	84
101	F	MS	1	2	12	40	STIM	to NUP	0	44	5.4	4	22.7	6.3	-71.4	3.7	0	84
101	F	MS	1	2	19	20	STIM	to RED	0	44	0.78	3	25.4	3.7	78.4	2.0	0	84
101	F	MS	1	2	19	20	STIM	to NUP	0	43	5.52	7	35.3	6.6	-50.8	1.1	0	78
101	F	MS	1	2	19	80	STIM	to RED	0	45	7.28	9	55.8	4.3	92.7	3.3	0	90
101	F	MS	1	2	19	80	STIM	to NUP	0	42	8.63	16	59.9	5.8	-165.1	7.6	0	72
101	F	MS	1	2	19	40	STIM	to RED	0	46	3.3	8	76.1	4.0	97.0	1.6	0	96
101	F	MS	1	2	19	40	STIM	to NUP	0	42	7.97	10	32.1	6.0	-84.7	0.9	0	72
101	F	MS	1	2	30	20	STIM	to RED	0	42	5.2	5	50.1	4.1	73.9	1.6	0	72
101	F	MS	1	2	30	20	STIM	to NUP	0	43	6.62	10	48.5	3.8	-66.4	3.6	0	78
101	F	MS	1	2	30	80	STIM	to RED	0	45	9.02	12	65.4	5.4	117.4	4.1	0	90
101	F	MS	1	2	30	80	STIM	to NUP	1	40	11.45	18	55.8	4.8	-103.4	11.0	1	60
101	F	MS	1	2	30	40	STIM	to RED	1	45	5.95	10	63.6	4.6	101.5	2.6	0	90
101	F	MS	1	2	30	40	STIM	to NUP	1	42	13.27	15	32.4	2.1	-81.5	9.8	0	72
101	F	MS	1	2	12	20	STIM	to RED	0	45	0	0	11.1	4.4	106.8	1.8	-1	90
101	F	MS	1	2	12	20	STIM	to NUP	0	45	-1	4	15.6	6.6	-58.6	2.2	0	90
101	F	MS	1	2	12	80	STIM	to RED	0	45	1.2	4	52.2	3.3	106.7	2.0	0	90
101	F	MS	1	2	12	80	STIM	to NUP	0	44.5	3.87	6	36.0	5.8	-106.0	4.8	0	87

101	F	MS	1	2	12	40	STIM	to RED	0	45	0.95	3	38.4	3.8	105.6	1.5	0	90
101	F	MS	1	2	12	40	STIM	to NUP	0	44	2.28	6	14.2	5.2	-78.2	0.4	0	84
101	F	MS	1	2	19	20	STIM	to RED	0	45	1.93	6	49.3	3.5	82.2	1.5	0	90
101	F	MS	1	2	19	20	STIM	to NUP	0	45	4.17	8	15.5	5.3	-45.9	3.1	0	90
101	F	MS	1	2	19	80	STIM	to RED	0	45	7.45	10	38.1	4.8	104.7	3.6	0	90
101	F	MS	1	2	19	80	STIM	to NUP	0	44	10.52	15	32.7	5.3	-90.3	5.4	0	84
101	F	MS	1	2	19	40	STIM	to RED	0	45	8.05	9	33.7	4.8	106.6	2.9	0	90
101	F	MS	1	2	19	40	STIM	to NUP	0	43	13.37	17	28.6	3.9	-95.5	5.4	0	78
101	F	MS	1	2	30	20	STIM	to RED	0	44	3.32	7	51.4	4.2	75.8	2.0	0	84
101	F	MS	1	2	30	20	STIM	to NUP	0	42	4.22	10	29.6	6.1	-57.1	4.0	0	72
101	F	MS	1	2	30	80	STIM	to RED	0	45	10.1	12	40.2	3.7	89.0	4.0	0	90
101	F	MS	1	2	30	80	STIM	to NUP	1	41	14.97	20	25.8	4.1	-104.7	11.7	1	66
101	F	MS	1	2	30	40	STIM	to RED	0	44	6.78	10	51.5	5.5	92.6	3.1	-1	84
101	F	MS	1	2	30	40	STIM	to NUP	1	42	12.55	16	26.5	4.8	-70.2	6.1	1	72
101	F	MS	1	2	23	80	POST	to RED	0	45	5.02	10	38.9	5.6	88.8	3.7	-1	90
101	F	MS	1	2	23	80	POST	to NUP	0	44	9.95	12	16.5	6.9	-103.2	10.2	0	84
101	F	MS	1	2	23	80	POST	to RED	0	45	6.4	10	54.3	3.7	106.2	6.7	0	90
101	F	MS	1	2	23	80	POST	to NUP	0	45	9.8	12	38.4	4.9	-75.9	8.3	0	90
101	F	MS	1	2	23	80	POST	to RED	0	45	9.23	9	51.4	6.1	110.2	2.7	0	90
101	F	MS	1	2	23	80	POST	to NUP	0	44	8.53	10	24.3	6.5	-98.1	7.2	0	84
101	F	MS	1	2	0	80	post	to RED	0	45		2					0	90
101	F	MS	1	2	0	80	post	to NUP	0	45		3					0	90
101	F	MS	1	2	0	80	post	to RED	0	45		0					0	90
101	F	MS	1	2	0	80	post	to NUP	0	45		0					0	90
101	F	MS	1	2	0	80	post	to RED	0	45		0					0	90
101	F	MS	1	2	0	80	post	to NUP	0	45		0					0	90
102	M	nMS	3	1	0	80	pre	to RED	0	45		0						90
102	M	nMS	3	1	0	80	pre	to NUP	0	45		0					0	90
102	M	nMS	3	1	0	80	pre	to RED	0	45		0					0	90
102	M	nMS	3	1	0	80	pre	to NUP	0	45		0					0	90
102	M	nMS	3	1	0	80	pre	to RED	0	45		0					0	90
102	M	nMS	3	1	0	80	pre	to NUP	0	45		0					0	90
102	M	nMS	3	1	23	80	PRE	to RED	0	45	3	10	28.6	3.5	85.7	3.6	0	90
102	M	nMS	3	1	23	80	PRE	to NUP	0	45	9.63	13	43.1	5.8	-101.6	7.7	0	90
102	M	nMS	3	1	23	80	PRE	to RED	0	45	4.27	2	47.6	3.5	59.4	2.8	0	90
102	M	nMS	3	1	23	80	PRE	to NUP	0	45	7.33	12	48.2	4.6	-92.7	6.7	0	90
102	M	nMS	3	1	23	80	PRE	to RED	0	45	3.53	2	31.5	3.5	82.3	2.6	0	90
102	M	nMS	3	1	23	80	PRE	to NUP	0	45	5.87	13	29.2	4.4	-82.7	9.0	0	90
102	M	nMS	3	1	12	20	STIM	to RED	0	45	0	0	5.7	3.8	72.8	9.3	0	90
102	M	nMS	3	1	12	20	STIM	to NUP	0	45	0	0	14.0	4.0	-54.4	0.9	0	90
102	M	nMS	3	1	12	80	STIM	to RED	0	45	2.08	1	22.1	3.8	86.4	2.4	0	90
102	M	nMS	3	1	12	80	STIM	to NUP	0	45	3.22	8	32.2	4.6	-96.6	4.3	0	90
102	M	nMS	3	1	12	40	STIM	to RED	0	45	1.55	1	14.0	4.0	66.9	10.6	0	90
102	M	nMS	3	1	12	40	STIM	to NUP	0	45	2.6	10	28.1	5.3	-72.8	3.6	0	90
102	M	nMS	3	1	19	20	STIM	to RED	0	45	1.58	1	13.7	2.4	46.6	5.6	0	90
102	M	nMS	3	1	19	20	STIM	to NUP	0	45	2.18	6	11.4	4.9	-47.6	2.6	0	90
102	M	nMS	3	1	19	80	STIM	to RED	0	45	3.58	9	25.5	4.1	56.0	3.3	0	90
102	M	nMS	3	1	19	80	STIM	to NUP	0	45	6.08	15	29.9	5.8	-99.0	6.3	0	90
102	M	nMS	3	1	19	40	STIM	to RED	0	45	2.07	10	17.9	2.5	65.6	2.7	0	90
102	M	nMS	3	1	19	40	STIM	to NUP	0	45	3.97	13	23.0	4.1	-68.3	3.9	0	90
102	M	nMS	3	1	30	20	STIM	to RED	0	45	1.57	7	13.8	3.1	52.4	1.8	0	90
102	M	nMS	3	1	30	20	STIM	to NUP	0	45	2.63	13	20.2	5.3	-45.8	2.6	0	90
102	M	nMS	3	1	30	80	STIM	to RED	0	45	3.77	14	33.5	4.2	61.5	4.0	0	90
102	M	nMS	3	1	30	80	STIM	to NUP	0	45	11.9	18	22.8	5.5	-95.1	9.2	0	90
102	M	nMS	3	1	30	40	STIM	to RED	0	45	2.37	10	25.3	3.6	57.5	2.3	0	90
102	M	nMS	3	1	30	40	STIM	to NUP	0	42	7	14	27.5	4.8	-65.5	6.4	0	72
102	M	nMS	3	1	12	20	STIM	to RED	0	45	1.4	2	4.1	2.3	51.8	9.3	0	90
102	M	nMS	3	1	12	20	STIM	to NUP	0	45	0.98	2	23.4	3.2	-42.9	2.6	0	90
102	M	nMS	3	1	12	80	STIM	to RED	0	45	3.27	8	23.2	3.0	62.8	3.8	0	90
102	M	nMS	3	1	12	80	STIM	to NUP	0	45	5.25	13	22.1	4.5	-87.7	5.2	0	90
102	M	nMS	3	1	12	40	STIM	to RED	0	45	2.57	10	15.9	2.9	61.2	1.6	0	90
102	M	nMS	3	1	12	40	STIM	to NUP	0	45	2.72	10	17.6	4.2	-63.9	2.0	0	90
102	M	nMS	3	1	19	20	STIM	to RED	0	45	1.4	6	8.9	3.2	54.1	11.6	0	90
102	M	nMS	3	1	19	20	STIM	to NUP	0	45	2.78	9	12.2	5.3	-72.0	7.7	0	90
102	M	nMS	3	1	19	80	STIM	to RED	0	45	3.87	11	44.5	3.6	62.8	5.0	0	90
102	M	nMS	3	1	19	80	STIM	to NUP	0	45	7.05	16	26.4	5.0	-87.7	6.2	0	90

102	M	nMS	3	1	19	40	STIM	to RED	0	45	2.58	10	27.5	2.9	68.1	1.9	0	90
102	M	nMS	3	1	19	40	STIM	to NUP	0	45	4.5	14	18.1	5.0	-68.4	4.6	0	90
102	M	nMS	3	1	30	20	STIM	to RED	1	45	3.63	10	15.0	2.4	59.2	2.6	1	90
102	M	nMS	3	1	30	20	STIM	to NUP	0	45	2.37	10	28.6	3.7	-54.3	4.8	-1	90
102	M	nMS	3	1	30	80	STIM	to RED	0	45	4.57	13	13.5	2.3	61.1	6.7	0	90
102	M	nMS	3	1	30	80	STIM	to NUP	1	45	10.65	19	16.4	3.5	-84.6	7.7	1	90
102	M	nMS	3	1	30	40	STIM	to RED	0	45	3.65	12	19.5	2.8	53.9	3.9	-1	90
102	M	nMS	3	1	30	40	STIM	to NUP	0	35	7.47	15	22.2	2.0	-71.6	7.3	0	30
102	M	nMS	3	1	23	80	POST	to RED	0	45	3.1	10	18.2	4.9	74.8	5.0	0	90
102	M	nMS	3	1	23	80	POST	to NUP	0	45	5.92	15	34.7	3.1	-82.3	8.2	0	90
102	M	nMS	3	1	23	80	POST	to RED	0	45	3	9	24.0	4.3	91.7	3.2	0	90
102	M	nMS	3	1	23	80	POST	to NUP	0	43	7.13	13	23.2	3.7	-74.3	3.4	0	78
102	M	nMS	3	1	23	80	POST	to RED	0	45	3.57	9	28.7	4.8	67.0	3.7	0	90
102	M	nMS	3	1	23	80	POST	to NUP	0	44	5.48	14	20.3	3.9	-75.7	6.0	0	84
102	M	nMS	3	1	0	80	post	to RED	0	45		0					0	90
102	M	nMS	3	1	0	80	post	to NUP	0	45		0					0	90
102	M	nMS	3	1	0	80	post	to RED	0	45		0					0	90
102	M	nMS	3	1	0	80	post	to NUP	0	45		0					0	90
102	M	nMS	3	1	0	80	post	to RED	0	45		0					0	90
102	M	nMS	3	1	0	80	post	to NUP	0	45		0					0	90
102	M	nMS	3	2	0	80	pre	to RED	0	45		0						90
102	M	nMS	3	2	0	80	pre	to NUP	0	45		0					0	90
102	M	nMS	3	2	0	80	pre	to RED	0	45		0					0	90
102	M	nMS	3	2	0	80	pre	to NUP	0	45		0					0	90
102	M	nMS	3	2	0	80	pre	to RED	0	45		0					0	90
102	M	nMS	3	2	0	80	pre	to NUP	0	45		0					0	90
102	M	nMS	3	2	23	80	PRE	to RED	0	45	3.08	5	25.6	4.2	101.1	5.5	0	90
102	M	nMS	3	2	23	80	PRE	to NUP	0	45	3.48	11	45.8	2.9	-94.8	8.0	0	90
102	M	nMS	3	2	23	80	PRE	to RED	0	45	2.88	5	63.9	4.2	105.9	2.1	0	90
102	M	nMS	3	2	23	80	PRE	to NUP	0	45	4.07	13	33.7	3.7	-86.2	7.3	0	90
102	M	nMS	3	2	23	80	PRE	to RED	0	45	4.35	8	48.6	3.8	64.4	3.2	0	90
102	M	nMS	3	2	23	80	PRE	to NUP	0	45	4.6	13	41.5	3.5	-85.2	7.6	0	90
102	M	nMS	3	2	12	20	STIM	to RED	0	45	0.98	1	8.6	1.7	73.5		0	90
102	M	nMS	3	2	12	20	STIM	to NUP	0	45	1.55	1	19.5	2.9	-51.5	1.3	0	90
102	M	nMS	3	2	12	80	STIM	to RED	0	45	2.67	2	34.7	3.7	90.4	1.9	0	90
102	M	nMS	3	2	12	80	STIM	to NUP	0	45	2.27	3	46.4	3.9	-93.4	4.7	0	90
102	M	nMS	3	2	12	40	STIM	to RED	0	45	1.38	1	19.1	2.2	76.2	2.3	0	90
102	M	nMS	3	2	12	40	STIM	to NUP	0	45	2.83	3	20.4	4.1	-60.1	2.1	0	90
102	M	nMS	3	2	19	20	STIM	to RED	0	45	1.37	2	16.2	3.4	60.7	10.7	0	90
102	M	nMS	3	2	19	20	STIM	to NUP	0	45	1.5	2	17.5	3.3	-58.6	2.1	0	90
102	M	nMS	3	2	19	80	STIM	to RED	0	45	3.88	9	39.8	4.0	78.1	2.7	0	90
102	M	nMS	3	2	19	80	STIM	to NUP	0	45	5.18	13	33.2	4.4	-95.4	8.7	0	90
102	M	nMS	3	2	19	40	STIM	to RED	0	45	1.38	11	33.0	2.3	55.7	1.2	0	90
102	M	nMS	3	2	19	40	STIM	to NUP	0	42	4.1	13	25.0	3.9	-65.0	3.3	0	72
102	M	nMS	3	2	30	20	STIM	to RED	0	45	1.42	8	19.3	4.4	73.5	2.6	0	90
102	M	nMS	3	2	30	20	STIM	to NUP	0	44	4.18	15	26.9	4.9	-57.1	1.3	0	84
102	M	nMS	3	2	30	80	STIM	to RED	0	45	4.88	16	68.0	2.7	67.0	3.5	0	90
102	M	nMS	3	2	30	80	STIM	to NUP	0	45	6.57	18	38.5	4.7	-83.8	6.4	0	90
102	M	nMS	3	2	30	40	STIM	to RED	0	45	4.78	15	35.8	3.3	56.4	4.3	0	90
102	M	nMS	3	2	30	40	STIM	to NUP	0	39	6.12	18	31.8	4.6	-68.5	4.9	0	54
102	M	nMS	3	2	12	20	STIM	to RED	0	45	1.1	1	20.7	3.4	59.5	1.7	0	90
102	M	nMS	3	2	12	20	STIM	to NUP	0	45	1.6	1	16.3	3.8	-43.6		0	90
102	M	nMS	3	2	12	80	STIM	to RED	0	45	2.65	1	36.7	3.5	71.7	1.8	0	90
102	M	nMS	3	2	12	80	STIM	to NUP	0	45	3.28	5	29.6	4.3	-89.3	5.8	0	90
102	M	nMS	3	2	12	40	STIM	to RED	0	45	1.98	2	24.1	2.3	60.3	2.0	0	90
102	M	nMS	3	2	12	40	STIM	to NUP	0	45	1.97	2	22.6	2.8	-74.0	1.9	0	90
102	M	nMS	3	2	19	20	STIM	to RED	0	45	0	0	16.2	3.1	54.1	2.6	0	90
102	M	nMS	3	2	19	20	STIM	to NUP	0	45	1.78	1	24.1	4.7	-47.9	4.9	0	90
102	M	nMS	3	2	19	80	STIM	to RED	0	45	4.18	4	28.6	3.1	81.5	5.7	0	90
102	M	nMS	3	2	19	80	STIM	to NUP	0	44	5.45	12	40.9	4.2	-98.2	7.9	0	84
102	M	nMS	3	2	19	40	STIM	to RED	0	45	2.53	7	31.2	2.2	54.9	2.6	0	90
102	M	nMS	3	2	19	40	STIM	to NUP	0	44	4.37	10	21.4	3.8	-61.3	1.4	0	84
102	M	nMS	3	2	30	20	STIM	to RED	0	45	1.6	4	17.6	4.7	56.0	2.3	0	90
102	M	nMS	3	2	30	20	STIM	to NUP	0	45	2.03	5	29.6	2.9	-52.0	8.1	0	90
102	M	nMS	3	2	30	80	STIM	to RED	0	45	4.9	10	42.4	3.3	81.5	5.1	0	90
102	M	nMS	3	2	30	80	STIM	to NUP	0	45	8.05	18	30.3	4.3	-84.3	9.7	0	90

102	M	nMS	3	2	30	40	STIM	to RED	0	45	4.47	11	25.1	3.0	69.5	5.4	0	90
102	M	nMS	3	2	30	40	STIM	to NUP	0	40	4.77	15	34.1	3.0	-67.1	7.9	0	60
102	M	nMS	3	2	23	80	POST	to RED	0	45	4.18	8	27.7	4.1	77.7	3.0	0	90
102	M	nMS	3	2	23	80	POST	to NUP	0	45	5.82	15	20.7	4.1	-81.3	4.7	0	90
102	M	nMS	3	2	23	80	POST	to RED	0	45	3.65	8	42.7	3.7	86.1	2.8	0	90
102	M	nMS	3	2	23	80	POST	to NUP	0	44	5.93	15	23.6	3.9	-85.5	9.9	0	84
102	M	nMS	3	2	23	80	POST	to RED	0	45	3.7	8	26.7	3.6	71.8	6.5	0	90
102	M	nMS	3	2	23	80	POST	to NUP	0	45	5.45	13	32.4	4.0	-93.4	8.4	0	90
102	M	nMS	3	2	0	80	post	to RED	0	45		0					0	90
102	M	nMS	3	2	0	80	post	to NUP	0	45		0					0	90
102	M	nMS	3	2	0	80	post	to RED	0	45		0					0	90
102	M	nMS	3	2	0	80	post	to NUP	0	45		0					0	90
102	M	nMS	3	2	0	80	post	to RED	0	45		0					0	90
102	M	nMS	3	2	0	80	post	to NUP	0	45		0					0	90
103	M	nMS	2	1	0	80	pre	to RED	0	45		0						90
103	M	nMS	2	1	0	80	pre	to NUP	0	45		0					0	90
103	M	nMS	2	1	0	80	pre	to RED	0	45		0					0	90
103	M	nMS	2	1	0	80	pre	to NUP	0	45		0					0	90
103	M	nMS	2	1	0	80	pre	to RED	0	46		0					0	96
103	M	nMS	2	1	0	80	pre	to NUP	0	45		0					0	90
103	M	nMS	2	1	23	80	PRE	to RED	0	46	3.87	10	93.2	4.5	96.8	3.9	0	96
103	M	nMS	2	1	23	80	PRE	to NUP	0	45	8.3	12	64.4	4.5	-113.8	6.0	0	90
103	M	nMS	2	1	23	80	PRE	to RED	0	46	7.05	5	47.1	5.1	91.0	5.8	0	96
103	M	nMS	2	1	23	80	PRE	to NUP	0	45	6.97	11	56.9	4.0	-118.9	6.0	0	90
103	M	nMS	2	1	23	80	PRE	to RED	0	45	2.78	6	80.3	5.8	89.1	8.9	0	90
103	M	nMS	2	1	23	80	PRE	to NUP	0	45	5.87	7	57.2	4.5	-135.6	5.2	0	90
103	M	nMS	2	1	12	20	STIM	to RED	0	45	0.78	1	20.7	3.9	86.6	6.5	0	90
103	M	nMS	2	1	12	20	STIM	to NUP	0	45	2.22	1	21.5	3.9	-71.9	0.9	0	90
103	M	nMS	2	1	12	80	STIM	to RED	0	46	3.12	3	58.0	6.0	108.1	1.8	0	96
103	M	nMS	2	1	12	80	STIM	to NUP	0	45	3.83	4	45.3	6.1	-134.5	3.3	0	90
103	M	nMS	2	1	12	40	STIM	to RED	0	45	1.47	2	55.8	5.1	113.7	2.2	0	90
103	M	nMS	2	1	12	40	STIM	to NUP	0	45	3.03	2	38.2	3.5	-77.7	1.9	0	90
103	M	nMS	2	1	19	20	STIM	to RED	0	45	1.4	1	59.1	5.2	78.2	1.8	0	90
103	M	nMS	2	1	19	20	STIM	to NUP	0	45	2.12	3	38.3	4.5	-63.7	1.2	0	90
103	M	nMS	2	1	19	80	STIM	to RED	0	45	4	5	84.7	4.9	123.5	5.5	0	90
103	M	nMS	2	1	19	80	STIM	to NUP	1	45	6.18	6	36.5	4.1	-156.2	8.0	1	90
103	M	nMS	2	1	19	40	STIM	to RED	0	45	3.68	3	63.3	5.6	83.9	3.0	-1	90
103	M	nMS	2	1	19	40	STIM	to NUP	0	45	3.63	3	61.9	3.6	-80.6	3.7	0	90
103	M	nMS	2	1	30	20	STIM	to RED	0	43	3.12	2	66.9	5.4	85.2	2.1	0	78
103	M	nMS	2	1	30	20	STIM	to NUP	0	45	3.8	2	47.2	4.0	-46.0	3.1	0	90
103	M	nMS	2	1	30	80	STIM	to RED	1	45	5.42	9	78.0	4.1	74.8	7.3	1	90
103	M	nMS	2	1	30	80	STIM	to NUP	2	45	6.07	7	50.9	4.0	-112.6	8.4	1	90
103	M	nMS	2	1	30	40	STIM	to RED	2	45	5.68	4	73.8	5.6	75.6	5.1	0	90
103	M	nMS	2	1	30	40	STIM	to NUP	2	45	5.1	3	40.0	3.7	-92.1	7.5	0	90
103	M	nMS	2	1	12	20	STIM	to RED	0	45	0	0	28.3	4.5	90.7	1.7	-2	90
103	M	nMS	2	1	12	20	STIM	to NUP	0	45	1.67	0.5	32.9	3.9	-66.7	0.6	0	90
103	M	nMS	2	1	12	80	STIM	to RED	0	45	4.47	1	58.3	4.2	134.5	3.9	0	90
103	M	nMS	2	1	12	80	STIM	to NUP	0	45	3.33	2	34.1	3.6	-115.4	5.5	0	90
103	M	nMS	2	1	12	40	STIM	to RED	0	45	3.4	2	43.5	4.5	91.3	1.7	0	90
103	M	nMS	2	1	12	40	STIM	to NUP	0	45	3.48	1	28.9	4.7	-91.5	0.7	0	90
103	M	nMS	2	1	19	20	STIM	to RED	1	45	2.55	2	46.3	4.5	84.8	1.6	1	90
103	M	nMS	2	1	19	20	STIM	to NUP	1	45	2.42	1	25.4	3.3	-42.6	1.2	0	90
103	M	nMS	2	1	19	80	STIM	to RED	1	45	5.55	4	50.2	3.2	103.4	3.8	0	90
103	M	nMS	2	1	19	80	STIM	to NUP	1	45	6.4	2	35.2	4.3	-110.3	6.5	0	90
103	M	nMS	2	1	19	40	STIM	to RED	0	45	3.52	2	38.5	4.3	60.7	6.3	-1	90
103	M	nMS	2	1	19	40	STIM	to NUP	0	45	3.92	2	32.0	4.1	-61.7	2.6	0	90
103	M	nMS	2	1	30	20	STIM	to RED	1	45	1.53	1	66.7	4.4	90.7	4.5	1	90
103	M	nMS	2	1	30	20	STIM	to NUP	2	45	3.95	2	26.5	3.8	-56.1	2.1	1	90
103	M	nMS	2	1	30	80	STIM	to RED	0	45	5.98	4	67.2	3.9	108.2	7.6	-2	90
103	M	nMS	2	1	30	80	STIM	to NUP	0	45	6.03	3	31.3	3.7	-92.4	7.5	0	90
103	M	nMS	2	1	30	40	STIM	to RED	0	45	4.83	2	45.6	4.2	65.2	7.7	0	90
103	M	nMS	2	1	30	40	STIM	to NUP	0	45	4.55	2	29.5	3.1	-82.3	9.3	0	90
103	M	nMS	2	1	23	80	POST	to RED	0	46	3.88	1	64.1	4.3	79.7	4.0	0	96
103	M	nMS	2	1	23	80	POST	to NUP	1	45	5.95	1	42.1	4.1	-102.8	6.1	1	90
103	M	nMS	2	1	23	80	POST	to RED	1	45	5.4	1	41.8	5.2	76.0	5.2	0	90
103	M	nMS	2	1	23	80	POST	to NUP	0	45	0	0	49.2	4.6	-92.6	7.1	-1	90

103	M	nMS	2	1	23	80	POST	to RED	0	45	5.1	1	48.8	5.1	102.1	4.1	0	90
103	M	nMS	2	1	23	80	POST	to NUP	0	45	4.92	1	52.0	2.9	-103.3	8.6	0	90
103	M	nMS	2	1	0	80	post	to RED	0	45		0					0	90
103	M	nMS	2	1	0	80	post	to NUP	0	45		0					0	90
103	M	nMS	2	1	0	80	post	to RED	0	45		0					0	90
103	M	nMS	2	1	0	80	post	to NUP	0	45		0					0	90
103	M	nMS	2	1	0	80	post	to RED	0	45		0					0	90
103	M	nMS	2	1	0	80	post	to NUP	0	45		0					0	90
103	M	nMS	2	2	0	80	pre	to RED	0	45		0						90
103	M	nMS	2	2	0	80	pre	to NUP	0	45		0					0	90
103	M	nMS	2	2	0	80	pre	to RED	0	45		0					0	90
103	M	nMS	2	2	0	80	pre	to NUP	0	45		0					0	90
103	M	nMS	2	2	0	80	pre	to RED	0	45		0					0	90
103	M	nMS	2	2	0	80	pre	to NUP	0	45		0					0	90
103	M	nMS	2	2	23	80	PRE	to RED	0	45	3.15	2	59.5	3.8	86.5	5.7	0	90
103	M	nMS	2	2	23	80	PRE	to NUP	0	45	4.57	2	36.7	3.5	-81.0	5.9	0	90
103	M	nMS	2	2	23	80	PRE	to RED	0	45	2.15	1	55.2	4.6	93.3	1.9	0	90
103	M	nMS	2	2	23	80	PRE	to NUP	0	45	4.8	2	47.9	4.8	-126.4	7.0	0	90
103	M	nMS	2	2	23	80	PRE	to RED	1	45	4.67	2	42.6	4.6	74.3	7.1	1	90
103	M	nMS	2	2	23	80	PRE	to NUP	1	45	4.77	2	32.9	4.9	-60.1	3.3	0	90
103	M	nMS	2	2	12	20	STIM	to RED	0	45	0	0	25.1	4.8	65.7	1.4	-1	90
103	M	nMS	2	2	12	20	STIM	to NUP	0	45	0	0	15.9	4.4	-44.7	0.9	0	90
103	M	nMS	2	2	12	80	STIM	to RED	0	45	3.8	1	42.5	4.9	137.1	2.6	0	90
103	M	nMS	2	2	12	80	STIM	to NUP	0	45	4.45	1	29.2	6.1	-60.1	1.0	0	90
103	M	nMS	2	2	12	40	STIM	to RED	0	45	1.87	1	32.1	3.9	62.9	3.5	0	90
103	M	nMS	2	2	12	40	STIM	to NUP	1	45	3.9	1	29.7	4.1	-69.6	0.6	1	90
103	M	nMS	2	2	19	20	STIM	to RED	1	45	0	0	41.4	5.1	77.9	1.8	0	90
103	M	nMS	2	2	19	20	STIM	to NUP	1	45	3.33	1	25.7	4.1	-43.8	3.5	0	90
103	M	nMS	2	2	19	80	STIM	to RED	1	45	4.18	1	37.8	4.0	69.6	6.4	0	90
103	M	nMS	2	2	19	80	STIM	to NUP	1	45	6.27	2	49.8	4.1	-78.4	5.5	0	90
103	M	nMS	2	2	19	40	STIM	to RED	1	45	2.87	1	45.4	3.8	54.5	6.9	0	90
103	M	nMS	2	2	19	40	STIM	to NUP	1	45	2.93	1	23.5	3.9	-62.2	4.9	0	90
103	M	nMS	2	2	30	20	STIM	to RED	0	45	0	0	63.5	3.1	90.9	3.5	-1	90
103	M	nMS	2	2	30	20	STIM	to NUP	1	45	3.12	1	36.6	5.2	-47.6	1.2	1	90
103	M	nMS	2	2	30	80	STIM	to RED	1	45	4.75	2	47.7	4.3	73.2	8.9	0	90
103	M	nMS	2	2	30	80	STIM	to NUP	1	45	6.47	2	43.4	4.2	-71.6	8.6	0	90
103	M	nMS	2	2	30	40	STIM	to RED	1	45	2.32	1	40.7	5.6	60.2	3.3	0	90
103	M	nMS	2	2	30	40	STIM	to NUP	1	45	5.23	1	25.1	4.7	-77.7	6.5	0	90
103	M	nMS	2	2	12	20	STIM	to RED	0	45	0	0	27.2	4.8	91.1	2.4	-1	90
103	M	nMS	2	2	12	20	STIM	to NUP	0	45	0	0	16.6	3.3	-65.9	1.4	0	90
103	M	nMS	2	2	12	80	STIM	to RED	0	45	0	0	42.0	3.7	73.3	4.1	0	90
103	M	nMS	2	2	12	80	STIM	to NUP	0	45	3.12	1	28.9	3.8	-104.0	4.2	0	90
103	M	nMS	2	2	12	40	STIM	to RED	0	45	0	0	24.8	3.5	70.7	5.3	0	90
103	M	nMS	2	2	12	40	STIM	to NUP	0	45	0	0	33.4	3.8	-58.4	1.3	0	90
103	M	nMS	2	2	19	20	STIM	to RED	0	45	0	0	35.5	3.3	82.7	3.4	0	90
103	M	nMS	2	2	19	20	STIM	to NUP	0	45	0	0	18.2	4.2	-53.5	6.1	0	90
103	M	nMS	2	2	19	80	STIM	to RED	0	45	0	0	54.3	3.6	78.3	4.7	0	90
103	M	nMS	2	2	19	80	STIM	to NUP	0	45	3.42	1	49.1	4.0	-69.9	6.3	0	90
103	M	nMS	2	2	19	40	STIM	to RED	0	45	0	0	45.6	3.2	60.7	5.5	0	90
103	M	nMS	2	2	19	40	STIM	to NUP	0	45	2.6	1	29.5	5.1	-74.1	1.5	0	90
103	M	nMS	2	2	30	20	STIM	to RED	1	45	0	0	48.0	3.7	74.0	5.2	1	90
103	M	nMS	2	2	30	20	STIM	to NUP	1	45	1.7	1	33.2	4.3	-92.7	2.6	0	90
103	M	nMS	2	2	30	80	STIM	to RED	0	45	3.77	2	42.2	4.4			-1	90
103	M	nMS	2	2	30	80	STIM	to NUP	1	45	3.38	1	61.4	4.2			1	90
103	M	nMS	2	2	30	40	STIM	to RED	1	45	3	1	56.7	4.0	81.5	4.0	0	90
103	M	nMS	2	2	30	40	STIM	to NUP	1	45	4.52	1	57.2	4.2	-61.0	5.2	0	90
103	M	nMS	2	2	23	80	POST	to RED	0	45	4.15	1	84.8	4.4	68.4	3.8	-1	90
103	M	nMS	2	2	23	80	POST	to NUP	0	45	3.93	1	27.8	4.4	-69.5	7.0	0	90
103	M	nMS	2	2	23	80	POST	to RED	1	45	0	0	65.4	4.9	66.8	3.8	1	90
103	M	nMS	2	2	23	80	POST	to NUP	0	45	3.57	1			-73.9	9.7	-1	90
103	M	nMS	2	2	23	80	POST	to RED	1	45	4.7	1	42.5	4.5	72.2	4.4	1	90
103	M	nMS	2	2	23	80	POST	to NUP	0	45	3.6	1	32.5	4.2	-53.7	5.8	-1	90
103	M	nMS	2	2	0	80	post	to RED	0	45		0					0	90
103	M	nMS	2	2	0	80	post	to NUP	0	45		0					0	90
103	M	nMS	2	2	0	80	post	to RED	0	45		0					0	90
103	M	nMS	2	2	0	80	post	to NUP	0	45		0					0	90

103	M	nMS	2	2	0	80	post	to RED	0	45		0					0	90
103	M	nMS	2	2	0	80	post	to NUP	0	45		0					0	90
104	M	MS	2	1	0	80	pre	to RED	0	45		0						90
104	M	MS	2	1	0	80	pre	to NUP	0	45		0					0	90
104	M	MS	2	1	0	80	pre	to RED	0	45		0					0	90
104	M	MS	2	1	0	80	pre	to NUP	0	45		0					0	90
104	M	MS	2	1	0	80	pre	to RED	0	45		0					0	90
104	M	MS	2	1	0	80	pre	to NUP	0	45		0					0	90
104	M	MS	2	1	23	80	PRE	to RED	0	45	3.28	10	59.5	4.7	112.2	2.9	0	90
104	M	MS	2	1	23	80	PRE	to NUP	0	45	3.75	10	67.4	4.4	-86.6	4.7	0	90
104	M	MS	2	1	23	80	PRE	to RED	0	45	3.25	10	57.9	4.3	90.0	4.2	0	90
104	M	MS	2	1	23	80	PRE	to NUP	2	45	3.92	10	62.3	5.1	-78.4	4.5	2	90
104	M	MS	2	1	23	80	PRE	to RED	1	45	4.23	10	58.1	4.4	90.9	3.3	-1	90
104	M	MS	2	1	23	80	PRE	to NUP	0	45	4.25	9	51.7	4.4	-97.3	4.9	-1	90
104	M	MS	2	1	12	20	STIM	to RED	0	45	0	0	11.5	3.8	110.1	1.6	0	90
104	M	MS	2	1	12	20	STIM	to NUP	0	45	0	0	17.8	3.8	-82.3	2.2	0	90
104	M	MS	2	1	12	80	STIM	to RED	0	45	0.87	2	23.1	4.7	94.3	1.4	0	90
104	M	MS	2	1	12	80	STIM	to NUP	0	45	1.55	2	36.6	4.5	-89.6	2.8	0	90
104	M	MS	2	1	12	40	STIM	to RED	0	40	0	0	17.2	4.8	89.6	0.7	0	60
104	M	MS	2	1	12	40	STIM	to NUP	0	40	0	0	25.2	4.0	-86.1	2.3	0	60
104	M	MS	2	1	19	20	STIM	to RED	0	45	0	0	21.0	4.3	100.4	2.0	0	90
104	M	MS	2	1	19	20	STIM	to NUP	0	45	0.35	2	26.4	3.9	-64.6	0.7	0	90
104	M	MS	2	1	19	80	STIM	to RED	0	45	4.95	10	46.1	3.8	78.7	2.5	0	90
104	M	MS	2	1	19	80	STIM	to NUP	0	45	5.52	15	60.8	4.4	-103.2	5.0	0	90
104	M	MS	2	1	19	40	STIM	to RED	0	45	1.52	5	33.5	4.0	104.0	0.7	0	90
104	M	MS	2	1	19	40	STIM	to NUP	0	45	2	5	49.5	4.0	-86.6	3.1	0	90
104	M	MS	2	1	30	20	STIM	to RED	5	45	1.53	7	22.6	3.9	73.1	0.5	5	90
104	M	MS	2	1	30	20	STIM	to NUP	7	45	2.48	5	35.7	4.3	-88.8	3.4	2	90
104	M	MS	2	1	30	80	STIM	to RED	7	45	5.87	15	102.5	3.6	90.9	3.4	0	90
104	M	MS	2	1	30	80	STIM	to NUP	10	45	5.92	30	53.7	3.9	-88.3	9.7	3	90
104	M	MS	2	1	30	40	STIM	to RED	7	45	2.43	10	60.8	3.6	106.1	1.8	-3	90
104	M	MS	2	1	30	40	STIM	to NUP	7	45	4.28	15	39.7	4.4	-68.5	4.2	0	90
104	M	MS	2	1	12	20	STIM	to RED	3	45	0	0	8.8	3.0	85.9	0.5	-4	90
104	M	MS	2	1	12	20	STIM	to NUP	1	45	0	0	34.9	4.0	-87.8	0.9	-2	90
104	M	MS	2	1	12	80	STIM	to RED	0	45	0.83	2	23.2	2.8	78.7	1.0	-1	90
104	M	MS	2	1	12	80	STIM	to NUP	0	45	0	0	38.0	4.4	-152.1	3.1	0	90
104	M	MS	2	1	12	40	STIM	to RED	0	45	0	0	21.2	3.6	106.3	2.1	0	90
104	M	MS	2	1	12	40	STIM	to NUP	0	45	0	0	28.3	3.3	-76.4	4.2	0	90
104	M	MS	2	1	19	20	STIM	to RED	0	45	0	0	16.0	3.2	82.6	0.7	0	90
104	M	MS	2	1	19	20	STIM	to NUP	1	45	0	0	30.1	4.1	-76.1	1.7	1	90
104	M	MS	2	1	19	80	STIM	to RED	1	45	2.65	10	63.7	3.0	99.5	1.4	0	90
104	M	MS	2	1	19	80	STIM	to NUP	2	45	3.68	13	62.4	3.7	-87.8	2.2	1	90
104	M	MS	2	1	19	40	STIM	to RED	1	45	0	0	30.3	3.6	77.3	1.3	-1	90
104	M	MS	2	1	19	40	STIM	to NUP	2	45	2.25	5	21.8	3.6	-95.8	7.7	1	90
104	M	MS	2	1	30	20	STIM	to RED	5	45	2.22	5	21.9	3.1	91.0	0.7	3	90
104	M	MS	2	1	30	20	STIM	to NUP	4	45	0	0	46.6	3.5	-64.4	2.8	-1	90
104	M	MS	2	1	30	80	STIM	to RED	4	45	6.95	25	96.9	2.6	85.4	3.3	0	90
104	M	MS	2	1	30	80	STIM	to NUP	7	45	4.78	18	47.6	3.0	-112.1	12.5	3	90
104	M	MS	2	1	30	40	STIM	to RED	3	45	2.47	8	66.8	2.7	70.6	1.5	-4	90
104	M	MS	2	1	30	40	STIM	to NUP	4	45	2.2	8	67.9	2.6	-93.4	4.8	1	90
104	M	MS	2	1	23	80	POST	to RED	2	45	3.05	12	77.9	2.8	99.3	1.9	-2	90
104	M	MS	2	1	23	80	POST	to NUP	3	45	3.15	15	49.1	2.6	-93.9	8.0	1	90
104	M	MS	2	1	23	80	POST	to RED	1	45	2.9	12	36.0	3.2	95.0	3.4	-2	90
104	M	MS	2	1	23	80	POST	to NUP	1	45	2.32	15	33.6	2.4	-124.5	2.2	0	90
104	M	MS	2	1	23	80	POST	to RED	0	45	3.28	10	38.9	3.0	103.4	2.5	-1	90
104	M	MS	2	1	23	80	POST	to NUP	0	45	1.97	10	46.2	2.8	-116.6	6.7	0	90
104	M	MS	2	1	0	80	post	to RED	0	45		0					0	90
104	M	MS	2	1	0	80	post	to NUP	0	45		0					0	90
104	M	MS	2	1	0	80	post	to RED	0	45		0					0	90
104	M	MS	2	1	0	80	post	to NUP	0	45		0					0	90
104	M	MS	2	1	0	80	post	to RED	0	45		0					0	90
104	M	MS	2	1	0	80	post	to NUP	0	45		0					0	90
104	M	MS	2	2	0	80	pre	to RED	0	45		0			97.3			90
104	M	MS	2	2	0	80	pre	to NUP	0	45		0			-102.1		0	90
104	M	MS	2	2	0	80	pre	to RED	0	45		0			99.9		0	90
104	M	MS	2	2	0	80	pre	to NUP	0	45		0			-74.6		0	90

104	M	MS	2	2	0	80	pre	to RED	0	45		0			78.9		0	90
104	M	MS	2	2	0	80	pre	to NUP	0	45		0			-132.5		0	90
104	M	MS	2	2	23	80	PRE	to RED	0	45		10			97.3		0	90
104	M	MS	2	2	23	80	PRE	to NUP	0	45		10			-102.1		0	90
104	M	MS	2	2	23	80	PRE	to RED	0	45		5			99.9		0	90
104	M	MS	2	2	23	80	PRE	to NUP	0	45		7			-74.6		0	90
104	M	MS	2	2	23	80	PRE	to RED	0	45		5			78.9		0	90
104	M	MS	2	2	23	80	PRE	to NUP	0	45		7			-132.5		0	90
104	M	MS	2	2	12	20	STIM	to RED	0	45		0			92.1		0	90
104	M	MS	2	2	12	20	STIM	to NUP	0	45		0			-90.5		0	90
104	M	MS	2	2	12	80	STIM	to RED	0	45		1			81.8		0	90
104	M	MS	2	2	12	80	STIM	to NUP	0	45		3			-79.4		0	90
104	M	MS	2	2	12	40	STIM	to RED	0	45		0			99.7		0	90
104	M	MS	2	2	12	40	STIM	to NUP	0	45		0			-69.5		0	90
104	M	MS	2	2	19	20	STIM	to RED	0	45		0			86.2		0	90
104	M	MS	2	2	19	20	STIM	to NUP	0	45		0			-75.1		0	90
104	M	MS	2	2	19	80	STIM	to RED	0	45		1			91.1		0	90
104	M	MS	2	2	19	80	STIM	to NUP	1	45		7			-112.4		1	90
104	M	MS	2	2	19	40	STIM	to RED	0	45		1			89.7		-1	90
104	M	MS	2	2	19	40	STIM	to NUP	0	45		1			-95.0		0	90
104	M	MS	2	2	30	20	STIM	to RED	0	45		0			69.9		0	90
104	M	MS	2	2	30	20	STIM	to NUP	0	45		1			-69.2		0	90
104	M	MS	2	2	30	80	STIM	to RED	0	45		10			82.1		0	90
104	M	MS	2	2	30	80	STIM	to NUP	2	45		12			-117.2		2	90
104	M	MS	2	2	30	40	STIM	to RED	1	45		2			92.9		-1	90
104	M	MS	2	2	30	40	STIM	to NUP	1	45		3			-94.0		0	90
104	M	MS	2	2	12	20	STIM	to RED	0	45		0			92.1		-1	90
104	M	MS	2	2	12	20	STIM	to NUP	0	45		0			-90.5		0	90
104	M	MS	2	2	12	80	STIM	to RED	0	45		0			81.8		0	90
104	M	MS	2	2	12	80	STIM	to NUP	0	45		1			-79.4		0	90
104	M	MS	2	2	12	40	STIM	to RED	0	45		0			99.7		0	90
104	M	MS	2	2	12	40	STIM	to NUP	0	45		0			-69.5		0	90
104	M	MS	2	2	19	20	STIM	to RED	0	45		0			86.2		0	90
104	M	MS	2	2	19	20	STIM	to NUP	0	45		0			-75.1		0	90
104	M	MS	2	2	19	80	STIM	to RED	0	45		1			91.1		0	90
104	M	MS	2	2	19	80	STIM	to NUP	0	45		2			-112.4		0	90
104	M	MS	2	2	19	40	STIM	to RED	0	45		1			89.7		0	90
104	M	MS	2	2	19	40	STIM	to NUP	0	45		1			-95.0		0	90
104	M	MS	2	2	30	20	STIM	to RED	0	45		0			69.9		0	90
104	M	MS	2	2	30	20	STIM	to NUP	0	45		0			-69.2		0	90
104	M	MS	2	2	30	80	STIM	to RED	2	45		10			82.1		2	90
104	M	MS	2	2	30	80	STIM	to NUP	2	45		8			-117.2		0	90
104	M	MS	2	2	30	40	STIM	to RED	0	45		1			92.9		-2	90
104	M	MS	2	2	30	40	STIM	to NUP	0	45		3			-94.0		0	90
104	M	MS	2	2	23	80	POST	to RED	0	45		4			93.0		0	90
104	M	MS	2	2	23	80	POST	to NUP	0	45		3			-76.8		0	90
104	M	MS	2	2	23	80	POST	to RED	0	45		2			94.7		0	90
104	M	MS	2	2	23	80	POST	to NUP	0	45		3			-85.3		0	90
104	M	MS	2	2	23	80	POST	to RED	0	45		2			95.7		0	90
104	M	MS	2	2	23	80	POST	to NUP	0	45		2			-86.8		0	90
104	M	MS	2	2	0	80	post	to RED	0	45		0					0	90
104	M	MS	2	2	0	80	post	to NUP	0	45		0					0	90
104	M	MS	2	2	0	80	post	to RED	0	45		0					0	90
104	M	MS	2	2	0	80	post	to NUP	0	45		0					0	90
104	M	MS	2	2	0	80	post	to RED	0	45		0					0	90
104	M	MS	2	2	0	80	post	to NUP	0	45		0					0	90
105	M	nMS	1	1	0	80	pre	to RED	0	45		0						90
105	M	nMS	1	1	0	80	pre	to NUP	0	45		0					0	90
105	M	nMS	1	1	0	80	pre	to RED	0	45		0					0	90
105	M	nMS	1	1	0	80	pre	to NUP	0	45		0					0	90
105	M	nMS	1	1	0	80	pre	to RED	0	45		0					0	90
105	M	nMS	1	1	0	80	pre	to NUP	0	45		0					0	90
105	M	nMS	1	1	23	80	PRE	to RED	0	45	0	0	48.0	4.3	45.1	4.5	0	90
105	M	nMS	1	1	23	80	PRE	to NUP	2	40	1.45	10	24.4	3.9	-94.8	12.0	2	60
105	M	nMS	1	1	23	80	PRE	to RED	0	45	2.3	10	24.5	4.3	111.2	4.1	-2	90
105	M	nMS	1	1	23	80	PRE	to NUP	0	40	4	15	44.8	4.5	-129.1	4.4	0	60

105	M	nMS	1	1	23	80	PRE	to RED	0	40	1.8	12	18.4	4.4	74.7	4.0	0	60
105	M	nMS	1	1	23	80	PRE	to NUP	0	45	8.18	17	19.5	4.1	-153.2	4.0	0	90
105	M	nMS	1	1	12	20	STIM	to RED	0	45	0	0	4.7	2.3	105.2		0	90
105	M	nMS	1	1	12	20	STIM	to NUP	0	45	0.42	5	12.2	2.6	-85.5	2.5	0	90
105	M	nMS	1	1	12	80	STIM	to RED	0	45	3.45	3	23.5	4.4	73.2	2.6	0	90
105	M	nMS	1	1	12	80	STIM	to NUP	0	45	5.33	7	24.6	4.2	-121.7	4.5	0	90
105	M	nMS	1	1	12	40	STIM	to RED	0	45	1.25	7	14.6	3.5	60.0	0.6	0	90
105	M	nMS	1	1	12	40	STIM	to NUP	0	40	4.05	8	19.1	3.6	-70.9	1.3	0	60
105	M	nMS	1	1	19	20	STIM	to RED	0	42	0.97	4	11.6	3.2	52.5	2.9	0	72
105	M	nMS	1	1	19	20	STIM	to NUP	0	40	2	5	16.4	2.9	-85.0	4.5	0	60
105	M	nMS	1	1	19	80	STIM	to RED	0	45	5.18	8	34.8	4.3	59.7	3.4	0	90
105	M	nMS	1	1	19	80	STIM	to NUP	0	45	4.77	10	40.4	4.3	-116.1	3.5	0	90
105	M	nMS	1	1	19	40	STIM	to RED	0	45	2.78	3	27.8	4.6	55.4	1.5	0	90
105	M	nMS	1	1	19	40	STIM	to NUP	0	45	3.17	8	28.2	2.8	-67.7	5.2	0	90
105	M	nMS	1	1	30	20	STIM	to RED	0	45	0.82	4	27.2	3.9	59.5	0.8	0	90
105	M	nMS	1	1	30	20	STIM	to NUP	2	45	2.5	4	32.9	4.6	-94.9	0.5	2	90
105	M	nMS	1	1	30	80	STIM	to RED	0	45	3.85	4	36.0	4.6	50.2	6.1	-2	90
105	M	nMS	1	1	30	80	STIM	to NUP	0	45	6.7	12	57.0	4.7	-109.4	2.5	0	90
105	M	nMS	1	1	30	40	STIM	to RED	0	45	1.92	7	47.2	4.8	71.0	1.1	0	90
105	M	nMS	1	1	30	40	STIM	to NUP	0	45	6.95	12	41.4	4.7	-79.7	2.3	0	90
105	M	nMS	1	1	12	20	STIM	to RED	0	45	0.85	1	9.8	3.4	74.5	0.5	0	90
105	M	nMS	1	1	12	20	STIM	to NUP	0	45	0.6	1	12.6	4.1	-68.2	2.5	0	90
105	M	nMS	1	1	12	80	STIM	to RED	0	45	2.67	2	26.9	4.1	86.8	2.5	0	90
105	M	nMS	1	1	12	80	STIM	to NUP	0	45	2.28	3	33.3	3.2	-108.2	1.5	0	90
105	M	nMS	1	1	12	40	STIM	to RED	0	45	1.13	1	20.4	3.2	80.0	1.0	0	90
105	M	nMS	1	1	12	40	STIM	to NUP	0	45	1.43	1	19.3	2.8	-88.4	1.1	0	90
105	M	nMS	1	1	19	20	STIM	to RED	0	45	0	0	18.2	3.7	73.8	0.8	0	90
105	M	nMS	1	1	19	20	STIM	to NUP	4	45	1.35	4	13.6	3.7	-84.9	0.7	4	90
105	M	nMS	1	1	19	80	STIM	to RED	3	45	3.25	6	31.1	4.3		3.6	-1	90
105	M	nMS	1	1	19	80	STIM	to NUP	2	45	4.1	9	32.7	4.8		0.7	-1	90
105	M	nMS	1	1	19	40	STIM	to RED	0	45	2	5	18.7	3.9	78.6	1.6	-2	90
105	M	nMS	1	1	19	40	STIM	to NUP	0	45	4.28	6	26.1	3.9	-102.5	1.1	0	90
105	M	nMS	1	1	30	20	STIM	to RED	1	40	0.8	3	19.1	3.8	62.4	0.4	1	60
105	M	nMS	1	1	30	20	STIM	to NUP	2	42	6.07	4	27.4	4.4	-64.0	1.0	1	72
105	M	nMS	1	1	30	80	STIM	to RED	0	45	3.95	8	53.3	4.2	52.1	5.7	-2	90
105	M	nMS	1	1	30	80	STIM	to NUP	0	42	5.05	13	39.3	4.5	-84.4	6.1	0	72
105	M	nMS	1	1	30	40	STIM	to RED	0	45	5.13	10	30.9	4.4	75.5	2.7	0	90
105	M	nMS	1	1	30	40	STIM	to NUP	0	45	6.58	15	34.9	3.9	-69.5	4.4	0	90
105	M	nMS	1	1	23	80	POST	to RED	0	40	3.15	5	36.1	5.8	53.6	3.8	0	60
105	M	nMS	1	1	23	80	POST	to NUP	2	42	5.33	7	43.2	4.9	-103.9	1.4	2	72
105	M	nMS	1	1	23	80	POST	to RED	2	45	4	7	33.6	6.4	64.6	2.4	0	90
105	M	nMS	1	1	23	80	POST	to NUP	0	45	6.85	8	42.4	4.2	-70.9	5.5	-2	90
105	M	nMS	1	1	23	80	POST	to RED	0	45	2.87	4	40.2	5.2	89.6	2.9	0	90
105	M	nMS	1	1	23	80	POST	to NUP	0	45	4.43	7	43.9	5.2	-93.4	2.4	0	90
105	M	nMS	1	1	0	80	post	to RED	0	50		2					0	120
105	M	nMS	1	1	0	80	post	to NUP	0	45		4					0	90
105	M	nMS	1	1	0	80	post	to RED	0	45		1					0	90
105	M	nMS	1	1	0	80	post	to NUP	1	45		3					1	90
105	M	nMS	1	1	0	80	post	to RED	0	45		1					-1	90
105	M	nMS	1	1	0	80	post	to NUP	0	45		0					0	90
105	M	nMS	1	2	0	80	pre	to RED	0	45		0						90
105	M	nMS	1	2	0	80	pre	to NUP	0	45		0					0	90
105	M	nMS	1	2	0	80	pre	to RED	0	45		0					0	90
105	M	nMS	1	2	0	80	pre	to NUP	0	45		0					0	90
105	M	nMS	1	2	0	80	pre	to RED	0	45		0					0	90
105	M	nMS	1	2	0	80	pre	to NUP	0	45		0					0	90
105	M	nMS	1	2	23	80	PRE	to RED	0	45	2.13	3	61.8	5.0	85.5	2.9	0	90
105	M	nMS	1	2	23	80	PRE	to NUP	0	45	6.83	9	38.7	5.0	-101.8	4.4	0	90
105	M	nMS	1	2	23	80	PRE	to RED	0	45	3.08	3	49.2	5.3	55.5	2.8	0	90
105	M	nMS	1	2	23	80	PRE	to NUP	0	45	5.35	7	38.4	4.2	-102.1	4.5	0	90
105	M	nMS	1	2	23	80	PRE	to RED	0	45	2.42	3	42.6	5.0	79.9	2.5	0	90
105	M	nMS	1	2	23	80	PRE	to NUP	0	45	2.88	5	57.0	4.6	-96.5	3.1	0	90
105	M	nMS	1	2	12	20	STIM	to RED	0	45	0.82	1	14.5	4.1	75.6	0.4	0	90
105	M	nMS	1	2	12	20	STIM	to NUP	0	45	0.65	2	9.5	3.8	-82.3	0.5	0	90
105	M	nMS	1	2	12	80	STIM	to RED	0	45	2.83	2	35.8	4.6	97.8	0.6	0	90
105	M	nMS	1	2	12	80	STIM	to NUP	0	45	4.48	4	40.3	4.4	-104.7	0.7	0	90

105	M	nMS	1	2	12	40	STIM	to RED	0	45	1.67	1	19.6	4.0	85.1	0.8	0	90
105	M	nMS	1	2	12	40	STIM	to NUP	0	45	2.3	2	21.8	4.0	-93.7	0.6	0	90
105	M	nMS	1	2	19	20	STIM	to RED	0	45	0.4	1	21.6	3.9	69.6	0.7	0	90
105	M	nMS	1	2	19	20	STIM	to NUP	0	45	1.02	3	21.0	4.0	-80.8	0.5	0	90
105	M	nMS	1	2	19	80	STIM	to RED	0	45	3.65	3	40.4	3.7	81.0	2.9	0	90
105	M	nMS	1	2	19	80	STIM	to NUP	0	45	4.4	4	43.0	5.4	-111.3	0.4	0	90
105	M	nMS	1	2	19	40	STIM	to RED	0	45	2.4	2.5	29.8	4.8	80.9	1.6	0	90
105	M	nMS	1	2	19	40	STIM	to NUP	0	45	3.7	3	42.9	3.5	-73.6	-0.1	0	90
105	M	nMS	1	2	30	20	STIM	to RED	0	45	1.53	2	29.8	2.8	69.0	0.6	0	90
105	M	nMS	1	2	30	20	STIM	to NUP	0	40	2.77	4	30.2	3.3	-83.8	2.2	0	60
105	M	nMS	1	2	30	80	STIM	to RED	0	45	3.75	6	53.2	3.8	59.6	7.0	0	90
105	M	nMS	1	2	30	80	STIM	to NUP	0	45	4.63	11	60.6	3.5	-128.1	8.1	0	90
105	M	nMS	1	2	30	40	STIM	to RED	0	45	2.45	6	42.9	3.3	76.2	3.0	0	90
105	M	nMS	1	2	30	40	STIM	to NUP	0	45	3.47	5	32.1	3.5	-93.4	4.6	0	90
105	M	nMS	1	2	12	20	STIM	to RED	0	45	0	0	14.4	3.1	53.1	0.5	0	90
105	M	nMS	1	2	12	20	STIM	to NUP	0	45	1.02	0.5	21.3	3.8	-95.5	0.2	0	90
105	M	nMS	1	2	12	80	STIM	to RED	0	45	2.47	2	31.4	3.8	100.4	2.0	0	90
105	M	nMS	1	2	12	80	STIM	to NUP	0	45	1.63	2.5	37.4	3.9	-109.4	2.6	0	90
105	M	nMS	1	2	12	40	STIM	to RED	0	45	0	0	25.7	2.9	78.0	0.2	0	90
105	M	nMS	1	2	12	40	STIM	to NUP	0	45	1.4	0.3	26.7	3.9	-80.0	0.6	0	90
105	M	nMS	1	2	19	20	STIM	to RED	0	45	0.83	0.2	23.3	2.9	78.2	0.5	0	90
105	M	nMS	1	2	19	20	STIM	to NUP	0	45	1.15	0.5	28.5	3.7	-87.6	0.9	0	90
105	M	nMS	1	2	19	80	STIM	to RED	0	45	2.4	0.5	46.6	4.7	57.4	1.7	0	90
105	M	nMS	1	2	19	80	STIM	to NUP	0	45	3.88	4	52.8	5.0	-102.8	2.4	0	90
105	M	nMS	1	2	19	40	STIM	to RED	0	45	1.32	2	31.7	4.6	69.6	0.6	0	90
105	M	nMS	1	2	19	40	STIM	to NUP	0	45	1.27	4	44.0	3.9	-87.2	1.4	0	90
105	M	nMS	1	2	30	20	STIM	to RED	0	43	1.58	2	40.3	3.6	75.2	0.6	0	78
105	M	nMS	1	2	30	20	STIM	to NUP	2	45	0.97	4	42.6	3.2	-74.6	1.5	2	90
105	M	nMS	1	2	30	80	STIM	to RED	2	45	5.42	7	45.4	3.9	74.2	6.2	0	90
105	M	nMS	1	2	30	80	STIM	to NUP	0	45	5.57	11	45.8	4.0	-74.2	7.8	-2	90
105	M	nMS	1	2	30	40	STIM	to RED	0	43	1.37	4	43.9	3.6	76.4	4.9	0	78
105	M	nMS	1	2	30	40	STIM	to NUP	0	45	4.87	8	56.0	3.1	-80.8	2.9	0	90
105	M	nMS	1	2	23	80	POST	to RED	0	45	2.42	5	57.9	4.0	81.2	3.4	0	90
105	M	nMS	1	2	23	80	POST	to NUP	2	45	3.67	4	38.6	4.1	-108.0	5.8	2	90
105	M	nMS	1	2	23	80	POST	to RED	0	45	2.3	3	37.9	4.4	66.5	5.3	-2	90
105	M	nMS	1	2	23	80	POST	to NUP	1	45	3.92	3	54.8	4.1	-106.8	1.8	1	90
105	M	nMS	1	2	23	80	POST	to RED	0	45	2.95	3	66.3	4.8	63.6	2.3	-1	90
105	M	nMS	1	2	23	80	POST	to NUP	3	45	4.7	5	39.8	4.2	-94.9	5.3	3	90
105	M	nMS	1	2	0	80	post	to RED	0	50		0.5					-3	120
105	M	nMS	1	2	0	80	post	to NUP	0	45		2					0	90
105	M	nMS	1	2	0	80	post	to RED	0	45		0					0	90
105	M	nMS	1	2	0	80	post	to NUP	0	45		1					0	90
105	M	nMS	1	2	0	80	post	to RED	0	45		0					0	90
105	M	nMS	1	2	0	80	post	to NUP	0	45		0.1					0	90
106	F	nMS	1	1	0	80	pre	to RED	0	45		0						90
106	F	nMS	1	1	0	80	pre	to NUP	0	45		0					0	90
106	F	nMS	1	1	0	80	pre	to RED	0	45		0					0	90
106	F	nMS	1	1	0	80	pre	to NUP	0	45		0					0	90
106	F	nMS	1	1	0	80	pre	to RED	0	45		0					0	90
106	F	nMS	1	1	0	80	pre	to NUP	0	45		0					0	90
106	F	nMS	1	1	23	80	PRE	to RED	0	45	3.98	10	75.4	5.2	65.4	4.6	0	90
106	F	nMS	1	1	23	80	PRE	to NUP	0	40	2.03	15	55.3	4.6	-107.1	10.1	0	60
106	F	nMS	1	1	23	80	PRE	to RED	0	45	2.72	8	161.7	5.4	117.7	1.0	0	90
106	F	nMS	1	1	23	80	PRE	to NUP	0	41	13.72	15	80.3	6.4	-94.4	3.8	0	66
106	F	nMS	1	1	23	80	PRE	to RED	0	50	4.48	16	102.8	5.9	110.9	2.5	0	120
106	F	nMS	1	1	23	80	PRE	to NUP	0	38	13.93	14	77.5	7.6	-96.8	3.0	0	48
106	F	nMS	1	1	12	20	STIM	to RED	0	46	1.52	7	21.8	4.5	74.4	1.8	0	96
106	F	nMS	1	1	12	20	STIM	to NUP	0	44	1.98	8	19.4	4.6	-96.1	0.5	0	84
106	F	nMS	1	1	12	80	STIM	to RED	0	45	7.78	8	65.1	5.0	90.6	1.1	0	90
106	F	nMS	1	1	12	80	STIM	to NUP	0	41	11.68	8	54.0	5.1	-111.6	3.6	0	66
106	F	nMS	1	1	12	40	STIM	to RED	0	45	7.83	9	40.4	4.6	113.5	0.1	0	90
106	F	nMS	1	1	12	40	STIM	to NUP	0	43	10.4	8	41.4	5.5	-72.0	0.2	0	78
106	F	nMS	1	1	19	20	STIM	to RED	0	47	6.62	8	32.2	4.5	75.0	1.2	0	102
106	F	nMS	1	1	19	20	STIM	to NUP	0	42	11.82	8	26.5	4.9	-69.3	1.5	0	72
106	F	nMS	1	1	19	80	STIM	to RED	0	49	14.53	9	96.5	4.6	80.4	1.5	0	114
106	F	nMS	1	1	19	80	STIM	to NUP	0	40	16.1	12	54.3	3.8	-106.1	7.1	0	60

106	F	nMS	1	1	19	40	STIM	to RED	0	47	9.18	10	51.0	4.5	79.7	1.8	0	102
106	F	nMS	1	1	19	40	STIM	to NUP	0	41	13.72	10	69.9	3.8	-82.8	2.8	0	66
106	F	nMS	1	1	30	20	STIM	to RED	0	46	7.98	9	57.7	4.2	58.5	2.0	0	96
106	F	nMS	1	1	30	20	STIM	to NUP	0	39	20.25	10	40.8	4.2	-95.6	4.1	0	54
106	F	nMS	1	1	30	80	STIM	to RED	0	53	19.65	10	104.5	4.1	65.1	4.4	0	138
106	F	nMS	1	1	30	80	STIM	to NUP	0	36	17.53	12	61.1	5.4	-124.5	8.1	0	36
106	F	nMS	1	1	30	40	STIM	to RED	0	52	12.97	10	104.9	3.6	90.1	1.8	0	132
106	F	nMS	1	1	30	40	STIM	to NUP	0	34	15.82	11	83.3	4.1	-119.2	5.1	0	24
106	F	nMS	1	1	12	20	STIM	to RED	0	45	2.35	8	27.0	2.7	72.7	0.8	0	90
106	F	nMS	1	1	12	20	STIM	to NUP	0	44	2.47	8	25.3	5.5	-83.6	2.3	0	84
106	F	nMS	1	1	12	80	STIM	to RED	0	45	8.33	7	59.2	4.8	94.3	1.4	0	90
106	F	nMS	1	1	12	80	STIM	to NUP	0	42	14.73	8	34.0	3.8	-96.4	6.1	0	72
106	F	nMS	1	1	12	40	STIM	to RED	0	46	7.02	9	37.9	3.2	85.8	0.6	0	96
106	F	nMS	1	1	12	40	STIM	to NUP	0	43	8.7	8	35.1	3.8	-66.1	4.2	0	78
106	F	nMS	1	1	19	20	STIM	to RED	0	47	5.93	8	37.8	3.6	60.7	1.0	0	102
106	F	nMS	1	1	19	20	STIM	to NUP	0	41	14.27	8	35.3	4.1	-97.1	1.9	0	66
106	F	nMS	1	1	19	80	STIM	to RED	0	47	14.63	6	83.5	3.9	73.2	3.1	0	102
106	F	nMS	1	1	19	80	STIM	to NUP	0	41	20.92	8	47.9	4.4	-115.3	6.1	0	66
106	F	nMS	1	1	19	40	STIM	to RED	0	46	15.08	7	49.3	2.7	124.9	2.6	0	96
106	F	nMS	1	1	19	40	STIM	to NUP	1	40	19.92	8	39.1	3.6	-81.3	1.9	1	60
106	F	nMS	1	1	30	20	STIM	to RED	1	48	17.03	10	31.8	3.9	65.8	3.0	0	108
106	F	nMS	1	1	30	20	STIM	to NUP	2	38	20.9	11	62.6	4.4	-91.5	1.7	1	48
106	F	nMS	1	1	30	80	STIM	to RED	1	52	19.42	12	64.5	3.8	78.2	5.0	-1	132
106	F	nMS	1	1	30	80	STIM	to NUP	2	40	22.52	13	32.4	3.1	-78.1	11.7	1	60
106	F	nMS	1	1	30	40	STIM	to RED	2	49	20.55	11	59.2	3.9	111.6	3.9	0	114
106	F	nMS	1	1	30	40	STIM	to NUP	3	37	27.78	12	36.8	3.4	-103.3	9.4	1	42
106	F	nMS	1	1	23	80	POST	to RED	2	45	14.65	9	88.9	3.3	89.6	3.6	-1	90
106	F	nMS	1	1	23	80	POST	to NUP	2	38	21.85	10	43.5	4.1	-93.9	4.8	0	48
106	F	nMS	1	1	23	80	POST	to RED	2	46	11.87	8	77.4	4.7	116.2	3.1	0	96
106	F	nMS	1	1	23	80	POST	to NUP	3	40	17.48	10	32.9	3.7	-112.6	11.6	1	60
106	F	nMS	1	1	23	80	POST	to RED	1	45	18.07	8	44.1	4.0	145.1	5.9	-2	90
106	F	nMS	1	1	23	80	POST	to NUP	3	43	20.65	10	64.2	3.5	-143.0	6.8	2	78
106	F	nMS	1	1	0	80	post	to RED	0	45		2					-3	90
106	F	nMS	1	1	0	80	post	to NUP	0	46		1					0	96
106	F	nMS	1	1	0	80	post	to RED	0	46		2					0	96
106	F	nMS	1	1	0	80	post	to NUP	0	46		0					0	96
106	F	nMS	1	1	0	80	post	to RED	0	45		2					0	90
106	F	nMS	1	1	0	80	post	to NUP	0	45		2					0	90
106	F	nMS	1	2	0	80	pre	to RED	0	45		0						90
106	F	nMS	1	2	0	80	pre	to NUP	0	45		0					0	90
106	F	nMS	1	2	0	80	pre	to RED	0	45		0					0	90
106	F	nMS	1	2	0	80	pre	to NUP	0	45		0					0	90
106	F	nMS	1	2	0	80	pre	to RED	0	45		0					0	90
106	F	nMS	1	2	0	80	pre	to NUP	0	45		0					0	90
106	F	nMS	1	2	23	80	PRE	to RED	0	47	10.38	7	53.1	5.1	83.1	3.1	0	102
106	F	nMS	1	2	23	80	PRE	to NUP	0	41	15.7	7	51.4	4.8	-70.6	5.5	0	66
106	F	nMS	1	2	23	80	PRE	to RED	0	47	11.6	6	87.0	4.6	86.4	2.3	0	102
106	F	nMS	1	2	23	80	PRE	to NUP	0	40	15.8	8	69.6	3.6	-99.7	5.4	0	60
106	F	nMS	1	2	23	80	PRE	to RED	0	46	8.8	6	112.8	4.6	106.8	1.2	0	96
106	F	nMS	1	2	23	80	PRE	to NUP	0	41	12.82	8	50.6	3.8	-83.1	7.9	0	66
106	F	nMS	1	2	12	20	STIM	to RED	0	45	1.47	3	24.2	3.1	71.1	0.4	0	90
106	F	nMS	1	2	12	20	STIM	to NUP	0	44	0.98	5	19.5	3.6	-77.2	2.4	0	84
106	F	nMS	1	2	12	80	STIM	to RED	0	45	4.13	5	46.7	4.2	83.4	1.4	0	90
106	F	nMS	1	2	12	80	STIM	to NUP	0	43	7.53	5	40.9	4.5	-114.2	4.0	0	78
106	F	nMS	1	2	12	40	STIM	to RED	0	46	4.05	4	31.2	3.6	91.2	0.5	0	96
106	F	nMS	1	2	12	40	STIM	to NUP	0	43.5	5.33	5	42.4	4.4	-108.4	0.7	0	81
106	F	nMS	1	2	19	20	STIM	to RED	0	46	5.87	6	29.1	4.3	64.3	0.9	0	96
106	F	nMS	1	2	19	20	STIM	to NUP	0	43	7.72	6	32.8	3.9	-86.3	1.2	0	78
106	F	nMS	1	2	19	80	STIM	to RED	0	46	9.35	6	32.5	4.0	96.9	6.4	0	96
106	F	nMS	1	2	19	80	STIM	to NUP	0	41	12.52	7	36.3	4.1	-123.4	5.3	0	66
106	F	nMS	1	2	19	40	STIM	to RED	0	46	8.92	6	47.2	4.4	134.2	3.4	0	96
106	F	nMS	1	2	19	40	STIM	to NUP	0	41	13.58	6	45.5	4.1	-141.3	5.9	0	66
106	F	nMS	1	2	30	20	STIM	to RED	0	47	7.58	7	60.5	3.6	61.9	1.6	0	102
106	F	nMS	1	2	30	20	STIM	to NUP	0	38	12.37	7	66.3	3.4	-88.8	3.1	0	48
106	F	nMS	1	2	30	80	STIM	to RED	0	46	12.8	8	82.5	3.5	150.7	4.4	0	96
106	F	nMS	1	2	30	80	STIM	to NUP	0	35	20.77	9	51.6	3.5	-66.7	8.2	0	30

106	F	nMS	1	2	30	40	STIM	to RED	0	45	10.73	7	69.8	3.6	126.4	3.1	0	90
106	F	nMS	1	2	30	40	STIM	to NUP	0	37	14.82	8	39.8	2.9	-64.9	8.2	0	42
106	F	nMS	1	2	12	20	STIM	to RED	0	45	1.87	1	19.6	3.0	53.8	0.6	0	90
106	F	nMS	1	2	12	20	STIM	to NUP	0	44.5	5.58	1	26.4	4.2	-61.4	1.9	0	87
106	F	nMS	1	2	12	80	STIM	to RED	0	46	0.75	1	44.2	4.0	101.5	1.3	0	96
106	F	nMS	1	2	12	80	STIM	to NUP	0	44	8.92	3	38.8	3.5	-88.0	8.7	0	84
106	F	nMS	1	2	12	40	STIM	to RED	0	45	3	2	48.1	3.9	85.5	0.8	0	90
106	F	nMS	1	2	12	40	STIM	to NUP	0	44	5.6	2	31.9	4.0	-59.0	1.7	0	84
106	F	nMS	1	2	19	20	STIM	to RED	0	46	1.28	4	28.9	3.9	60.0	2.2	0	96
106	F	nMS	1	2	19	20	STIM	to NUP	0	42	6.63	5	40.7	3.2	-65.6	2.3	0	72
106	F	nMS	1	2	19	80	STIM	to RED	0	46	6.37	4	35.9	3.5	94.9	5.9	0	96
106	F	nMS	1	2	19	80	STIM	to NUP	0	44	7.83	5	40.1	3.7	-104.2	7.2	0	84
106	F	nMS	1	2	19	40	STIM	to RED	0	45	4.5	3	43.3	4.2	72.0	1.4	0	90
106	F	nMS	1	2	19	40	STIM	to NUP	0	42	10.98	4.5	44.3	3.2	-67.3	3.2	0	72
106	F	nMS	1	2	30	20	STIM	to RED	0	46	2.28	4	53.3	3.2	59.2	2.7	0	96
106	F	nMS	1	2	30	20	STIM	to NUP	0	43	7.85	4	42.3	3.4	-82.9	3.5	0	78
106	F	nMS	1	2	30	80	STIM	to RED	0	46.5	8.72	5	62.6	3.2	105.6	4.1	0	99
106	F	nMS	1	2	30	80	STIM	to NUP	0	43	13.58	5	56.3	3.8	-63.5	5.9	0	78
106	F	nMS	1	2	30	40	STIM	to RED	0	48	9.32	5	60.3	4.2	56.0	3.1	0	108
106	F	nMS	1	2	30	40	STIM	to NUP	0	40	13.42	5	37.1	3.4	-69.9	7.3	0	60
106	F	nMS	1	2	23	80	POST	to RED	0	46.5	6.6	2	44.9	3.6	105.4	5.1	0	99
106	F	nMS	1	2	23	80	POST	to NUP	0	44	12.87	3	38.5	4.2	-55.6	5.7	0	84
106	F	nMS	1	2	23	80	POST	to RED	0	45	7.12	1	34.5	4.3	122.0	4.6	0	90
106	F	nMS	1	2	23	80	POST	to NUP	0	43	13.15	3	68.2	4.4	-89.0	4.7	0	78
106	F	nMS	1	2	23	80	POST	to RED	0	46	8.38	2	50.6	4.1	101.1	4.2	0	96
106	F	nMS	1	2	23	80	POST	to NUP	0	44	9.47	3	48.2	3.7	-102.6	7.1	0	84
106	F	nMS	1	2	0	80	post	to RED	0	45		0					0	90
106	F	nMS	1	2	0	80	post	to NUP	0	45		0					0	90
106	F	nMS	1	2	0	80	post	to RED	0	45		0					0	90
106	F	nMS	1	2	0	80	post	to NUP	0	45		0					0	90
106	F	nMS	1	2	0	80	post	to RED	0	45		0					0	90
106	F	nMS	1	2	0	80	post	to NUP	0	45		0					0	90
107	M	nMS	1	1	0	80	pre	to RED	0	45		0						90
107	M	nMS	1	1	0	80	pre	to NUP	0	45		0					0	90
107	M	nMS	1	1	0	80	pre	to RED	0	45		0					0	90
107	M	nMS	1	1	0	80	pre	to NUP	0	45		0					0	90
107	M	nMS	1	1	0	80	pre	to RED	0	45		0					0	90
107	M	nMS	1	1	0	80	pre	to NUP	0	45		0					0	90
107	M	nMS	1	1	23	80	PRE	to RED	0	45	0.55	10			104.6		0	90
107	M	nMS	1	1	23	80	PRE	to NUP	0	45	0.8	20			-72.0		0	90
107	M	nMS	1	1	23	80	PRE	to RED	0	45	0.35	12			190.9		0	90
107	M	nMS	1	1	23	80	PRE	to NUP	0	45	0.23	20			-72.9		0	90
107	M	nMS	1	1	23	80	PRE	to RED	0	45	9.27	12			140.6		0	90
107	M	nMS	1	1	23	80	PRE	to NUP	0	42	11.37	20			-125.1		0	72
107	M	nMS	1	1	12	20	STIM	to RED	0	45	0	0			44.9		0	90
107	M	nMS	1	1	12	20	STIM	to NUP	0	45	0.57	8			-68.4		0	90
107	M	nMS	1	1	12	80	STIM	to RED	0	45	4.87	5			102.3		0	90
107	M	nMS	1	1	12	80	STIM	to NUP	0	45	9.33	10			-108.5		0	90
107	M	nMS	1	1	12	40	STIM	to RED	0	45	4.02	7			89.6		0	90
107	M	nMS	1	1	12	40	STIM	to NUP	0	45	5.77	8			-94.5		0	90
107	M	nMS	1	1	19	20	STIM	to RED	0	45	1	3			85.6		0	90
107	M	nMS	1	1	19	20	STIM	to NUP	0	40	3.53	5			-42.2		0	60
107	M	nMS	1	1	19	80	STIM	to RED	0	45	5.4	15			102.1		0	90
107	M	nMS	1	1	19	80	STIM	to NUP	0	42	8.75	20			-132.8		0	72
107	M	nMS	1	1	19	40	STIM	to RED	0	45	6.42	10			74.0		0	90
107	M	nMS	1	1	19	40	STIM	to NUP	0	38	8.22	18			-134.0		0	48
107	M	nMS	1	1	30	20	STIM	to RED	0	45	2.07	8			55.6		0	90
107	M	nMS	1	1	30	20	STIM	to NUP	0	35	4.4	5			-71.8		0	30
107	M	nMS	1	1	30	80	STIM	to RED	0	45	3.1	15			84.9		0	90
107	M	nMS	1	1	30	80	STIM	to NUP	0	37	8.42	22			-113.6		0	42
107	M	nMS	1	1	30	40	STIM	to RED	0	45	2.38	10			167.4		0	90
107	M	nMS	1	1	30	40	STIM	to NUP	0	35	1.03	17			-150.2		0	30
107	M	nMS	1	1	12	20	STIM	to RED	0	45	0	0			72.3		0	90
107	M	nMS	1	1	12	20	STIM	to NUP	0	45	0.35	1			-86.0		0	90
107	M	nMS	1	1	12	80	STIM	to RED	0	45	1.22	5			97.6		0	90
107	M	nMS	1	1	12	80	STIM	to NUP	0	45	4.22	9			-105.6		0	90

107	M	nMS	1	1	12	40	STIM	to RED	0	45	0.73	4			102.6		0	90
107	M	nMS	1	1	12	40	STIM	to NUP	0	45	0.93	4			-92.4		0	90
107	M	nMS	1	1	19	20	STIM	to RED	0	45	0	0			69.4		0	90
107	M	nMS	1	1	19	20	STIM	to NUP	0	45	0.75	5			-90.9		0	90
107	M	nMS	1	1	19	80	STIM	to RED	0	45	3.28	8			102.2		0	90
107	M	nMS	1	1	19	80	STIM	to NUP	0	43	2.58	15			-77.4		0	78
107	M	nMS	1	1	19	40	STIM	to RED	0	45	1.17	5			112.8		0	90
107	M	nMS	1	1	19	40	STIM	to NUP	0	43	2.03	12			-61.3		0	78
107	M	nMS	1	1	30	20	STIM	to RED	0	45	0	0			76.9		0	90
107	M	nMS	1	1	30	20	STIM	to NUP	0	45	0	0			-74.5		0	90
107	M	nMS	1	1	30	80	STIM	to RED	0	45	1.33	7			97.9		0	90
107	M	nMS	1	1	30	80	STIM	to NUP	1	42	7.22	15			-84.8		1	72
107	M	nMS	1	1	30	40	STIM	to RED	0	45	1.22	12			113.6		-1	90
107	M	nMS	1	1	30	40	STIM	to NUP	2	44	1.1	12			-81.0		2	84
107	M	nMS	1	1	23	80	POST	to RED	1	45	1.03	2			127.6		-1	90
107	M	nMS	1	1	23	80	POST	to NUP	1	45	3.37	10			-80.4		0	90
107	M	nMS	1	1	23	80	POST	to RED	0	45	0.88	5			90.3		-1	90
107	M	nMS	1	1	23	80	POST	to NUP	1	43	0.87	5			-111.8		1	78
107	M	nMS	1	1	23	80	POST	to RED	0	45	1.27	3			94.5		-1	90
107	M	nMS	1	1	23	80	POST	to NUP	1	45	3.38	5			-105.6		1	90
107	M	nMS	1	1	0	80	post	to RED	0	45		0					-1	90
107	M	nMS	1	1	0	80	post	to NUP	0	45		0					0	90
107	M	nMS	1	1	0	80	post	to RED	0	45		0					0	90
107	M	nMS	1	1	0	80	post	to NUP	0	45		0					0	90
107	M	nMS	1	1	0	80	post	to RED	0	45		0					0	90
107	M	nMS	1	1	0	80	post	to NUP	0	45		0					0	90
107	M	nMS	1	2	0	80	pre	to RED	0	45		0						90
107	M	nMS	1	2	0	80	pre	to NUP	0	45		0					0	90
107	M	nMS	1	2	0	80	pre	to RED	0	45		0					0	90
107	M	nMS	1	2	0	80	pre	to NUP	0	45		0					0	90
107	M	nMS	1	2	0	80	pre	to RED	0	45		0					0	90
107	M	nMS	1	2	0	80	pre	to NUP	0	45		0					0	90
107	M	nMS	1	2	23	80	PRE	to RED	0	45	0.42	10			114.3		0	90
107	M	nMS	1	2	23	80	PRE	to NUP	0	42	1.67	13			-106.9		0	72
107	M	nMS	1	2	23	80	PRE	to RED	0	45	0.35	10			107.1		0	90
107	M	nMS	1	2	23	80	PRE	to NUP	0	45	6.27	15			-109.2		0	90
107	M	nMS	1	2	23	80	PRE	to RED	0	45	1.52	10			154.6		0	90
107	M	nMS	1	2	23	80	PRE	to NUP	0	45	4.35	14			-110.0		0	90
107	M	nMS	1	2	12	20	STIM	to RED	0	45	0	0			87.3		0	90
107	M	nMS	1	2	12	20	STIM	to NUP	0	45	0	0			-69.3		0	90
107	M	nMS	1	2	12	80	STIM	to RED	0	45	0	0			256.5		0	90
107	M	nMS	1	2	12	80	STIM	to NUP	0	44	0.35	2			-115.3		0	84
107	M	nMS	1	2	12	40	STIM	to RED	0	45	0	0			114.1		0	90
107	M	nMS	1	2	12	40	STIM	to NUP	0	45	2.53	1			-108.0		0	90
107	M	nMS	1	2	19	20	STIM	to RED	0	45	0.52	1					0	90
107	M	nMS	1	2	19	20	STIM	to NUP	0	42	0	0					0	72
107	M	nMS	1	2	19	80	STIM	to RED	0	45	0.73	5			110.7		0	90
107	M	nMS	1	2	19	80	STIM	to NUP	0	43	1.07	11			-106.4		0	78
107	M	nMS	1	2	19	40	STIM	to RED	0	45	0	0			81.4		0	90
107	M	nMS	1	2	19	40	STIM	to NUP	0	43	0.87	2			-83.6		0	78
107	M	nMS	1	2	30	20	STIM	to RED	0	45	0.25	2			71.7		0	90
107	M	nMS	1	2	30	20	STIM	to NUP	0	38	0	0			-86.7		0	48
107	M	nMS	1	2	30	80	STIM	to RED	0	45	1.53	8			85.9		0	90
107	M	nMS	1	2	30	80	STIM	to NUP	0	40	4.43	14			-86.6		0	60
107	M	nMS	1	2	30	40	STIM	to RED	0	45	0.9	3			69.1		0	90
107	M	nMS	1	2	30	40	STIM	to NUP	0	43	0.83	5			-118.9		0	78
107	M	nMS	1	2	12	20	STIM	to RED	0	45	0	0			77.0		0	90
107	M	nMS	1	2	12	20	STIM	to NUP	0	45	0	0			-104.8		0	90
107	M	nMS	1	2	12	80	STIM	to RED	0	45	0	0			86.8		0	90
107	M	nMS	1	2	12	80	STIM	to NUP	0	45	0.78	4			-106.6		0	90
107	M	nMS	1	2	12	40	STIM	to RED	0	45	0	0			80.6		0	90
107	M	nMS	1	2	12	40	STIM	to NUP	0	43	0.6	4			-95.5		0	78
107	M	nMS	1	2	19	20	STIM	to RED	0	45	0	0			106.9		0	90
107	M	nMS	1	2	19	20	STIM	to NUP	0	43	0	0			-136.6		0	78
107	M	nMS	1	2	19	80	STIM	to RED	0	45	0	0			174.7		0	90
107	M	nMS	1	2	19	80	STIM	to NUP	0	45	0.68	1			-150.5		0	90

107	M	nMS	1	2	19	40	STIM	to RED	0	45	0	0			124.3		0	90
107	M	nMS	1	2	19	40	STIM	to NUP	0	44	0	0			-91.4		0	84
107	M	nMS	1	2	30	20	STIM	to RED	0	45	-1	1			85.0		0	90
107	M	nMS	1	2	30	20	STIM	to NUP	0	43	0	0			-101.2		0	78
107	M	nMS	1	2	30	80	STIM	to RED	0	45	0.57	4			133.0		0	90
107	M	nMS	1	2	30	80	STIM	to NUP	0	44	0.68	3			-82.2		0	84
107	M	nMS	1	2	30	40	STIM	to RED	0	45	0.4	1			66.2		0	90
107	M	nMS	1	2	30	40	STIM	to NUP	0	43	0	0			-99.2		0	78
107	M	nMS	1	2	23	80	POST	to RED	0	45	0.27	1			114.7		0	90
107	M	nMS	1	2	23	80	POST	to NUP	0	45	0.5	3			-121.1		0	90
107	M	nMS	1	2	23	80	POST	to RED	0	45	0	0			153.2		0	90
107	M	nMS	1	2	23	80	POST	to NUP	0	45	0.27	2			-117.6		0	90
107	M	nMS	1	2	23	80	POST	to RED	0	45	0.28	1			91.9		0	90
107	M	nMS	1	2	23	80	POST	to NUP	0	45	0.27	2			-137.0		0	90
107	M	nMS	1	2	0	80	post	to RED	0	45		0					0	90
107	M	nMS	1	2	0	80	post	to NUP	0	45		0					0	90
107	M	nMS	1	2	0	80	post	to RED	0	45		0					0	90
107	M	nMS	1	2	0	80	post	to NUP	0	45		0					0	90
107	M	nMS	1	2	0	80	post	to RED	0	45		0					0	90
107	M	nMS	1	2	0	80	post	to NUP	0	45		0					0	90
109	M	nMS	2	1	0	80	pre	to RED	0	45		0						90
109	M	nMS	2	1	0	80	pre	to NUP	0	45		0					0	90
109	M	nMS	2	1	0	80	pre	to RED	0	45		0					0	90
109	M	nMS	2	1	0	80	pre	to NUP	0	45		0					0	90
109	M	nMS	2	1	0	80	pre	to RED	0	45		0					0	90
109	M	nMS	2	1	0	80	pre	to NUP	0	45		0					0	90
109	M	nMS	2	1	23	80	PRE	to RED	1	40	7.8	10					1	60
109	M	nMS	2	1	23	80	PRE	to NUP	1	45	8	10					0	90
109	M	nMS	2	1	23	80	PRE	to RED	0	45	10	10					-1	90
109	M	nMS	2	1	23	80	PRE	to NUP	0	45	11.3	10					0	90
109	M	nMS	2	1	23	80	PRE	to RED	0	45	7.32	10					0	90
109	M	nMS	2	1	23	80	PRE	to NUP	0	45	9.17	10					0	90
109	M	nMS	2	1	12	20	STIM	to RED	0	45	0	0					0	90
109	M	nMS	2	1	12	20	STIM	to NUP	0	45	0.47	3					0	90
109	M	nMS	2	1	12	80	STIM	to RED	0	45	1.53	5					0	90
109	M	nMS	2	1	12	80	STIM	to NUP	0	45	1.65	5					0	90
109	M	nMS	2	1	12	40	STIM	to RED	0	45	0	0					0	90
109	M	nMS	2	1	12	40	STIM	to NUP	0	45	0	0					0	90
109	M	nMS	2	1	19	20	STIM	to RED	0	45	0.73	2					0	90
109	M	nMS	2	1	19	20	STIM	to NUP	0	45	0	0					0	90
109	M	nMS	2	1	19	80	STIM	to RED	0	45	5.75	7					0	90
109	M	nMS	2	1	19	80	STIM	to NUP	0	45	2.03	7					0	90
109	M	nMS	2	1	19	40	STIM	to RED	0	45	1.35	5					0	90
109	M	nMS	2	1	19	40	STIM	to NUP	0	45	1.4	4					0	90
109	M	nMS	2	1	30	20	STIM	to RED	1	45	2.52	5					1	90
109	M	nMS	2	1	30	20	STIM	to NUP	0	45	0.88	4					-1	90
109	M	nMS	2	1	30	80	STIM	to RED	0	45	8.93	10					0	90
109	M	nMS	2	1	30	80	STIM	to NUP	0	45	8.9	10					0	90
109	M	nMS	2	1	30	40	STIM	to RED	0	45	5.33	10					0	90
109	M	nMS	2	1	30	40	STIM	to NUP	0	45	4.43	7					0	90
109	M	nMS	2	1	12	20	STIM	to RED	0	45	0	0					0	90
109	M	nMS	2	1	12	20	STIM	to NUP	0	45	1.4	1					0	90
109	M	nMS	2	1	12	80	STIM	to RED	0	45	2.12	5					0	90
109	M	nMS	2	1	12	80	STIM	to NUP	0	45	4.78	4					0	90
109	M	nMS	2	1	12	40	STIM	to RED	0	45	0	0					0	90
109	M	nMS	2	1	12	40	STIM	to NUP	0	45	1.57	1					0	90
109	M	nMS	2	1	19	20	STIM	to RED	0	45	1.28	2					0	90
109	M	nMS	2	1	19	20	STIM	to NUP	0	45	1.02	2					0	90
109	M	nMS	2	1	19	80	STIM	to RED	0	45	3.75	5					0	90
109	M	nMS	2	1	19	80	STIM	to NUP	0	45	2.68	5					0	90
109	M	nMS	2	1	19	40	STIM	to RED	0	45	2.67	3					0	90
109	M	nMS	2	1	19	40	STIM	to NUP	0	45	2.95	2					0	90
109	M	nMS	2	1	30	20	STIM	to RED	0	40	1.72	4					0	60
109	M	nMS	2	1	30	20	STIM	to NUP	0	45	1.6	4					0	90
109	M	nMS	2	1	30	80	STIM	to RED	0	45	9.75	9					0	90
109	M	nMS	2	1	30	80	STIM	to NUP	0	45	6.23	10					0	90

109	M	nMS	2	1	30	40	STIM	to RED	0	45	3.97	5					0	90
109	M	nMS	2	1	30	40	STIM	to NUP	1	45	2.95	10					1	90
109	M	nMS	2	1	23	80	POST	to RED	0	45	3.6	5					-1	90
109	M	nMS	2	1	23	80	POST	to NUP	0	45	2.85	4					0	90
109	M	nMS	2	1	23	80	POST	to RED	0	45	3.47	2					0	90
109	M	nMS	2	1	23	80	POST	to NUP	0	45	3.77	2					0	90
109	M	nMS	2	1	23	80	POST	to RED	0	45	3.68	2					0	90
109	M	nMS	2	1	23	80	POST	to NUP	0	45	0	0					0	90
109	M	nMS	2	1	0	80	post	to RED	0	45		1					0	90
109	M	nMS	2	1	0	80	post	to NUP	0	45		1					0	90
109	M	nMS	2	1	0	80	post	to RED	0	45		0					0	90
109	M	nMS	2	1	0	80	post	to NUP	0	45		0					0	90
109	M	nMS	2	1	0	80	post	to RED	0	45		0					0	90
109	M	nMS	2	1	0	80	post	to NUP	0	45		0					0	90
109	M	nMS	2	2	0	80	pre	to RED	0	45		0						90
109	M	nMS	2	2	0	80	pre	to NUP	0	45		0					0	90
109	M	nMS	2	2	0	80	pre	to RED	0	45		0					0	90
109	M	nMS	2	2	0	80	pre	to NUP	0	45		0					0	90
109	M	nMS	2	2	0	80	pre	to RED	0	45		0					0	90
109	M	nMS	2	2	0	80	pre	to NUP	0	45		0					0	90
109	M	nMS	2	2	23	80	PRE	to RED	0	45	2.52	8					0	90
109	M	nMS	2	2	23	80	PRE	to NUP	0	45	4.27	10					0	90
109	M	nMS	2	2	23	80	PRE	to RED	0	45	3.6	10					0	90
109	M	nMS	2	2	23	80	PRE	to NUP	0	45	3.28	7					0	90
109	M	nMS	2	2	23	80	PRE	to RED	0	45	3.77	5					0	90
109	M	nMS	2	2	23	80	PRE	to NUP	0	45	2.22	5					0	90
109	M	nMS	2	2	12	20	STIM	to RED	0	45	0	0					0	90
109	M	nMS	2	2	12	20	STIM	to NUP	0	45	1.47	1					0	90
109	M	nMS	2	2	12	80	STIM	to RED	0	45	5.1	3					0	90
109	M	nMS	2	2	12	80	STIM	to NUP	0	45	2.05	2					0	90
109	M	nMS	2	2	12	40	STIM	to RED	0	45	2.3	2					0	90
109	M	nMS	2	2	12	40	STIM	to NUP	1	45	1.88	1					1	90
109	M	nMS	2	2	19	20	STIM	to RED	1	45	1	3					0	90
109	M	nMS	2	2	19	20	STIM	to NUP	0	45	0	0					-1	90
109	M	nMS	2	2	19	80	STIM	to RED	0	45	4.37	5					0	90
109	M	nMS	2	2	19	80	STIM	to NUP	0	45	2.52	3					0	90
109	M	nMS	2	2	19	40	STIM	to RED	0	45	0	0					0	90
109	M	nMS	2	2	19	40	STIM	to NUP	0	45	2.23	2					0	90
109	M	nMS	2	2	30	20	STIM	to RED	0	42.5	1.12	4					0	75
109	M	nMS	2	2	30	20	STIM	to NUP	0	45	0	0					0	90
109	M	nMS	2	2	30	80	STIM	to RED	0	45	5.07	8					0	90
109	M	nMS	2	2	30	80	STIM	to NUP	0	45	3.8	8					0	90
109	M	nMS	2	2	30	40	STIM	to RED	2	45	1.95	4					2	90
109	M	nMS	2	2	30	40	STIM	to NUP	3	45	2.48	2					1	90
109	M	nMS	2	2	12	20	STIM	to RED	2	45	0	0					-1	90
109	M	nMS	2	2	12	20	STIM	to NUP	0	45	0	0					-2	90
109	M	nMS	2	2	12	80	STIM	to RED	0	45	2.77	4					0	90
109	M	nMS	2	2	12	80	STIM	to NUP	0	45	3.03	3					0	90
109	M	nMS	2	2	12	40	STIM	to RED	0	45	2.12	1					0	90
109	M	nMS	2	2	12	40	STIM	to NUP	0	45	1.63	2					0	90
109	M	nMS	2	2	19	20	STIM	to RED	0	45	1.2	1					0	90
109	M	nMS	2	2	19	20	STIM	to NUP	0	45	0	0					0	90
109	M	nMS	2	2	19	80	STIM	to RED	0	45	4	5					0	90
109	M	nMS	2	2	19	80	STIM	to NUP	0	45	2.8	4					0	90
109	M	nMS	2	2	19	40	STIM	to RED	0	45	1.65	2					0	90
109	M	nMS	2	2	19	40	STIM	to NUP	0	45	2.2	3					0	90
109	M	nMS	2	2	30	20	STIM	to RED	2	45	1.55	2					2	90
109	M	nMS	2	2	30	20	STIM	to NUP	0	45	1.3	3					-2	90
109	M	nMS	2	2	30	80	STIM	to RED	0	45	4.42	8					0	90
109	M	nMS	2	2	30	80	STIM	to NUP	0	45	4.73	10					0	90
109	M	nMS	2	2	30	40	STIM	to RED	0	45	3.65	8					0	90
109	M	nMS	2	2	30	40	STIM	to NUP	2	45	3.22	6					2	90
109	M	nMS	2	2	23	80	POST	to RED	0	45	2.82	4					-2	90
109	M	nMS	2	2	23	80	POST	to NUP	0	45	3.67	5					0	90
109	M	nMS	2	2	23	80	POST	to RED	0	45	3.25	4					0	90
109	M	nMS	2	2	23	80	POST	to NUP	3	45	2.87	4					3	90

109	M	nMS	2	2	23	80	POST	to RED	0	45	3.15	3					-3	90
109	M	nMS	2	2	23	80	POST	to NUP	0	45	2.63	2					0	90
109	M	nMS	2	2	0	80	post	to RED	0	45		0					0	90
109	M	nMS	2	2	0	80	post	to NUP	0	45		0					0	90
109	M	nMS	2	2	0	80	post	to RED	0	45		0					0	90
109	M	nMS	2	2	0	80	post	to NUP	0	45		0					0	90
109	M	nMS	2	2	0	80	post	to RED	0	45		0					0	90
109	M	nMS	2	2	0	80	post	to NUP	0	45		0					0	90
110	M	nMS	3	1	0	80	pre	to RED	0	45		0						90
110	M	nMS	3	1	0	80	pre	to NUP	0	45		0					0	90
110	M	nMS	3	1	0	80	pre	to RED	0	45		0					0	90
110	M	nMS	3	1	0	80	pre	to NUP	0	45		0					0	90
110	M	nMS	3	1	0	80	pre	to RED	0	45		0					0	90
110	M	nMS	3	1	0	80	pre	to NUP	0	45		0					0	90
110	M	nMS	3	1	23	80	PRE	to RED	1	45	0	0	45.1	5.3	86.8	8.2	1	90
110	M	nMS	3	1	23	80	PRE	to NUP	0	46	8.28	10	54.9	5.9	-92.1	5.8	-1	96
110	M	nMS	3	1	23	80	PRE	to RED	0	45	6.68	7	55.3	6.7	123.8	10.3	0	90
110	M	nMS	3	1	23	80	PRE	to NUP	0	45	9.35	10	41.0	5.9	-102.8	9.0	0	90
110	M	nMS	3	1	23	80	PRE	to RED	0	44	6.83	6	52.1	4.2	78.6	10.2	0	84
110	M	nMS	3	1	23	80	PRE	to NUP	0	45	10.87	9	36.7	6.6	-103.1	3.9	0	90
110	M	nMS	3	1	12	20	STIM	to RED	0	47	0	0	45.1	3.1	81.4	2.7	0	102
110	M	nMS	3	1	12	20	STIM	to NUP	0	45	0.68	1	31.7	4.2	-83.3	1.7	0	90
110	M	nMS	3	1	12	80	STIM	to RED	0	45	0	0	38.7	4.6	72.8	5.7	0	90
110	M	nMS	3	1	12	80	STIM	to NUP	0	45	2.48	1	39.0	5.0	-80.1	4.8	0	90
110	M	nMS	3	1	12	40	STIM	to RED	1	45	0	0	43.4	4.8	86.6	3.6	1	90
110	M	nMS	3	1	12	40	STIM	to NUP	0	45	3.3	1	38.5	4.6	-69.4	2.5	-1	90
110	M	nMS	3	1	19	20	STIM	to RED	0	45	0.82	1	45.5	5.1	75.4	5.1	0	90
110	M	nMS	3	1	19	20	STIM	to NUP	0	44	5.52	2	26.5	4.3	-61.9	4.6	0	84
110	M	nMS	3	1	19	80	STIM	to RED	0	46	7.22	3	30.9	4.1	95.7	11.7	0	96
110	M	nMS	3	1	19	80	STIM	to NUP	0	45	11.48	3	44.5	5.1	-88.7	10.5	0	90
110	M	nMS	3	1	19	40	STIM	to RED	0	45	3.08	3	54.2	5.1	79.3	4.1	0	90
110	M	nMS	3	1	19	40	STIM	to NUP	0	45	8.28	3	33.1	4.0	-74.7	6.8	0	90
110	M	nMS	3	1	30	20	STIM	to RED	0	43	3.45	2	50.2	3.6	71.0	4.1	0	78
110	M	nMS	3	1	30	20	STIM	to NUP	0	44	9.25	3	57.3	4.6	-80.4	4.4	0	84
110	M	nMS	3	1	30	80	STIM	to RED	0	45	15.37	6	32.0	3.6	80.1	0.0	0	90
110	M	nMS	3	1	30	80	STIM	to NUP	1	45	16.97	8	26.5	4.1	-98.3	2.2	1	90
110	M	nMS	3	1	30	40	STIM	to RED	0	45	7.12	5	31.6	4.6	98.9	9.9	-1	90
110	M	nMS	3	1	30	40	STIM	to NUP	0	45	13.27	4	42.9	4.3	-88.8	8.2	0	90
110	M	nMS	3	1	12	20	STIM	to RED	0	45	0	0	38.1	4.3	79.5	2.3	0	90
110	M	nMS	3	1	12	20	STIM	to NUP	0	45	0	0	24.9	4.9	-70.5	1.1	0	90
110	M	nMS	3	1	12	80	STIM	to RED	0	45	0	0	54.1	5.1	88.7	3.5	0	90
110	M	nMS	3	1	12	80	STIM	to NUP	0	45	8.9	1	43.2	3.7	-111.6	11.6	0	90
110	M	nMS	3	1	12	40	STIM	to RED	0	45	2.42	1	30.1	4.4	80.6	6.0	0	90
110	M	nMS	3	1	12	40	STIM	to NUP	0	45	0	0	38.3	4.5	-97.6	2.5	0	90
110	M	nMS	3	1	19	20	STIM	to RED	0	45	0	0	31.7	4.7	64.1	1.1	0	90
110	M	nMS	3	1	19	20	STIM	to NUP	1	45	0	0	21.1	3.9	-69.0	2.9	1	90
110	M	nMS	3	1	19	80	STIM	to RED	1	45	14.28	4	32.3	4.3	107.4	11.7	0	90
110	M	nMS	3	1	19	80	STIM	to NUP	1	45	11.83	3	47.0	5.3	-83.9	6.4	0	90
110	M	nMS	3	1	19	40	STIM	to RED	2	45	7.67	1	41.0	4.5	77.7	6.8	1	90
110	M	nMS	3	1	19	40	STIM	to NUP	1	45	1.85	2	54.2	4.5	-84.9	3.5	-1	90
110	M	nMS	3	1	30	20	STIM	to RED	0	45	6.78	1	52.1	4.4	70.6	3.8	-1	90
110	M	nMS	3	1	30	20	STIM	to NUP	1	45	5.65	1	57.5	4.7	-80.5	4.6	1	90
110	M	nMS	3	1	30	80	STIM	to RED	3	45	12.77	5	36.6	3.7	73.2	9.3	2	90
110	M	nMS	3	1	30	80	STIM	to NUP	2	44	13.95	3	47.1	5.5	-81.5	10.2	-1	84
110	M	nMS	3	1	30	40	STIM	to RED	1	45	11.73	5	30.3	4.2	94.7	7.8	-1	90
110	M	nMS	3	1	30	40	STIM	to NUP	2	45	10.12	4	32.4	4.2	-75.2	11.1	1	90
110	M	nMS	3	1	23	80	POST	to RED	0	45	5.42	3	51.0	5.1	158.6	7.0	-2	90
110	M	nMS	3	1	23	80	POST	to NUP	1	45	12.57	5	44.7	4.7	-100.1	8.4	1	90
110	M	nMS	3	1	23	80	POST	to RED	1	45	11.32	4	43.7	5.0	86.6	9.1	0	90
110	M	nMS	3	1	23	80	POST	to NUP	3	45	14.97	5	33.8	4.2	-95.8	10.6	2	90
110	M	nMS	3	1	23	80	POST	to RED	2	45	16.08	4	40.5	4.0	78.4	11.3	-1	90
110	M	nMS	3	1	23	80	POST	to NUP	1	45	18.45	3	46.1	4.8	-94.0	9.3	-1	90
110	M	nMS	3	1	0	80	post	to RED	1	45		0					0	90
110	M	nMS	3	1	0	80	post	to NUP	2	45		0					1	90
110	M	nMS	3	1	0	80	post	to RED	1	45		0					-1	90
110	M	nMS	3	1	0	80	post	to NUP	1	45		0					0	90

110	M	nMS	3	1	0	80	post	to RED	1	45		0					0	90
110	M	nMS	3	1	0	80	post	to NUP	1	45		0					0	90
110	M	nMS	3	2	0	80	pre	to RED	0	45		0						90
110	M	nMS	3	2	0	80	pre	to NUP	0	45		0					0	90
110	M	nMS	3	2	0	80	pre	to RED	0	45		0					0	90
110	M	nMS	3	2	0	80	pre	to NUP	0	45		0					0	90
110	M	nMS	3	2	0	80	pre	to RED	0	45		0					0	90
110	M	nMS	3	2	0	80	pre	to NUP	0	45		0					0	90
110	M	nMS	3	2	23	80	PRE	to RED	1	45	5.73	3	37.8	3.9	107.7	10.5	1	90
110	M	nMS	3	2	23	80	PRE	to NUP	0	45	13.3	6	30.3	3.9	-89.7	13.2	-1	90
110	M	nMS	3	2	23	80	PRE	to RED	0	45	6.03	3	37.1	4.3	78.7	10.9	0	90
110	M	nMS	3	2	23	80	PRE	to NUP	1	45	17.95	7	31.4	3.9	-79.2	8.6	1	90
110	M	nMS	3	2	23	80	PRE	to RED	1	45	9.85	4	34.4	4.2	108.9	9.5	0	90
110	M	nMS	3	2	23	80	PRE	to NUP	0	45	16.2	5.5	30.7	3.8	-86.4	4.0	-1	90
110	M	nMS	3	2	12	20	STIM	to RED	0	46	0	0	35.6	4.2	101.3	7.5	0	96
110	M	nMS	3	2	12	20	STIM	to NUP	0	45	0	0	35.3	3.9	-89.4	5.2	0	90
110	M	nMS	3	2	12	80	STIM	to RED	0	45	0	0	107.6	4.6	114.5	1.4	0	90
110	M	nMS	3	2	12	80	STIM	to NUP	1	45	5.1	4	66.2	5.1	-86.7	2.4	1	90
110	M	nMS	3	2	12	40	STIM	to RED	0	45	1.3	1	46.9	4.4	97.1	1.3	-1	90
110	M	nMS	3	2	12	40	STIM	to NUP	0	45	0	0	29.4	5.2	-82.3	2.2	0	90
110	M	nMS	3	2	19	20	STIM	to RED	3	45	0.82	1	39.6	4.6	79.7	3.2	3	90
110	M	nMS	3	2	19	20	STIM	to NUP	2	45	0.77	4	23.2	4.0	-77.2	5.7	-1	90
110	M	nMS	3	2	19	80	STIM	to RED	1	45	8.73	1	48.6	3.6	90.4	10.1	-1	90
110	M	nMS	3	2	19	80	STIM	to NUP	1	45	10.12	5	41.1	4.4	-104.6	2.5	0	90
110	M	nMS	3	2	19	40	STIM	to RED	2	45	7.1	2	26.5	4.1	72.9	11.7	1	90
110	M	nMS	3	2	19	40	STIM	to NUP	2	45	8.53	1	24.1	4.1	-80.7	7.7	0	90
110	M	nMS	3	2	30	20	STIM	to RED	1	45	0.92	1	40.7	3.8	75.7	7.3	-1	90
110	M	nMS	3	2	30	20	STIM	to NUP	1	45	0	0	41.7	4.3	-67.7	4.3	0	90
110	M	nMS	3	2	30	80	STIM	to RED	2	45	10.68	5	21.7	3.5	109.7	8.0	1	90
110	M	nMS	3	2	30	80	STIM	to NUP	2	45	17.7	12	35.9	4.1	-98.1	6.6	0	90
110	M	nMS	3	2	30	40	STIM	to RED	1	45	10.12	6	29.1	4.4	75.9	10.8	-1	90
110	M	nMS	3	2	30	40	STIM	to NUP	0	45	6.37	3	78.4	4.6	-73.8	5.2	-1	90
110	M	nMS	3	2	12	20	STIM	to RED	0	45	0	0	32.3	4.8	82.3	2.3	0	90
110	M	nMS	3	2	12	20	STIM	to NUP	0	45	0	0	15.5	4.5	-66.5	2.7	0	90
110	M	nMS	3	2	12	80	STIM	to RED	1	45	0	0	54.3	4.5	79.9	5.3	1	90
110	M	nMS	3	2	12	80	STIM	to NUP	1	45	6.9	2	31.2	4.3	-78.9	7.6	0	90
110	M	nMS	3	2	12	40	STIM	to RED	1	45	0	0	32.4	4.2	103.9	5.1	0	90
110	M	nMS	3	2	12	40	STIM	to NUP	1	45	6.8	1	32.6	4.7	-75.8	-0.2	0	90
110	M	nMS	3	2	19	20	STIM	to RED	1	45	6.55	1	20.5	3.9	69.9	9.8	0	90
110	M	nMS	3	2	19	20	STIM	to NUP	1	45	0	0	33.4	4.2	-74.7	2.6	0	90
110	M	nMS	3	2	19	80	STIM	to RED	1	45	7.83	2	32.4	4.1	89.2	9.7	0	90
110	M	nMS	3	2	19	80	STIM	to NUP	1	45	9.58	1	52.3	4.4	-104.1	8.8	0	90
110	M	nMS	3	2	19	40	STIM	to RED	0	45	6.02	1	54.1	4.2	88.3	4.8	-1	90
110	M	nMS	3	2	19	40	STIM	to NUP	0	45	4.8	2	44.4	4.6	-63.6	4.7	0	90
110	M	nMS	3	2	30	20	STIM	to RED	2	45	7.63	2	70.2	4.1	67.8	3.4	2	90
110	M	nMS	3	2	30	20	STIM	to NUP	3	45	2.73	1	40.7	5.0	-73.6	1.2	1	90
110	M	nMS	3	2	30	80	STIM	to RED	2	45	9.6	4	37.2	4.3	78.4	12.2	-1	90
110	M	nMS	3	2	30	80	STIM	to NUP	2	45	16.28	9	45.8	4.4	-88.7	13.3	0	90
110	M	nMS	3	2	30	40	STIM	to RED	1	45	8.15	4	78.1	4.7	84.4	5.6	-1	90
110	M	nMS	3	2	30	40	STIM	to NUP	1	45	11.33	2	53.6	4.6	-79.4	6.5	0	90
110	M	nMS	3	2	23	80	POST	to RED	1	45	7.2	2	61.9	5.5	83.8	6.4	0	90
110	M	nMS	3	2	23	80	POST	to NUP	0	45	11.22	4	66.5	5.4	-112.8	8.1	-1	90
110	M	nMS	3	2	23	80	POST	to RED	0	45	16.58	2	87.7	5.3	96.2	4.9	0	90
110	M	nMS	3	2	23	80	POST	to NUP	0	45	17.37	4	38.6	5.1	-108.0	10.6	0	90
110	M	nMS	3	2	23	80	POST	to RED	0	45	12.33	2	74.8	5.4	100.3	5.7	0	90
110	M	nMS	3	2	23	80	POST	to NUP	0	45	12.57	2	33.6	5.1	-108.1	11.3	0	90
110	M	nMS	3	2	0	80	post	to RED	0	45		0					0	90
110	M	nMS	3	2	0	80	post	to NUP	0	45		0					0	90
110	M	nMS	3	2	0	80	post	to RED	0	45		0					0	90
110	M	nMS	3	2	0	80	post	to NUP	0	45		0					0	90
110	M	nMS	3	2	0	80	post	to RED	0	45		0					0	90
110	M	nMS	3	2	0	80	post	to NUP	0	45		0					0	90
111	M	nMS	1	1	0	80	pre	to RED	0	45		0						90
111	M	nMS	1	1	0	80	pre	to NUP	0	45		0					0	90
111	M	nMS	1	1	0	80	pre	to RED	0	45		0					0	90
111	M	nMS	1	1	0	80	pre	to NUP	0	45		0					0	90

111	M	nMS	1	1	0	80	pre	to RED	0	45		0					0	90
111	M	nMS	1	1	0	80	pre	to NUP	0	45		0					0	90
111	M	nMS	1	1	23	80	PRE	to RED	0	48	4.27	10	52.0	5.7	98.8	4.6	0	108
111	M	nMS	1	1	23	80	PRE	to NUP	0	43	9.88	13	76.3	5.3	-104.8	2.8	0	78
111	M	nMS	1	1	23	80	PRE	to RED	0	47	7.45	10	70.3	5.7	90.0	6.7	0	102
111	M	nMS	1	1	23	80	PRE	to NUP	0	43	10.53	14			-81.4	10.5	0	78
111	M	nMS	1	1	23	80	PRE	to RED	0	46	3.55	7	58.0	5.5	98.7	6.8	0	96
111	M	nMS	1	1	23	80	PRE	to NUP	0	42	10.37	12	53.8	5.1	-94.6	4.3	0	72
111	M	nMS	1	1	12	20	STIM	to RED	0	47	0	0	39.1	4.8	81.2	0.6	0	102
111	M	nMS	1	1	12	20	STIM	to NUP	0	44	0.78	2	19.4	4.9	-73.6	0.5	0	84
111	M	nMS	1	1	12	80	STIM	to RED	0	46	1.52	1	48.6	4.5	82.0	3.9	0	96
111	M	nMS	1	1	12	80	STIM	to NUP	0	44	3.27	2	41.4	3.6	-117.0	4.4	0	84
111	M	nMS	1	1	12	40	STIM	to RED	0	46	0	0	36.4	3.6	74.1	5.0	0	96
111	M	nMS	1	1	12	40	STIM	to NUP	0	44	3.13	2	26.6	3.6	-98.4	2.6	0	84
111	M	nMS	1	1	19	20	STIM	to RED	0	47	1.17	1	39.1	3.9	86.7	3.3	0	102
111	M	nMS	1	1	19	20	STIM	to NUP	0	43	3.1	2	26.7	3.8	-67.9	2.1	0	78
111	M	nMS	1	1	19	80	STIM	to RED	0	46	3.48	3	58.9	4.2	78.3	6.2	0	96
111	M	nMS	1	1	19	80	STIM	to NUP	0	43	6.33	8	55.0	3.9	-101.7	5.4	0	78
111	M	nMS	1	1	19	40	STIM	to RED	0	45	1.78	2	53.3	4.2	85.5	4.2	0	90
111	M	nMS	1	1	19	40	STIM	to NUP	1	44	3.85	5	42.6	3.7	-84.8	4.2	1	84
111	M	nMS	1	1	30	20	STIM	to RED	0	43	3.57	1	48.2	4.2	71.8	4.6	-1	78
111	M	nMS	1	1	30	20	STIM	to NUP	0	41	4.17	5	31.8	3.9	-51.9	3.1	0	66
111	M	nMS	1	1	30	80	STIM	to RED	0	43	7.67	10	55.5	4.8	81.3	10.3	0	78
111	M	nMS	1	1	30	80	STIM	to NUP	0	39	12.92	16	75.0	4.7	-98.6	4.3	0	54
111	M	nMS	1	1	30	40	STIM	to RED	0	43	6.88	5	54.9	5.0	90.9	6.4	0	78
111	M	nMS	1	1	30	40	STIM	to NUP	0	40	10.82	15	45.9	4.3	-60.8	4.1	0	60
111	M	nMS	1	1	12	20	STIM	to RED	0	47	0	0	35.0	3.1	68.6	0.7	0	102
111	M	nMS	1	1	12	20	STIM	to NUP	0	47	0	0	19.3	3.0	-66.9	0.5	0	102
111	M	nMS	1	1	12	80	STIM	to RED	0	47	1.9	0.5	49.2	4.5	77.3	4.0	0	102
111	M	nMS	1	1	12	80	STIM	to NUP	1	45	1	1	53.6	3.7	-104.8	2.3	1	90
111	M	nMS	1	1	12	40	STIM	to RED	0	45	0	0	43.3	4.4	75.6	2.0	-1	90
111	M	nMS	1	1	12	40	STIM	to NUP	0	45.5	2.45	1	31.5	3.9	-89.0	1.4	0	93
111	M	nMS	1	1	19	20	STIM	to RED	0	45	1.3	0.5	32.1	5.7	68.6	3.8	0	90
111	M	nMS	1	1	19	20	STIM	to NUP	0	44.5	2.77	1	35.9	3.5	-56.8	0.7	0	87
111	M	nMS	1	1	19	80	STIM	to RED	0	46	1.85	1	68.7	4.1	85.2	4.3	0	96
111	M	nMS	1	1	19	80	STIM	to NUP	0	44	6.22	6	53.8	4.6	-102.4	3.7	0	84
111	M	nMS	1	1	19	40	STIM	to RED	0	45	4.15	2	52.4	4.0	91.6	4.6	0	90
111	M	nMS	1	1	19	40	STIM	to NUP	1	44	6.05	6	45.5	4.3	-90.2	1.8	1	84
111	M	nMS	1	1	30	20	STIM	to RED	0	44	2.73	1	42.7	4.2	72.8	2.8	-1	84
111	M	nMS	1	1	30	20	STIM	to NUP	1	42	4.15	4	27.8	3.4	-59.0	4.0	1	72
111	M	nMS	1	1	30	80	STIM	to RED	0	44	6.05	4	46.9	4.4	74.5	8.7	-1	84
111	M	nMS	1	1	30	80	STIM	to NUP	1	40	14.68	19	39.8	3.9	-85.6	9.5	1	60
111	M	nMS	1	1	30	40	STIM	to RED	0	43.5	4.13	2	61.2	4.1	89.2	4.4	-1	81
111	M	nMS	1	1	30	40	STIM	to NUP	2	41	10.95	16	53.0	4.0	-82.2	3.2	2	66
111	M	nMS	1	1	23	80	POST	to RED	0	47	0	0	57.8	4.4	76.6	4.2	-2	102
111	M	nMS	1	1	23	80	POST	to NUP	1	44	4.97	3	57.9	4.2	-97.1	5.3	1	84
111	M	nMS	1	1	23	80	POST	to RED	0	46	0	0	53.5	4.5	79.7	5.5	-1	96
111	M	nMS	1	1	23	80	POST	to NUP	0.5	44	9.77	5	53.3	4.9	-90.3	2.2	0.5	84
111	M	nMS	1	1	23	80	POST	to RED	0	47	0	0	68.6	4.9	123.5	4.3	-0.5	102
111	M	nMS	1	1	23	80	POST	to NUP	1	44	8.35	4	58.0	4.4	-103.8	4.8	1	84
111	M	nMS	1	1	0	80	post	to RED	0	48		0					-1	108
111	M	nMS	1	1	0	80	post	to NUP	0	47		0.5					0	102
111	M	nMS	1	1	0	80	post	to RED	0	47		0					0	102
111	M	nMS	1	1	0	80	post	to NUP	0	46		0					0	96
111	M	nMS	1	1	0	80	post	to RED	0	46		0					0	96
111	M	nMS	1	1	0	80	post	to NUP	0	45.5		0					0	93
111	M	nMS	1	2	0	80	pre	to RED	0	45		0						90
111	M	nMS	1	2	0	80	pre	to NUP	0	45		0					0	90
111	M	nMS	1	2	0	80	pre	to RED	0	45		0					0	90
111	M	nMS	1	2	0	80	pre	to NUP	0	45		0					0	90
111	M	nMS	1	2	0	80	pre	to RED	0	45		0					0	90
111	M	nMS	1	2	0	80	pre	to NUP	0	45		0					0	90
111	M	nMS	1	2	23	80	PRE	to RED	0	43	4.18	4	59.1	4.1	89.5	6.2	0	78
111	M	nMS	1	2	23	80	PRE	to NUP	0	42	8.47	8	71.8	4.4	-102.4	3.8	0	72
111	M	nMS	1	2	23	80	PRE	to RED	0	44	3.08	2.5	33.7	4.1	93.1	7.8	0	84
111	M	nMS	1	2	23	80	PRE	to NUP	0	42	7.8	6	37.0	4.0	-105.6	7.7	0	72

111	M	nMS	1	2	23	80	PRE	to RED	0	44	2.45	2	64.6	4.0	84.7	5.5	0	84
111	M	nMS	1	2	23	80	PRE	to NUP	0	43	8.95	6	44.8	3.4	-84.8	8.3	0	78
111	M	nMS	1	2	12	20	STIM	to RED	0	46	0	0	37.1	4.0	64.5	1.0	0	96
111	M	nMS	1	2	12	20	STIM	to NUP	0	45	0.48	0.5	29.0	3.2	-68.1	-0.1	0	90
111	M	nMS	1	2	12	80	STIM	to RED	0	45	0	0	42.8	3.7	83.6	3.2	0	90
111	M	nMS	1	2	12	80	STIM	to NUP	0	45	2.6	1.5	41.6	3.6	-98.0	4.0	0	90
111	M	nMS	1	2	12	40	STIM	to RED	0	45	0	0	26.7	3.8	93.3	3.3	0	90
111	M	nMS	1	2	12	40	STIM	to NUP	0.5	45	2.43	1	29.3	3.9	-80.4	1.2	0.5	90
111	M	nMS	1	2	19	20	STIM	to RED	0	44	0	0	36.8	3.5	53.2	5.4	-0.5	84
111	M	nMS	1	2	19	20	STIM	to NUP	0	43	1.22	1	22.9	4.2	-56.1	1.1	0	78
111	M	nMS	1	2	19	80	STIM	to RED	0	45	1.58	1	38.8	3.5	92.2	6.1	0	90
111	M	nMS	1	2	19	80	STIM	to NUP	0	43	7.52	6	36.6	4.1	-105.1	1.8	0	78
111	M	nMS	1	2	19	40	STIM	to RED	0	44	3.6	2	43.6	4.0	91.1	5.7	0	84
111	M	nMS	1	2	19	40	STIM	to NUP	0	43	5.38	4	21.3	3.9	-97.2	3.4	0	78
111	M	nMS	1	2	30	20	STIM	to RED	0	42	2.23	1	54.1	3.8	88.6	3.4	0	72
111	M	nMS	1	2	30	20	STIM	to NUP	0	39	5.05	4	33.6	4.2	-62.3	0.8	0	54
111	M	nMS	1	2	30	80	STIM	to RED	0	43	8.28	6	59.9	4.6	76.2	6.4	0	78
111	M	nMS	1	2	30	80	STIM	to NUP	0	38	12.95	15	60.0	4.5	-89.9	6.1	0	48
111	M	nMS	1	2	30	40	STIM	to RED	0	40	7.75	4	54.5	5.4	87.1	7.6	0	60
111	M	nMS	1	2	30	40	STIM	to NUP	0	39	10.93	12	37.1	3.8	-122.8	3.5	0	54
111	M	nMS	1	2	12	20	STIM	to RED	0	48	0	0	34.0	4.3	76.5	2.1	0	108
111	M	nMS	1	2	12	20	STIM	to NUP	0	46	0	0	17.1	3.9	-77.2	1.8	0	96
111	M	nMS	1	2	12	80	STIM	to RED	0	47	0	0	42.9	4.8	90.8	3.9	0	102
111	M	nMS	1	2	12	80	STIM	to NUP	0	45	1.38	1	38.0	3.4	-108.6	3.1	0	90
111	M	nMS	1	2	12	40	STIM	to RED	0	45	0	0	33.4	3.6	78.0	4.3	0	90
111	M	nMS	1	2	12	40	STIM	to NUP	0	45	2.12	0.5	20.8	4.0	-99.5	2.5	0	90
111	M	nMS	1	2	19	20	STIM	to RED	0	44	0	0	47.4	3.8	68.5	2.1	0	84
111	M	nMS	1	2	19	20	STIM	to NUP	0	44	0	0	17.0	3.5	-88.1	1.7	0	84
111	M	nMS	1	2	19	80	STIM	to RED	0	45	2.72	0.5	49.8	4.4	82.9	5.1	0	90
111	M	nMS	1	2	19	80	STIM	to NUP	0	44	5.9	2	64.5	3.7	-93.3	1.9	0	84
111	M	nMS	1	2	19	40	STIM	to RED	0	44.5	1.08	1	43.4	4.4	87.3	4.2	0	87
111	M	nMS	1	2	19	40	STIM	to NUP	1	44	4.85	2	30.6	3.7	-95.5	2.7	1	84
111	M	nMS	1	2	30	20	STIM	to RED	0	43	4.37	1	44.9	4.1	67.6	3.9	-1	78
111	M	nMS	1	2	30	20	STIM	to NUP	1	41	5.48	2.5	22.3	4.1	-66.6	1.1	1	66
111	M	nMS	1	2	30	80	STIM	to RED	0	42	7.83	5	52.0	4.6	76.8	10.0	-1	72
111	M	nMS	1	2	30	80	STIM	to NUP	0	39	12.2	12	27.7	3.8	-99.5	8.6	0	54
111	M	nMS	1	2	30	40	STIM	to RED	0	41	4.48	3	55.2	4.4	77.6	5.6	0	66
111	M	nMS	1	2	30	40	STIM	to NUP	0	40	7.82	6	36.8	3.8	-93.2	3.5	0	60
111	M	nMS	1	2	23	80	POST	to RED	0	46	2.1	1	46.4	5.0	83.6	5.4	0	96
111	M	nMS	1	2	23	80	POST	to NUP	1	45	6.4	5	29.8	3.9	-105.3	6.4	1	90
111	M	nMS	1	2	23	80	POST	to RED	0	45	1.43	1	51.6	4.2	89.3	5.6	-1	90
111	M	nMS	1	2	23	80	POST	to NUP	1	44	9.27	6	36.9	3.4	-120.5	4.6	1	84
111	M	nMS	1	2	23	80	POST	to RED	0	44	2.48	1	53.4	4.4	103.2	5.8	-1	84
111	M	nMS	1	2	23	80	POST	to NUP	0	44	2.97	2	47.6	3.6	-120.8	4.8	0	84
111	M	nMS	1	2	0	80	post	to RED	0	47		0					0	102
111	M	nMS	1	2	0	80	post	to NUP	0	46		0					0	96
111	M	nMS	1	2	0	80	post	to RED	0	46		0					0	96
111	M	nMS	1	2	0	80	post	to NUP	0	45.5		0					0	93
111	M	nMS	1	2	0	80	post	to RED	0	46		0					0	96
111	M	nMS	1	2	0	80	post	to NUP	0	45		0					0	90
113	M	MS	2	1	0	80	pre	to RED	0	45		0						90
113	M	MS	2	1	0	80	pre	to NUP	0	45		0					0	90
113	M	MS	2	1	0	80	pre	to RED	0	45		0					0	90
113	M	MS	2	1	0	80	pre	to NUP	0	45		0					0	90
113	M	MS	2	1	0	80	pre	to RED	0	45		0					0	90
113	M	MS	2	1	0	80	pre	to NUP	0	45		0					0	90
113	M	MS	2	1	23	80	PRE	to RED	0	45	4.07	10	87.3	5.4	89.4	4.1	0	90
113	M	MS	2	1	23	80	PRE	to NUP	0	45	9.83	15	88.7	5.7	-66.8	2.1	0	90
113	M	MS	2	1	23	80	PRE	to RED	0	45	5.08	10	64.7	4.7	83.2	6.5	0	90
113	M	MS	2	1	23	80	PRE	to NUP	1	45	9.58	14	56.5	4.7	-73.3	5.1	1	90
113	M	MS	2	1	23	80	PRE	to RED	0	45	3.6	9	51.3	4.7	88.6	7.8	-1	90
113	M	MS	2	1	23	80	PRE	to NUP	1	45	8.07	12	58.1	4.6	-65.2	4.3	1	90
113	M	MS	2	1	12	20	STIM	to RED	0	45	0	0	22.8	3.5	53.8	1.8	-1	90
113	M	MS	2	1	12	20	STIM	to NUP	0	45	1.87	3	21.8	3.5	-76.0	3.5	0	90
113	M	MS	2	1	12	80	STIM	to RED	1	45	2.72	5	41.0	3.9	103.7	6.9	1	90
113	M	MS	2	1	12	80	STIM	to NUP	1	45	4.37	10	57.2	4.9	-93.7	0.9	0	90

113	M	MS	2	1	12	40	STIM	to RED	1	45	0.9	2	36.3	4.8	104.6	2.6	0	90
113	M	MS	2	1	12	40	STIM	to NUP	0	45	2.22	5	30.0	3.5	-83.4	1.6	-1	90
113	M	MS	2	1	19	20	STIM	to RED	0	45	0.57	3	43.1	3.1	79.2	4.8	0	90
113	M	MS	2	1	19	20	STIM	to NUP	1	45	2.97	5	35.5	3.8	-55.4	-0.4	1	90
113	M	MS	2	1	19	80	STIM	to RED	1	45	5.93	10	60.0	4.4	95.8	6.2	0	90
113	M	MS	2	1	19	80	STIM	to NUP	1	45	5.25	10	85.1	4.6	-97.7	2.7	0	90
113	M	MS	2	1	19	40	STIM	to RED	1	45	1.9	5	38.8	4.5	87.8	5.8	0	90
113	M	MS	2	1	19	40	STIM	to NUP	1	45	5.32	7	49.3	3.9	-72.7	2.0	0	90
113	M	MS	2	1	30	20	STIM	to RED	1	45	1.78	3	46.5	3.6	65.1	4.9	0	90
113	M	MS	2	1	30	20	STIM	to NUP	2	45	2.17	8	51.2	4.4	-59.9	0.7	1	90
113	M	MS	2	1	30	80	STIM	to RED	2	45	8.03	7	71.7	4.5	105.0	6.8	0	90
113	M	MS	2	1	30	80	STIM	to NUP	4	45	15.88	15	58.3	4.7	-94.3	8.0	2	90
113	M	MS	2	1	30	40	STIM	to RED	4	45	7.37	5	38.7	4.0	94.3	6.9	0	90
113	M	MS	2	1	30	40	STIM	to NUP	4	45	17.07	5	40.0	3.7	-70.6	6.1	0	90
113	M	MS	2	1	12	20	STIM	to RED	2	45	0	0	31.9	3.2	70.2	0.9	-2	90
113	M	MS	2	1	12	20	STIM	to NUP	2	45	0	0	23.6	3.5	-62.8	2.5	0	90
113	M	MS	2	1	12	80	STIM	to RED	2	45	0.98	2	55.8	4.3		2.3	0	90
113	M	MS	2	1	12	80	STIM	to NUP	2	45	3.3	4	28.8	3.2		6.2	0	90
113	M	MS	2	1	12	40	STIM	to RED	2	45	0	0	33.6	3.8	70.9	3.3	0	90
113	M	MS	2	1	12	40	STIM	to NUP	3	45	5.48	3	26.0	4.3	-59.7	-0.2	1	90
113	M	MS	2	1	19	20	STIM	to RED	2	45	0.77	2	34.9	3.5	56.6	1.8	-1	90
113	M	MS	2	1	19	20	STIM	to NUP	3	45	3.95	5	18.9	4.4	-36.7	3.1	1	90
113	M	MS	2	1	19	80	STIM	to RED	3	45	3.48	5	58.2	3.5	80.5	5.5	0	90
113	M	MS	2	1	19	80	STIM	to NUP	4	45	7.72	5	34.6	4.2	-80.1	7.3	1	90
113	M	MS	2	1	19	40	STIM	to RED	6	45	3.47	5	41.5	3.9	69.5	4.7	2	90
113	M	MS	2	1	19	40	STIM	to NUP	6	45	5.82	7	37.4	3.2	-45.1	2.7	0	90
113	M	MS	2	1	30	20	STIM	to RED	6	45	0	0	43.4	3.6	42.2	3.5	0	90
113	M	MS	2	1	30	20	STIM	to NUP	6	45	2.9	4	37.0	3.8	-40.7	1.8	0	90
113	M	MS	2	1	30	80	STIM	to RED	7	45	5.28	10	56.7	3.4	59.4	9.4	1	90
113	M	MS	2	1	30	80	STIM	to NUP	8	45	10.25	8	59.9	3.2	-64.6	10.3	1	90
113	M	MS	2	1	30	40	STIM	to RED	8	45	3.35	5	77.8	4.6	55.8	2.8	0	90
113	M	MS	2	1	30	40	STIM	to NUP	9	45	5.17	7	60.0	3.5	-45.5	2.2	1	90
113	M	MS	2	1	23	80	POST	to RED	7	45	1.5	4	96.4	4.0	65.6	3.6	-2	90
113	M	MS	2	1	23	80	POST	to NUP	6	45	4.62	5	42.6	3.5	-70.4	8.0	-1	90
113	M	MS	2	1	23	80	POST	to RED	6	45	3.18	5	80.4	4.5	90.0	3.7	0	90
113	M	MS	2	1	23	80	POST	to NUP	7	45	4.85	5	53.1	3.7	-82.4	5.0	1	90
113	M	MS	2	1	23	80	POST	to RED	6	45	1.07	3	42.0	3.2	69.1	6.7	-1	90
113	M	MS	2	1	23	80	POST	to NUP	6	45	5.3	4			-72.2	0.8	0	90
113	M	MS	2	1	0	80	post	to RED	5	45		0					-1	90
113	M	MS	2	1	0	80	post	to NUP	5	45		0					0	90
113	M	MS	2	1	0	80	post	to RED	4	45		0					-1	90
113	M	MS	2	1	0	80	post	to NUP	3	45		0					-1	90
113	M	MS	2	1	0	80	post	to RED	2	45		0					-1	90
113	M	MS	2	1	0	80	post	to NUP	3	45		0					1	90
113	M	MS	2	2	0	80	pre	to RED	0	45		0						90
113	M	MS	2	2	0	80	pre	to NUP	0	45		0					0	90
113	M	MS	2	2	0	80	pre	to RED	0	45		0					0	90
113	M	MS	2	2	0	80	pre	to NUP	0	45		0					0	90
113	M	MS	2	2	0	80	pre	to RED	0	45		0					0	90
113	M	MS	2	2	0	80	pre	to NUP	0	45		0					0	90
113	M	MS	2	2	23	80	PRE	to RED	0	45	3.69	8	26.9	3.7	100.3	6.1	0	90
113	M	MS	2	2	23	80	PRE	to NUP	0	45	5.36	13	28.7	3.8	-81.6	7.5	0	90
113	M	MS	2	2	23	80	PRE	to RED	1	45	4.48	8	49.5	4.0	80.6	3.4	1	90
113	M	MS	2	2	23	80	PRE	to NUP	1	45	6.87	12	39.2	3.6	-70.4	5.7	0	90
113	M	MS	2	2	23	80	PRE	to RED	1	45	3.26	7	26.9	3.7	90.2	5.4	0	90
113	M	MS	2	2	23	80	PRE	to NUP	1	45	6.23	10	54.0	3.4	-88.9	4.2	0	90
113	M	MS	2	2	12	20	STIM	to RED	1	45	0	0	20.9	2.6	66.9	1.5	0	90
113	M	MS	2	2	12	20	STIM	to NUP	3	45	0	0	10.3	2.9	-85.2	0.6	2	90
113	M	MS	2	2	12	80	STIM	to RED	1	45	1.13	2	28.4	3.2	75.7	1.5	-2	90
113	M	MS	2	2	12	80	STIM	to NUP	1	45	1.18	4	32.3	3.8	-86.4	-0.2	0	90
113	M	MS	2	2	12	40	STIM	to RED	1	45	2.88	1	26.1	3.3	92.4	2.0	0	90
113	M	MS	2	2	12	40	STIM	to NUP	1	45	2.05	3	20.8	3.7	-70.7	-0.1	0	90
113	M	MS	2	2	19	20	STIM	to RED	1	45	0	0	17.5	3.4	49.4	0.6	0	90
113	M	MS	2	2	19	20	STIM	to NUP	1	45	1.63	3	18.4	3.2	-87.0	2.8	0	90
113	M	MS	2	2	19	80	STIM	to RED	2	45	2.43	5	49.8	3.5		4.4	1	90
113	M	MS	2	2	19	80	STIM	to NUP	2	45	5.48	7	56.1	3.8		1.8	0	90

113	M	MS	2	2	19	40	STIM	to RED	2	45	2.28	3	31.4	3.7	62.5	4.0	0	90
113	M	MS	2	2	19	40	STIM	to NUP	3	45	5.38	4	24.8	3.6	-53.9	2.4	1	90
113	M	MS	2	2	30	20	STIM	to RED	3	45	1.67	4	36.7	3.2	45.4	3.6	0	90
113	M	MS	2	2	30	20	STIM	to NUP	3	45	4.22	5	29.7	4.5	-48.5	1.5	0	90
113	M	MS	2	2	30	80	STIM	to RED	3	45	5.23	7	79.6	3.6	68.7	1.3	0	90
113	M	MS	2	2	30	80	STIM	to NUP	4	45	10.2	13	32.2	3.8	-66.2	7.2	1	90
113	M	MS	2	2	30	40	STIM	to RED	5	45	3.38	7	28.5	3.9	57.7	4.7	1	90
113	M	MS	2	2	30	40	STIM	to NUP	5	45	5.53	7	53.7	3.9	-50.5	0.9	0	90
113	M	MS	2	2	12	20	STIM	to RED	5	45	0.4	1	23.1	3.3	69.3	0.8	0	90
113	M	MS	2	2	12	20	STIM	to NUP	4	45	0.65	1	16.4	2.9	-52.5	0.0	-1	90
113	M	MS	2	2	12	80	STIM	to RED	4	45	1.52	4	31.3	3.4	105.0	2.3	0	90
113	M	MS	2	2	12	80	STIM	to NUP	4	45	2.57	6	33.1	3.1	-109.0	3.8	0	90
113	M	MS	2	2	12	40	STIM	to RED	4	45	0.97	3	29.5	3.5	104.4	2.5	0	90
113	M	MS	2	2	12	40	STIM	to NUP	4	45	2.6	3	36.2	3.2	-70.1	1.0	0	90
113	M	MS	2	2	19	20	STIM	to RED	3	45	0.43	1	26.1	2.5	65.5	1.1	-1	90
113	M	MS	2	2	19	20	STIM	to NUP	3	45	1.5	3	27.0	3.5	-56.9	0.0	0	90
113	M	MS	2	2	19	80	STIM	to RED	3	45	3.67	7	54.9	3.9	93.9	2.4	0	90
113	M	MS	2	2	19	80	STIM	to NUP	4	45	4.32	7	39.6	5.0	-98.9	3.1	1	90
113	M	MS	2	2	19	40	STIM	to RED	4	45	2.08	5	40.9	3.9	66.2	3.2	0	90
113	M	MS	2	2	19	40	STIM	to NUP	4	45	1.28	5	38.3	4.3	-66.8	-0.3	0	90
113	M	MS	2	2	30	20	STIM	to RED	3	45	1.55	5	26.1	3.9	55.9	1.7	-1	90
113	M	MS	2	2	30	20	STIM	to NUP	3	45	1.97	5	42.9	4.0	-59.0	0.1	0	90
113	M	MS	2	2	30	80	STIM	to RED	4	45	5.63	7	40.5	4.3	105.0	6.3	1	90
113	M	MS	2	2	30	80	STIM	to NUP	4	45	6.1	12	41.1	4.0	-104.2	7.7	0	90
113	M	MS	2	2	30	40	STIM	to RED	4	45	3.18	7	37.8	4.1	79.2	3.5	0	90
113	M	MS	2	2	30	40	STIM	to NUP	4	45	4.17	9	47.0	3.9	-69.1	1.1	0	90
113	M	MS	2	2	23	80	POST	to RED	4	45	1.43	8	33.7	4.5	83.5	3.9	0	90
113	M	MS	2	2	23	80	POST	to NUP	4	45	2.97	10			-77.8	2.0	0	90
113	M	MS	2	2	23	80	POST	to RED	4	45	2.85	8	38.6	4.1	71.1	5.7	0	90
113	M	MS	2	2	23	80	POST	to NUP	4	45	4.57	8	40.9	3.9	-62.3	5.1	0	90
113	M	MS	2	2	23	80	POST	to RED	4	45	3.63	7	39.5	3.6	82.3	4.9	0	90
113	M	MS	2	2	23	80	POST	to NUP	4	45	3.27	7	38.0	5.0	-72.7	1.5	0	90
113	M	MS	2	2	0	80	post	to RED	3	45		0					-1	90
113	M	MS	2	2	0	80	post	to NUP	3	45		0					0	90
113	M	MS	2	2	0	80	post	to RED	3	45		0					0	90
113	M	MS	2	2	0	80	post	to NUP	2	45		0					-1	90
113	M	MS	2	2	0	80	post	to RED	2	45		0					0	90
113	M	MS	2	2	0	80	post	to NUP	2	45		0					0	90
114	M	MS	1	1	0	80	pre	to RED	0	45		0						90
114	M	MS	1	1	0	80	pre	to NUP	0	45		0					0	90
114	M	MS	1	1	0	80	pre	to RED	0	45		0					0	90
114	M	MS	1	1	0	80	pre	to NUP	0	45		0					0	90
114	M	MS	1	1	0	80	pre	to RED	0	45		0					0	90
114	M	MS	1	1	0	80	pre	to NUP	0	45		0					0	90
114	M	MS	1	1	23	80	PRE	to RED	0	45	7.88	10	88.6	5.2	123.1	3.6	0	90
114	M	MS	1	1	23	80	PRE	to NUP	0	40	9.95	9	60.3	3.7	-96.0	7.8	0	60
114	M	MS	1	1	23	80	PRE	to RED	0	45	9.78	8	81.9	4.6	155.0	5.0	0	90
114	M	MS	1	1	23	80	PRE	to NUP	0	40	9.83	8	55.1	3.3	-106.7	5.9	0	60
114	M	MS	1	1	23	80	PRE	to RED	0	45	7.67	7	79.0	4.5	105.3	4.5	0	90
114	M	MS	1	1	23	80	PRE	to NUP	0	41	9.12	7	65.4	4.1	-104.2	7.0	0	66
114	M	MS	1	1	12	20	STIM	to RED	0	45	1.4	4	46.6	3.6	82.9	1.1	0	90
114	M	MS	1	1	12	20	STIM	to NUP	0	44	1.48	4	37.8	3.9	-110.9	0.6	0	84
114	M	MS	1	1	12	80	STIM	to RED	0	45	5.17	5	47.1	5.0	123.9	2.1	0	90
114	M	MS	1	1	12	80	STIM	to NUP	0	42	8.85	4.5	104.7	4.1	-131.2	0.9	0	72
114	M	MS	1	1	12	40	STIM	to RED	0	45	4.4	3	45.1	4.3	157.8	1.4	0	90
114	M	MS	1	1	12	40	STIM	to NUP	0	43	5.7	3	48.0	3.9	-163.3	1.0	0	78
114	M	MS	1	1	19	20	STIM	to RED	0	45	5.37	3	45.1	4.1	89.9	1.6	0	90
114	M	MS	1	1	19	20	STIM	to NUP	0	43	5.63	3	35.6	3.6	-85.6	2.6	0	78
114	M	MS	1	1	19	80	STIM	to RED	0	45	6.37	4	79.7	4.9	117.4	2.7	0	90
114	M	MS	1	1	19	80	STIM	to NUP	0	43	7.13	4	96.6	3.9	-91.3	3.4	0	78
114	M	MS	1	1	19	40	STIM	to RED	0	45	5.88	2	46.2	3.7	133.7	3.0	0	90
114	M	MS	1	1	19	40	STIM	to NUP	0	43	6.48	3	96.6	3.4	-113.9	1.0	0	78
114	M	MS	1	1	30	20	STIM	to RED	0	45	7.8	4	59.2	3.3	93.0	3.3	0	90
114	M	MS	1	1	30	20	STIM	to NUP	0	40	7.82	4	55.3	3.8	-98.5	2.6	0	60
114	M	MS	1	1	30	80	STIM	to RED	0	45	8.37	4	38.5	5.1	125.9	6.7	0	90
114	M	MS	1	1	30	80	STIM	to NUP	2.5	42	11.27	5	81.3	3.8	-133.3	6.4	2.5	72

114	M	MS	1	1	30	40	STIM	to RED	4	45	9.63	4	104.0	4.2	165.7	2.7	1.5	90
114	M	MS	1	1	30	40	STIM	to NUP	4	43	8.78	3	74.0	3.9	-123.9	4.1	0	78
114	M	MS	1	1	12	20	STIM	to RED	0	45	1.93	1	16.8	3.3	74.7	1.8	-4	90
114	M	MS	1	1	12	20	STIM	to NUP	1	44	1.12	1	26.6	4.5	-73.7	0.3	1	84
114	M	MS	1	1	12	80	STIM	to RED	0	45	1.1	1	33.1	4.7	88.6	2.6	-1	90
114	M	MS	1	1	12	80	STIM	to NUP	0	43	6.57	2	43.0	3.9	-85.6	4.9	0	78
114	M	MS	1	1	12	40	STIM	to RED	0	45	5.07	1	34.2	4.0	106.9	2.1	0	90
114	M	MS	1	1	12	40	STIM	to NUP	0	44	6	2	34.4	3.6	-121.0	2.3	0	84
114	M	MS	1	1	19	20	STIM	to RED	0	45	2.58	1	18.1	4.2	90.7	2.3	0	90
114	M	MS	1	1	19	20	STIM	to NUP	1	44	4.23	2	40.4	4.2	-82.4	0.5	1	84
114	M	MS	1	1	19	80	STIM	to RED	0	45	7.55	2.5	51.2	4.8	93.4	2.6	-1	90
114	M	MS	1	1	19	80	STIM	to NUP	4	42	9.88	4	60.6	4.0	-88.0	5.0	4	72
114	M	MS	1	1	19	40	STIM	to RED	2	45	4.7	3	58.5	3.7	112.3	2.1	-2	90
114	M	MS	1	1	19	40	STIM	to NUP	3	43	0.8	3	54.6	3.3	-93.2	2.8	1	78
114	M	MS	1	1	30	20	STIM	to RED	0	45	4.35	3	66.2	3.3	80.8	1.1	-3	90
114	M	MS	1	1	30	20	STIM	to NUP	3	43	5.12	3	45.7	3.8	-81.1	2.4	3	78
114	M	MS	1	1	30	80	STIM	to RED	4	45	8.37	3	48.5	3.1	70.9	6.9	1	90
114	M	MS	1	1	30	80	STIM	to NUP	4	43	11.47	4	51.1	5.1	-118.5	4.6	0	78
114	M	MS	1	1	30	40	STIM	to RED	4	45	5.63	2	67.4	3.9	115.7	3.6	0	90
114	M	MS	1	1	30	40	STIM	to NUP	5	43	7.53	4	42.0	4.3	-113.1	6.4	1	78
114	M	MS	1	1	23	80	POST	to RED	3	45	0.5	3	52.6	3.9	82.8	4.7	-2	90
114	M	MS	1	1	23	80	POST	to NUP	4	43	10.4	4	49.4	4.4	-87.7	7.4	1	78
114	M	MS	1	1	23	80	POST	to RED	2	45	4.28	2	62.1	4.8	83.4	2.1	-2	90
114	M	MS	1	1	23	80	POST	to NUP	3	43	0.5	4	68.9	3.9	-85.0	6.9	1	78
114	M	MS	1	1	23	80	POST	to RED	3	45	0.4	2	62.4	4.8	83.7	2.2	0	90
114	M	MS	1	1	23	80	POST	to NUP	4	43	8.67	3	73.9	3.6	-113.0	6.6	1	78
114	M	MS	1	1	0	80	post	to RED	0	45		0					-4	90
114	M	MS	1	1	0	80	post	to NUP	0	45		0					0	90
114	M	MS	1	1	0	80	post	to RED	0	45		0					0	90
114	M	MS	1	1	0	80	post	to NUP	0	45		0					0	90
114	M	MS	1	1	0	80	post	to RED	0	45		0					0	90
114	M	MS	1	1	0	80	post	to NUP	0	45		0					0	90
114	M	MS	1	2	0	80	pre	to RED	0	45		0						90
114	M	MS	1	2	0	80	pre	to NUP	0	45		0					0	90
114	M	MS	1	2	0	80	pre	to RED	0	45		0					0	90
114	M	MS	1	2	0	80	pre	to NUP	0	45		0					0	90
114	M	MS	1	2	0	80	pre	to RED	0	45		0					0	90
114	M	MS	1	2	0	80	pre	to NUP	0	45		0					0	90
114	M	MS	1	2	23	80	PRE	to RED	0	47	6.72	4	49.9	4.6	151.3	4.5	0	102
114	M	MS	1	2	23	80	PRE	to NUP	0	42	8.75	4	84.3	3.6	-95.1	5.0	0	72
114	M	MS	1	2	23	80	PRE	to RED	0	47	8.32	4			103.9	2.2	0	102
114	M	MS	1	2	23	80	PRE	to NUP	0	43	8.53	4	76.4	3.5	-119.3	4.1	0	78
114	M	MS	1	2	23	80	PRE	to RED	0	46	7.72	3	52.3	5.3	123.4	3.8	0	96
114	M	MS	1	2	23	80	PRE	to NUP	0	43	7.15	3	56.0	4.9	-105.9	6.7	0	78
114	M	MS	1	2	12	20	STIM	to RED	0	45	0	0	21.6	3.4	105.8	2.5	0	90
114	M	MS	1	2	12	20	STIM	to NUP	0	45	0	0	21.7	3.9	-92.9	2.0	0	90
114	M	MS	1	2	12	80	STIM	to RED	0	45	2.23	1	28.3	4.6	91.2	3.9	0	90
114	M	MS	1	2	12	80	STIM	to NUP	0	45	4.85	1	65.1	2.9	-123.2	2.8	0	90
114	M	MS	1	2	12	40	STIM	to RED	0	45	1.4	0.5	32.0	4.2	153.8	2.7	0	90
114	M	MS	1	2	12	40	STIM	to NUP	0	45	1.9	0.5	37.8	3.9	-94.4	2.2	0	90
114	M	MS	1	2	19	20	STIM	to RED	0	45	0.65	0.5	30.6	3.6	89.4	2.9	0	90
114	M	MS	1	2	19	20	STIM	to NUP	0	45	1.4	0.5	41.5	3.7	-81.0	0.9	0	90
114	M	MS	1	2	19	80	STIM	to RED	0	46	5.1	2	63.5	3.8	111.4	3.0	0	96
114	M	MS	1	2	19	80	STIM	to NUP	0	44	8.58	2	52.3	3.7	-114.1	6.9	0	84
114	M	MS	1	2	19	40	STIM	to RED	0	45	3.28	1	100.6	3.9	125.7	0.5	0	90
114	M	MS	1	2	19	40	STIM	to NUP	0	45	5.4	1	50.2	3.7	-92.5	2.1	0	90
114	M	MS	1	2	30	20	STIM	to RED	0	45	3.9	1	48.7	5.0	66.4	1.0	0	90
114	M	MS	1	2	30	20	STIM	to NUP	0	45	3.5	1	42.3	4.9	-87.6	0.8	0	90
114	M	MS	1	2	30	80	STIM	to RED	0	47	7.43	4	31.9	4.4	126.9	7.0	0	102
114	M	MS	1	2	30	80	STIM	to NUP	0	43	10.75	4	52.1	3.7	-95.1	8.0	0	78
114	M	MS	1	2	30	40	STIM	to RED	0	45	3.9	2	81.6	3.7	131.1	2.8	0	90
114	M	MS	1	2	30	40	STIM	to NUP	0	43	5.07	2	90.3	3.8	-111.7	4.9	0	78
114	M	MS	1	2	12	20	STIM	to RED	0	45	0	0	24.7	4.0	81.3	0.8	0	90
114	M	MS	1	2	12	20	STIM	to NUP	0	45	0	0	22.5	4.6	-64.4	0.1	0	90
114	M	MS	1	2	12	80	STIM	to RED	0	45	0	0	34.2	4.1	107.9	3.4	0	90
114	M	MS	1	2	12	80	STIM	to NUP	0	45	4.55	1	57.7	5.1	-133.2	5.2	0	90

114	M	MS	1	2	12	40	STIM	to RED	0	45	0	0	43.2	4.1	99.5	1.7	0	90
114	M	MS	1	2	12	40	STIM	to NUP	0	45	2.92	1	34.9	3.5	-81.9	1.4	0	90
114	M	MS	1	2	19	20	STIM	to RED	0	45	0	0	22.6	4.1	85.1	1.2	0	90
114	M	MS	1	2	19	20	STIM	to NUP	0	45	0	0	36.1	4.5	-76.6	2.2	0	90
114	M	MS	1	2	19	80	STIM	to RED	0	45	4.68	1	26.9	4.0	120.7	6.6	0	90
114	M	MS	1	2	19	80	STIM	to NUP	0	45	9.2	1.5	50.1	3.3	-84.4	6.9	0	90
114	M	MS	1	2	19	40	STIM	to RED	0	45	2.35	1	44.5	3.7	121.5	2.7	0	90
114	M	MS	1	2	19	40	STIM	to NUP	0	45	4.93	1	34.6	4.5	-94.4	4.1	0	90
114	M	MS	1	2	30	20	STIM	to RED	0	45	2.32	1	44.5	4.1	78.3	1.9	0	90
114	M	MS	1	2	30	20	STIM	to NUP	0	45	6.28	1	43.7	4.3	-74.2	0.7	0	90
114	M	MS	1	2	30	80	STIM	to RED	0	46	7.6	3	45.8	4.2	109.1	6.8	0	96
114	M	MS	1	2	30	80	STIM	to NUP	0	45	11.37	5	92.6	4.5	-98.6	5.4	0	90
114	M	MS	1	2	30	40	STIM	to RED	0	45	7.3	2	56.2	3.8	92.8	3.4	0	90
114	M	MS	1	2	30	40	STIM	to NUP	0	43	6.35	2	81.0	3.4	-95.0	4.3	0	78
114	M	MS	1	2	23	80	POST	to RED	0	45	3.47	2	53.7	4.1	122.0	4.4	0	90
114	M	MS	1	2	23	80	POST	to NUP	0	44	7.43	2	77.9	5.2	-98.4	5.4	0	84
114	M	MS	1	2	23	80	POST	to RED	0	45	3.97	1	39.6	4.1	110.0	4.3	0	90
114	M	MS	1	2	23	80	POST	to NUP	0	45	5.45	2	83.0	3.7	-90.7	6.0	0	90
114	M	MS	1	2	23	80	POST	to RED	1	45	4.48	1	46.3	4.4	118.6	3.5	1	90
114	M	MS	1	2	23	80	POST	to NUP	0	45	8.17	2	77.5	3.6	-90.6	5.7	-1	90
114	M	MS	1	2	0	80	post	to RED	0	45		0					0	90
114	M	MS	1	2	0	80	post	to NUP	0	45		0					0	90
114	M	MS	1	2	0	80	post	to RED	0	45		0					0	90
114	M	MS	1	2	0	80	post	to NUP	0	45		0					0	90
114	M	MS	1	2	0	80	post	to RED	0	45		0					0	90
114	M	MS	1	2	0	80	post	to NUP	0	45		0					0	90
115	M	nMS	1	1	0	80	pre	to RED	0	45		0						90
115	M	nMS	1	1	0	80	pre	to NUP	0	45		0					0	90
115	M	nMS	1	1	0	80	pre	to RED	0	45		0					0	90
115	M	nMS	1	1	0	80	pre	to NUP	0	45		0					0	90
115	M	nMS	1	1	0	80	pre	to RED	0	45		0					0	90
115	M	nMS	1	1	0	80	pre	to NUP	0	45		0					0	90
115	M	nMS	1	1	23	80	PRE	to RED	0	40	0	0	59.5	3.8	104.0	3.3	0	60
115	M	nMS	1	1	23	80	PRE	to NUP	0	45	2.28	10	53.2	4.9	-68.7	2.6	0	90
115	M	nMS	1	1	23	80	PRE	to RED	0	42	0	0	39.3	3.3	109.8	3.3	0	72
115	M	nMS	1	1	23	80	PRE	to NUP	0	45	0.42	13	39.0	4.6	-68.9	5.8	0	90
115	M	nMS	1	1	23	80	PRE	to RED	0	45	2.07	5	62.3	3.5	90.4	2.2	0	90
115	M	nMS	1	1	23	80	PRE	to NUP	0	45	2.62	10	41.5	4.6	-61.6	0.7	0	90
115	M	nMS	1	1	12	20	STIM	to RED	0	50	0	0	15.4	3.0	65.2	1.6	0	120
115	M	nMS	1	1	12	20	STIM	to NUP	0	45	0	0	9.9	2.4	-74.0	2.0	0	90
115	M	nMS	1	1	12	80	STIM	to RED	0	50	1.38	3	28.9	3.5	79.0	1.5	0	120
115	M	nMS	1	1	12	80	STIM	to NUP	0	40	2.3	7	37.3	4.0	-79.1	1.5	0	60
115	M	nMS	1	1	12	40	STIM	to RED	0	40	0	0	25.3	3.3	74.7	0.9	0	60
115	M	nMS	1	1	12	40	STIM	to NUP	0	37	0.63	10	27.8	3.4	-65.1	1.9	0	42
115	M	nMS	1	1	19	20	STIM	to RED	0	40	0.63	8	20.7	4.0	60.3	0.7	0	60
115	M	nMS	1	1	19	20	STIM	to NUP	0	37	0.72	11	16.4	3.9	-53.5	1.5	0	42
115	M	nMS	1	1	19	80	STIM	to RED	0	43	2.42	12	36.6	3.6	88.8	1.8	0	78
115	M	nMS	1	1	19	80	STIM	to NUP	0	40	2.78	7	21.9	4.2	-70.5	3.2	0	60
115	M	nMS	1	1	19	40	STIM	to RED	0	37	0.97	10	29.8	3.9	69.4	1.5	0	42
115	M	nMS	1	1	19	40	STIM	to NUP	0	40	0.85	6	34.4	4.3	-52.3	1.6	0	60
115	M	nMS	1	1	30	20	STIM	to RED	0	35	0.6	15	30.3	4.0	57.8	0.9	0	30
115	M	nMS	1	1	30	20	STIM	to NUP	0	33	2.73	15	31.1	4.4	-60.9	0.9	0	18
115	M	nMS	1	1	30	80	STIM	to RED	0	33	2.63	16	53.2	3.7	66.6	2.0	0	18
115	M	nMS	1	1	30	80	STIM	to NUP	0	33	4.97	15	43.0	4.3	-67.9	0.6	0	18
115	M	nMS	1	1	30	40	STIM	to RED	2	33	0.6	14	40.1	4.1	85.1	1.6	2	18
115	M	nMS	1	1	30	40	STIM	to NUP	2	32	2.47	13	29.4	3.6	-69.6	1.9	0	12
115	M	nMS	1	1	12	20	STIM	to RED	1	48	0.5	4	13.4	2.3	55.2	1.1	-1	108
115	M	nMS	1	1	12	20	STIM	to NUP	0	49	0.65	3	31.7	4.3	-61.6	0.9	-1	114
115	M	nMS	1	1	12	80	STIM	to RED	0	43	1.17	8	31.9	4.0	77.9	1.3	0	78
115	M	nMS	1	1	12	80	STIM	to NUP	0	43	1.45	8	28.9	4.0	-72.1	2.1	0	78
115	M	nMS	1	1	12	40	STIM	to RED	0	42	1	5	23.6	3.3	68.0	2.0	0	72
115	M	nMS	1	1	12	40	STIM	to NUP	0	45	0.8	4	20.6	3.2	-54.2	1.6	0	90
115	M	nMS	1	1	19	20	STIM	to RED	0	48	0.47	10	23.9	3.7	53.9	1.2	0	108
115	M	nMS	1	1	19	20	STIM	to NUP	0	43	1.02	11	30.5	3.7	-58.1	6.6	0	78
115	M	nMS	1	1	19	80	STIM	to RED	0	47	0.85	12	17.6	3.1	75.8	5.9	0	102
115	M	nMS	1	1	19	80	STIM	to NUP	0	43	-1	14	42.5	4.3	-79.8	4.1	0	78

115	M	nMS	1	1	19	40	STIM	to RED	0	48	0.68	7	24.7	3.5	80.0	3.6	0	108
115	M	nMS	1	1	19	40	STIM	to NUP	0	41	0.78	10	34.4	3.4	-54.9	1.4	0	66
115	M	nMS	1	1	30	20	STIM	to RED	0	39	0.58	12	26.3	3.6	63.5	2.1	0	54
115	M	nMS	1	1	30	20	STIM	to NUP	0	37	0.43	12	27.4	3.5	-59.9	1.3	0	42
115	M	nMS	1	1	30	80	STIM	to RED	0	39	1.7	13	44.6	3.6	73.4	2.6	0	54
115	M	nMS	1	1	30	80	STIM	to NUP	4	41	3.5	15	35.9	4.6	-68.7	4.8	4	66
115	M	nMS	1	1	30	40	STIM	to RED	2	42	0.62	17	39.7	3.8	80.4	1.6	-2	72
115	M	nMS	1	1	30	40	STIM	to NUP	1	37	3.4	14	19.4	4.4	-56.2	6.4	-1	42
115	M	nMS	1	1	23	80	POST	to RED	4	40	1.42	16	42.0	4.3	81.8	1.3	3	60
115	M	nMS	1	1	23	80	POST	to NUP	2	45	3.47	12	36.0	4.4	-83.9	5.1	-2	90
115	M	nMS	1	1	23	80	POST	to RED	0	43	1.97	13	31.6	3.9	76.6	2.0	-2	78
115	M	nMS	1	1	23	80	POST	to NUP	0	44	3.53	15	31.4	3.5	-70.3	7.0	0	84
115	M	nMS	1	1	23	80	POST	to RED	0	48	0.73	15	24.2	4.0	88.9	3.9	0	108
115	M	nMS	1	1	23	80	POST	to NUP	0	43	2.88	17	43.2	4.5	-67.6	1.5	0	78
115	M	nMS	1	1	0	80	post	to RED	0	48		0					0	108
115	M	nMS	1	1	0	80	post	to NUP	0	50		0					0	120
115	M	nMS	1	1	0	80	post	to RED	0	47		0					0	102
115	M	nMS	1	1	0	80	post	to NUP	0	48		0					0	108
115	M	nMS	1	1	0	80	post	to RED	0	45		0					0	90
115	M	nMS	1	1	0	80	post	to NUP	0	48		0					0	108
115	M	nMS	1	2	0	80	pre	to RED	0	45		0						90
115	M	nMS	1	2	0	80	pre	to NUP	0	45		0					0	90
115	M	nMS	1	2	0	80	pre	to RED	0	45		0					0	90
115	M	nMS	1	2	0	80	pre	to NUP	0	45		0					0	90
115	M	nMS	1	2	0	80	pre	to RED	0	45		0					0	90
115	M	nMS	1	2	0	80	pre	to NUP	0	45		0					0	90
115	M	nMS	1	2	23	80	PRE	to RED	0	43	0	0	68.8	5.5	81.6	3.2	0	78
115	M	nMS	1	2	23	80	PRE	to NUP	0	43	0.88	4	48.0	4.3	-72.6	9.3	0	78
115	M	nMS	1	2	23	80	PRE	to RED	0	41	0.62	3	41.6	4.6	89.5	7.9	0	66
115	M	nMS	1	2	23	80	PRE	to NUP	0	45	1.23	5	46.1	4.0	-102.4	6.2	0	90
115	M	nMS	1	2	23	80	PRE	to RED	0	46	1.65	3	42.4	4.8	91.3	6.4	0	96
115	M	nMS	1	2	23	80	PRE	to NUP	0	42	2.18	4	41.8	4.4	-68.5	6.3	0	72
115	M	nMS	1	2	12	20	STIM	to RED	0	46	0	0	20.9	4.2	56.8	2.2	0	96
115	M	nMS	1	2	12	20	STIM	to NUP	0	47	0	0	17.1	3.3	-65.3	0.8	0	102
115	M	nMS	1	2	12	80	STIM	to RED	0	45	0	0	54.8	4.4	75.0	2.0	0	90
115	M	nMS	1	2	12	80	STIM	to NUP	0	46	0	0	41.1	5.3	-76.2	2.0	0	96
115	M	nMS	1	2	12	40	STIM	to RED	0	47	0	0	31.4	4.4	61.9	2.0	0	102
115	M	nMS	1	2	12	40	STIM	to NUP	0	45	0	0	27.2	4.1	-61.0	1.8	0	90
115	M	nMS	1	2	19	20	STIM	to RED	0	43	0.37	1	35.8	3.7	50.9	0.8	0	78
115	M	nMS	1	2	19	20	STIM	to NUP	0	43	0	0	27.6	4.4	-40.0	1.2	0	78
115	M	nMS	1	2	19	80	STIM	to RED	0	46	0.67	4	35.2	4.2	69.6	5.6	0	96
115	M	nMS	1	2	19	80	STIM	to NUP	0	42	1.85	4	46.2	4.3	-75.5	5.2	0	72
115	M	nMS	1	2	19	40	STIM	to RED	0	46	0.62	2	21.0	3.4	84.2	8.1	0	96
115	M	nMS	1	2	19	40	STIM	to NUP	0	42	0.37	3	33.4	3.5	-45.7	11.3	0	72
115	M	nMS	1	2	30	20	STIM	to RED	0	41	1.08	6	54.4	3.6	43.6	0.9	0	66
115	M	nMS	1	2	30	20	STIM	to NUP	0	40	0.62	5	41.3	4.2	-56.4	3.3	0	60
115	M	nMS	1	2	30	80	STIM	to RED	0	48	0.52	7	77.2	4.0	81.6	5.0	0	108
115	M	nMS	1	2	30	80	STIM	to NUP	0	40	0.37	12	63.3	3.8	-66.3	8.0	0	60
115	M	nMS	1	2	30	40	STIM	to RED	0	40	0.77	7	41.6	4.2	81.3	1.1	0	60
115	M	nMS	1	2	30	40	STIM	to NUP	0	38	0.3	3	51.4	4.0	-63.5	1.1	0	48
115	M	nMS	1	2	12	20	STIM	to RED	0	48	0	0	17.5	3.1	58.8	2.5	0	108
115	M	nMS	1	2	12	20	STIM	to NUP	0	46	0	0	35.7	3.8	-60.4	0.7	0	96
115	M	nMS	1	2	12	80	STIM	to RED	0	47	0.35	1	35.1	4.2	73.5	1.2	0	102
115	M	nMS	1	2	12	80	STIM	to NUP	0	44	0	0	27.4	4.8	-74.1	2.2	0	84
115	M	nMS	1	2	12	40	STIM	to RED	0	45	0	0	36.7	4.2	75.8	2.1	0	90
115	M	nMS	1	2	12	40	STIM	to NUP	0	42	0	0	35.8	4.0	-66.9	6.4	0	72
115	M	nMS	1	2	19	20	STIM	to RED	0	41	0	0	28.6	4.0	72.1	0.7	0	66
115	M	nMS	1	2	19	20	STIM	to NUP	0	41	0	0	40.5	3.9	-45.8	10.3	0	66
115	M	nMS	1	2	19	80	STIM	to RED	0	46	0.42	3	28.3	4.0	84.7	5.5	0	96
115	M	nMS	1	2	19	80	STIM	to NUP	0	44	1.23	2	41.9	3.7	-84.8	13.3	0	84
115	M	nMS	1	2	19	40	STIM	to RED	0	44	0.3	3	30.4	3.9	66.2	3.6	0	84
115	M	nMS	1	2	19	40	STIM	to NUP	0	42	0.52	1	39.5	3.9	-45.0	3.2	0	72
115	M	nMS	1	2	30	20	STIM	to RED	0	38	0	0	20.3	4.0	80.2	3.1	0	48
115	M	nMS	1	2	30	20	STIM	to NUP	0	35	0.73	8	21.8	4.1	-57.8	4.3	0	30
115	M	nMS	1	2	30	80	STIM	to RED	0	43	1.38	13	29.8	3.4	83.6	6.0	0	78
115	M	nMS	1	2	30	80	STIM	to NUP	0	40	0.55	11	48.2	4.6	-64.0	5.1	0	60

115	M	nMS	1	2	30	40	STIM	to RED	0	44	0.37	7	46.3	3.8	84.4	2.7	0	84
115	M	nMS	1	2	30	40	STIM	to NUP	0	37	0.6	7	30.2	3.8	-59.6	1.7	0	42
115	M	nMS	1	2	23	80	POST	to RED	0	40	1.1	8	43.9	3.5	70.8	4.0	0	60
115	M	nMS	1	2	23	80	POST	to NUP	0	40	0.87	6	58.5	3.3	-83.5	4.9	0	60
115	M	nMS	1	2	23	80	POST	to RED	0	46	0.97	4	53.6	3.1	61.2	2.6	0	96
115	M	nMS	1	2	23	80	POST	to NUP	0	43	0.9	2			-60.6	2.0	0	78
115	M	nMS	1	2	23	80	POST	to RED	0	45	1.63	1			82.3	3.4	0	90
115	M	nMS	1	2	23	80	POST	to NUP	0	40	0	0			-75.5	3.9	0	60
115	M	nMS	1	2	0	80	post	to RED	0	50		1					0	120
115	M	nMS	1	2	0	80	post	to NUP	0	50		0					0	120
115	M	nMS	1	2	0	80	post	to RED	0	47		0					0	102
115	M	nMS	1	2	0	80	post	to NUP	0	46		0					0	96
115	M	nMS	1	2	0	80	post	to RED	0	47		0					0	102
115	M	nMS	1	2	0	80	post	to NUP	0	47		0					0	102
116	M	MS	1	1	0	80	pre	to RED	0	45		0						90
116	M	MS	1	1	0	80	pre	to NUP	0	45		0					0	90
116	M	MS	1	1	0	80	pre	to RED	0	45		0					0	90
116	M	MS	1	1	0	80	pre	to NUP	0	45		0					0	90
116	M	MS	1	1	0	80	pre	to RED	0	45		0					0	90
116	M	MS	1	1	0	80	pre	to NUP	0	45		0					0	90
116	M	MS	1	1	23	80	PRE	to RED	0	50	1.18	10	74.8	5.7	105.0	5.5	0	120
116	M	MS	1	1	23	80	PRE	to NUP	0	43	10.82	11	64.6	4.9	-97.9	5.6	0	78
116	M	MS	1	1	23	80	PRE	to RED	0	40	12.6	9	46.2	5.4	84.6	9.2	0	60
116	M	MS	1	1	23	80	PRE	to NUP	0	42	10.97	10	63.3	6.3	-103.1	1.6	0	72
116	M	MS	1	1	23	80	PRE	to RED	0	47	13.58	11	84.3	5.9	103.7	3.5	0	102
116	M	MS	1	1	23	80	PRE	to NUP	0	43	11.57	9	48.6	4.7	-133.4	8.5	0	78
116	M	MS	1	1	12	20	STIM	to RED	0	45	2.08	2	22.5	3.8	84.6	0.6	0	90
116	M	MS	1	1	12	20	STIM	to NUP	0	45	3.15	3	11.5	4.8	-57.3	0.7	0	90
116	M	MS	1	1	12	80	STIM	to RED	0	46	11.15	5	38.6	5.0	76.2	4.5	0	96
116	M	MS	1	1	12	80	STIM	to NUP	0	44	10.8	6	36.2	5.1	-106.3	0.2	0	84
116	M	MS	1	1	12	40	STIM	to RED	0	45.5	7.43	3.5	46.7	4.1	84.2	1.0	0	93
116	M	MS	1	1	12	40	STIM	to NUP	0	44	5.15	4	17.8	3.8	-99.5	1.6	0	84
116	M	MS	1	1	19	20	STIM	to RED	0	46	8.9	4	38.3	4.8	102.7	1.0	0	96
116	M	MS	1	1	19	20	STIM	to NUP	0	44	5.72	3.5	25.0	3.7	-83.4	3.1	0	84
116	M	MS	1	1	19	80	STIM	to RED	0	47	13.43	7	63.8	4.9	95.6	4.2	0	102
116	M	MS	1	1	19	80	STIM	to NUP	1	43	9.1	9	71.0	4.5	-91.4	4.9	1	78
116	M	MS	1	1	19	40	STIM	to RED	1	45	11.38	6	69.2	4.3	104.4	1.3	0	90
116	M	MS	1	1	19	40	STIM	to NUP	1	44	12.8	5	30.8	5.1	-93.9	1.9	0	84
116	M	MS	1	1	30	20	STIM	to RED	3	48	14.67	7	59.2	4.7	85.9	1.4	2	108
116	M	MS	1	1	30	20	STIM	to NUP	3	40	16.9	7	33.3	5.1	-76.0	0.8	0	60
116	M	MS	1	1	30	80	STIM	to RED	4	50	17.85	12	75.9	4.4	105.0	6.6	1	120
116	M	MS	1	1	30	80	STIM	to NUP	4	40	17.22	13	63.5	4.6	-90.9	6.1	0	60
116	M	MS	1	1	30	40	STIM	to RED	3	47	13.95	8	45.7	3.8	95.3	10.5	-1	102
116	M	MS	1	1	30	40	STIM	to NUP	4	42	10.97	8	39.3	4.2	-100.6	2.3	1	72
116	M	MS	1	1	12	20	STIM	to RED	0	45.5	0.85	3	21.0	3.7	52.1	0.4	-4	93
116	M	MS	1	1	12	20	STIM	to NUP	4	44.5	0.97	3	14.3	4.6	-51.2	0.7	4	87
116	M	MS	1	1	12	80	STIM	to RED	3	47	10.98	7	56.5	4.5	78.5	1.3	-1	102
116	M	MS	1	1	12	80	STIM	to NUP	3	44	9.88	6	28.3	4.7	-68.5	4.1	0	84
116	M	MS	1	1	12	40	STIM	to RED	4	46.5	6.62	6	40.8	3.5	87.4	1.0	1	99
116	M	MS	1	1	12	40	STIM	to NUP	4	44	6.4	6	39.7	4.2	-54.2	0.7	0	84
116	M	MS	1	1	19	20	STIM	to RED	3	47	11.62	6	37.1	3.6	47.0	1.7	-1	102
116	M	MS	1	1	19	20	STIM	to NUP	3	44	6.02	4	19.0	3.7	-50.4	2.9	0	84
116	M	MS	1	1	19	80	STIM	to RED	4	46.5	11.72	10	77.2	4.5	82.3	2.9	1	99
116	M	MS	1	1	19	80	STIM	to NUP	4	44	16.12	7	43.9	4.6	-81.9	1.4	0	84
116	M	MS	1	1	19	40	STIM	to RED	5	46	11.13	7	69.5	3.9	98.1	1.7	1	96
116	M	MS	1	1	19	40	STIM	to NUP	4	44	10.08	7	33.0	4.4	-62.4	0.3	-1	84
116	M	MS	1	1	30	20	STIM	to RED	6	48	6.98	6	46.1	4.5	66.8	1.4	2	108
116	M	MS	1	1	30	20	STIM	to NUP	6	42	9.08	9	19.9	3.6	-39.3	1.5	0	72
116	M	MS	1	1	30	80	STIM	to RED	8	49	16.57	13	109.7	4.5	65.7	3.6	2	114
116	M	MS	1	1	30	80	STIM	to NUP	8	40	11.98	15	73.4	5.8	-74.1	6.9	0	60
116	M	MS	1	1	30	40	STIM	to RED	7	48	14.08	11	84.0	4.4	105.0	2.5	-1	108
116	M	MS	1	1	30	40	STIM	to NUP	8	42	11.45	10	81.2	4.9	-73.9	3.2	1	72
116	M	MS	1	1	23	80	POST	to RED	6	47.5	10.23	10	65.4	4.5	105.0	4.8	-2	105
116	M	MS	1	1	23	80	POST	to NUP	5	42	17.4	11	46.5	4.4	-99.8	6.1	-1	72
116	M	MS	1	1	23	80	POST	to RED	8	47	3.22	10	73.1	4.4	91.8	3.3	3	102
116	M	MS	1	1	23	80	POST	to NUP	9	43	17	10	32.4	4.1	-105.2	1.6	1	78

116	M	MS	1	1	23	80	POST	to RED	8	47	12.95	11	100.3	3.8	73.7	4.3	-1	102
116	M	MS	1	1	23	80	POST	to NUP	8	43	18.75	10	42.7	4.7	-81.9	2.1	0	78
116	M	MS	1	1	0	80	post	to RED	3	45.5		2					-5	93
116	M	MS	1	1	0	80	post	to NUP	3	46		2					0	96
116	M	MS	1	1	0	80	post	to RED	2.5	45.5		0					-0.5	93
116	M	MS	1	1	0	80	post	to NUP	2	45		0					-0.5	90
116	M	MS	1	1	0	80	post	to RED	2	45		0					0	90
116	M	MS	1	1	0	80	post	to NUP	1	45		0					-1	90
116	M	MS	1	2	0	80	pre	to RED	0	45		0						90
116	M	MS	1	2	0	80	pre	to NUP	0	45		0					0	90
116	M	MS	1	2	0	80	pre	to RED	0	45		0					0	90
116	M	MS	1	2	0	80	pre	to NUP	0	45		0					0	90
116	M	MS	1	2	0	80	pre	to RED	0	45		0					0	90
116	M	MS	1	2	0	80	pre	to NUP	0	45		0					0	90
116	M	MS	1	2	23	80	PRE	to RED	0	47	14.22	10	77.1	4.8	105.0	4.0	0	102
116	M	MS	1	2	23	80	PRE	to NUP	0	44.5	13.75	10.5	78.4	4.1	-104.0	4.0	0	87
116	M	MS	1	2	23	80	PRE	to RED	0	46	13.55	10.5	47.7	4.1	82.1	5.4	0	96
116	M	MS	1	2	23	80	PRE	to NUP	0	44	13.28	11.5	78.9	3.9	-86.9	3.3	0	84
116	M	MS	1	2	23	80	PRE	to RED	0	46	14.6	11	40.2	4.3	96.0	5.0	0	96
116	M	MS	1	2	23	80	PRE	to NUP	0	44	10.5	12	69.1	3.9	-119.7	7.6	0	84
116	M	MS	1	2	12	20	STIM	to RED	0	45.5	0.65	3	17.1	4.0	80.2	0.6	0	93
116	M	MS	1	2	12	20	STIM	to NUP	0	45	1.07	2	9.0	3.2	-60.1	0.6	0	90
116	M	MS	1	2	12	80	STIM	to RED	0	45.5	3.68	6.5	42.5	3.8	102.9	1.9	0	93
116	M	MS	1	2	12	80	STIM	to NUP	0	44.5	3.43	5	29.0	4.1	-120.8	4.2	0	87
116	M	MS	1	2	12	40	STIM	to RED	0	45	1.88	4.5	30.7	3.6	79.6	1.1	0	90
116	M	MS	1	2	12	40	STIM	to NUP	0	44.5	2.87	5	29.2	3.8	-80.0	3.5	0	87
116	M	MS	1	2	19	20	STIM	to RED	0	45.5	3.6	3	39.3	3.9	48.7	1.0	0	93
116	M	MS	1	2	19	20	STIM	to NUP	0	45	2.28	3.5	17.8	3.6	-81.3	1.2	0	90
116	M	MS	1	2	19	80	STIM	to RED	0	46	8.72	5	43.8	3.5	105.0	3.3	0	96
116	M	MS	1	2	19	80	STIM	to NUP	0	43	13.05	12	94.2	3.3	-86.1	6.1	0	78
116	M	MS	1	2	19	40	STIM	to RED	0	45.5	4.22	3	49.0	3.6	87.8	2.4	0	93
116	M	MS	1	2	19	40	STIM	to NUP	0	44	4.87	6	34.0	3.9	-69.1	0.7	0	84
116	M	MS	1	2	30	20	STIM	to RED	0	46.5	6.32	6	41.1	4.1	50.8	2.7	0	99
116	M	MS	1	2	30	20	STIM	to NUP	2	43	6.43	10	41.7	3.9	-73.9	3.6	2	78
116	M	MS	1	2	30	80	STIM	to RED	2	48	11.7	15	88.8	4.0	82.1	4.7	0	108
116	M	MS	1	2	30	80	STIM	to NUP	2	42	12.4	19	103.1	5.3	-111.1	4.8	0	72
116	M	MS	1	2	30	40	STIM	to RED	1	47	6.03	5	55.7	4.0	94.3	4.7	-1	102
116	M	MS	1	2	30	40	STIM	to NUP	3	43	10.4	10	44.7	4.3	-123.1	3.4	2	78
116	M	MS	1	2	12	20	STIM	to RED	0	45	0.57	1	22.1	3.3	42.4	2.5	-3	90
116	M	MS	1	2	12	20	STIM	to NUP	0	45	0	0	17.5	3.3	-40.1	1.0	0	90
116	M	MS	1	2	12	80	STIM	to RED	0	45.5	3.55	3	33.8	3.5	65.5	2.2	0	93
116	M	MS	1	2	12	80	STIM	to NUP	0	45	4.77	3	17.9	3.7	-60.9	8.1	0	90
116	M	MS	1	2	12	40	STIM	to RED	0	45	3.6	2	49.3	3.5	55.2	0.5	0	90
116	M	MS	1	2	12	40	STIM	to NUP	0	45	1.97	2.5	26.1	4.5	-67.4	2.3	0	90
116	M	MS	1	2	19	20	STIM	to RED	0	45.5	0.97	1.5	26.9	3.8	42.8	1.3	0	93
116	M	MS	1	2	19	20	STIM	to NUP	0	44.5	1.57	2	17.9	4.0	-44.3	4.0	0	87
116	M	MS	1	2	19	80	STIM	to RED	0	47	8.58	5	34.4	3.8	67.6	8.4	0	102
116	M	MS	1	2	19	80	STIM	to NUP	1	44	6.17	7	32.0	4.0	-63.2	6.8	1	84
116	M	MS	1	2	19	40	STIM	to RED	0	45	3.78	3	65.1	3.4	58.4	2.3	-1	90
116	M	MS	1	2	19	40	STIM	to NUP	0	44	2.63	3	23.4	3.2	-59.0	1.3	0	84
116	M	MS	1	2	30	20	STIM	to RED	0	46.5	7.6	4	64.1	3.3	50.4	1.3	0	99
116	M	MS	1	2	30	20	STIM	to NUP	0	43	5.58	3	25.2	3.6	-45.2	5.8	0	78
116	M	MS	1	2	30	80	STIM	to RED	0	47	15.82	13	89.7	3.5	63.8	5.3	0	102
116	M	MS	1	2	30	80	STIM	to NUP	0	42	4.08	15	42.6	3.4	-72.0	5.5	0	72
116	M	MS	1	2	30	40	STIM	to RED	0	46	5.62	8	80.8	4.1	54.6	2.4	0	96
116	M	MS	1	2	30	40	STIM	to NUP	0	43.5	8.72	6	17.9	3.4	-61.3	3.4	0	81
116	M	MS	1	2	23	80	POST	to RED	0	45.5	4.95	6	67.8	3.5	105.0	2.9	0	93
116	M	MS	1	2	23	80	POST	to NUP	0	44.5	4.35	5			-82.3	0.8	0	87
116	M	MS	1	2	23	80	POST	to RED	0	45.5	2.73	6	73.7	3.8	102.5	2.5	0	93
116	M	MS	1	2	23	80	POST	to NUP	0	44	9.6	6	28.5	3.6	-76.9	1.7	0	84
116	M	MS	1	2	23	80	POST	to RED	0	46.5	7.73	7	65.9	3.7	82.1	3.8	0	99
116	M	MS	1	2	23	80	POST	to NUP	0	44	5.33	8	42.6	4.0	-81.7	3.1	0	84
116	M	MS	1	2	0	80	post	to RED	0	46		1					0	96
116	M	MS	1	2	0	80	post	to NUP	0	45.5		0.5					0	93
116	M	MS	1	2	0	80	post	to RED	0	45.75		0					0	94.5
116	M	MS	1	2	0	80	post	to NUP	0	45		0					0	90

116	M	MS	1	2	0	80	post	to RED	0	45.5		0					0	93
116	M	MS	1	2	0	80	post	to NUP	0	45		0					0	90
117	M	MS	1	1	0	80	pre	to RED	0	45		0						90
117	M	MS	1	1	0	80	pre	to NUP	0	45		0					0	90
117	M	MS	1	1	0	80	pre	to RED	0	45		0					0	90
117	M	MS	1	1	0	80	pre	to NUP	0	45		0					0	90
117	M	MS	1	1	0	80	pre	to RED	0	45		0					0	90
117	M	MS	1	1	0	80	pre	to NUP	0	45		0					0	90
117	M	MS	1	1	23	80	PRE	to RED	0	45	0.37	10	56.5	8.4	105.0	5.3	0	90
117	M	MS	1	1	23	80	PRE	to NUP	0	41	0.35	9	144.6	7.9	-79.4	1.6	0	66
117	M	MS	1	1	23	80	PRE	to RED	0	45	2.52	9	79.1	8.6	64.5	3.2	0	90
117	M	MS	1	1	23	80	PRE	to NUP	0	45	4.63	10	95.2	6.4	-72.0	5.2	0	90
117	M	MS	1	1	23	80	PRE	to RED	0	45	2.47	8	70.0	7.4	74.6	4.9	0	90
117	M	MS	1	1	23	80	PRE	to NUP	0	45	3.45	10	80.4	5.9	-71.8	6.4	0	90
117	M	MS	1	1	12	40	STIM	to RED	0	45	0.65	4	36.9	5.5	105.0	1.7	0	90
117	M	MS	1	1	12	40	STIM	to NUP	0	45	1.32	5	39.7	4.4	-71.8	1.5	0	90
117	M	MS	1	1	12	20	STIM	to RED	0	45	0.67	1	20.5	3.9	65.7	1.5	0	90
117	M	MS	1	1	12	20	STIM	to NUP	0	45	0.88	1	11.8	3.9	-64.5	4.8	0	90
117	M	MS	1	1	12	80	STIM	to RED	0	45	1.3	3	43.2	7.8	81.5	2.0	0	90
117	M	MS	1	1	12	80	STIM	to NUP	0	45	2	5	56.1	6.4	-92.6	3.8	0	90
117	M	MS	1	1	19	40	STIM	to RED	0	45	1.28	4	60.3	5.8	74.3	1.6	0	90
117	M	MS	1	1	19	40	STIM	to NUP	0	45	1.55	5	78.7	6.8	-68.7	1.0	0	90
117	M	MS	1	1	19	20	STIM	to RED	0	45	0.53	1	24.0	5.4	55.4	1.0	0	90
117	M	MS	1	1	19	20	STIM	to NUP	0	45	0.65	2	28.2	6.4	-79.4	1.9	0	90
117	M	MS	1	1	19	80	STIM	to RED	0	48	0.83	9	60.9	8.2	88.8	2.7	0	108
117	M	MS	1	1	19	80	STIM	to NUP	0	45	1.78	10	80.5	7.0	-66.8	6.9	0	90
117	M	MS	1	1	30	40	STIM	to RED	0	45	1.22	5	66.8	6.6	94.1	3.3	0	90
117	M	MS	1	1	30	40	STIM	to NUP	0	45	1.93	7	65.9	5.1	-48.9	6.1	0	90
117	M	MS	1	1	30	20	STIM	to RED	0	45	1.12	1	53.5	5.3	56.1	0.9	0	90
117	M	MS	1	1	30	20	STIM	to NUP	0	45	0.63	3	46.9	6.6	-47.3	1.1	0	90
117	M	MS	1	1	30	80	STIM	to RED	0	48	4.3	12	79.1	8.6	59.4	4.2	0	108
117	M	MS	1	1	30	80	STIM	to NUP	0	45	3.95	14	103.8	6.6	-80.0	8.7	0	90
117	M	MS	1	1	12	40	STIM	to RED	0	48	0.98	3	47.5	4.4	74.6	1.4	0	108
117	M	MS	1	1	12	40	STIM	to NUP	0	48	1.35	2	43.7	4.8	-78.5	1.2	0	108
117	M	MS	1	1	12	20	STIM	to RED	0	48	0.58	1	31.0	5.1	69.1	0.8	0	108
117	M	MS	1	1	12	20	STIM	to NUP	0	46	0.87	1	21.9	4.8	-56.9	1.0	0	96
117	M	MS	1	1	12	80	STIM	to RED	0	48	1.6	4	50.4	5.6	72.2	1.5	0	108
117	M	MS	1	1	12	80	STIM	to NUP	0	45	2.57	7	62.4	6.8	-78.5	2.5	0	90
117	M	MS	1	1	19	40	STIM	to RED	0	45	1.23	3	68.5	5.2	105.0	1.2	0	90
117	M	MS	1	1	19	40	STIM	to NUP	1	45	2.02	4	48.5	5.6	-75.2	5.0	1	90
117	M	MS	1	1	19	20	STIM	to RED	2	45	0.9	1	29.5	5.7	77.7	0.7	1	90
117	M	MS	1	1	19	20	STIM	to NUP	3	45	0.57	2	41.4	6.2	-62.0	0.9	1	90
117	M	MS	1	1	19	80	STIM	to RED	4	45	2.32	7	54.4	7.8	60.3	2.1	1	90
117	M	MS	1	1	19	80	STIM	to NUP	6	45	2.28	11	76.6	7.5	-67.4	6.4	2	90
117	M	MS	1	1	30	40	STIM	to RED	4	45	2.55	8	83.6	6.2	78.5	2.0	-2	90
117	M	MS	1	1	30	40	STIM	to NUP	4	45	1.52	8	59.5	6.5	-68.0	3.3	0	90
117	M	MS	1	1	30	20	STIM	to RED	4	45	0.83	1	36.4	5.2	48.7	1.7	0	90
117	M	MS	1	1	30	20	STIM	to NUP	4	45	0.88	3	52.5	5.4	-86.3	0.8	0	90
117	M	MS	1	1	30	80	STIM	to RED	4	45	1.62	8	67.2	7.7	76.4	6.9	0	90
117	M	MS	1	1	30	80	STIM	to NUP	4	45	3.08	10	76.0	5.4	-90.9	10.4	0	90
117	M	MS	1	1	23	80	POST	to RED	4	45	1.33	8	68.9	7.1	101.9	2.8	0	90
117	M	MS	1	1	23	80	POST	to NUP	4	45	1.27	8	78.9	7.8	-93.5	5.4	0	90
117	M	MS	1	1	23	80	POST	to RED	6	45	1.28	7	58.2	7.8	93.0	4.0	2	90
117	M	MS	1	1	23	80	POST	to NUP	7	45	1.85	9	80.2	7.5	-98.3	7.4	1	90
117	M	MS	1	1	23	80	POST	to RED	7	45	2.35	7	63.2	6.5	105.0	3.4	0	90
117	M	MS	1	1	23	80	POST	to NUP	7	45	3.48	9	77.8	6.5	-127.3	7.3	0	90
117	M	MS	1	1	0	80	post	to RED	5	45		0					-2	90
117	M	MS	1	1	0	80	post	to NUP	5	45		0					0	90
117	M	MS	1	1	0	80	post	to RED	5	45		0					0	90
117	M	MS	1	1	0	80	post	to NUP	5	45		0					0	90
117	M	MS	1	1	0	80	post	to RED	5	45		0					0	90
117	M	MS	1	1	0	80	post	to NUP	5	45		0					0	90
117	M	MS	1	2	0	80	pre	to RED	0	45		0						90
117	M	MS	1	2	0	80	pre	to NUP	0	45		0					0	90
117	M	MS	1	2	0	80	pre	to RED	0	45		0					0	90
117	M	MS	1	2	0	80	pre	to NUP	0	45		0					0	90

117	M	MS	1	2	0	80	pre	to RED	0	45		0					0	90
117	M	MS	1	2	0	80	pre	to NUP	0	45		0					0	90
117	M	MS	1	2	23	80	PRE	to RED	0	45	1.1	4	77.2	6.5	99.8	4.3	0	90
117	M	MS	1	2	23	80	PRE	to NUP	0	45	1.17	7	56.6	7.0	-89.3	4.8	0	90
117	M	MS	1	2	23	80	PRE	to RED	0	45	1.35	5	61.2	6.9	84.8	2.2	0	90
117	M	MS	1	2	23	80	PRE	to NUP	0	45	3.08	10	77.3	5.2	-112.8	5.8	0	90
117	M	MS	1	2	23	80	PRE	to RED	0	45	1.65	7	49.8	6.1	105.0	6.4	0	90
117	M	MS	1	2	23	80	PRE	to NUP	0	45	2.28	10	89.3	6.5	-94.1	2.8	0	90
117	M	MS	1	2	12	40	STIM	to RED	0	48	0.88	3	28.6	4.3	86.7	3.8	0	108
117	M	MS	1	2	12	40	STIM	to NUP	0	48	1.33	4	37.8	5.0	-51.2	1.0	0	108
117	M	MS	1	2	12	20	STIM	to RED	0	48	0.53	1	27.2	3.5	72.9	1.1	0	108
117	M	MS	1	2	12	20	STIM	to NUP	0	45	0.55	2	23.2	3.8	-45.4	3.7	0	90
117	M	MS	1	2	12	80	STIM	to RED	0	45	0.7	4	68.6	4.7	105.0	2.2	0	90
117	M	MS	1	2	12	80	STIM	to NUP	0	45	1.42	7	68.3	5.8	-62.2	1.1	0	90
117	M	MS	1	2	19	40	STIM	to RED	0	40	1.6	5	55.3	4.5	48.9	2.7	0	60
117	M	MS	1	2	19	40	STIM	to NUP	0	40	1.38	6	47.2	5.4	-53.6	0.9	0	60
117	M	MS	1	2	19	20	STIM	to RED	0	45	0.58	2	33.4	4.6	46.2	2.0	0	90
117	M	MS	1	2	19	20	STIM	to NUP	0	45	0.47	2	40.0	4.3	-42.2	-0.1	0	90
117	M	MS	1	2	19	80	STIM	to RED	0	45	1.27	7	48.3	4.6	76.9	6.4	0	90
117	M	MS	1	2	19	80	STIM	to NUP	0	45	1.57	7	53.2	4.8	-64.5	3.5	0	90
117	M	MS	1	2	30	40	STIM	to RED	0	40	1.65	8	77.4	5.8	59.2	4.7	0	60
117	M	MS	1	2	30	40	STIM	to NUP	0	40	1.87	10	67.6	5.6	-60.1	4.7	0	60
117	M	MS	1	2	30	20	STIM	to RED	0	40	0.98	3	39.8	4.7	58.4	1.4	0	60
117	M	MS	1	2	30	20	STIM	to NUP	0	40	0.58	4	37.8	5.2	-43.5	0.8	0	60
117	M	MS	1	2	30	80	STIM	to RED	0	40	2.85	11	70.1	6.3	67.4	8.1	0	60
117	M	MS	1	2	30	80	STIM	to NUP	0	40	3.78	12	70.5	4.9	-58.2	10.7	0	60
117	M	MS	1	2	12	40	STIM	to RED	0	48	0.95	4	29.3	5.6	55.9	0.6	0	108
117	M	MS	1	2	12	40	STIM	to NUP	0	48	0.67	4	20.5	4.3	-71.4	4.2	0	108
117	M	MS	1	2	12	20	STIM	to RED	0	48	0.5	2	19.7	5.3	49.4	0.9	0	108
117	M	MS	1	2	12	20	STIM	to NUP	0	48	0.52	1	22.8	4.9	-37.0	-0.4	0	108
117	M	MS	1	2	12	80	STIM	to RED	0	48	1.23	5	45.9	5.2	105.0	3.3	0	108
117	M	MS	1	2	12	80	STIM	to NUP	0	48	1.37	6	31.4	5.0	-67.8	3.2	0	108
117	M	MS	1	2	19	40	STIM	to RED	0	45	1.17	4	21.0	4.9	69.1	3.0	0	90
117	M	MS	1	2	19	40	STIM	to NUP	0	45	1.17	5	39.1	5.4	-63.4	-0.2	0	90
117	M	MS	1	2	19	20	STIM	to RED	0	45	0.67	4	19.1	3.9	61.3	2.5	0	90
117	M	MS	1	2	19	20	STIM	to NUP	0	45	0.78	3	16.1	3.8	-45.4	1.6	0	90
117	M	MS	1	2	19	80	STIM	to RED	0	45	1.67	9	51.6	4.9	67.8	5.3	0	90
117	M	MS	1	2	19	80	STIM	to NUP	0	45	3.48	10	40.9	4.8	-63.8	8.9	0	90
117	M	MS	1	2	30	40	STIM	to RED	0	40	1.88	9	59.2	5.7	62.2	5.3	0	60
117	M	MS	1	2	30	40	STIM	to NUP	0	40	1.33	9	39.7	5.0	-68.3	6.4	0	60
117	M	MS	1	2	30	20	STIM	to RED	0	35	1.8	7	30.9	4.8	45.8	4.3	0	30
117	M	MS	1	2	30	20	STIM	to NUP	0	35	0.62	4	30.4	5.3	-35.3	0.5	0	30
117	M	MS	1	2	30	80	STIM	to RED	0	35	2.35	11	59.4	6.7	60.5	7.4	0	30
117	M	MS	1	2	30	80	STIM	to NUP	0	35	3.1	13	85.3	6.2	-78.1	8.1	0	30
117	M	MS	1	2	23	80	POST	to RED	0	40	2.82	9	34.0	5.5	74.8	11.1	0	60
117	M	MS	1	2	23	80	POST	to NUP	0	40	2.67	10	31.7	6.0	-60.3	3.8	0	60
117	M	MS	1	2	23	80	POST	to RED	0	40	1.92	9	50.3	5.8	84.2	6.1	0	60
117	M	MS	1	2	23	80	POST	to NUP	0	40	3.45	11	64.4	5.4	-90.5	7.7	0	60
117	M	MS	1	2	23	80	POST	to RED	0	40	1.7	9			105.0	6.4	0	60
117	M	MS	1	2	23	80	POST	to NUP	0	40	2.5	10	65.9	6.1	-72.7	2.5	0	60
117	M	MS	1	2	0	80	post	to RED	0	45		0					0	90
117	M	MS	1	2	0	80	post	to NUP	0	45		0					0	90
117	M	MS	1	2	0	80	post	to RED	0	45		0					0	90
117	M	MS	1	2	0	80	post	to NUP	0	45		0					0	90
117	M	MS	1	2	0	80	post	to RED	0	45		0					0	90
117	M	MS	1	2	0	80	post	to NUP	0	45		0					0	90
118	M	nMS	2	1	0	80	pre	to RED	0	45		0						90
118	M	nMS	2	1	0	80	pre	to NUP	0	45		0					0	90
118	M	nMS	2	1	0	80	pre	to RED	0	45		0					0	90
118	M	nMS	2	1	0	80	pre	to NUP	0	45		0					0	90
118	M	nMS	2	1	0	80	pre	to RED	0	45		0					0	90
118	M	nMS	2	1	0	80	pre	to NUP	0	45		0					0	90
118	M	nMS	2	1	23	80	PRE	to RED	0	45		10					0	90
118	M	nMS	2	1	23	80	PRE	to NUP	0	45		10					0	90
118	M	nMS	2	1	23	80	PRE	to RED	0	45		10					0	90
118	M	nMS	2	1	23	80	PRE	to NUP	0	45		10					0	90

118	M	nMS	2	1	23	80	PRE	to RED	0	45		10					0	90
118	M	nMS	2	1	23	80	PRE	to NUP	0	45		8					0	90
118	M	nMS	2	1	12	40	STIM	to RED	0	45		0					0	90
118	M	nMS	2	1	12	40	STIM	to NUP	0	45		2					0	90
118	M	nMS	2	1	12	20	STIM	to RED	0	45		1					0	90
118	M	nMS	2	1	12	20	STIM	to NUP	0	45		0					0	90
118	M	nMS	2	1	12	80	STIM	to RED	0	45		8					0	90
118	M	nMS	2	1	12	80	STIM	to NUP	0	43		8					0	78
118	M	nMS	2	1	19	40	STIM	to RED	0	44		9					0	84
118	M	nMS	2	1	19	40	STIM	to NUP	0	45		7					0	90
118	M	nMS	2	1	19	20	STIM	to RED	0	45		1					0	90
118	M	nMS	2	1	19	20	STIM	to NUP	0	45		0					0	90
118	M	nMS	2	1	19	80	STIM	to RED	0	45		7					0	90
118	M	nMS	2	1	19	80	STIM	to NUP	0	45	5	7					0	90
118	M	nMS	2	1	30	40	STIM	to RED	0	44		8					0	84
118	M	nMS	2	1	30	40	STIM	to NUP	0	45		8					0	90
118	M	nMS	2	1	30	20	STIM	to RED	0	45		3					0	90
118	M	nMS	2	1	30	20	STIM	to NUP	0	45		2					0	90
118	M	nMS	2	1	30	80	STIM	to RED	0	45		10					0	90
118	M	nMS	2	1	30	80	STIM	to NUP	0	45		9					0	90
118	M	nMS	2	1	12	40	STIM	to RED	0	45		2					0	90
118	M	nMS	2	1	12	40	STIM	to NUP	0	45		1					0	90
118	M	nMS	2	1	12	20	STIM	to RED	0	45		0					0	90
118	M	nMS	2	1	12	20	STIM	to NUP	0	45		0					0	90
118	M	nMS	2	1	12	80	STIM	to RED	0	45		3					0	90
118	M	nMS	2	1	12	80	STIM	to NUP	0	45		2					0	90
118	M	nMS	2	1	19	40	STIM	to RED	0	45		3					0	90
118	M	nMS	2	1	19	40	STIM	to NUP	0	45		3					0	90
118	M	nMS	2	1	19	20	STIM	to RED	0	45		1					0	90
118	M	nMS	2	1	19	20	STIM	to NUP	0	45		1					0	90
118	M	nMS	2	1	19	80	STIM	to RED	0	45		5					0	90
118	M	nMS	2	1	19	80	STIM	to NUP	0	45		3					0	90
118	M	nMS	2	1	30	40	STIM	to RED	0	45		8					0	90
118	M	nMS	2	1	30	40	STIM	to NUP	0	45		7					0	90
118	M	nMS	2	1	30	20	STIM	to RED	0	45		2					0	90
118	M	nMS	2	1	30	20	STIM	to NUP	0	45		1.5					0	90
118	M	nMS	2	1	30	80	STIM	to RED	0	45		9					0	90
118	M	nMS	2	1	30	80	STIM	to NUP	0	45		9					0	90
118	M	nMS	2	1	23	80	POST	to RED	0	45		4					0	90
118	M	nMS	2	1	23	80	POST	to NUP	0	45		4					0	90
118	M	nMS	2	1	23	80	POST	to RED	0	45		3					0	90
118	M	nMS	2	1	23	80	POST	to NUP	0	45		3					0	90
118	M	nMS	2	1	23	80	POST	to RED	0	45		3					0	90
118	M	nMS	2	1	23	80	POST	to NUP	0	45		2.5					0	90
118	M	nMS	2	1	0	80	post	to RED	0	45		0					0	90
118	M	nMS	2	1	0	80	post	to NUP	0	45		0					0	90
118	M	nMS	2	1	0	80	post	to RED	0	45		0					0	90
118	M	nMS	2	1	0	80	post	to NUP	0	45		0					0	90
118	M	nMS	2	1	0	80	post	to RED	0	45		0					0	90
118	M	nMS	2	1	0	80	post	to NUP	0	45		0					0	90
118	M	nMS	2	2	0	80	pre	to RED	0	45		0						90
118	M	nMS	2	2	0	80	pre	to NUP	0	45		0					0	90
118	M	nMS	2	2	0	80	pre	to RED	0	45		0					0	90
118	M	nMS	2	2	0	80	pre	to NUP	0	45		0					0	90
118	M	nMS	2	2	0	80	pre	to RED	0	45		0					0	90
118	M	nMS	2	2	0	80	pre	to NUP	0	45		0					0	90
118	M	nMS	2	2	23	80	PRE	to RED	0	45		6					0	90
118	M	nMS	2	2	23	80	PRE	to NUP	0	45		6					0	90
118	M	nMS	2	2	23	80	PRE	to RED	0	45		6					0	90
118	M	nMS	2	2	23	80	PRE	to NUP	0	45		6					0	90
118	M	nMS	2	2	23	80	PRE	to RED	0	45		6					0	90
118	M	nMS	2	2	23	80	PRE	to NUP	0	45		6					0	90
118	M	nMS	2	2	12	40	STIM	to RED	0	45		2					0	90
118	M	nMS	2	2	12	40	STIM	to NUP	0	45		2.5					0	90
118	M	nMS	2	2	12	20	STIM	to RED	0	45		1.5					0	90
118	M	nMS	2	2	12	20	STIM	to NUP	0	45		1					0	90

118	M	nMS	2	2	12	80	STIM	to RED	0	45		1.5					0	90
118	M	nMS	2	2	12	80	STIM	to NUP	0	45		2					0	90
118	M	nMS	2	2	19	40	STIM	to RED	0	45		4					0	90
118	M	nMS	2	2	19	40	STIM	to NUP	0	45		4					0	90
118	M	nMS	2	2	19	20	STIM	to RED	0	45		4					0	90
118	M	nMS	2	2	19	20	STIM	to NUP	0	45		2					0	90
118	M	nMS	2	2	19	80	STIM	to RED	0	45		6					0	90
118	M	nMS	2	2	19	80	STIM	to NUP	0	45		5					0	90
118	M	nMS	2	2	30	40	STIM	to RED	0	45		6					0	90
118	M	nMS	2	2	30	40	STIM	to NUP	0	45		5					0	90
118	M	nMS	2	2	30	20	STIM	to RED	0	45		4					0	90
118	M	nMS	2	2	30	20	STIM	to NUP	0	45		3					0	90
118	M	nMS	2	2	30	80	STIM	to RED	0	45		7					0	90
118	M	nMS	2	2	30	80	STIM	to NUP	0	45		6					0	90
118	M	nMS	2	2	12	40	STIM	to RED	0	45		1					0	90
118	M	nMS	2	2	12	40	STIM	to NUP	0	45		1					0	90
118	M	nMS	2	2	12	20	STIM	to RED	0	45		0					0	90
118	M	nMS	2	2	12	20	STIM	to NUP	0	45		0					0	90
118	M	nMS	2	2	12	80	STIM	to RED	0	45		3					0	90
118	M	nMS	2	2	12	80	STIM	to NUP	0	45		2					0	90
118	M	nMS	2	2	19	40	STIM	to RED	0	45		5					0	90
118	M	nMS	2	2	19	40	STIM	to NUP	0	45		4					0	90
118	M	nMS	2	2	19	20	STIM	to RED	0	45		1					0	90
118	M	nMS	2	2	19	20	STIM	to NUP	0	45		2					0	90
118	M	nMS	2	2	19	80	STIM	to RED	0	45		5					0	90
118	M	nMS	2	2	19	80	STIM	to NUP	0	45		4					0	90
118	M	nMS	2	2	30	40	STIM	to RED	0	45		5					0	90
118	M	nMS	2	2	30	40	STIM	to NUP	0	45		5					0	90
118	M	nMS	2	2	30	20	STIM	to RED	0	45		3					0	90
118	M	nMS	2	2	30	20	STIM	to NUP	0	45		1					0	90
118	M	nMS	2	2	30	80	STIM	to RED	0	45		7					0	90
118	M	nMS	2	2	30	80	STIM	to NUP	0	45		7					0	90
118	M	nMS	2	2	23	80	POST	to RED	0	45		4					0	90
118	M	nMS	2	2	23	80	POST	to NUP	0	45		4					0	90
118	M	nMS	2	2	23	80	POST	to RED	0	45		4					0	90
118	M	nMS	2	2	23	80	POST	to NUP	0	45		4					0	90
118	M	nMS	2	2	23	80	POST	to RED	0	45		3					0	90
118	M	nMS	2	2	23	80	POST	to NUP	0	45		4					0	90
118	M	nMS	2	2	0	80	post	to RED	0	45		0					0	90
118	M	nMS	2	2	0	80	post	to NUP	0	45		0					0	90
118	M	nMS	2	2	0	80	post	to RED	0	45		0					0	90
118	M	nMS	2	2	0	80	post	to NUP	0	45		0					0	90
118	M	nMS	2	2	0	80	post	to RED	0	45		0					0	90
118	M	nMS	2	2	0	80	post	to NUP	0	45		0					0	90
119	F	MS	1	1	0	80	pre	to RED	0	45		0						90
119	F	MS	1	1	0	80	pre	to NUP	0	45		0					0	90
119	F	MS	1	1	0	80	pre	to RED	0	45		0					0	90
119	F	MS	1	1	0	80	pre	to NUP	0	45		0					0	90
119	F	MS	1	1	0	80	pre	to RED	0	45		0					0	90
119	F	MS	1	1	0	80	pre	to NUP	0	45		0					0	90
119	F	MS	1	1	23	80	PRE	to RED	0	46	1.6	10	92.4	5.8	128.8	2.8	0	96
119	F	MS	1	1	23	80	PRE	to NUP	0	46.5	4.45	10	72.6	4.1	-99.9	9.0	0	99
119	F	MS	1	1	23	80	PRE	to RED	0	46	2.85	10	69.8	4.8	138.2	6.5	0	96
119	F	MS	1	1	23	80	PRE	to NUP	0	46	3.52	10	51.6	4.3	-89.7	8.4	0	96
119	F	MS	1	1	23	80	PRE	to RED	0	46	4.55	10	63.8	4.5	126.5	5.8	0	96
119	F	MS	1	1	23	80	PRE	to NUP	0	46	5.45	11	62.6	3.0	-102.6	8.3	0	96
119	F	MS	1	1	12	40	STIM	to RED	0	45	0.4	5	69.1	4.6	154.7	1.7	0	90
119	F	MS	1	1	12	40	STIM	to NUP	0	45	1.18	6	64.9	4.2	-74.8	1.4	0	90
119	F	MS	1	1	12	20	STIM	to RED	0	41	1.07	0.5	46.5	4.3	67.2	0.8	0	66
119	F	MS	1	1	12	20	STIM	to NUP	0	45	0.97	5	43.2	4.7	-80.0	0.6	0	90
119	F	MS	1	1	12	80	STIM	to RED	0	45	0.85	2	34.2	4.4	146.6	8.3	0	90
119	F	MS	1	1	12	80	STIM	to NUP	0	45	3.38	4	60.8	3.7	-122.9	7.3	0	90
119	F	MS	1	1	19	40	STIM	to RED	0	45	0.28	5	36.3	4.4	119.7	4.6	0	90
119	F	MS	1	1	19	40	STIM	to NUP	0	46	1.95	7	92.0	3.7	-82.9	4.0	0	96
119	F	MS	1	1	19	20	STIM	to RED	0	47.5	0.58	5	33.5	3.2	81.6	5.2	0	105
119	F	MS	1	1	19	20	STIM	to NUP	0	47	0.75	5	53.2	3.5	-101.1	1.5	0	102

119	F	MS	1	1	19	80	STIM	to RED	0	48	3.77	7	41.9	3.6	145.9	7.4	0	108
119	F	MS	1	1	19	80	STIM	to NUP	0	50	5.43	9	55.8	4.7	-98.7	3.2	0	120
119	F	MS	1	1	30	40	STIM	to RED	0	46	0.5	12	67.2	4.5	112.5	4.6	0	96
119	F	MS	1	1	30	40	STIM	to NUP	2	46	2	13	55.5	4.0	-108.2	11.2	2	96
119	F	MS	1	1	30	20	STIM	to RED	0	46	0.72	10	67.6	3.9	80.5	3.2	-2	96
119	F	MS	1	1	30	20	STIM	to NUP	2.5	46.5	2.52	14	67.8	4.0	-67.7	5.2	2.5	99
119	F	MS	1	1	30	80	STIM	to RED	0	47	1.57	12	66.7	4.1	113.3	6.4	-2.5	102
119	F	MS	1	1	30	80	STIM	to NUP	5	47	28.93	12	29.0	3.8	-55.1	13.0	5	102
119	F	MS	1	1	12	40	STIM	to RED	2	45.5	0.43	5	48.6	4.8	103.3	1.5	-3	93
119	F	MS	1	1	12	40	STIM	to NUP	2	45	0.92	2	55.4	4.7	-66.1	3.1	0	90
119	F	MS	1	1	12	20	STIM	to RED	0	46	0.43	1	25.8	4.4	79.0	3.6	-2	96
119	F	MS	1	1	12	20	STIM	to NUP	2	45	0.98	1	27.1	3.5	-50.2	3.0	2	90
119	F	MS	1	1	12	80	STIM	to RED	2	46	1.53	3	20.7	3.6	119.4	9.4	0	96
119	F	MS	1	1	12	80	STIM	to NUP	3	45	0.72	5	76.3	3.7	-101.5	5.2	1	90
119	F	MS	1	1	19	40	STIM	to RED	2	48	1.38	7	44.8	3.8	110.0	2.4	-1	108
119	F	MS	1	1	19	40	STIM	to NUP	4	47	2.78	9	45.9	3.9	-67.4	6.7	2	102
119	F	MS	1	1	19	20	STIM	to RED	4	47	0.6	10	33.7	3.7	60.4	2.8	0	102
119	F	MS	1	1	19	20	STIM	to NUP	4	48	0.35	10	44.5	3.7	-67.5	3.0	0	108
119	F	MS	1	1	19	80	STIM	to RED	4	48	2.95	11	34.9	4.1	104.2	11.4	0	108
119	F	MS	1	1	19	80	STIM	to NUP	5	50	1.6	13	38.6	4.6	-81.7	8.8	1	120
119	F	MS	1	1	30	40	STIM	to RED	4	50	4.55	14	35.3	3.4	96.8	8.1	-1	120
119	F	MS	1	1	30	40	STIM	to NUP	6	50	3.13	15	48.6	4.3	-90.3	7.1	2	120
119	F	MS	1	1	30	20	STIM	to RED	6	52	1.95	14	59.6	4.6	74.1	2.8	0	132
119	F	MS	1	1	30	20	STIM	to NUP	7	50	5.17	17	61.9	4.0	-46.1	5.0	1	120
119	F	MS	1	1	30	80	STIM	to RED	6	50	1.68	15	66.8	3.9	107.3	6.0	-1	120
119	F	MS	1	1	30	80	STIM	to NUP	10	50	7.57	17	88.8	3.8	-94.8	10.6	4	120
119	F	MS	1	1	23	80	POST	to RED	10	48	1.6	12			112.2	2.6	0	108
119	F	MS	1	1	23	80	POST	to NUP	11	46	4.93	12	51.0	4.0	-102.6	9.3	1	96
119	F	MS	1	1	23	80	POST	to RED	10	46	6.03	10	46.9	3.8	111.5	6.1	-1	96
119	F	MS	1	1	23	80	POST	to NUP	11	47	5.15	12	51.3	3.5	-92.7	9.1	1	102
119	F	MS	1	1	23	80	POST	to RED	10	46	3.7	10	44.0	3.8	133.5	7.4	-1	96
119	F	MS	1	1	23	80	POST	to NUP	10	46	0.6	10	65.6	3.1	-82.0	9.3	0	96
119	F	MS	1	1	0	80	post	to RED	0	45		0					-10	90
119	F	MS	1	1	0	80	post	to NUP	0	45		0					0	90
119	F	MS	1	1	0	80	post	to RED	0	45		0					0	90
119	F	MS	1	1	0	80	post	to NUP	0	45		0					0	90
119	F	MS	1	1	0	80	post	to RED	0	45		0					0	90
119	F	MS	1	1	0	80	post	to NUP	0	45		0					0	90
119	F	MS	1	2	0	80	pre	to RED	0	45		0						90
119	F	MS	1	2	0	80	pre	to NUP	0	45		0					0	90
119	F	MS	1	2	0	80	pre	to RED	0	45		0					0	90
119	F	MS	1	2	0	80	pre	to NUP	0	45		0					0	90
119	F	MS	1	2	0	80	pre	to RED	0	45		0					0	90
119	F	MS	1	2	0	80	pre	to NUP	0	45		0					0	90
119	F	MS	1	2	23	80	PRE	to RED	0	46	2.33	5	65.4	3.7	51.5	6.0	0	96
119	F	MS	1	2	23	80	PRE	to NUP	0	46	1.83	4.5	73.6	4.5	-37.8	3.9	0	96
119	F	MS	1	2	23	80	PRE	to RED	0	47	3.33	4	75.4	4.3	29.0	5.4	0	102
119	F	MS	1	2	23	80	PRE	to NUP	0	47	3.07	6	67.5	4.1	-27.5	5.1	0	102
119	F	MS	1	2	23	80	PRE	to RED	0	46	1.33	4	74.3	3.8	105.0	5.3	0	96
119	F	MS	1	2	23	80	PRE	to NUP	0	47	3.68	4	67.6	4.1	-104.2	8.3	0	102
119	F	MS	1	2	12	40	STIM	to RED	0	46	0.25	2	70.6	4.3	122.6	1.5	0	96
119	F	MS	1	2	12	40	STIM	to NUP	0	45	1.88	3	57.0	3.8	-85.6	2.9	0	90
119	F	MS	1	2	12	20	STIM	to RED	0	46	0.88	2	44.7	3.3	76.9	1.2	0	96
119	F	MS	1	2	12	20	STIM	to NUP	0	46	0.68	3	18.0	3.8	-76.7	3.2	0	96
119	F	MS	1	2	12	80	STIM	to RED	0	46	1.03	2	59.1	3.8	118.7	4.2	0	96
119	F	MS	1	2	12	80	STIM	to NUP	0	46	1.25	2	57.3	3.7	-149.3	5.4	0	96
119	F	MS	1	2	19	40	STIM	to RED	0	47	0.47	1	44.8	3.9	121.9	4.9	0	102
119	F	MS	1	2	19	40	STIM	to NUP	1	47	2.4	2	54.6	3.9	-98.8	4.3	1	102
119	F	MS	1	2	19	20	STIM	to RED	0	47	0	0	34.6	3.8	72.8	3.6	-1	102
119	F	MS	1	2	19	20	STIM	to NUP	0	47	0.85	2	33.2	3.8	-92.6	5.5	0	102
119	F	MS	1	2	19	80	STIM	to RED	0	47	2.28	3	62.2	3.9	120.9	6.6	0	102
119	F	MS	1	2	19	80	STIM	to NUP	0	47	2.4	4	84.4	4.5	-99.8	0.5	0	102
119	F	MS	1	2	30	40	STIM	to RED	0	50	1.12	2	73.9	3.8	137.8	5.2	0	120
119	F	MS	1	2	30	40	STIM	to NUP	0	47.5	2.35	3	72.1	3.8	-109.9	6.4	0	105
119	F	MS	1	2	30	20	STIM	to RED	0	48	0.37	1	86.7	4.1	79.3	1.5	0	108
119	F	MS	1	2	30	20	STIM	to NUP	1	48	0.78	2	26.6	3.9	-88.9	3.3	1	108

119	F	MS	1	2	30	80	STIM	to RED	0	46	4.3	5	77.3	3.7	111.0	6.2	-1	96
119	F	MS	1	2	30	80	STIM	to NUP	3	47	4.38	7	100.8	4.5	-99.2	0.2	3	102
119	F	MS	1	2	12	40	STIM	to RED	0	46	0	0	80.5	3.4	118.6	1.3	-3	96
119	F	MS	1	2	12	40	STIM	to NUP	0	46	0	0	37.8	3.3	-94.6	5.2	0	96
119	F	MS	1	2	12	20	STIM	to RED	0	48	0	0	37.5	3.5	88.9	1.1	0	108
119	F	MS	1	2	12	20	STIM	to NUP	0	48	0	0	26.4	3.5	-74.9	2.8	0	108
119	F	MS	1	2	12	80	STIM	to RED	0	49	1.07	1	59.9	3.1	122.7	5.5	0	114
119	F	MS	1	2	12	80	STIM	to NUP	0	48	0.67	1	57.2	3.2	-113.3	5.9	0	108
119	F	MS	1	2	19	40	STIM	to RED	0	48	0.48	2	106.5	3.3	126.1	1.5	0	108
119	F	MS	1	2	19	40	STIM	to NUP	1	47	0.33	2	88.6	3.5	-110.6	3.5	1	102
119	F	MS	1	2	19	20	STIM	to RED	0	50	0.48	4	57.9	3.4	96.3	1.9	-1	120
119	F	MS	1	2	19	20	STIM	to NUP	0	49	0.52	2	38.1	3.8	-90.2	2.8	0	114
119	F	MS	1	2	19	80	STIM	to RED	0	47	0.45	3	64.2	3.8	118.7	5.0	0	102
119	F	MS	1	2	19	80	STIM	to NUP	2	48	1.65	5	37.8	3.2	-110.6	10.1	2	108
119	F	MS	1	2	30	40	STIM	to RED	0	50	0.93	10	119.8	3.5	113.3	3.1	-2	120
119	F	MS	1	2	30	40	STIM	to NUP	2	48	3.58	10	98.7	3.5	-74.5	6.5	2	108
119	F	MS	1	2	30	20	STIM	to RED	0	51	0.23	7	63.0	3.9	75.9	3.4	-2	126
119	F	MS	1	2	30	20	STIM	to NUP	2	49	0.55	9	60.4	3.7	-93.2	1.6	2	114
119	F	MS	1	2	30	80	STIM	to RED	0	48	2.05	10	62.9	3.7	124.0	6.7	-2	108
119	F	MS	1	2	30	80	STIM	to NUP	2	48	1.72	10	61.6	3.8	-98.1	7.6	2	108
119	F	MS	1	2	23	80	POST	to RED	0	47	0.62	9	61.4	3.6	112.0	5.8	-2	102
119	F	MS	1	2	23	80	POST	to NUP	0	48	2.42	9			-102.4	3.9	0	108
119	F	MS	1	2	23	80	POST	to RED	0	47	0.77	9	64.8	3.6	115.5	6.7	0	102
119	F	MS	1	2	23	80	POST	to NUP	0	47	1.45	8	55.4	3.5	-82.5	10.6	0	102
119	F	MS	1	2	23	80	POST	to RED	0	46	0.28	10	72.7	3.6	106.2	5.5	0	96
119	F	MS	1	2	23	80	POST	to NUP	0	46	1.27	11	85.5	3.5	-104.9	7.3	0	96
119	F	MS	1	2	0	80	post	to RED	0	45		0					0	90
119	F	MS	1	2	0	80	post	to NUP	0	45		0					0	90
119	F	MS	1	2	0	80	post	to RED	0	45		0					0	90
119	F	MS	1	2	0	80	post	to NUP	0	45		0					0	90
119	F	MS	1	2	0	80	post	to RED	0	45		0					0	90
119	F	MS	1	2	0	80	post	to NUP	0	45		0					0	90
121	M	nMS	1	1	0	80	pre	to RED	0	45		0						90
121	M	nMS	1	1	0	80	pre	to NUP	0	45		0					0	90
121	M	nMS	1	1	0	80	pre	to RED	0	45		0					0	90
121	M	nMS	1	1	0	80	pre	to NUP	0	45		0					0	90
121	M	nMS	1	1	0	80	pre	to RED	0	45		0					0	90
121	M	nMS	1	1	0	80	pre	to NUP	0	45		0					0	90
121	M	nMS	1	1	23	80	PRE	to RED	0	42	12.97	10	61.8	5.7	105.0	8.2	0	72
121	M	nMS	1	1	23	80	PRE	to NUP	0	45	12.33	10	59.9	5.6	-117.0	14.9	0	90
121	M	nMS	1	1	23	80	PRE	to RED	0	40	13.45	8.5	38.4	6.5	93.0	13.3	0	60
121	M	nMS	1	1	23	80	PRE	to NUP	0	50	15.17	11	49.6	5.3	-104.0	14.2	0	120
121	M	nMS	1	1	23	80	PRE	to RED	0	47	14.13	7	52.3	6.4	86.3	12.3	0	102
121	M	nMS	1	1	23	80	PRE	to NUP	0	50	11.43	6.5	86.7	4.5	-108.6	16.1	0	120
121	M	nMS	1	1	12	40	STIM	to RED	0	45	0	0	36.4	5.0	101.2	2.3	0	90
121	M	nMS	1	1	12	40	STIM	to NUP	0	45	0.75	2	25.8	4.3	-88.8	11.5	0	90
121	M	nMS	1	1	12	20	STIM	to RED	0	47	2.03	2	18.1	5.2	105.0	1.0	0	102
121	M	nMS	1	1	12	20	STIM	to NUP	0	47	2.77	2	15.4	4.0	-75.0	2.2	0	102
121	M	nMS	1	1	12	80	STIM	to RED	0	50	4.97	2.5	40.1	5.3	74.8	2.1	0	120
121	M	nMS	1	1	12	80	STIM	to NUP	0	45	9.9	2	45.5	5.5	-96.2	9.0	0	90
121	M	nMS	1	1	19	40	STIM	to RED	0	47.5	7.65	3.5	50.0	5.5	94.7	2.9	0	105
121	M	nMS	1	1	19	40	STIM	to NUP	0	50	10.97	3	38.4	4.5	-74.3	17.1	0	120
121	M	nMS	1	1	19	20	STIM	to RED	0	45	4.65	2	29.5	4.8	84.0	0.3	0	90
121	M	nMS	1	1	19	20	STIM	to NUP	0	45	4.62	2	24.1	3.6	-90.1	2.7	0	90
121	M	nMS	1	1	19	80	STIM	to RED	0	40	14.17	3.5	50.4	6.1	95.3	6.4	0	60
121	M	nMS	1	1	19	80	STIM	to NUP	0	50	16.58	3.5	55.1	5.4	-85.9	11.6	0	120
121	M	nMS	1	1	30	40	STIM	to RED	0	50	10.98	7	41.1	5.7	87.2	7.0	0	120
121	M	nMS	1	1	30	40	STIM	to NUP	0	40	17.07	7	62.3	5.4	-72.7	8.0	0	60
121	M	nMS	1	1	30	20	STIM	to RED	0	40	7.43	4	37.2	5.7	74.1	2.5	0	60
121	M	nMS	1	1	30	20	STIM	to NUP	0	40	6.87	2	31.7	4.4	-93.9	5.3	0	60
121	M	nMS	1	1	30	80	STIM	to RED	0	50	16.52	8	49.3	4.7	85.3	12.4	0	120
121	M	nMS	1	1	30	80	STIM	to NUP	0	45	24.12	9.5	79.3	5.3	-146.6	20.1	0	90
121	M	nMS	1	1	12	40	STIM	to RED	0	45	5.1	1	31.8	4.9	105.0	3.7	0	90
121	M	nMS	1	1	12	40	STIM	to NUP	0	45	6.53	2	34.1	4.7	-82.7	14.0	0	90
121	M	nMS	1	1	12	20	STIM	to RED	0	40	0	0	22.1	5.3	72.0	0.8	0	60
121	M	nMS	1	1	12	20	STIM	to NUP	0	45	5.83	2	30.4	4.5	-74.3	0.5	0	90

121	M	nMS	1	1	12	80	STIM	to RED	0	50	10.67	5	51.3	5.9	84.4	1.3	0	120
121	M	nMS	1	1	12	80	STIM	to NUP	0	50	11.9	3	48.0	6.2	-93.7	2.9	0	120
121	M	nMS	1	1	19	40	STIM	to RED	0	50	8.38	4.5	41.7	5.6	68.9	1.9	0	120
121	M	nMS	1	1	19	40	STIM	to NUP	1	47.5	11.45	3	39.9	6.0	-78.1	7.5	1	105
121	M	nMS	1	1	19	20	STIM	to RED	0	50	8.27	2.5	23.2	4.7	78.1	1.2	-1	120
121	M	nMS	1	1	19	20	STIM	to NUP	0	40	10.63	4	23.1	4.8	-72.5	1.4	0	60
121	M	nMS	1	1	19	80	STIM	to RED	1	50	14.45	4.5	33.7	4.0	84.4	14.0	1	120
121	M	nMS	1	1	19	80	STIM	to NUP	1	50	16.67	4	43.4	3.7	-93.7	12.4	0	120
121	M	nMS	1	1	30	40	STIM	to RED	1	50	10.95	4.5	42.8	4.9	99.1	7.4	0	120
121	M	nMS	1	1	30	40	STIM	to NUP	1	40	16.22	4	29.5	5.2	-72.9	12.4	0	60
121	M	nMS	1	1	30	20	STIM	to RED	1	47	7.8	3	35.1	4.7	95.8	3.8	0	102
121	M	nMS	1	1	30	20	STIM	to NUP	0	42	9.05	2	29.6	3.4	-71.0	10.4	-1	72
121	M	nMS	1	1	30	80	STIM	to RED	1	48	17.17	7.5	36.0	4.6	93.7	14.9	1	108
121	M	nMS	1	1	30	80	STIM	to NUP	0	50	23.2	11	67.6	5.9	-94.3	10.8	-1	120
121	M	nMS	1	1	23	80	POST	to RED	0	52	12.7	6.5	60.0	6.2	100.6	7.4	0	132
121	M	nMS	1	1	23	80	POST	to NUP	0	40	18.65	6	58.1	5.7	-97.2	11.6	0	60
121	M	nMS	1	1	23	80	POST	to RED	0	42	15.12	5.5	48.7	5.5	96.2	9.1	0	72
121	M	nMS	1	1	23	80	POST	to NUP	1	48	20.7	5	52.9	6.3	-142.0	7.0	1	108
121	M	nMS	1	1	23	80	POST	to RED	1	40	13.27	6			105.0	10.3	0	60
121	M	nMS	1	1	23	80	POST	to NUP	0	48	19.1	6			-94.9	16.9	-1	108
121	M	nMS	1	1	0	80	post	to RED	0	45		0					0	90
121	M	nMS	1	1	0	80	post	to NUP	0	45		0.5					0	90
121	M	nMS	1	1	0	80	post	to RED	0	45		0					0	90
121	M	nMS	1	1	0	80	post	to NUP	0	45		0					0	90
121	M	nMS	1	1	0	80	post	to RED	0	45		0					0	90
121	M	nMS	1	1	0	80	post	to NUP	0	45		0					0	90
121	M	nMS	1	2	0	80	pre	to RED	0	45		0						90
121	M	nMS	1	2	0	80	pre	to NUP	0	45		0					0	90
121	M	nMS	1	2	0	80	pre	to RED	0	45		0					0	90
121	M	nMS	1	2	0	80	pre	to NUP	0	45		0					0	90
121	M	nMS	1	2	0	80	pre	to RED	0	45		0					0	90
121	M	nMS	1	2	0	80	pre	to NUP	0	45		0					0	90
121	M	nMS	1	2	23	80	PRE	to RED	0	50	5.67	5	52.7	5.3	95.6	7.1	0	120
121	M	nMS	1	2	23	80	PRE	to NUP	0	52	9.92	6	51.6	6.8	-128.1	10.2	0	132
121	M	nMS	1	2	23	80	PRE	to RED	0	50	11.28	5.5	46.8	5.5	105.0	7.0	0	120
121	M	nMS	1	2	23	80	PRE	to NUP	0	50	12.05	5	46.0	6.4	-133.4	9.8	0	120
121	M	nMS	1	2	23	80	PRE	to RED	0	50	10.97	5	44.9	5.3	77.7	11.4	0	120
121	M	nMS	1	2	23	80	PRE	to NUP	0	40	12.4	5	47.4	6.1	-115.5	12.2	0	60
121	M	nMS	1	2	12	40	STIM	to RED	0	45	3.15	2	36.8	4.0	25.0	2.0	0	90
121	M	nMS	1	2	12	40	STIM	to NUP	0	45	5.58	2.5	38.7	4.2	-24.4	1.4	0	90
121	M	nMS	1	2	12	20	STIM	to RED	0	45	0	0	26.4	3.6	27.1	1.2	0	90
121	M	nMS	1	2	12	20	STIM	to NUP	0	45	3.62	2	21.7	3.8	-21.4	1.4	0	90
121	M	nMS	1	2	12	80	STIM	to RED	0	47	9.15	3.5	42.7	3.7	22.1	4.4	0	102
121	M	nMS	1	2	12	80	STIM	to NUP	0	45	9.97	3.5	44.7	3.8	-30.2	9.3	0	90
121	M	nMS	1	2	19	40	STIM	to RED	0	50	9.77	4	42.8	4.1	28.1	3.5	0	120
121	M	nMS	1	2	19	40	STIM	to NUP	0	40	1.77	4	41.9	3.7	-20.6	10.5	0	60
121	M	nMS	1	2	19	20	STIM	to RED	0	40	5.47	2.5	34.3	3.8	23.9	1.6	0	60
121	M	nMS	1	2	19	20	STIM	to NUP	0	47	5.02	1	32.2	3.8	-19.1	2.3	0	102
121	M	nMS	1	2	19	80	STIM	to RED	0	50	12.73	6	40.0	3.9	23.5	10.0	0	120
121	M	nMS	1	2	19	80	STIM	to NUP	0	42	15.78	7	52.0	4.7	-24.8	11.1	0	72
121	M	nMS	1	2	30	40	STIM	to RED	0	35	9	7.5	59.9	4.3	22.3	4.8	0	30
121	M	nMS	1	2	30	40	STIM	to NUP	0	40	7.8	6	40.2	4.1	-21.8	9.2	0	60
121	M	nMS	1	2	30	20	STIM	to RED	0	40	8.45	4	44.8	4.1	16.4	2.7	0	60
121	M	nMS	1	2	30	20	STIM	to NUP	0	42	8.23	4	37.8	4.0	-26.5	6.5	0	72
121	M	nMS	1	2	30	80	STIM	to RED	0	35	10.92	9	73.0	4.1	116.3	8.9	0	30
121	M	nMS	1	2	30	80	STIM	to NUP	0	40	18	12	68.8	4.9	-29.2	15.9	0	60
121	M	nMS	1	2	12	40	STIM	to RED	0	45	1.88	4	33.9	3.8			0	90
121	M	nMS	1	2	12	40	STIM	to NUP	0	45	4.65	2	39.3	4.6			0	90
121	M	nMS	1	2	12	20	STIM	to RED	0	45	0	0	21.3	3.6			0	90
121	M	nMS	1	2	12	20	STIM	to NUP	0	45	0	0	23.0	3.3			0	90
121	M	nMS	1	2	12	80	STIM	to RED	0	50	6.28	3	44.1	4.5			0	120
121	M	nMS	1	2	12	80	STIM	to NUP	0	45	9.97	4	57.1	4.6			0	90
121	M	nMS	1	2	19	40	STIM	to RED	0	40	7.97	4	24.4	4.6			0	60
121	M	nMS	1	2	19	40	STIM	to NUP	0	47	8.15	4.5	44.2	4.8			0	102
121	M	nMS	1	2	19	20	STIM	to RED	0	45	6.47	2.5	36.5	4.5			0	90
121	M	nMS	1	2	19	20	STIM	to NUP	0	40	8.35	3	24.6	3.9			0	60

121	M	nMS	1	2	19	80	STIM	to RED	0	48	10.18	5	40.5	4.3			0	108
121	M	nMS	1	2	19	80	STIM	to NUP	0	40	12.75	5	66.7	4.5			0	60
121	M	nMS	1	2	30	40	STIM	to RED	0	35	6.65	4	62.8	5.0			0	30
121	M	nMS	1	2	30	40	STIM	to NUP	0	35	13.6	6	46.6	5.6			0	30
121	M	nMS	1	2	30	20	STIM	to RED	0	40	7	3	49.6	4.6			0	60
121	M	nMS	1	2	30	20	STIM	to NUP	0	35	6.77	3.5	36.4	4.6			0	30
121	M	nMS	1	2	30	80	STIM	to RED	0	40	12.88	7	58.3	4.2			0	60
121	M	nMS	1	2	30	80	STIM	to NUP	0	35	15.58	7	69.0	4.6			0	30
121	M	nMS	1	2	23	80	POST	to RED	0	45	10.47	5.5	50.4	4.3	93.9	9.0	0	90
121	M	nMS	1	2	23	80	POST	to NUP	0	45	15.05	5	46.6	4.0	-188.2	19.8	0	90
121	M	nMS	1	2	23	80	POST	to RED	0	47	8.43	5	39.5	4.8	98.5	9.4	0	102
121	M	nMS	1	2	23	80	POST	to NUP	0	45	12.93	6	78.0	4.8	-111.7	13.6	0	90
121	M	nMS	1	2	23	80	POST	to RED	0	45	9.78	5	44.3	5.0	105.0	8.5	0	90
121	M	nMS	1	2	23	80	POST	to NUP	0	40	14.68	5	42.5	4.0	-112.1	15.2	0	60
121	M	nMS	1	2	0	80	post	to RED	0	45		0.5					0	90
121	M	nMS	1	2	0	80	post	to NUP	0	45		0					0	90
121	M	nMS	1	2	0	80	post	to RED	0	45		0					0	90
121	M	nMS	1	2	0	80	post	to NUP	0	45		0					0	90
121	M	nMS	1	2	0	80	post	to RED	0	45		0					0	90
121	M	nMS	1	2	0	80	post	to NUP	0	45		0					0	90
122	F	nMS	2	1	0	80	pre	to RED	0	45		0						90
122	F	nMS	2	1	0	80	pre	to NUP	0	45		0					0	90
122	F	nMS	2	1	0	80	pre	to RED	0	45		0					0	90
122	F	nMS	2	1	0	80	pre	to NUP	0	45		0					0	90
122	F	nMS	2	1	0	80	pre	to RED	0	45		0					0	90
122	F	nMS	2	1	0	80	pre	to NUP	0	45		0					0	90
122	F	nMS	2	1	23	80	PRE	to RED	0	45	1.5	10	78.1	5.2	131.7	5.2	0	90
122	F	nMS	2	1	23	80	PRE	to NUP	1	45	0.48	10	139.9	5.7	-95.0	4.1	1	90
122	F	nMS	2	1	23	80	PRE	to RED	0	45	4.12	10	89.4	4.5	102.6	5.8	-1	90
122	F	nMS	2	1	23	80	PRE	to NUP	0	45	5.17	10	90.4	4.3	-131.2	9.2	0	90
122	F	nMS	2	1	23	80	PRE	to RED	0	45	4.37	10			92.1	2.7	0	90
122	F	nMS	2	1	23	80	PRE	to NUP	0	45	4.42	10	86.4	3.9	-125.9	6.9	0	90
122	F	nMS	2	1	12	40	STIM	to RED	0	45	1.42	7	53.2	4.9	107.9	0.6	0	90
122	F	nMS	2	1	12	40	STIM	to NUP	0	45	3.8	7	61.0	4.8	-117.9	3.1	0	90
122	F	nMS	2	1	12	20	STIM	to RED	0	45	2.5	5	27.0	5.2	82.3	0.9	0	90
122	F	nMS	2	1	12	20	STIM	to NUP	0	45	2.58	5	36.4	4.7	-66.3	0.4	0	90
122	F	nMS	2	1	12	80	STIM	to RED	0	45	3.8	7	70.8	5.6	156.6	0.6	0	90
122	F	nMS	2	1	12	80	STIM	to NUP	0	45	4.52	7	72.5	5.1	-96.1	4.5	0	90
122	F	nMS	2	1	19	40	STIM	to RED	0	45	4.68	8	56.6	4.4	124.9	3.5	0	90
122	F	nMS	2	1	19	40	STIM	to NUP	0	45	4.17	8	49.5	5.3	-105.9	1.3	0	90
122	F	nMS	2	1	19	20	STIM	to RED	0	45	2.92	7	50.0	4.8	76.3	1.3	0	90
122	F	nMS	2	1	19	20	STIM	to NUP	0	45	3.95	7	52.9	5.1	-74.8	2.0	0	90
122	F	nMS	2	1	19	80	STIM	to RED	0	45	4.9	8	64.9	4.8	109.6	4.6	0	90
122	F	nMS	2	1	19	80	STIM	to NUP	0	45	4.77	8	48.3	4.6	-128.9	6.7	0	90
122	F	nMS	2	1	30	40	STIM	to RED	0	45	5.48	9	74.4	4.8	103.8	4.0	0	90
122	F	nMS	2	1	30	40	STIM	to NUP	0	40	6.7	10	77.4	4.1	-117.6	7.9	0	60
122	F	nMS	2	1	30	20	STIM	to RED	0	45	5	10	68.8	4.1	73.1	3.8	0	90
122	F	nMS	2	1	30	20	STIM	to NUP	0	45	3.73	9	78.5	4.4	-89.4	2.6	0	90
122	F	nMS	2	1	30	80	STIM	to RED	0	45	5.57	9	86.3	4.9	89.7	4.4	0	90
122	F	nMS	2	1	30	80	STIM	to NUP	0	45	7.82	10	76.1	4.5	-87.3	4.3	0	90
122	F	nMS	2	1	12	40	STIM	to RED	0	45	1.33	3	68.3	3.5	133.6	0.4	0	90
122	F	nMS	2	1	12	40	STIM	to NUP	0	45	3.08	4	63.9	4.8	-107.7	1.5	0	90
122	F	nMS	2	1	12	20	STIM	to RED	0	45	1.08	3	32.5	4.5	89.3	0.5	0	90
122	F	nMS	2	1	12	20	STIM	to NUP	0	45	1.88	3	33.3	4.1	-65.9	0.7	0	90
122	F	nMS	2	1	12	80	STIM	to RED	0	45	2.9	4	79.0	3.9	136.4	1.6	0	90
122	F	nMS	2	1	12	80	STIM	to NUP	0	45	2.1	4	70.9	4.5	-128.8	3.4	0	90
122	F	nMS	2	1	19	40	STIM	to RED	0	45	3.33	5	66.7	4.7	103.8	1.4	0	90
122	F	nMS	2	1	19	40	STIM	to NUP	0	45	2.62	6	76.4	4.5	-96.8	4.2	0	90
122	F	nMS	2	1	19	20	STIM	to RED	0	45	2.77	5	51.0	4.2	56.9	0.8	0	90
122	F	nMS	2	1	19	20	STIM	to NUP	0	45	1.88	5	45.1	4.2	-74.4	2.3	0	90
122	F	nMS	2	1	19	80	STIM	to RED	1	45	4.42	7	65.7	3.7	111.2	3.8	1	90
122	F	nMS	2	1	19	80	STIM	to NUP	1	45	5.18	7	65.9	3.9	-124.1	6.7	0	90
122	F	nMS	2	1	30	40	STIM	to RED	0	45	3.33	7	106.0	3.6	96.9	2.5	-1	90
122	F	nMS	2	1	30	40	STIM	to NUP	0	45	6.42	11	88.9	3.8	-106.6	6.8	0	90
122	F	nMS	2	1	30	20	STIM	to RED	0	45	4.22	9	65.9	4.0	61.4	0.7	0	90
122	F	nMS	2	1	30	20	STIM	to NUP	0	45	3.78	7	62.2	4.7	-83.0	1.6	0	90

122	F	nMS	2	1	30	80	STIM	to RED	0	45	4.68	12	106.2	3.3	174.6	5.6	0	90
122	F	nMS	2	1	30	80	STIM	to NUP	0	45	8.88	12	106.7	3.5	-133.2	8.8	0	90
122	F	nMS	2	1	23	80	POST	to RED	0	45	3.52	7	62.9	3.7	111.6	4.9	0	90
122	F	nMS	2	1	23	80	POST	to NUP	0	45	5.15	7	78.4	5.0	-125.2	6.0	0	90
122	F	nMS	2	1	23	80	POST	to RED	0	45	6.4	7	68.8	3.8	106.2	5.6	0	90
122	F	nMS	2	1	23	80	POST	to NUP	0	45	5.03	7	54.5	4.3	-117.4	4.1	0	90
122	F	nMS	2	1	23	80	POST	to RED	0	45	6.62	7	76.7	4.1	162.2	4.3	0	90
122	F	nMS	2	1	23	80	POST	to NUP	0	45	7.7	7	68.7	3.4	-95.2	6.1	0	90
122	F	nMS	2	1	0	80	post	to RED	0	45		0					0	90
122	F	nMS	2	1	0	80	post	to NUP	0	45		0					0	90
122	F	nMS	2	1	0	80	post	to RED	0	45		0					0	90
122	F	nMS	2	1	0	80	post	to NUP	0	45		0					0	90
122	F	nMS	2	1	0	80	post	to RED	0	45		0					0	90
122	F	nMS	2	1	0	80	post	to NUP	0	45		0					0	90
122	F	nMS	2	2	0	80	pre	to RED	0	45		0						90
122	F	nMS	2	2	0	80	pre	to NUP	0	45		0					0	90
122	F	nMS	2	2	0	80	pre	to RED	0	45		0					0	90
122	F	nMS	2	2	0	80	pre	to NUP	0	45		0					0	90
122	F	nMS	2	2	0	80	pre	to RED	0	45		0					0	90
122	F	nMS	2	2	0	80	pre	to NUP	0	45		0					0	90
122	F	nMS	2	2	23	80	PRE	to RED	0	45	1.68	7			130.7	3.7	0	90
122	F	nMS	2	2	23	80	PRE	to NUP	0	45	3.63	8			-183.4	4.4	0	90
122	F	nMS	2	2	23	80	PRE	to RED	0	45	5.33	7	67.4	4.6	144.1	3.4	0	90
122	F	nMS	2	2	23	80	PRE	to NUP	0	45	5.07	8	90.4	4.7	-148.1	3.1	0	90
122	F	nMS	2	2	23	80	PRE	to RED	0	45	4.58	7	77.3	4.4	179.0	3.8	0	90
122	F	nMS	2	2	23	80	PRE	to NUP	0	45	5.92	7	58.1	3.7	-121.6	5.4	0	90
122	F	nMS	2	2	12	40	STIM	to RED	0	45	0.77	3	48.6	3.6	135.6	0.7	0	90
122	F	nMS	2	2	12	40	STIM	to NUP	0	45	1.68	2	48.7	3.9	-128.7	0.8	0	90
122	F	nMS	2	2	12	20	STIM	to RED	0	45	0.83	2	24.1	3.8	79.9	0.3	0	90
122	F	nMS	2	2	12	20	STIM	to NUP	0	45	0.5	2	33.1	3.8	-87.1	0.4	0	90
122	F	nMS	2	2	12	80	STIM	to RED	0	45	1.97	4	47.9	3.8	145.9	1.3	0	90
122	F	nMS	2	2	12	80	STIM	to NUP	0	45	2.1	3	43.5	4.5	-131.3	2.5	0	90
122	F	nMS	2	2	19	40	STIM	to RED	0	45	2.65	6	58.9	4.5	113.6	1.4	0	90
122	F	nMS	2	2	19	40	STIM	to NUP	0	45	6.1	7	68.5	3.3	-137.8	3.7	0	90
122	F	nMS	2	2	19	20	STIM	to RED	0	45	3.05	6	33.9	3.5	82.9	2.4	0	90
122	F	nMS	2	2	19	20	STIM	to NUP	0	45	2.92	6	55.2	4.0	-81.8	2.7	0	90
122	F	nMS	2	2	19	80	STIM	to RED	0	45	4.63	7	44.7	3.9	137.2	5.1	0	90
122	F	nMS	2	2	19	80	STIM	to NUP	0	45	7.03	8	56.7	4.4	-123.2	1.5	0	90
122	F	nMS	2	2	30	40	STIM	to RED	0	45	4.9	11	95.6	3.3	137.3	3.9	0	90
122	F	nMS	2	2	30	40	STIM	to NUP	0	45	6.03	11	54.6	3.7	-104.4	6.6	0	90
122	F	nMS	2	2	30	20	STIM	to RED	0	45	4.08	11	67.2	3.0	79.3	3.6	0	90
122	F	nMS	2	2	30	20	STIM	to NUP	0	45	4.27	10	34.2	3.6	-88.7	8.2	0	90
122	F	nMS	2	2	30	80	STIM	to RED	0	45	8.12	11	43.7	3.2	121.6	7.1	0	90
122	F	nMS	2	2	30	80	STIM	to NUP	0	45	7.95	11	29.3	2.8	-143.8	9.0	0	90
122	F	nMS	2	2	12	40	STIM	to RED	0	45	0.65	1	37.2	3.7	117.5	0.7	0	90
122	F	nMS	2	2	12	40	STIM	to NUP	0	45	0.63	1	59.9	3.6	-95.0	1.3	0	90
122	F	nMS	2	2	12	20	STIM	to RED	0	45	0.67	1	32.2	3.6	80.4	0.2	0	90
122	F	nMS	2	2	12	20	STIM	to NUP	0	45	0.42	1	29.5	3.2	-86.8	2.5	0	90
122	F	nMS	2	2	12	80	STIM	to RED	0	45	0.75	1	45.2	3.3	138.9	3.1	0	90
122	F	nMS	2	2	12	80	STIM	to NUP	0	45	7.17	2	37.4	3.8	-108.3	5.9	0	90
122	F	nMS	2	2	19	40	STIM	to RED	0	45	5.5	6	41.3	3.7	122.2	2.3	0	90
122	F	nMS	2	2	19	40	STIM	to NUP	0	45	6.9	7	41.3	3.6	-91.7	7.4	0	90
122	F	nMS	2	2	19	20	STIM	to RED	0	45	1.75	6	36.5	3.3	75.4	2.6	0	90
122	F	nMS	2	2	19	20	STIM	to NUP	0	45	1.18	4	30.1	3.4	-72.7	2.6	0	90
122	F	nMS	2	2	19	80	STIM	to RED	0	45	4.85	7	50.5	3.1	134.5	5.9	0	90
122	F	nMS	2	2	19	80	STIM	to NUP	0	45	7.05	8	47.6	3.1	-138.1	7.3	0	90
122	F	nMS	2	2	30	40	STIM	to RED	0	45	8.37	9	38.8	3.3	93.5	6.2	0	90
122	F	nMS	2	2	30	40	STIM	to NUP	0	45	5.82	10	58.2	3.1	-113.2	5.9	0	90
122	F	nMS	2	2	30	20	STIM	to RED	0	45	6.5	9	44.3	3.9	74.1	0.6	0	90
122	F	nMS	2	2	30	20	STIM	to NUP	0	45	5.35	9	64.2	3.3	-85.4	2.4	0	90
122	F	nMS	2	2	30	80	STIM	to RED	0	45	5.77	10	67.2	3.5	95.2	4.6	0	90
122	F	nMS	2	2	30	80	STIM	to NUP	0	45	6.92	10	67.2	3.7	-134.3	2.8	0	90
122	F	nMS	2	2	23	80	POST	to RED	0	45	4.82	6	70.8	4.2	95.8	2.7	0	90
122	F	nMS	2	2	23	80	POST	to NUP	0	45	7.63	7	40.7	4.0	-118.5	7.8	0	90
122	F	nMS	2	2	23	80	POST	to RED	0	45	5.43	7	46.5	3.8	112.0	4.4	0	90
122	F	nMS	2	2	23	80	POST	to NUP	0	45	6.53	7	66.0	3.7	-136.8	5.2	0	90

122	F	nMS	2	2	23	80	POST	to RED	0	45	6.57	7	55.0	3.8	124.6	4.7	0	90
122	F	nMS	2	2	23	80	POST	to NUP	0	45	5.45	7	91.8	3.2	-116.3	5.6	0	90
122	F	nMS	2	2	0	80	post	to RED	0	45		0					0	90
122	F	nMS	2	2	0	80	post	to NUP	0	45		0					0	90
122	F	nMS	2	2	0	80	post	to RED	0	45		0					0	90
122	F	nMS	2	2	0	80	post	to NUP	0	45		0					0	90
122	F	nMS	2	2	0	80	post	to RED	0	45		0					0	90
122	F	nMS	2	2	0	80	post	to NUP	0	45		0					0	90
123	F	nMS	2	1	0	80	pre	to RED	0	45		0						90
123	F	nMS	2	1	0	80	pre	to NUP	0	45		0					0	90
123	F	nMS	2	1	0	80	pre	to RED	0	45		0					0	90
123	F	nMS	2	1	0	80	pre	to NUP	0	45		0					0	90
123	F	nMS	2	1	0	80	pre	to RED	0	45		0					0	90
123	F	nMS	2	1	0	80	pre	to NUP	0	45		0					0	90
123	F	nMS	2	1	23	80	PRE	to RED	0	45	14.12	10	70.7	6.4	140.2	1.4	0	90
123	F	nMS	2	1	23	80	PRE	to NUP	0	45	17.92	14	121.1	3.5	-132.7	2.5	0	90
123	F	nMS	2	1	23	80	PRE	to RED	0	45	12.33	9	60.1	6.8	118.6	3.4	0	90
123	F	nMS	2	1	23	80	PRE	to NUP	0	45	15.6	13	90.1	3.9	-145.6	3.6	0	90
123	F	nMS	2	1	23	80	PRE	to RED	0	45	10.65	7	63.0	6.6	103.4	3.7	0	90
123	F	nMS	2	1	23	80	PRE	to NUP	0	45	12.88	12	53.9	4.2	-120.0	6.1	0	90
123	F	nMS	2	1	12	40	STIM	to RED	0	45	1.02	2	39.3	4.2	135.7	1.1	0	90
123	F	nMS	2	1	12	40	STIM	to NUP	0	45	3.02	1	32.9	4.7	-90.2	0.7	0	90
123	F	nMS	2	1	12	20	STIM	to RED	0	45	0	0	23.2	4.2	74.7	1.3	0	90
123	F	nMS	2	1	12	20	STIM	to NUP	0	45	0	0	25.0	4.3	-71.6	0.1	0	90
123	F	nMS	2	1	12	80	STIM	to RED	0	45	5.78	3	40.5	5.6	120.9	0.8	0	90
123	F	nMS	2	1	12	80	STIM	to NUP	0	45	6.07	3	51.6	4.8	-112.3	1.1	0	90
123	F	nMS	2	1	19	40	STIM	to RED	0	45	6.12	5	65.3	5.4	88.3	0.9	0	90
123	F	nMS	2	1	19	40	STIM	to NUP	0	45	7.32	5	56.3	4.6	-96.6	0.9	0	90
123	F	nMS	2	1	19	20	STIM	to RED	0	45	4.83	2	53.0	5.4	80.1	1.1	0	90
123	F	nMS	2	1	19	20	STIM	to NUP	0	45	3.55	2	47.0	3.8	-80.5	-0.1	0	90
123	F	nMS	2	1	19	80	STIM	to RED	0	45	10.4	6	37.6	5.6	96.6	4.4	0	90
123	F	nMS	2	1	19	80	STIM	to NUP	0	45	13.75	6	53.5	4.4	-97.5	3.0	0	90
123	F	nMS	2	1	30	40	STIM	to RED	0	45	6.97	4	69.9	5.8	111.5	2.7	0	90
123	F	nMS	2	1	30	40	STIM	to NUP	0	45	11.6	6	80.2	4.9	-64.5	1.3	0	90
123	F	nMS	2	1	30	20	STIM	to RED	0	45	6.45	2	37.7	6.2	72.3	0.2	0	90
123	F	nMS	2	1	30	20	STIM	to NUP	0	45	5.97	2	49.5	3.7	-47.5	0.6	0	90
123	F	nMS	2	1	30	80	STIM	to RED	0	45	12.77	9	40.1	5.6	82.7	6.4	0	90
123	F	nMS	2	1	30	80	STIM	to NUP	0	45	15.15	12	82.8	4.8	-92.2	4.2	0	90
123	F	nMS	2	1	12	40	STIM	to RED	0	45	0	0	35.1	4.4	76.5	1.7	0	90
123	F	nMS	2	1	12	40	STIM	to NUP	0	45	0	0	39.2	4.1	-74.4	-0.2	0	90
123	F	nMS	2	1	12	20	STIM	to RED	0	45	0	0	22.3	4.0	76.0	1.1	0	90
123	F	nMS	2	1	12	20	STIM	to NUP	0	45	0	0	16.7	3.4	-76.2	2.7	0	90
123	F	nMS	2	1	12	80	STIM	to RED	0	45	8.28	2	15.7	4.0	95.6	8.8	0	90
123	F	nMS	2	1	12	80	STIM	to NUP	0	45	8.7	2	46.2	3.8	-111.5	1.1	0	90
123	F	nMS	2	1	19	40	STIM	to RED	0	45	7.37	3	14.1	3.6	63.1	5.5	0	90
123	F	nMS	2	1	19	40	STIM	to NUP	0	45	8.22	3	28.5	4.2	-55.0	1.0	0	90
123	F	nMS	2	1	19	20	STIM	to RED	0	45	0.52	1	34.9	4.2	79.9	1.5	0	90
123	F	nMS	2	1	19	20	STIM	to NUP	0	45	1.78	1	32.8	3.7	-77.1	0.6	0	90
123	F	nMS	2	1	19	80	STIM	to RED	0	45	10.1	5	15.8	3.6	68.4	4.9	0	90
123	F	nMS	2	1	19	80	STIM	to NUP	0	45	13.62	6	67.5	4.2	-105.8	2.3	0	90
123	F	nMS	2	1	30	40	STIM	to RED	0	45	9.28	7	29.2	3.6	91.4	8.6	0	90
123	F	nMS	2	1	30	40	STIM	to NUP	0	45	10.85	7	34.3	4.0	-52.8	2.3	0	90
123	F	nMS	2	1	30	20	STIM	to RED	0	45	3	4	38.3	4.5	82.7	4.1	0	90
123	F	nMS	2	1	30	20	STIM	to NUP	0	45	5.97	4	32.6	3.9	-79.5	0.4	0	90
123	F	nMS	2	1	30	80	STIM	to RED	0	45	9.95	9	28.4	4.0	83.5	8.1	0	90
123	F	nMS	2	1	30	80	STIM	to NUP	0	45	15.75	9	75.0	4.6	-86.0	4.5	0	90
123	F	nMS	2	1	23	80	POST	to RED	0	45	3.65	3	40.6	4.7	86.6	3.3	0	90
123	F	nMS	2	1	23	80	POST	to NUP	0	45	12.28	4	21.8	3.2	-64.4	10.3	0	90
123	F	nMS	2	1	23	80	POST	to RED	0	45	8.07	3	23.0	3.8	83.7	10.2	0	90
123	F	nMS	2	1	23	80	POST	to NUP	0	45	11.48	4	18.4	3.9	-74.8	3.6	0	90
123	F	nMS	2	1	23	80	POST	to RED	0	45	4.62	2	45.3	3.8	82.5	6.6	0	90
123	F	nMS	2	1	23	80	POST	to NUP	0	45	9.77	3	43.5	4.3	-76.4	3.7	0	90
123	F	nMS	2	1	0	80	post	to RED	0	45		0					0	90
123	F	nMS	2	1	0	80	post	to NUP	0	45		0					0	90
123	F	nMS	2	1	0	80	post	to RED	0	45		0					0	90
123	F	nMS	2	1	0	80	post	to NUP	0	45		0					0	90

123	F	nMS	2	1	0	80	post	to RED	0	45		0					0	90
123	F	nMS	2	1	0	80	post	to NUP	0	45		0					0	90
123	F	nMS	2	2	0	80	pre	to RED	0	45		0						90
123	F	nMS	2	2	0	80	pre	to NUP	0	45		0					0	90
123	F	nMS	2	2	0	80	pre	to RED	0	45		0					0	90
123	F	nMS	2	2	0	80	pre	to NUP	0	45		0					0	90
123	F	nMS	2	2	0	80	pre	to RED	0	45		0					0	90
123	F	nMS	2	2	0	80	pre	to NUP	0	45		0					0	90
123	F	nMS	2	2	23	80	PRE	to RED	0	45	6.12	5	79.1	4.2	113.4	2.9	0	90
123	F	nMS	2	2	23	80	PRE	to NUP	0	45	13.17	9	98.6	4.5	-95.2	2.5	0	90
123	F	nMS	2	2	23	80	PRE	to RED	0	45	7.82	4	62.5	4.7	58.7	4.4	0	90
123	F	nMS	2	2	23	80	PRE	to NUP	0	45	11.95	7	82.3	4.8	-78.5	2.0	0	90
123	F	nMS	2	2	23	80	PRE	to RED	0	45	9.62	4			87.4	5.5	0	90
123	F	nMS	2	2	23	80	PRE	to NUP	0	45	11.08	5			-73.0	8.5	0	90
123	F	nMS	2	2	12	40	STIM	to RED	0	45	2.8	2	44.1	3.7	70.4	1.9	0	90
123	F	nMS	2	2	12	40	STIM	to NUP	0	45	3.9	2	32.7	4.3	-73.2	-0.4	0	90
123	F	nMS	2	2	12	20	STIM	to RED	0	45	0	0	38.2	4.4	79.4	0.9	0	90
123	F	nMS	2	2	12	20	STIM	to NUP	0	45	-1	0.5	16.1	3.2	-107.7	1.8	0	90
123	F	nMS	2	2	12	80	STIM	to RED	0	45	8.37	2	31.4	3.0	118.3	7.3	0	90
123	F	nMS	2	2	12	80	STIM	to NUP	0	45	6.37	2	42.4	4.0	-109.2	1.3	0	90
123	F	nMS	2	2	19	40	STIM	to RED	0	45	4.22	3.5	44.5	4.7	107.2	5.1	0	90
123	F	nMS	2	2	19	40	STIM	to NUP	0	45	7.05	4	56.0	3.1	-81.3	3.3	0	90
123	F	nMS	2	2	19	20	STIM	to RED	0	45	1.85	1.5	40.7	3.7	80.0	0.8	0	90
123	F	nMS	2	2	19	20	STIM	to NUP	0	45	2.82	1.5	30.2	3.4	-86.9	6.6	0	90
123	F	nMS	2	2	19	80	STIM	to RED	0	45	6.92	3	36.6	4.5	78.3	6.2	0	90
123	F	nMS	2	2	19	80	STIM	to NUP	0	45	8.03	3	45.9	3.9	-93.4	5.6	0	90
123	F	nMS	2	2	30	40	STIM	to RED	0	45	6.58	5	43.5	4.7	97.7	5.9	0	90
123	F	nMS	2	2	30	40	STIM	to NUP	0	45	6.47	6	47.1	4.7	-83.3	4.6	0	90
123	F	nMS	2	2	30	20	STIM	to RED	0	45	4.65	2	26.5	3.7	70.7	2.3	0	90
123	F	nMS	2	2	30	20	STIM	to NUP	0	45	7.12	3	40.2	3.4	-58.8	0.9	0	90
123	F	nMS	2	2	30	80	STIM	to RED	0	45	7.85	4	41.7	3.5	90.8	10.2	0	90
123	F	nMS	2	2	30	80	STIM	to NUP	0	45	13.82	6	63.3	4.5	-100.4	5.3	0	90
123	F	nMS	2	2	12	40	STIM	to RED	0	45	2.73	0.5	45.0	3.5	105.4	2.2	0	90
123	F	nMS	2	2	12	40	STIM	to NUP	0	45	1.65	0.5	32.1	3.8	-93.9	4.6	0	90
123	F	nMS	2	2	12	20	STIM	to RED	0	45	0	0	23.4	3.7	82.1	1.3	0	90
123	F	nMS	2	2	12	20	STIM	to NUP	0	45	0	0	33.1	3.3	-63.6	1.3	0	90
123	F	nMS	2	2	12	80	STIM	to RED	0	45	4.12	1	57.1	4.7	90.9	1.2	0	90
123	F	nMS	2	2	12	80	STIM	to NUP	0	45	5.25	1	52.1	3.1	-82.8	4.4	0	90
123	F	nMS	2	2	19	40	STIM	to RED	0	45	3.2	1	40.7	3.8	53.5	3.7	0	90
123	F	nMS	2	2	19	40	STIM	to NUP	0	45	5.62	1.5	37.9	3.5	-75.5	4.9	0	90
123	F	nMS	2	2	19	20	STIM	to RED	0	45	0	0	48.0	3.9	84.4	0.8	0	90
123	F	nMS	2	2	19	20	STIM	to NUP	0	45	0	0	29.4	3.0	-73.1	0.2	0	90
123	F	nMS	2	2	19	80	STIM	to RED	0	45	4.98	0.5	68.4	4.0	67.5	4.6	0	90
123	F	nMS	2	2	19	80	STIM	to NUP	0	45	7.37	1	46.8	3.8	-76.4	9.2	0	90
123	F	nMS	2	2	30	40	STIM	to RED	0	45	4.2	3	54.1	4.6	100.5	3.5	0	90
123	F	nMS	2	2	30	40	STIM	to NUP	0	45	13.27	3.5	40.7	3.6	-74.0	2.5	0	90
123	F	nMS	2	2	30	20	STIM	to RED	0	45	0.48	0.25	44.6	3.4	91.9	3.2	0	90
123	F	nMS	2	2	30	20	STIM	to NUP	0	45	0.73	0.25	37.4	3.6	-74.5	4.9	0	90
123	F	nMS	2	2	30	80	STIM	to RED	0	45	5.43	1	78.8	4.2	91.6	7.1	0	90
123	F	nMS	2	2	30	80	STIM	to NUP	0	45	13.42	3	63.8	4.2	-81.4	2.2	0	90
123	F	nMS	2	2	23	80	POST	to RED	0	45	5.78	2	42.7	4.5	68.1	4.7	0	90
123	F	nMS	2	2	23	80	POST	to NUP	0	45	10.82	4	45.7	5.1	-84.3	2.1	0	90
123	F	nMS	2	2	23	80	POST	to RED	0	45	-1	0.5	56.4	3.9	81.3	7.6	0	90
123	F	nMS	2	2	23	80	POST	to NUP	0	45	7.45	3	51.7	4.3	-87.4	1.3	0	90
123	F	nMS	2	2	23	80	POST	to RED	0	45	5.73	2	66.5	4.3	70.0	5.4	0	90
123	F	nMS	2	2	23	80	POST	to NUP	0	45	5.03	2	65.2	4.6	-83.4	1.2	0	90
123	F	nMS	2	2	0	80	post	to RED	0	45		0					0	90
123	F	nMS	2	2	0	80	post	to NUP	0	45		0					0	90
123	F	nMS	2	2	0	80	post	to RED	0	45		0					0	90
123	F	nMS	2	2	0	80	post	to NUP	0	45		0					0	90
123	F	nMS	2	2	0	80	post	to RED	0	45		0					0	90
123	F	nMS	2	2	0	80	post	to NUP	0	45		0					0	90